DOCTOR OF PHILOSOPHY

Bio-optical studies of coastal waters

Kratzer,, Susanne

Award date:
2000

Awarding institution:
University of Wales, Bangor

Bio-optical studies of coastal waters

by

Susanne Kratzer

A thesis in partial fulfilment of the requirements of the University of Wales

for the degree of Doctor of Philosophy

University of Wales, Bangor

School of Ocean Sciences

Menai Bridge

Anglesey

LL59 5ey

UK

Abstract

Most bio-optical work and remote sensing for the estimation of biomass and productivity has concentrated on clear ocean waters (optical Case-1 waters). Coastal waters (optical Case-2 waters), however, tend to be the most productive areas of the world oceans, and it is therefore important to estimate biomass here. However, because of the presence of suspended particulate matter (SPM), and coloured dissolved organic matter (CDOM) coastal waters are optically very complicated, and remote sensing imagery from coastal waters is difficult to interpret.

A study of bio-optical properties of coastal waters is reported using the Menai Strait and the open Baltic Sea as examples. Both in situ and laboratory methods were applied. Laboratory methods focused on spectrophotometric measurements of optically-active in-water constituents (OICs) and a four-channel colour sensor (CS) was used for in situ measurements of upwelling irradiance.

The Menai Strait was optically dominated by SPM, whereas in the open Baltic Sea CDOM was the prime optical determinant. Multiple regression analysis (MRA) and a semi-empirical model (Harker, 1997) were applied to interpret the CS data, and to investigate the possibility of deriving OICs from CS measurements. The MRA algorithms were regional.

The semi-empirical model was tested using data from a 9-month deployment of the CS in the Menai Strait. MRA was used to derive a time series of OICs. When inverted, the resulting algorithm provided good estimation of SPM. For chlorophyll and SPM, a time series was produced that agreed with historical data. For CDOM no satisfactory algorithm could be derived, because CDOM absorption was relatively small in the Menai Strait. Chlorophyll a had a seasonal signal, and SPM showed a seasonal as well as a tidal signal, whereas CDOM was highest in summer.

The Harker model was adapted to the Baltic Sea. The model results were best when assuming backscatter to be spectrally neutral. The MRA yielded good predictive algorithms for chlorophyll and CDOM in the open Baltic Sea. A high correlation was found between chlorophyll and SPM. CDOM absorption was higher in summer than in spring.

Complementary chromatic adaptation of Baltic Sea cyanobacteria was investigated, and suggestions for algorithm development were made.

This PhD thesis is dedicated to the sun

- and all the chlorophyll molecules on Earth.

Table of contents

List of figures and tables

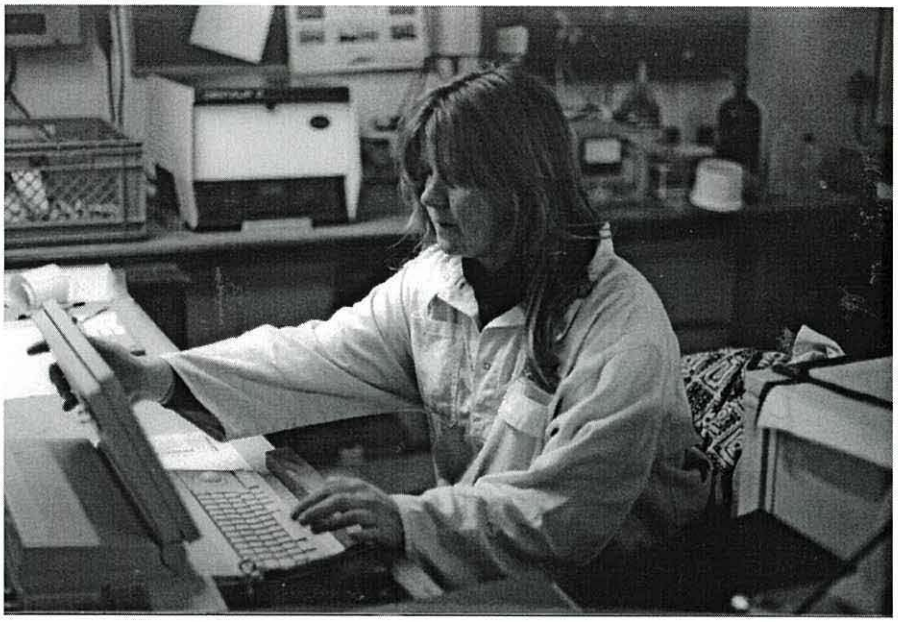

Acknowledgements

This work was funded by MAFF (UK Ministry of Agriculture Fisheries and Food), RESE (Remote Sensing of the Environment, a Swedish MISTRA project), and the Swedish National Space Board.

This is a truly European thesis, and I am afraid it involved a lot of jetting around between Wales, Sweden and Scotland, and using up of precious fossil fuels. I am sorry for this, and for the trees that got used up during the write-up of this thesis.

This thesis would not have been completed without the love and support of many people. I am very grateful to my friends and colleagues who contributed in all various ways.

I am grateful to Paul Tett, Dave Bowers and Ian Lukas for their joint supervision. Great thanks to Paul for getting me interested in oceanography in the first place, and for guiding me during my writing-up of the thesis. Thanks for your incredible patience! Thanks to Dave for your cheerfulness and for getting me into modelling. Thanks for running various versions of the model for me (see chapter 5). Thanks to Ian Lucas for letting me use his microscope, and for providing moral support and advice. Thanks to Peter Williams for providing me with a really nice lab space and for letting me take part in his PhD student seminars. Thanks for making me feel like a part of your group! Thanks to Gay Mitchelson-Jacob for her support and for taking part in the supervising-committee. Thanks a lot to Andy Yule for statistical advice in Chapter 4. I would like to thank Sinclair Buchan for writing a manuscript with Dave and me. Special thanks to Anne Hammerstein for her friendship and her continuous practical and moral support and humour during cruises. Thanks for looking after the colour sensors, and me. You made all the difference! Thanks to Ray Wilton for providing information about the construction and the electronics of the colour sensors. Many thanks to Gwyn Roberts, Dave Gill, Elwyn Jones, Berwyn Roberts and Sonja Wiese for support during the Menai Strait time series. Thanks a lot to Vivian Ellis and Sandy Hague for technical advice during the years I spent in Menai Bridge. Thanks to Margaret Jones for sorting out the finances of our MAFF project.

Many thanks to Dave Mills from CEFAS in Lowestoft for giving me the opportunity to take part in several cruises within the Jonus II program, and for lending instrumentation, as well as for all the interesting discussions. Thanks to Alison Reeve and Jenny Taylor for analysing the salinity samples (Chapter 5), and for good company during cruises. Thanks to Ali for her hospitality and for letting me stay in her house in Lowestoft many times.

Thanks to Ray Barlow for access to the PML HPLC system. Many thanks to Denise Cummings for teaching me how to use the HPLC system, and how to process the data. Great thanks to Gerald Moore and Jim Aiken for letting me use excellent optical calibration facilities in PML. Special thanks to Gerald for teaching me how to calibrate a colour sensor.

Thanks to my German friends, Barbara Peterson, Tanja Mohr, Anuschka Heckers, Antje Lorch, and Katrin Urban, for keeping in touch. Thanks to my friends Peter Hope Jones, Ivor Richards, Jilly Thomas, Cathrine Dromer, Elisabeth and Peter Depner, Hazel Manual, Helen Gilbert and Ellen Sieg for support during difficult times in Wales. Great thanks to my dear friends Anna and Christopher Nixon for being themselves, and for their incredible faith. Thanks for making me feel home in your house many times.

Special thanks to my current boss Bertil Håkansson for his support and for producing the temperature-depth chart for the Gotland time series. Thanks to our head of department, Leif Wastenson, for letting me use all the facilities at the Department of Physical Geography, Stockholm University. Thanks to Berit Berggren for looking after our finances. Great thanks to Eva Petersdotter for being so positive, and ever so helpful!
Great thanks to my colleagues Peter Land and Ove Rud for all the helpful comments and discussions about remote sensing. Thanks to Peter for proof reading and for joining in with the modelling in chapter 6. Thanks to Niklas Strömbeck for providing the map of the stations in the Baltic Sea, and for joining in with the fieldwork. Thanks to Don Pierson for his help. Thanks to the crew of RV Argos for support during Baltic Sea cruises, in particular to Bodil Thorstensson for being ever so supportive, and to Eva-Gun Thelén for measuring the humus content from the Argos cruise in August 1998. Great thanks to Lars Westin, the director of the field station in Ar for providing excellent laboratory facilities in Gotland, and for being himself. Special thanks to Henrik Lindh (SMHI) for setting up the raft with me in the north of Gotland, and to Herbert Hammerin for taking me out on his boat Special thanks to Leif Lundgren, who has been very helpful. Thanks to Jenny Degerholm and Erik Söderbeck for providing me with cyanobacteria cultures, and to Birgitta Bergman for providing a photograph of *Nodularia spumigena*. Special thanks to Alve Henricson, the captain of Searcher, and his crew, especially to Ola Fjelddahl. Thanks to Petra Ammenberg and Ajit Subramaniam for joining the Searcher cruise.
Thanks to Maj-Liz Nordberg, Tina Ekström, and Miho Ishii for being ever so nice colleagues, and for cheering me up during difficult times in Stockholm. Thanks to my friend Elaine Rowan, and all the members of the late-lunch club at the Department of Physical Geography, Stockholm University. Thanks to my friends Lotta Wiener and Kumiko Holm for looking after me in Sweden.
I express my gratitude to my family, in particular to my sisters Andrea and Michaela Kratzer who gave me continuous telephone support from Germany both to Britain and Sweden.
I express my love and gratitude to Alan Brown for his consistent love and support over the last five years. Thanks for deploying the buoys with me at the station in Gotland, for helping me transport equipment to Gotland, for proof reading my thesis, and helping me print out the first draft. Thanks for taking an interest in my work, and for all the helpful discussions.
Thanks to my examiners, Alison Weeks and Sarah Jones, for the great discussion during my viva, and for the helpful comments!
During the course of this work I came to realise what it means to look at things from different perspectives. During the Searcher cruise I swam in a toxic cyanobacteria bloom, and the understanding I gained from this was as valid as looking at different satellite images. I learnt that an understanding of phytoplankton ecology is only possible if we use different approaches and different scales of observation.
Ki-Aikido helped me to find a good balance between physical and academic work. Thanks to Ivor Richards, who got me interested in Ki-Aikido. I am grateful to Joshigasaki Sensei who made me understand the congruity of perception and meditation, and how to keep mind and body unified (even when in the middle of a committee meeting, or when giving a talk in front of many people). My nicest experience of meditation was when I was floating in a surface accumulation, and felt as one with the cyanobacteria. It certainly felt warm and sunny!

Chapter 1 - Introduction

Measurements with in situ radiometers in combination with optical measurements in the laboratory provide a powerful tool to distinguish different water masses optically, and to derive concentrations of optically-active in-water constituents (OICs), such as phytoplankton, suspended particulate matter (SPM) and coloured dissolved organic matter (CDOM). The combination of both satellite remote sensing, and in-water measurements can provide valuable information about the productivity of the world ocean, the global carbon budget, as well as information about large-scale ocean dynamics. Radiometers can be used for deriving time series of OICs, and for modelling and ground-truthing of satellite remote sensing imagery. Theoretically, it should be possible to invert the process, and to derive information about OICs from satellite imagery. The work presented in this thesis concentrates on in-water optical measurements, and discusses implications for remote sensing applications.

1.1 Remote sensing and marine optics

The photic zone is the illuminated surface layer of the sea wherein the absorption of heat energy by water and light energy by phytoplankton helps to regulate many aspects of the global environment (Tett 1990). It is also the layer of the sea that determines the surface optical properties (ocean colour) which in principle makes it possible to monitor these environmental properties optically.

Light can be broadly classified into infrared (IR) with wavelength greater than 760 nm, ultraviolet (UV) with wavelength less than 390 nm, and visible with intermediate wavelengths (Parsons *et al.* 1990). The visible light is the most important fraction for biological aspects such as photosynthesis and visual sense of organisms: light energy required by algal photosynthesis is restricted to wavelengths between circa 400 and 700 nm. Radiation at this wavelength range is therefore called 'photo-synthetically active radiation' (PAR). Blue photons have got more energy than red photons, and therefore, PAR is often expressed in terms of the energy per Einstein, E, ranging from 170 to 300 kJ/E (an Einstein is a mole of photons: 6.022×10^{23}). Plants are able to convert this light energy into chemical energy by means of photosynthetic fixation of CO_2. This has the profoundest consequences for life on Earth, helping to determine global climate and chemical composition of oceans and the atmosphere, as well as the nature of marine food chains and the abundance of marine organisms.

After penetrating through the atmosphere, sunlight must find its way across the air-water interface to become available in the aquatic ecosystem. A part of it will be reflected back into the atmosphere. The proportion of the incident light which is reflected is dependant on the zenith angle of the incident light and the sea state. It increases from 2% for vertically incident light on a flat water surface to 100% as the beam approaches grazing incidence (Kirk 1994).

Dera and Stramski measured the short-term fluctuations in downward irradiance under a wind-disturbed sea surface (Dera and Stramski 1986). Their results show how strongly the changes in wind-speed may influence the refraction of solar rays on the wind-disturbed water surface. Furthermore, when solar rays are focused by wave crests, the instantaneous irradiance (measured in milliseconds) in the top few meters of the water column can exceed the average irradiance (averaged over minutes) by a factor of five. There are also strong fluctuations in instantaneous daylight irradiance caused by clouds. A few clouds in an otherwise clear sky increase the amount of diffuse irradiance at the Earth's surface, provided they do not obscure the sun. They may increase the total irradiance by 5-10%. However, a deep layer of cloud may transmit only 10% of the solar radiation.

Light that penetrates the sea surface bends abruptly at the air-water interface (refraction), changing the angular distribution of light under water. Irradiance and light quality change dramatically with depth in the water column: the downwelling and upwelling irradiances decrease exponentially with depth (Tett 1990) but the rate of decrease is wavelength dependent. In clear ocean water blue light is absorbed much less than red light, and at any particular depth the irradiance is a larger fraction of its surface value in the blue than at longer wavelengths (Falkowski 1980). Physicists have studied the optical properties of the ocean for several decades. The pioneer work was done by Jerlov during the Swedish deep-sea expedition in 1947-1948. This resulted in Jerlov's optical classification into the oceanic water types I (the clearest natural waters), II, III and the coastal water types 1 to 9 (see Figure 8.6, Chapter 8). In oceanic water type I the maximum transmittance occurs in the blue at 475 nm and amounts to 98.2% per metre. At 310 nm it is still 86% which means that ultraviolet plays a considerable part in clear water optics. Conversely, in coastal water type 9 the maximum transmittance occurs in the yellow-green at about 575 nm and is only 56%. This means that the maximum transmittance decreases and shifts from blue to green when moving from type I to type 9 water. Transmittance in the red at 675 nm ranges from 66% for type I to

40% for type 9. Infrared (>700 nm) is totally absorbed within the first few centimetres of the surface.

The current water type in an area can be estimated from transmittance in a narrow waveband and then the spectral distribution of the light at any depth can be calculated, with certain precautions, from the transmittance data given by Jerlov's system of water types. The geographical distribution for these water types has been determined for a number of ocean areas. Many stations measured in the Pacific represent type I, and clearer water has been found in the Sargasso Sea. Type III prevails in upwelling areas. Jerlov's classification remains purely descriptive as only the variations in the optical properties are quantified, without the causes being identified or quantitatively assessed.

In 1961, Preisendorfer introduced a system which separated optical properties into two categories - inherent and apparent (Kirk, 1994). Apparent optical properties (AOPs), e.g. radiance and irradiance, are those affected by a change in the radiance distribution, while inherent optical properties (IOPs) are independent of changes in the radiance distribution and depend only on the substances within the aquatic medium. Examples for IOPs are the absorption coefficient, the scattering coefficient and the volume scattering function (VSF).

Smith and Baker (1978) coined the expression 'bio-optical state of ocean water' to acknowledge the fact that the optical properties of the ocean waters are tightly subordinated to the abundance of pigmented algal cells. It was also recognised that in many situations not only phytoplankton but also their detrital products play a predominant role in determining the optical properties of oceanic waters. These detrital products are mainly particulates but there may also be dissolved fractions which are collectively known as yellow substance, Gelbstoff, or coloured dissolved organic matter (CDOM). The particulate fraction is called suspended particulate matter (SPM), or TSS (total suspended solids) which can be partitioned into an organic or an inorganic fraction. The inorganic fraction is also called mineral suspended solids (MSS; Gallegos *et al.* 1990), and the organic fraction is also called organic suspended solids (OSS).

The light absorption taking place in aquatic ecosystems can be mainly attributed to four components: the water itself, CDOM, the photosynthetic biota (phytoplankton and macrophytes where present) and inanimate particulate matter. The scattering is mostly caused by particles and water itself. Phytoplankton and large particles scatter mostly in a forward direction. The backscatter is relatively small. Inorganic particles have in

general low absorption, but relatively high backscattering. The backscattering of phytoplankton, as for other particles, depends mostly on the cell size rather than on the species. Particles lager than about 5 μm in diameter backscatter light nearly wavelength independently, and their backscattering coefficient is proportional to their concentration. Particles in the range of 1-5 μm in diameter cause backscattering that is roughly inversely proportional to wavelength.

Morel and Prieur (1977) introduced a new system which divides marine water optically into two categories. They defined Case-1 waters as those with a high phytoplankton concentration compared to that of other particles, which means that the light field is determined merely by the optical properties of phytoplankton (particularly pigment absorption), and the optical properties of the water. Oceanic waters are usually Case-1 waters but some coastal waters can also be Case-1, for example along arid coasts, in the absence of terrigenous influx and in areas void of resuspended sediments. More than 98% of the world ocean water, ranging from oligotrophic to eutrophic waters, are presumably Case-1 waters (Morel 1988). Some waters may exhibit special optical properties even though they satisfy the requirements for Case-1, e.g. red tides and coccolithophorid blooms. Morel termed these 'anomalous' Case-1 waters.

Coastal and continental shelf areas comprise only 10% of the total ocean area. Nevertheless, they provide roughly half of the oceanic new production (Walsh *et al.* 1981). These areas tend to be higher in pigment concentration, but also include significant amounts of coloured terrigenous constituents, such as CDOM and suspended sediments. Waters in which the optical properties are dominated by factors other than phytoplankton, and their products, for instance highly scattering inorganic particles, are defined as Case-2 waters (Morel and Prieur 1977).

There have been many studies to develop remote sensing algorithms to estimate the chlorophyll concentrations (used as a proxy for phytoplankton biomass or total pigment concentration) in Case-1 waters. Most of these algorithms are based on colour ratios, such as the blue-green ratio (Gordon and Morel 1983). Using ratios it is possible to eliminate unwanted effects such as absolute calibration errors or factors with a weak wavelength dependence, and therefore they are a suitable tool for remote sensing. However, in Case-2 waters, the same algorithms can not be applied as there are two or more substances present, which have different optical properties and do not necessarily co-vary with chlorophyll a concentration (Mueller and Austin 1995). This leads to

significant problems when developing algorithms for the estimation of chlorophyll in Case-2 waters. In practice, only those water types for which the blue-green ratio algorithms for chlorophyll concentration could be applied have been treated as Case-1. Conversely, water masses that should belong to the Case-1 water type but for which the standard blue-green ratio algorithm is inapplicable have been redefined as Case-2 (Mueller and Austin 1995). An example of these anomalous Case-1 conditions is during coccolithophorid blooms, in which detached coccoliths[1] dominate scattering and therefore reflectance, invalidating the relationship between the blue-green ratio and pigment concentration.

In the SeaWiFS protocols (Mueller and Austin 1995) the term 'Case-1 waters' refers to 'ordinary open ocean Case-1 waters', wherein absorption and scattering are dominated by phytoplankton and covarying CDOM concentrations, and where global blue-green colour ratio algorithms for retrieving chlorophyll a concentration and the downwelling diffuse attenuation coefficient at 490 nm K(490) work well. Most oceanic waters belong to this case.

Water masses may be categorised as Case-1 if:

- CDOM absorption at 380 nm is less than 0.1 m^{-1}
- total SPM concentration is less than 0.5 g m^{-3}
- the measured water-leaving radiance, L_w (λ), predicts fluorometrically measured chlorophyll a concentration within 35%; and the attenuation coefficient, K_d (490) within 20%

All other water masses which do not satisfy these criteria are grouped by Müller and Austin (1995) as Case-2 waters. Water masses with wide diversity of bio-optical characteristics may be found in this category, like the coccolithophorid blooms. Case-2 water masses also include coastal areas in which CDOM of terrestrial origin contributes

---

[1] Coccoliths are tiny calcium plates that make up the shells of coccolithophorids

a strong absorption component. Phytoplankton blooms with unusual accessory pigment concentrations, like red tides, may require the use of special regional ocean colour algorithms. The fourth category of Case-2 waters is 'classical extreme Case-2 waters' where attenuation is dominated by inorganic particles, dependent on their chemical and geological composition.

1.2 Some terms used in optical oceanography:

Irradiance or flux density (sometimes just called flux) is defined as the power incident on or radiated by a surface per unit surface area, usually denoted E (SI unit W m^{-2}). Radiance, light intensity or radiant intensity is the power incident on or radiated by a surface in a given direction, per unit surface area and solid angle, often denoted L or sometimes I (W m^{-2} sr^{-1}). These definitions (Morel and Smith 1982) may be applied to an arbitrary spectral distribution, e.g. the solar spectrum or an instrument's spectral response. Spectral irradiance and radiance are these quantities per unit wavelength (or occasionally frequency) interval.

Remote sensing instruments by their nature sample light from a given point on the sea surface in a particular direction, hence measure radiance (Kirk 1994). The measure that is most often used for remote sensing of ocean colour is the 'water leaving radiance', which is the radiance exiting the water surface, in the direction of the sensor, that has penetrated into the water and hence has been influenced by the water optical properties. Recently the use of the term 'reflectance' has become widespread, and new satellite sensors may be calibrated in this way.

The transmittance of a layer is the proportion of irradiance incident on the layer that is transmitted through the layer. This may be diffuse transmittance, which considers all irradiance exiting the far side of the layer as transmitted, or direct (or beam) transmittance, in which only undeviated irradiance is considered transmitted. Attenuance is the proportion of incident irradiance that is not transmitted, and may also be defined as diffuse or direct. Similarly, the absorbance of a layer is the proportion absorbed by the layer, and the scatterance is that scattered. These quantities, spectral or otherwise, may be related to inherent properties of a medium by considering a collimated beam of irradiance E normally incident on an infinitesimally thin layer δz of the medium, which undergoes a direct attenuation $-\delta E$. The attenuation coefficient c of the medium is defined as the attenuance per unit thickness and hence as:

$$c = -\delta E\,(E\delta z)^{-1} \qquad (m^{-1}) \qquad \text{(equation 1.1)}$$

We may similarly define the absorption coefficient a and the scattering coefficient b in terms of the absorbance $-\delta E_a$ and scattance $-\delta E_b$. Since beam attenuance consists of absorbance and scatterance it follows that for very thin layers $\delta E = \delta E_a + \delta E_b$, hence:

$$c = a + b \qquad (m^{-1}) \qquad \text{(equation 1.2)}$$

Scattering is often highly anisotropic, and its geometric behaviour is described by the volume scattering function. Consider an infinitesimally thin slab δx illuminated normally by collimated light of irradiance E from direction Ω_0. The light scattered into direction Ω will have a radiance $\delta L(\Omega_0,\Omega)$. The volume scattering function β is then defined as:

$$\beta(\Omega_0,\Omega) = \delta L(\Omega_0,\Omega) / (E\delta x) \ (m^{-1}\ sr^{-1}) \qquad \text{(equation 1.3)}$$

The integral of β over all Ω is equal to b.

The spectral quantities $a(\lambda)$, $b(\lambda)$ and $\beta(\lambda,\Omega_0,\Omega)$ are used to describe the optical behaviour of a medium and together with $c(\lambda)$ are referred to as the primary inherent optical properties (IOPs) of the medium (Kirk, 1994).

It is also useful to distinguish between scattering in a forward direction and that in a backward direction. The scattering coefficient b can be partitioned into a forward scattering coefficient b_f, relating to light scattered through less than 90°, and a backward scattering coefficient (or backscattering coefficient) b_b, relating to light scattered through more than 90° (Kirk 1994):

$$b = b_f + b_b \qquad (m^{-1}) \qquad \text{(equation 1.4)}$$

Another term, the backscattering ratio, is often used in modelling the upwelling light field. It is the ratio of the backscattering coefficient to the total scattering coefficient (Ulloa *et al.* 1994) It is also called the normalised backward scattering coefficient.

Energy which enters the water from above and is transmitted downwards is known as downwelling irradiance, E_d. In the case of monochromatic light with uniform angular didtribution E_d diminishes in an approximately exponential manner with depth:

$$E_d(z) = E_d(0)\, e^{-k_d z} \quad \text{(Beer's Law)} \qquad \text{(equation 1.5)}$$

where $E_d(0)$ and $E_d(z)$ are the values of downward irradiance just below the surface and at depth z, respectively. Note that the rate of decrease is wavelength dependent. K_d is the average value of the diffuse attenuation coefficient for the downwelling light field c_d over any defined depth interval.

$c_d(z)$ is dependent on the angular distribution of the light and the attenuation coefficent:

$$c_d(z) = c(z) / \mu^{av}(z) \qquad \text{(equation 1.6),}$$

where $\mu^{av}(z)$ is the average cosine for the downwelling light at depth z (Kirk 1994). The average cosine may be regarded as the average value, in an infinitesimally small volume element at that point in the field, of the cosine of the zenith angle of all the downwelling photons in the volume element. It accounts for the difference in attenuation between laboratory (e.g. by a spectrophotometer) and in situ measurements (e.g. by a radiometer).

Changes in ocean colour are often described in terms of the spectral variation in sea surface reflectance, R. R may be described as the ratio of upward irradiance to downward irradiance just below the sea surface (Kirk, 1994):

$$R = E_u / E_d \qquad \text{(equation 1.7),}$$

where the upwelling irradiance, E_u, describes photons which travel upwards, having been diverted from their downward path.

R is strongly correlated with the ratio of backscattering to absorption:

$$R \approx f\ b_b\ (a + b_b)^{-1} \qquad \text{(equation 1.8)}$$

Usually, the backscatter is very small compared to the absorption ($a >> b_b$), and therefore:

$$R \approx f\ b_b / a \qquad \text{(equation 1.9)},$$

where Morel and Prieur (1977) found f to be equal to 0.33. However, f is dependent on the incident light field and the phase function (Morel and Gentili 1991). The phase function is the volume scattering function normalised to the total scattering coefficient (Kirk 1994).

For remote sensing, the radiance reflectance R_r is of importance. It takes the angular distribution of the upwelling light into account:

$$R_r = L_u(\Omega) / E_d \qquad \text{(equation 1.10)},$$

where $L_u(\Omega)$ is the upward radiance in some particular view direction Ω. For in-situ measurements this is usually the vertical. Both L_u and E_d may be measured just below or just above the water, and L_u above the water may include surface reflection, so care is needed when interpreting these measurements. Because only one view direction is used, the symbol is R_r, not $R_r(\Omega)$.

1.3 Optically-active in-water constituents (OICs): description and methods

1.3.1 Water

Pure water of sufficient depth is blue: this is clearly apparent in oceanic waters or in clear coastal waters which have little input from rivers and are infertile (Kirk 1994). This has two reasons: pure water absorption has a minimum in the blue to green, rising from about 550 nm and becoming quite significant in the red (Figure 2.2, Chapter 2), and the backscatter of pure water increases with decreasing wavelength. One metre of pure water will absorb about 35% of incident light at 680 nm. The absorption at the red end of the visible is really the tail end of a series of much stronger absorption bands in the IR. The contribution of water itself to the attenuation of PAR by absorption is consequently of importance only above 550 nm. The absorption properties of water in the UV are of considerable importance in oceanic and other clear waters: they have a marked influence on the penetration of UV radiation which has strongly inhibitory effects on phytoplankton photosynthesis in the surface layer. (Photo-inhibition is strongest in the UV with a peak at 250-260 nm).

It is very difficult to measure the absorption coefficient of pure water, and the reported values in the literature vary widely. The most commonly used spectra of the diffuse

attenuation coefficient of water, $K_{d(w)}$, and the absorption coefficient of water, a_w, are those proposed by Smith and Baker (1981). These are partly based on their own measurements of K_d in the clearest ocean waters, where K_d is slightly greater than the absorption coefficient. In the photosynthetic spectral region (380-700 nm), they use values based on laboratory measurements by Morel and Prieur (1977). Buitelveld *et al.* (1994) suggested a new spectrum for water attenuation, from measurements with a submersible absorption meter at temperatures from 2.5 to 40.5 °C. They found absorption in the wavelength range 300-550 nm to be lower than in Smith and Baker, and above 700 nm the spectrum had a different shape. A formula for the effect of temperature on the absorption spectrum was given. The spectrum given by Smith and Baker also seems to underestimate the absorption of inorganic salts. Another absorption spectrum for water was recently proposed by Pope and Fry (1997).

1.3.2 CDOM

Introduction

Decomposing plant tissue in the soil or in a water body is mainly broken down by microbial action (Kirk 1994). This process takes place within days or weeks and, ultimately, inorganic compounds like carbon dioxide, inorganic forms of nitrogen, sulphur and phosphorus are released into the water column. However, a complex group of compounds loosely referred to as 'humic substances', are also released during this process. These humic substances are what constitutes CDOM. They are very varied in molecular weight and structure: they are polymers of phenolic and benzenecarboxylic acids, together with aliphatic di- and monocarboxylic acids. Some are freely soluble (fulvic acids) and others are insoluble macromolecular aggregates (humic acids). The aromatic sub-units of CDOM may originate from the plant or may be generated *de novo* during microbial breakdown. Water originating from rainfall drains through soil, extracting humic substances which are carried into rivers and then into estuaries and the sea.

CDOM concentrations tend to be much higher in inland waters. It seems likely that most of the CDOM in inland waters is due to soluble humic substances leached from the soils in the catchment areas, but it can also be generated by decomposition of plant material within the water body. CDOM concentration is highest in waters draining from bogs or swamps and from humid tropical forests (Kirk, 1994).

The presence of CDOM in marine waters is not as readily apparent as in inland waters. Most of the soluble humic material in river water is precipitated when it comes into contact with sea water. A fraction of it remains in solution though, and most of the CDOM in coastal waters originates from land run off. In sea waters with lush brown algal beds, the algae might contribute significantly to the amount of CDOM: brown sea weeds actively excrete phenolic compounds for example, which are probably turned into CDOM by oxidation and polymerisation. It is not clear to what extent CDOM derives from phytoplankton decomposition. Measurements in the Baltic and the North Atlantic seem to refute this idea whereas investigations in the upwelling region west of South America indicate an immediate marine origin of the CDOM as the area has no input from rivers or land drainage (Kirk 1994). Kopelevich and Burenkov (1977) observed a strong correlation between the concentrations of CDOM and chlorophyll in productive oceanic waters. They proposed that there are two kinds of oceanic CDOM: a 'labile' component resulting from the recent decomposition of phytoplankton and a 'refractory' component of much greater age and stability. Bricaud et al. (1981) proposed that the refractive part of CDOM may reflect average biological activity over a long time.

Optical properties of CDOM

CDOM absorbs strongly at short wavelengths, causing a shift in the minimum of water absorption to longer wavelengths and imparting a yellow colour to the water. Its spectral absorption is generally characterised by an exponential decay with wavelength. It has negligible scattering. The concentration of CDOM is usually indicated by its absorption coefficient at 440 nm, g_{440} (Kirk, 1994):

$$g_{440} = a\,(440)\, e^{-0.014\,(\lambda-440)} \qquad (m^{-1}) \qquad \text{(equation 1.11)},$$

where λ is the wavelength in nm. However, Carder *et al.* (1991) showed that the absorption curve of fulvic acid differs from that of humic acid. They both decrease exponentially, but with exponents of -0.0189 nm^{-1} and -0.01105 nm^{-1}, respectively.

Quantification of CDOM

In most inland waters the CDOM absorption is sufficiently high to be measured with reasonable accuracy using a filtered water sample (0.2-0.4 μm pore size) in a 5 or 10 cm pathlength cell (Kirk 1994). In most marine waters, the concentration of CDOM is too low for the spectrophotometric method. Instead the absorption coefficient can be measured in the near-UV (350-400 nm) where absorption is higher. G_{440} can then be

determined by proportion, either from a typical CDOM absorption spectrum or by using the above exponential relationship. Fluorescence is another method of measuring CDOM which is an order of magnitude more sensitive than absorption and can be used to distinguish between CDOM from terrestrial and marine sources e.g. by using a scanning fluorometer (Coble and Brophy 1994). Using fingerprints of excitation and emission spectra CDOM can be categorised in this way.

If CDOM is isolated by filtration, any light scattering particles that pass through the filter will remain in the sample. Some backscatter is caused by heterotrophic bacteria in the submicrometer range (Ulloa *et al.* 1992). Most of the backscatter in the sea is due to small organic particles (Ulloa *et al.* 1994). Examination of sub-micrometer particles by transmission electron microscopy has shown that the greatest abundance of these particles occurs in the <0.12 μm size fraction (Wells and Goldberg 1992). It is not possible to measure these particles with the methods currently used in oceanography (e.g. resistive-pulse particle counters which have a lower limit of detection at 0.32 μm). Ulloa *et al.* (1994) used Mie theory to model the backscattering ratio of these organic particles, and found that the backscattering ratio is not only sensitive to the presence of sub-micrometer particles but also depends strongly on the size distribution. It is not affected significantly by absorption and does not vary with wavelength over the visible range. The presence of such particles will therefore add a constant amount to the CDOM spectrum.

1.3.3 SPM

Introduction

SPM should include all particulate matter in the water. In practise, it is usually defined as all matter that is collected by a 0.45 μm membrane filter (Mueller and Austin 1995). Hence SPM includes plankton.

Typical SPM samples collected on a filter are often brown in colour, probably due to free particles of humus or humic material bound to mineral particles (Kirk 1994). In shallow coastal waters SPM may come from bottom sediment resuspended by wave action. In oceanic waters well away from land or in productive waters some or all of the SPM may consist of phytoplankton and their degradation products (detritus), which may include an inorganic (e.g. frustules of diatoms or coccoliths of coccolithophorids) as well as an organic fraction.

Optical properties of SPM

According to Kirk (1994) the absorption spectrum of SPM is quite similar to that of CDOM: absorption is low at the red end of the visible and rises steadily as wavelength decreases into the blue and UV. SPM both absorbs and scatters, but it is usually not the dominant absorber and its primary effect on water colour usually comes from scattering. The scattering properties of SPM depend mostly on the particle size, but also on the shape and refractive index, and so are quite variable. Heterotrophic bacteria are much more efficient scatterers than absorbers and in natural waters, bacteria could contribute significantly to the scattering of light (Kopelevich *et al.* 1987; Morel and Ahn 1990; Stramski and Kiefer 1990). Bacteria can significantly affect *in situ* measurements of optical properties such as the attenuation coefficient (Spinrad *et al.* 1989).

Quantification and identification of SPM

Because of scattering, the absorption coefficient of SPM cannot be measured by normal spectrophotometry with long-pathlength cells. A widely used method is to resuspend material collected on a filter into a much smaller volume and then measure the absorption spectrum in a short-pathlength cell with an integrating sphere to measure scattering (Kirk 1994). From this, the SPM absorption coefficient in the original water body may be calculated. This, however, may include absorption due to phytoplankton pigments. The concentration of SPM is usually measured by gravimetric analysis (see Chapter 2).

1.4 Phytoplankton and phytoplankton pigments

1.4.1 Introduction

Most of the variations of the optical properties of Case-1 waters are due to absorption by phytoplankton pigments and scattering by phytoplankton and their products, with some effects due to fluorescence. Knowledge of the inherent optical properties of phytoplankton is therefore a necessary requirement for interpretation of ocean colour, as well as for models of light penetration, of light utilisation by phytoplankton and even of mixed-layer dynamics (Hoepffner and Sathyendranath 1992). The measurement or optical estimation of photosynthetic pigment concentration is often used to estimate algal biomass as well as productivity.

The word 'plankton' derives from the Greek planktos which means wanderer. This refers to the fact that planktonic organisms are drifters rather than powerful swimmers.

In 1887, Hensen defined plankton as including all organic matter (living and dead) which drifted or moved passively in water (Boney 1989). Today the collective term plankton is used for organisms drifting in the sea or in freshwater. They are kept in suspension by water movements and dispersed more by those movements than by their own activities. The phytoplankton are *photo*-autotrophs, mainly microscopic (eukaryotic) algae and (prokaryotic) cyanobacteria.

Marine phytoplankters have evolved a large variety of light harvesting and photosynthetic pigments. The three main groups of pigments that determine the bio-optical properties are the chlorophylls, the carotenoids and the phycobiliproteins (Rowan 1989). Marine algae used to be classified into three groups, 'brown', 'red' and 'green', on the basis of their colour. Some classification systems still use pigment composition as a primary character.

The 'green' phytoplankters (including PRASINOPHYCEAE (prasinophytes), CHLOROPHYCEAE (chlorophytes), EUGLENOPHCEAE (euglenophytes)[2] have a similar pigmentation to the 'higher plants' , they contain chlorophyll a, chlorophyll b and ß-carotene. All other groups contain chlorophyll a and ß-carotene but lack chlorophyll b. The brown coloured phytoplankters include CHRYSOPHYCEAE (yellow-brown or golden-brown algae), DINOPHYCEAE (dinoflagellates) and DIATOMOPHYCEAE (diatoms), which are also called BACILLARIOPHYCEAE, PRYMNESIOPHYCEAE (premnesiophytes), and RAPHIDOPHYCEAE (raphidophytes). They all contain chlorophyll c as well as chlorophyll a. Their characteristic brown colour derives from a mixture of xanthophyll pigments, of which fucoxanthin is the most important in brown seaweed, diatoms and the golden-brown algae, and premnisiophytes while peridinin is found in dinoflagellates. All the pigments so far mentioned are soluble in organic solvents, such as acetone or methanol. Water soluble proteinaceous pigments, the phycobilins, are present in some flagellates of the phylum CRYPTOPHYCEAE (cryptomonads) and are the major accessory pigments in the cyanobacteria (CYANOPHYCEAE; blue greens) and the red algae (RHODOPHYCEAE). The red pigment, phycoerythrin, predominates in most red

---

[2] The systematics used here are those used in the 'Atlas du Phytoplankton' (Sournia 1986; Ricard 1987; Chrétiennot-Dinet 1990) .

algae, and the blue-green pigment, phycocyanin, predominates in typical blue green algae. The balance between these pigments varies considerably within each group.

Marine phytoplankton is dominated by two groups of brown-coloured algae, the diatoms and the dinoflagellates. Cryptomonads and prymnesiophytes are also very common. In the late 1970s, the application of new techniques like flow cytometry to marine science led to the discovery of minute unicellular photosynthetic picoplankton as an essential part of the marine planktonic community. They occur in both oceanic and coastal waters. They include cyanobacteria as well as small eukaryotic flagellates. Sieburth *et al.* (1978) defined picoplankton as ranging from 0.2 to 2 μm. Picoplankton usually pass through filters with a nominal size of 1 μm which might account for their late discovery, but they can be retained by 0.2 μm filters.

Picoplanktonic cyanobacteria such as *Synechococcus* have been found to be widely distributed in oceanic waters and the contribution of these small prokaryotes to the primary production within dimly lit blue layers, like the deep chlorophyll maximum in Case-1 waters, has been emphasised by Glover *et al.* (1985).

Gieskes and Kraay (1983) discovered by HPLC a derivative of chlorophyll a with a concentration exceeding that of 'normal' chlorophyll a in oligotrophic waters and they associated it with unidentified particles below 1 μm. A few years later, red fluorescing bodies typically smaller than 0.8 μm were identified by flow cytometry in the same kind of waters. They were found to be extremely abundant and because of their unusual pigmentation, they were hypothesised to be free-living marine prochlorophytes [3] (Chrisholm *et al.* 1988). The name *Prochlorochoccus marinus* was recently given to an organism of this type isolated from the Sargasso Sea (Chrisholm *et al.* 1992). Numerically, prochlorophytes are the most abundant photosynthetic organisms. Both *Prochlorochoccus* and *Synechococcus* in association with picoeukaryotic algae often appear to be dominant in oligotrophic environments, and so in a major part of the world oceans. Consequently to understand the optical properties of oceanic waters, these small organisms must be studied.

---

[3]Prochlorophytes are also called prochlorobacteria or chlorooxybacteria. They are prokaryotic cells which resemble chloroplasts in morphology and in releasing oxygen in photosynthesis. Their gram-negative cell walls contain muramic acids and are sensitive to lysozyme. Their thylakoids are adjacent to the cell wall.

Cyanobacteria can be distinguished from other phytoplankton bacteria by their characteristic orange autofluorescence (Waterbury *et al.* 1979). Cyanobacteria possess phycobilins but no accessory chlorophylls. This leads to characteristic absorption bands in the yellow / orange part of the spectrum. In contrast, prochlorophytes do not contain phycobilins but divinyl derivatives of chlorophyll a and b, identified as being 8-diethyl, 8-vinyl compounds by Goericke and Repeta (1992). The absorption peaks of these pigments occur at wavelengths 10 nm higher than those of chlorophyll a and b, respectively. *Prochlorococcus* also contains a chlorophyll c-like pigment present in certain prasinophytes. Within the cells, total carotenoids are more concentrated in *Prochlorococcus* than in *Synechococcus*.

The scattering properties of cyanobacteria are those of a particle much larger than the wavelength of light, i.e. forward scattering predominates. Stramski and Morel (1990) found that for a cyanobacterium belonging to the genus *Synechocystis*, the scattering increases towards the blue end of the spectrum whereas the backscattering increases towards the red. Like many algal cells it is more efficient in scattering than in absorbing light. The scattering properties of *Prochlorococcus* are different. Morel *et al.* (1993) showed that in the blue the probability of a photon being absorbed by a *Prochlorococcus* cell exceeds that of being scattered. Such a combination has not been found for any other phytoplankton, which are consistently more efficient scatterers than absorbers. Compared to *Synechocystis* cells *Prochlorococcus* cells have a minute scattering signature. Their backscattering capacity remains negligible, even though their backscattering ratio is higher than those of other phytoplankton.

1.4.2 Plant Pigments

Chlorophyll a has long been recognised to be the main pigment in photosynthesis. All algal groups contain chlorophyll a and, with the exception of the photosynthetic prokaryotes, this pigment is contained in distinct cell organelles called chloroplasts. All other photosynthetic pigments in plants are considered to be accessory pigments. Most of the energy absorbed by the accessory pigments is transferred ultimately to chlorophyll a as it absorbs at a longer wavelength than any of the other pigments, and so requires less energy for excitation (Richter, 1988). Clusters of several hundred chlorophyll molecules are fixed to the thylakoid membranes of the chloroplasts by proteins (the antenna complex) in such a way as to harvest light energy falling on them, and to relay it to a special chlorophyll molecule in an associated photosystem. The pigments in the chloroplasts appear to be organised into two separate pigment-complex

systems, Photosystem I (PS I) and Photosystem II (PS II) both of which are inserted into the thylakoid membrane of the chloroplasts. The accessory pigments and the shorter wavelength forms of chlorophyll a are mainly found in PS II whereas in PS I there is a higher proportion of chlorophyll a absorbing at longer wavelengths (Lüning 1990).

The evolutionary origin of chloroplasts is currently explained in terms of endosymbiosis. The term endosymbiosis refers to a symbiotic association between cells of two or more different species, one inhabiting the other, the larger being host for the smaller. According to this theory, Margulis (1993) argues that heterotrophic prokaryotes symbiotically acquired fully developed, photo-autotrophic prokaryotes that became chloroplasts. The main argument for this theory is that chloroplasts seem to have a persistent individuality: like cells, nuclei or chromosomes they follow the law of genetic continuity. They contain DNA, messenger RNA as well as protein-synthesising systems. Also, there are striking similarities between existant photo-autotrophic bacteria and chloroplasts. It seems quite likely that cyanobacteria are free living prokaryotic codescendants of red algal chloroplasts as in both the chlorophyll a-phycobilisome-on-thylakoidsystems are very similar. Thus, the algal groups can be explained if one assumes that different phagotrophs acquired as food different photosynthetic prokaryotes. The former failed to digest the latter and the latter became chloroplasts. The symbionts co-evolved with their hosts and evidence of prior heterotrophy was severely reduced but not lost.

Chlorophylls

Each chlorophyll molecule comprises a magnesium-containing porphyrin group related to the prosthetic group of haemoglobin, ester-linked to a long phytol side chain (Richter 1988). There are several chlorophylls (a, b, c_1, c_2, c_3) with minor difference in chemical structure. During degradation processes, the phytol side chain can be removed by the enzyme chlorophyllase. The molecule is then called chlorophyllide. The magnesium ion in the centre of the chlorophyll molecule can be displaced by protons simply by adding weak acids. The products of this reaction are called phaophytins (coloured from olive green to brown). These are also products of natural degradation. If both the magnesium ion and the phytol chain are removed (e.g. by strong acids), the products are called phaeophorbides. Chlorophyllase can be activated by harvesting techniques (filtration and centrifugation) which may result in inaccuracies in *in vitro* chlorophyll a and chlorophyllide a measurements (Jeffrey and Hallegraeff 1987). Chlorophyllide a is

also one of the intermediates in the biosynthesis of chlorophyll a and under certain conditions (for instance changes in the physiological state of the phytoplankton or in nutrient status) a chemical exchange between these two pigments may occur. Unlike phaeophorbide a, chlorophyllide a is not a good indicator of senescence.

The fluorescence of chlorophyll a can be shown by dissolving it in organic solvents such as acetone, and exciting the solution with blue light. The fluorescence is an intense red but only about 30% of the energy of the absorbed blue radiation is re-emitted. The absorption spectrum of chlorophyll a in ether implies that only photons of wavelengths around 440 nm (blue) or 680 nm (red) can excite the fluorescence (Richter 1988). In both cases the emission in ether is around 669 nm.

As chlorophyll a is the only pigment occurring in all phytoplankton cells, it is used to estimate phytoplankton biomass applying a converting factor. This is possible due to its ability to fluoresce, and due to its distinct fluorescence maximum at 663 nm in acetone. The use of the correct excitation and emission filters will exclude all other pigments except chlorophyll a, chlorophyllide a, and some of the phaeopigments, especially phaeophytin a and phaeophorbide a. Phaeopigment concentration can be used as an index of the amount of dead plant material present.

Carotenoids

Carotenoids shade from yellow to red (Richter, 1988). They consist of C_{40} skeletons and absorb light because of their extended network of single and double bonds (they are polyenes). They are hydrophobic and dissolve well in organic media, thus can be extracted in acetone. They include carotenes (α, β, etc.) and xanthophylls (which are oxygen containing derivatives of carotenes; e.g. lutein, flavoxanthin, fucoxanthin, violaxanthin, zeaxanthin). The absorption maxima of the different carotenoids (in petrol) range from 450 nm to 500 nm. However, the *in vivo* peak of carotenoids may be shifted considerably upwards into the green part of the spectrum. For example, the in vivo peak of fucoxanthin, is at 545 nm, whereas the in vitro peak in 90% acetone is at 449 nm (Lüning 1990). Zeaxanthin and violaxanthin are photo protective pigments (Jeffrey *et al.* 1997).

Biliproteins

Photoautotrophic biliproteins (phycobiliproteins) act as important light-harvesting components for driving the photosynthetic reactions in two important taxa of marine photosynthetic microorganisms: the cyanobacteria and the cryptophyta. Therefore, they

are ideal marker pigments for these taxa. Phycobiliproteins are composed of pigments (phycobilins) covalently bound to specific proteins (the combination of the two is called a chromoprotein). Unlike chlorophylls and carotenoids, they are water soluble. They are not associated with detrital material and do not interfere with biomass estimates as they degrade almost immediately upon death of the cell (Stewart and Farmer 1984). There are different types of phycobiliproteins: the phycoerythrins, which contain phycoerythrobilin and are red, and the phycocyanins and allophycocyanins, which contain phycocyanobilin and are blue (see Chapter 7 for more detail about phycobiliproteins). They are organised into granules known as phycobilisomes, which are localised on the outer surface of the thylakoids and may be classified on the basis of absorbance spectra and taxonomic origin into many distinctive kinds (Siegelman and Kycia 1973).

C-phycocyanin is the characteristic pigment of cyanobacteria (Richter, 1988) with an absorption maximum at 618 nm (orange). R-phycocyanin can be found in cyanobacteria as well as in a few red algae species; it has peaks in absorbance at 552 nm (yellow) and 615 nm (orange). Allophycocyanins, which are found in small amounts in these two groups, absorb more in the red part of the spectrum (650-670 nm). In some cyanobacteria one can find phycoerythrocyanin, which has a peak of absorption in the yellow at 568 nm. R-phycoerythrin, the dominant pigment in red algae, and B-phycoerythrin, absorb in the yellow (between 540 nm and 570 nm). Because they have phycobiliproteins as accessory pigments, cyanobacteria and red algae are able to use the part of the visible spectrum which cannot be used by green plants and green algae. The extraction of phycobilins from cyanobacteria is difficult because of the special structure of the cell walls which is similar to that of gram-negative bacteria (Richter 1988).

1.4.3 Quantification and identification of plant pigments

Acetone soluble pigments

Chlorophylls and carotenoids are usually measured by extraction in 90% acetone. A method for estimating chlorophyll a by fluorometry due originally to Holm-Hansson is reviewed by Strickland and Parsons (1972) and Tett (1987). The main problem with this method is that other pigments (chlorophyllide a and phaeophorbide a) have the same fluorescence emission wavelength as chlorophyll a. However, an acidification step can help to distinguish phaeopigments.

Chlorophyll a can also be measured spectrophotometrically by the trichromatic method (Jeffrey and Humphrey 1975; Parsons, Maita *et al.* 1989). This method is more useful in terms of marine optics than the fluorometric method as it provides additional information about chlorophyll b and c, and about total carotenoid concentration (see Chapter2, section 2.3.3). However, the estimation of carotenoids is only a coarse indication (Jeffrey *et al.* 1997). Furthermore, it does not provide any information about the carotenoid composition, which is needed as they have a wide range of absorption bands. Jeffrey (1974) used thin layer chromatography (TLC) for the chemotaxonomic identification of phytoplankton and Gieskes and Kraay (1986) used high pressure liquid chromatography (HPLC) for the same purpose. With the advent of HPLC it is now possible to separate and quantify a wide range of chlorophyll and carotenoid pigments that can be used as chemotaxonomic signatures of the various microalgal classes contributing to the phytoplankton community (Barlow *et al.* 1993; Goericke and Repeta 1993; Johnsen *et al.* 1994). It has become an essential tool for the identification of picoplankton, which is difficult by more conventional methods (e.g. light or electron microscopy). For highly accurate determination of chlorophyll a, b and c, and carotenoid pigments, reverse phase C_{18} HPLC is recommended (Gieskes and Kraay 1983; Mantaura and Llewellyn 1983; Bidigare *et al.* 1989; Wright, Jeffrey *et al.* 1991; Jeffrey *et al.* 1997).

Water soluble pigments: phycobilins

In 1954 Shibata introduced a method of measuring the *in vivo* absorption spectra of living microorganisms in suspension (the Shibata technique, Jones and Myers, 1965). It is useful for comparing pigment concentration ratios of algae grown under varied environmental conditions. Jones and Myers (1965) determined the ratios of phycocyanins, chlorophyll a and carotenoids in the cyanobacterium *Anacystis nidulans* using this technique. Moreth and Yentsch (1970) developed a highly sensitive method for the extraction and fluorometric estimation of phycoerythrin in cultures of the marine cyanobacteria *Trichodesmium* but when applied to the mechanically more resistant cells of the cyanobacterium *Synechococcus* spp. this technique was not very successful (Glover *et al.* 1985). For a more quantitative determination biliproteins can be exteacted into a phosphate buffer by prolonged sonication. Stewart and Farmer (1984) described a technique for the extraction, identification and quantification of phycoerythrins and phycocyanins from cultures as well as from field samples, using a combination of grinding and enzymatic attack (lysozyme) to disrupt the cells.

Cyanobacteria can be directly counted by the autofluorescence technique (El Hag and Fogg 1986). The fluorescence cross section of phycobilins has been estimated to be an order of magnitude higher than that of chlorophyll (Houghton *et al.* 1983). Hoge and Swift (1990) suggested that upwelled water-leaving radiances also include physical scattering and absorption effects of photosynthetic accessory pigments such as phycoerythrin, and the fluorescence may consequently be remotely detected by laser fluorosensors using appropriate excitation and emission wavelengths.

Wyman (1992) introduced a laboratory method that estimates the concentration of marine *Synechococcus* spp by fluorescence. The method is based on the observation that glycerol uncouples phycoerythrin from energy transduction to other biliproteins of the phycobilisomes (Wyman *et al.* 1986; Heathcote *et al.* 1992). This gives a linear relationship between the *in vivo* fluorescence emission of phycoerythrin and the phycoerythrin cell content. Field samples from the Sargasso Sea were filtered onto 0.6 μm Nucleopore filters and the sediment was resuspended in 3 ml of 50% glycerol. Samples from the Celtic Sea were fractionated through 3- and 0.6 μm filters. The 3 μm filter was necessary to remove abundant larger phytoplankton, including phycoerythrin-rich cryptomonads. The steady state, *in vivo* fluorescence emission intensity of phycoerythrin arising from excitation at 520 nm was recorded at an emission wavelength of 570 nm, using a scanning fluorometer. Alternatively, a Turner Fluorometer, equipped with enhancer gates and fitted with appropriate filters (excitation at 520 nm and emission at 577 nm) can be used. Since the differences in the excitation and emission wavelengths is only 57 nm, the use of high-grade, narrow-bandwidth interference filters is essential to prevent excessive leakage of the excitation beam into the emission detector. The increase in phycoerythrin fluorescence intensity following the addition of glycerol was completed in 30-60 seconds.

1.4.4 *In vivo* spectra of phytoplankton

Introduction

Bio-optical models that relate optical properties to photosynthesis have been developed to predict primary production and phytoplankton growth by remote sensing (Sosik and Mitchell 1991). The spectral absorption coefficient of living phytoplankton is required for determining the energy useable for photosynthesis and so it is an essential parameter in bio-optical models developed to predict carbon fixation rates from pigment concentrations and available radiant energy (Kiefer and Mitchell 1983; Platt and Sathyendranath 1988; Morel and Gentili 1991). Physiological variability in pigment-

specific absorption can potentially be important in estimating the biomass of primary producers as well as the production realised by that biomass.

The chlorophyll-specific absorption coefficient, $a_{ph}^*(\lambda)$, allows an estimate of the amount of light absorbed by phytoplankton cells per unit chlorophyll a from knowledge of ambient irradiance. It can be calculated by dividing the absorption coefficient, $a(\lambda)$, by the chlorophyll concentration, [chl]:

$$a_{ph}^*(\lambda) = a(\lambda) / [chl], \qquad (m^2 (mg\ chl)^{-1}) \qquad \text{(equation 1.12)}.$$

There are differences in a_{ph}^* spectra among different species and within the same species caused by changes in growth irradiance, $E_0(\lambda)$. Changes in the abundance of accessory pigments relative to chlorophyll a can also contribute to the variability in $a_{ph}^*(\lambda)$. An investigation in the Western North Atlantic showed that the cell size seems to represent the major factor responsible for variability in the specific absorption coefficient at 440 nm (Yentsch and Phinney 1989). One of the factors influencing the chlorophyll-specific absorption coefficient is the pigment packaging effect. Pigments are not evenly distributed but are within discrete packages: chloroplasts, cells, a cell thallus or cell colonies (Kirk 1994). The absorbance spectrum of a cell or colony in suspension or of a segment of thallus will be found to differ noticeably from that of dispersed thylakoid fragments or pigments dissolved in a solution. The in vivo spectra will be found to have peaks which are less pronounced with respect to the valleys, and to have, overall, a lower specific absorption per unit pigment. This is due to mutual shading of pigments within the thylakoid membrane. When extracted in acetone or another solvent the overall absorption is higher than within the chloroplast. The packaging effect is proportionally greatest when absorption is strongest (Duysens 1956). The influence of the packaging effect on the absorption of light by phytoplankton populations was extensively studied (Morel and Bricaud 1981; Mitchell and Kiefer 1988; Kirk 1994). Pigment packaging effects vary with cell size and pigment content per cell.

Methods for measuring the in-vivo absorption of phytoplankton pigments

Yentsch (1957; 1962) and Trüper and Yentsch (1967) proposed to measure the absorption of particles retained on membrane or glass fibre filters. Later, Kirk (1980) and Weidemann and Bannister (1986) introduced pre-concentration techniques to measure absorption directly from suspensions. The pre-concentration technique,

though, is very time consuming and it is difficult to achieve quantification of the particles. Therefore, the glass fibre technique (also called filter pad technique) has been most intensively used to measure absorption by natural phytoplankton (Lewis *et al.* 1988; Yentsch and Phinney 1989; Garver *et al.* 1994). The filters may be stored in liquid nitrogen if there is no spectrophotometer available and scanned in a batch (Gieskes and Kraay 1983). Hoepffner and Sathyendranath (1992) froze all filters immediately after collection. In order to minimise pigment degradation they were thawed just before measuring absorption.

Absorbance, also referred to as optical density OD (λ) can be converted into the absorption coefficient a(λ) according to:

$$a(\lambda) = 2.3\ OD(\lambda)\ S\ V^{-1} \qquad \text{(equation 1.13)},$$

where 2.3 converts from $\log_{10}$ to $\log_e$, S is the area covered by particles on the slide and V is the filtered volume (m^3).

One of the main problems of using glass fibre filters, is that they are strong scatterers themselves. Multiple scattering within the filter and between the filter and particles occurs. Consequently it is necessary to determine the so called 'β-Factor', a dimensionless pathlength amplification factor (Butler 1962). Kiefer and Sohoo (1982) assumed β to be constant but Kishino *et al.* (1985) suggested that it varies with particle type and geometrical configuration. Bricaud and Stramski (1990) found β to be constant ($\approx$2) for high optical densities (OD > 0.2) of sample filters. This is why they suggested filtering a sufficient volume of water to yield a value for OD_f higher than at least 0.2 within the absorption bands. At lower optical densities β was shown to be highly variable and probably wavelength dependent. Mitchell (1990) recommended the use of a quadratic relationship between OD_f and OD_s (optical density of the suspension) for correcting the β-effect. Measurements performed by Cleveland and Weidemann (1993) on 48 phytoplankton species seem to confirm this approach and the result of their quadratic fit is close to that obtained by Mitchell. The prevailing practice is therefore to estimate β empirically through such polynomial expressions (Mueller and Austin 1995). In order to obtain the correction factors, the absorption coefficients of equivalent amounts of algal cultures in suspension and of algal cultures on filters are

measured. An empirical relationship may be established between the two measurements with a series of dilutions made from each culture.

Allali *et al.* (1995) proposed a new technique for measuring the spectral absorption coefficient which was developed from the 'filter-transfer-freeze (FTF) technique introduced by Hewes and Holm-Hansen (1983) for microscopic observation of nanoplankton (2-20 μm). This method consists of transferring algal cells from membrane filters onto microscopic slides, using dry ice freezing at -78 °C. The cells are subsequently embedded in a glycerine-gel medium for cell identification and counting. The method by Allali *et al.* works in a similar way: The sediment is filtered onto 25 mm polycarbonate (PC) Nucleopore filters (0.4 μm pore size). Filtration is stopped before the complete drying out of the filter so that a very thin layer of liquid remains on the filter. The filter is then carefully removed and quickly transferred onto 5μl of Nucleopore-filtered (0.2 μm) sea water placed onto a microscope slide, the sediment side of the filter facing down. The slide is then placed onto a metal box filled with liquid nitrogen. The material on the filter freezes instantaneously. After a few seconds, the slide is removed from the metal box. Just when the sediment starts to thaw, the filter can be peeled off from the sediment which stays on the slide. A cover slip with a diameter identical to that of the clearance area of the filter is placed onto the frozen sediment in order to trap the particles over the same diameter. Even though this method eliminates the pathlength amplification effect it is still necessary to deal with the scattering by the particles, e.g. by using an integrating sphere.

Another problem with measuring spectra of the phytoplankton *in vivo* is the presence of organic detritus and inorganic sediments which in general have an exponential absorption spectrum with high absorbance in the blue. This leads to a strong overlap with the spectrum of the phytoplankton fraction and, once the total particle absorption spectrum has been determined, it is useful to separate it into algal and non-algal components (see e.g. Chapter 5, section 5.3.2). Kishino *et al.* (1985) proposed a technique associated with the glass fibre filter method which allows separation of the signatures of the pigmented and non-pigmented components. After scanning the total sediment on the GF/F filter, it is immersed in methanol for pigment extraction. The absorption of the non-pigmented components may then be measured, and subtracted from the total absorption to get the spectrum of the phytoplankton pigments. Alternatively, Hoepffner and Sathyendranath (1992) used a mixture consisting of 6 parts by volume of 90% acetone and 4 parts of DMSO (dimethyl sulphoxide) to extract the

pigments. They allowed the solvents to flow passively through the filter which required an extracting period of 25-30 min. The extracted filters must be soaked again in filtered sea water before scanning the depigmented particles. 90% acetone is not very efficient for extraction of photosynthetic pigments in this manner as it always leaves a slight absorption at 675 nm (the absorption peak of chlorophyll a *in vivo*). Tassan and Ferrari (1995) used NaClO for bleaching the pigment instead. In all these methods, the absorption measured after pigment extraction includes not only detritus, but also depigmented algal cells. It may also include water soluble phycobilins which are not (or only weakly) extracted by methanol. Detrital phaeopigments, as well as other chlorophylls and carotenoids which may be present in zooplankton pellets (Kleppel and Pieper 1984) are extracted in methanol and therefore erroneously included as algal components.

It is difficult to interpret and classify the spectral absorption coefficients of natural phytoplankton *in vivo*, since they consist of an additive mixture of the spectra of all the pigments present. Several techniques have been used: Bidigare *et al.* (1989) used spectral derivative analysis to highlight the peaks, Sathyendranath *et al.* (1987) used multiple regression and Hoepffner and Sathyendranath (1991) used deconvolution of absorption spectra. Johnsen *et al.* (1994) determined a set of wavelengths that highlight, as accurately as possible, the bio-optical differences between light absorption spectra and could thus give an indication of the species composition. Thirty-one species, covering 10 main classes of phytoplankton were cultured at varying light intensities. Pigments of each species were isolated by means of HPLC and identified by several authentic standards. The *in vivo* absorption spectra were measured on GF/C or GF/F filters, depending on the size of the cells. The absorption spectra were corrected using the algorithm developed by Mitchell and Kiefer (1988). The chlorophyll a concentration was determined by HPLC, and also spectrophotometrically in order to normalise the *in vivo* spectra to chlorophyll a. The spectra were log transformed and normalised to chlorophyll a at 675 nm to minimise photoadaptational effects on the spectral characteristics due to differences in pigment composition and the package effect. Pigments were isolated by means of HPLC to obtain visible spectra of isolated pigments and hence to identify peaks and shoulders of the *in vivo* absorption spectra. The spectra were related to four classes of phytoplankton based on their complement of accessory chlorophylls (chlorophyll b, chlorophyll c_1 and c_2, chlorophyll c_3, and phytoplankton without accessory chlorophylls). The first class represented green algae

containing chlorophyll b (prasinophytes, euglenophytes and chlorophytes). The second class represented phytoplankters containing chlorophyll c_1 and/or chlorophyll c_2 (diatoms, premnesiophytes, chrysophytes, raphidophytes, dinoflagellates and cryptophytes). The third class were phytoplankters containing chlorophyll c_3 which also may posses chlorophyll c_1 and sometimes chlorophyll c_2 (mainly toxic and bloom-forming species). The fourth class were cyanobacteria, characterised by the lack of accessory chlorophylls. The authors attempted to identify a minimum set of wavelengths from which the plankton class could be determined from the absorption by stepwise discriminant analysis of the spectra reduced to 85 variables (every third nanometer from 400 to 652 nm). Data from wavelengths above 652 nm were excluded. A set of 3 wavelengths (481, 535 and 649 nm) yielded a prediction success of 93% for cells adapted to low light. When two more wavelengths were added (586 nm, indicating the red peak absorption maximum of chlorophyll c_3, and 628 nm, indicating the absorption peak of chlorophyll c_1 and c_2), the prediction success increased to 99%. The choice of these wavelengths in a radiometer may therefore be a step towards identifying different phytoplankton groups from radiometer data.

1.5 Colour sensor theory

Since 1991, the School of Ocean Sciences has been developing a colour sensor with four different optical channels. The channels were centered at 440, 490, 570, and 670 nm and were 10 nm wide (see Chapter 2 and 3). During the design of the instrument, self-shading was not taken into account. However, it was considered in relation to the model in section 6.2.

The 440 nm waveband corresponds to the peak of chlorophyll a in the blue but might also be influenced by high concentrations of CDOM and SPM which highly absorb in the blue part of the visible spectrum. Both chlorophyll a and b have a strong absorption band in the red and another stronger band in the blue region. Absorption is very low in the middle part, the green region of the spectrum, hence the green colour of the pigments. This part of the spectrum is sometimes referred to as the 'green window' (Lüning, 1990). Chlorophyll b and c, when present, as well as carotenoids and phycobiliproteins have the effect of increasing the absorption within this window, at both the long- and short-wavelength ends.

The 490 nm channel (cyan) of the colour sensor might give some indications of carotenoid concentrations as their peak of absorbance in organic solvents is in the range of 450 to 500 nm. However, the *in vivo* peak, is shifted, relative to the position of the peak in organic solvents, by about 40 nm towards longer wavelength. This may lead to a substantially increasing absorption in the green window (Lüning 1990). The pigments absorbing in the blue part of the spectrum seem to be part of certain light-harvesting pigment-proteins that feed their energy into the Photosystem II. They are usually summarised as light harvesting complex II (LHC II). They all contain chlorophyll a together with an accessory chlorophyll b or c, and in addition the major light-harvesting xanthophyll carotenoid(s) characteristic of the particular algal class. Their main absorption is in the blue-green part of the spectrum (400-550 nm), caused by the combination of chlorophyll and carotenoid bands.

The channel at 570 nm (green to yellow-green) was intended as a reference measurement of OICs. Figure 2.2 (Chapter 2) shows that the absorbance at 570 nm is low taking all optical constituents (including water) into account. The use of the 570 nm channel as reference channel may be complicated in waters dominated by cyanobacteria, or other biliprotein-containing algae as cryptomonads. Phycobilins have an absorption band in the green window of the chlorophyll absorption spectrum. The main absorption peaks are in the 612-645 nm range (orange) in the case of phycocyanins, and in the 544-568 nm range (yellow) in the case of phycoerythrins.

The 670 nm channel corresponds to the peak of absorbance of *in vivo* chlorophyll a. All algal classes have a peak in the red region of the spectrum due to their characteristic chlorophylls (see Figure 2.2).

Sea surface reflectance is defined as the ratio of upwelling to downwelling irradiance (equation 1.7, section 1.2). However, early work with the four-channel colour sensor showed that the cyan to green ratio of upwelling irradiance could be used to derive chlorophyll a in a range of waters in which phytoplankton pigments dominated light attenuation (Wild-Allen *et al.* 1997; Kratzer *et al.* 1997, Chapter 4). The explanation derives from equation 1.8, section 1.2. Assuming b_b to be spectrally neutral, and using ratios of two channels, the term b_b cancels out in equation 1.8, and the reflectance becomes solely dependant on upwelling irradiance and absorption (see Chapter 5).

1.6 Aims and objectives

The original aim of the work presented in this thesis was to extend the use of the UWB 4-channel colour sensor beyond estimates of bulk phytoplankton biomass, by testing the hypothesis that the instruments could be used to distinguish chromatically different phytoplankton groups. The work was to involve the estimation of chlorophyll a concentrations from the ratio of upwelling irradiance in the cyan and the green wavebands, thus allowing data from other colour-sensor wavebands to be used to identify the dominant type of phytoplankton. However, most of the work described here was done in coastal waters, where it proved impossible to derive chlorophyll a concentrations from simple colour ratios (as is discussed in more detail in Chapter 4), because of the optical effect of the high concentrations of SPM and CDOM which are characteristic of optical Case-2 waters. In effect, the need to identify chlorophyll separately from these other OICs used up the information from the other colour ratios, which had originally been intended for use in identifying type of phytoplankton. Therefore, a big portion of this work concentrated on the use of a four-channel colour sensor to estimate the main OICs of coastal waters. This was seen both as an important problem in its own right, and, also, a necessary first step towards optical monitoring of coastal phytoplankton quality. I chose two optically different coastal water bodies for this investigation: the Menai Strait (high in SPM), and the offshore waters of the Baltic Sea (high in CDOM). The choice of these two water bodies was partly a result of where I happened to work, but also represented two different types of optical Case-2 waters. The data from the Irish Sea have been analysed to a great extent, but are not included in this thesis because I took up a new position at the Department of Physical Geography, Stockholm University, which required to concentrate on the optical properties of the Baltic Sea.

In my Master thesis (Kratzer 1994) I investigated the bio-optical properties of phytoplankton from coastal and oceanic waters from the point of view of complementary chromatic adaptation (Lüning 1990). Phytoplankton may be able to adapt their accessory pigment composition to the prevailing light field, and this in turn may change the light field, again. It is possible, that not only the availability of nutrients and light govern the occurrence of a phytoplankton bloom, but that the quality of light is also an essential trigger for the dominance of a certain group or species. This hypothesis is followed up again in Chapter 7 using filamentous cyanobacteria in the Baltic Sea as a case study (Kratzer, 2000).

Some of the objectives of the work reported in this thesis derived from the MAFF contract that funded my PhD from 1995 to 1997.

The objectives can be summarised as follows:

I a) To write a short user manual for the UWB colour sensors (see appendix I).

b) To improve the spectral calibration of the colour sensors, and to perform an absolute calibration on one of the instruments (see Chapter 3).

c) To test the UWB colour sensor in different modes of deployment .

II a) To deploy the colour sensor in different coastal waters over periods of several weeks or months (see Chapters 4, 5, 6) in order to investigate its suitability for optical monitoring of water quality in coastal waters.

b) To test the hypothesis that the UWB 4-channel colour sensor can be used for *in situ* measurements of chlorophyll a and carotenoid concentrations in Case-1 waters (see Chapter 4).

c) To test and improve the model by Harker (1997) to predict reflectance ratios (Chapter 5), and to adapt it to the Baltic Sea (Chapter 6.2). Furthermore to explore how OICs can be derived from colour ratios (model inversion) in Case-2 waters (see Chapter 5 and 6).

d) To perform a detailed optical study of the following water masses:

- Menai Strait (Chapter 5)
- Open Baltic Sea (Chapter 6).

III) To investigate the possibility of complementary chromatic adaptation of the cyanobacteria *Nodularia spumigena* and *Aphanizomenon flos-aquae* to the optical properties in the open Baltic Sea (Chapter 7).

Chapter 2 - Methods

2.1 Colour Sensor: construction, calibration and use

The School of Ocean Sciences developed a 6-channel profiling colour sensor (CS) in 1981 (Mitchelson *et al.* 1986) which copied some of the features of the Coastal Zone Colour Scanner. Later, a more simple instrument was developed (CS1) with only two channels to estimate the phytoplankton chlorophyll concentration from the ratio of the blue to green submarine downwelling irradiance. The instrument was deployed in Loch Striven, Scotland, in 1991 with two recording fluorometers (Chelsea Instruments Aquatracka I) and proved to be as reliable as the *in vivo* fluorometers for the estimation of chlorophyll concentration (Tett *et al.* 2000). In 1991, another two instruments, CS2 and CS3 were developed with four different channels.

The instruments had a black cylindrical plastic housing (400 mm long, and 150 mm in diameter; weighing approx. 5 kg) with a translucent diffusing Perspex window acting as a cosine collector (Figure 2.1). The power supply consisted of a 9 V battery pack at the bottom of the instrument. This provided an operational lifetime of up to 3 months of intermittent sampling with a 10 min logging interval. There were four short tunnels under the diffuser to collimate the light. A photodiode was placed at the end of each tunnel, behind a narrow waveband interference filter (nominal Full-Width at Half-Maximum (FWHM): 10 nm). The central wavebands of the filters were nominally at 440, 490, 570 and 670 nm (see Table 3.1, Chapter 3). Apart from the channel at 570 nm, these matched some of the visible channels of SeaWiFS (Figure 2.2). The band at 570 nm was chosen according to early plans of the SeaWiFS project, with the intention of using 570 nm as the green reference channel. This channel was later moved to 555 nm. The Marine Optics Group (MOG) at the School of Ocean Sciences (SOS), however, decided to retain the channel at 570 as it seemed to correspond more closely (than 555 nm) to a part of the pigment absorption spectrum with low absorption by most phytoplankton fat-soluble pigments.

CS2 and CS3 had four silicon photodiodes with an area of $1 cm^2$. The signals from these were passed to a gain-controlled amplifier, and then to an A-D converter with a conversion time of about 250 μs (personal communication with Ray Wilton). Sampling was controlled by an internal 16 bit microcomputer. Each channel was initially sampled to determine the light level, and the gain of the amplifier was adjusted automatically for maximum signal, without swamping the A-D converter. Twenty

discrete samples were taken together with the gain settings over a period of one second. The average of these samples was stored for each band.

CS2 and CS3 both had problems with sensitivity when measuring upwelling irradiance. In the CS4 series of colour sensors (CS20, CS21, CS22, CS23, CS24) the optics were identical, but improved photocells (Texas Instruments, TSL220) were incorporated in order to improve sensitivity. By using long sample periods (~30-60 sec) relatively low light levels could be monitored which made the CS4 colour sensors better instruments for measuring upwelling light then the previous models. The CS4 series was also developed to simplify the electronics of CS2/3. It utilised a large area photodiode with a built-in current-to-frequency converter. The output of the sensor was a pulse train whose frequency was directly proportional to the irradiance on the photodiode. The pulses were counted and stored by the microcomputer for a predetermined sample period, which was set by the user before the deployment (see Appendix I).

CS20-CS22 were constructed with funding from the NERC LOIS Shelf Edge Study (SES). CS23 and CS24 were bought with funding from MAFF/CEFAS. CS23 was dedicated to this PhD project. Both instruments contained an internal pressure sensor for profiling purposes, but because of sensitivity problems of the colour sensors, the instrumets could only be used for profiling the downwelling irradiance (personal communication with Dave Bowers). In the context of this thesis, however, only upwelling irradiance measurements are reported, which did not require the use of the pressure sensor.

Figure 2.3a shows CS23 in downwelling profiling mode. CS23 and CS24 were also fitted with an external RS-232 connector which allowed for downloading and calibration without having to open the housing of the instruments. CS23 was comprehensively calibrated at Plymouth Marine Laboratory (PML).

2.2 Use of the colour sensors, and their deployment sites

Appendix I explains how to handle the colour sensor and how to change the settings and download the data. The colour sensors were designed for a sampling strategy that did not require an absolute calibration by using colour ratios, and by restricting measurements of upwelling irradiance to two hours before and after mid-day (Wild-Allen *et al.* 1997; Bowers *et al.* 2000). Previous work had shown that ratios of upwelling radiance are rather consistent when omitting measurements close to dawn and dusk (Smith *et al.* 1991; Abbott *et al.* 1995).

CS2 and CS3 were deployed to measure upwelling irradiance on ARGOS-traced drifters south-west of Gran Canaria, Canary Islands (Wild-Allen *et al.* 1997) and on a mooring in Loch Striven (Harker 1997). CS20-CS22 were deployed in upwelling mode in 1995 and 1996 at moorings in waters west of the Outer Hebrides as part of the NERC SES (Kratzer *et al.* 1997; Smith *et al.* 1997, and Smith 1999). CS20 was lost while deployed. Some of the results of these deployments are shown in Chapter 4 (Kratzer *et al.* 1997).

In 1996 CS3 was deployed in upwelling mode in the Menai Strait over a period of nine months at a depth of 50 cm below the surface. The results of this deployment are described in Chapter 5, and in Kratzer *et al.*, 2000. The time series from 1996 was compared to a time series in the 1960s (Buchan *et al.* 1967; Kratzer *et al.* ms).

CS21 and CS22 were deployed in upwelling mode at 1.1 m depth on a Smart biophysical mooring from 17 April to 3 July 1997 in the Western Irish Sea during a CEFAS cruise as a part of the JoNuS II program.

CS 23 and CS24 were used for CEFAS cruises in the Irish Sea and the North Sea in 1996 and 1997 (Figure 2.3a and 2.3b). Some of the results are presented in Chapter 4, and in Kratzer *et al.* (1997). CS23 was subsequently modified to be compatible with the AVHRR sensor: the blue channel (440 nm) was changed to a channel at 580-680 nm, and was used in PhD studies by Sean Gaffney.

CS 22 and CS 24 were used during Baltic Sea cruises in May/June 1998. CS22 was deployed on a floating frame, in upwelling mode, whereas CS24 was deployed on deck measuring downwelling irradiance. The data from these cruises was used to calibrate an optical model for the Baltic Sea as described in Chapter 6.2, and (Kratzer *et al.* 1998).

CS22 was deployed in July/August 1998 north of Gotland, 1 km off the coast close to Ar. The sensor was mounted in upwelling mode on a raft at a depth of about 25 cm below the surface. The results are discussed in Chapter 6.2. CS24 was stolen when deployed as a surface reference measuring downwelling irradiance on the pier in Ar.

Table 2.1 lists all the field work that was carried out during the study. Some related bio-optical measurements around the Canary Islands and Loch Striven have been discussed in Kratzer (1994; 'Diplomarbeit', German Masters thesis). Chapter 4 includes data which was collected during this previous study (see second part of Table 2.1), and which was analysed during the course of this PhD.

The data from the Searcher and Baltica cruises have not been analysed fully yet, but some qualitative and observational results are discussed in Chapters 6 and 7.

August 1999	Cruise on R.V. Searcher,	9 days
	cruise on R.V. Baltica.	2 days
July/August 1999:	Optical station in the north of Gotland.	2 weeks
March/April 1999:	Spring cruises on R.V. Baltica (SMF), Landsort Deep.	1 day weekly
August 1998:	SMHI cruise on R.V. Argos, Baltic Sea (Skagerrak, Kattegat, and Baltic Proper).	2 weeks
July/August 1998:	Optical station in the north of Gotland.	6 weeks
May/June 1998:	SMHI cruise on R.V. Argos across the Baltic Sea.	2 weeks
July 1997:	MAFF cruise on R.V. Cirolana (JONUS II Program), North Sea and Irish Sea	3 weeks
April 1997:	MAFF cruise on R.V. Cirolana (JONUS II), North Sea and Irish Sea.	3 weeks.
March-Nov. 1996:	Optical time series in the Menai Strait.	9 months
July 1996:	MAFF cruise on R.V. Cirolana (JONUS II), North Sea.	2 weeks
May 1996:	MAFF cruise on R.V. Cirolana (JONUS II), North Sea and Irish Sea.	3 weeks.
May 1995:	Shelf-Edge Study (SES) cruise on R.V. Charles Darwin, Outer Hebrides.	2 weeks
	before registration:	
March 1994:	UWB cruise on R.V. Prince Madog, Loch Striven.	1 week
August 1993:	R.V. Hesperides (Spanish Armada), Canary Islands.	10 days
May 1993:	MAFF cruise on R.V. Cirolana, Irish Sea.	2 weeks

Table 2.1 Cruises and setting-up of optical stations during the course of this PhD. The cruises in 1993/1994 were performed during a previous study (Kratzer 1994).

2.3 Water sampling and analysis

In order to compare the colour sensor measurements with the different OICs, as well as for in-water modelling, water samples were taken at each optical station during cruises, and as frequently as possible during deployment on a mooring. The samples were either measured on board the ship (Cirolana and Argos cruises), or were taken to the laboratory to be measured (Menai Strait time series, Gotland station). All water sampling and analysis was carried out according to standard protocols (Marine Optical Group, School of Ocean Sciences) which as far as possible followed the SeaWiFS protocols (Mueller and Austin 1995). Duplicate samples were taken for all measurements except the concentration of CDOM (because the measurements proved to be very consistent), and HPLC pigment measurements (because of cost). Water samples were filtered as soon as possible after collection, and usually analysed or extracted immediately. The bottles were always well shaken before filtration to avoid settling of phytoplankton and sediment. Filters for the HPLC analysis were stored in liquid nitrogen for up to 11 months, and processed at PML (Plymouth Marine

Laboratory). CDOM samples were filtered, and spectrophotometrically scanned when they had warmed to room temperature (~20°C). In a few cases where measurements could not be performed straight away the samples were kept in a refrigerator for up to one week.

In the Menai Strait water samples were taken from the surface only on the grounds that the water column was vertically well mixed by the strong turbulence of tidal flows (Harker 1997). In other cases, samples were taken at prescribed depths below the surface. A Secchi Disk reading was taken prior to sampling in order to be able to judge how much water volume would be needed for filtration. During cruises in spring and summer stratification could be expected, and therefore the Secchi reading was also used to decide the actual sampling depth corresponding to the prescribed 0.5 and 2.3 optical depth (these were set as standard depths by MOG).

2.3.1 Determination of Suspended Particulate Matter (SPM)

The concentration of SPM was measured gravimetrically (Strickland and Parsons 1972). 1-2 litres of sample were filtered through pre-weighed GF/F filters, which were then washed with 250 ml of distilled water to remove salts, baked overnight in an oven (100 °C), and kept in a dessicator until weighing. A balance weighing to 5 decimal places (i.e. precision of 10 μg) was used (Sartorius AG at SOS; and A&D at Systems Ecology, Stockholm University).

During cruises, the filters were first left to dry in air, and then kept in a dessicator before being baked. The dry weight was measured after baking. Then, the filters were combusted for 5 hours at 500 °C, which burnt off all organic suspended solids (OSS), and the weight was measured again. The difference between the combusted filters and the tare weight equalled the inorganic fraction, or mineral suspended solids (MSS). The organic fraction was calculated by taking the difference between the dry weight of the whole sediment and the inorganic fraction. The weighing and combustion of the filters was done in aluminium trays which were labelled so that the filters would not be confused. Handling of both filters and trays was done very carefully, using forceps, and in between handling the filters were sealed in plastic bags. During the handling of glass fibre filters it is difficult to avoid loss of bits of filter paper e.g. when taking the filters off the filtering apparatus. A handling correction was determined by processing blank filter papers.

All the trays from the Menai Strait samples were numbered with Tipp-Ex in order to

distinguish the trays from one another. The idea was that Tipp-Ex would not vanish with combustion, as writing with permanent markers does. However, it turned out that Tipp-Ex contained an organic fraction which itself had to be corrected for. In order to correct for this error, 10 replicas of blank filters were treated in the following way: for each blank, 2 litres of deionised water were filtered through pre-weighed GF/F filters. After that, the filters were weighed and treated in the same way as the sample filters. Both the inorganic and organic fraction were corrected for the mean value of those blank filters. The correction value were -1.6 (+/- 0.1) gm^{-3} for MSS, and 1.1 (+/- 0.1) gm^{-3} for OSS. For the Baltic Sea samples the trays were labelled by marking the aluminium trays with numbers using a scriber.

2.3.2 Spectrophotometric determination of coloured dissolved organic matter (CDOM)

CDOM was measured in 10 cm cuvettes with a dual beam scanning spectrophotometer (Shimadzu UV-1601 for Irish Sea and Menai Strait samples, UV-2401 for Baltic Sea samples). The sea water was collected in 500 ml amber bottles and filtered through 0.22 μm membrane filters. Glassware was used for filtration since plastic may degrade with time, adding to the optical signal of CDOM (Mueller and Austin 1995). Absorbance was measured optically against deionised water as a blank. The optical density (OD) was measured from 350 to 750 nm and the absorption of CDOM at a given wavelength was calculated from:

$$a_{CDOM} = (2.3026\ (OD\ ))\ L^{-1} \qquad m^{-1}$$

where L was the path length of the cuvette, in this case 0.1 m. The CDOM absorption coefficient at 440 nm, g_{440} as derived in Chapter 1, equation 1.11, was used as a proxy for the concentration of CDOM (Kirk 1994).

2.3.3 Spectrophotometric determination of pigments

For the spectrophotometric estimation of pigments (Jeffrey and Humphrey 1975; Parsons *et al.*, 1984), 1-2 l of sea water were filtered through a GF/F filter and the filter was extracted overnight in 90% acetone ($NaHCO_3$-neutralised) in darkness in a refrigerator. The sample was centrifuged at 3000 rpm. The extract's optical density was measured against a blank of 90% acetone using a dual beam scanning spectrophotometer (UV-1601 for Irish Sea and Menai Strait samples, UV-2401 for Baltic Sea samples). In some cases a single beam UV 1201 was used at SOS instead. The concentration of chlorophyll a was estimated using the trichromatic method, which

uses the optical density at 630 nm, 647 nm, and 664 nm, after correction by subtracting the reading at 750 nm. The total carotenoid concentration was determined from the optical density of the acetone extracts at 480 and 510 nm (Parsons *et al.* 1984). The optical densities were corrected by subtracting the 750 nm reading from the 664, 647 and 630 nm and by subtracting 2x the 750 nm reading from the 510 nm absorbance, and 3x the 750 nm reading from the 480 nm absorbance. The amount of pigment in the original sea water sample was derived from the equations given below:

$$(Ca) = (11.85\ OD_{664} - 1.54\ OD_{647} - 0.08\ OD_{630})\ L^{-1}$$

where OD stands for the corrected optical density at each wavelength, and Ca is the amount of chlorophyll a in µg per ml extract. L was the pathlength of the cuvette in centimeters, usually 1 cm.

The chlorophyll a concentration [Chl] was calculated as follows:

$$[Chl] = (Ca\ E)V^{-1} \qquad \mu g\ chl\ l^{-1}$$

where E was the volume of acetone in ml (10 ml), V was the volume of sea water in litres.

In the case of total carotenoids,

$$(Cp) = (7.6\ (OD_{480} - 1.49\ OD_{510}))\ l^{-1}$$

and the total carotenoid concentration [Carot] was calculated in the same way as stated above for chlorophyll:

$$[Carot] = (Cp\ E)\ V^{-1} \qquad \mu g\ carot\ l^{-1}$$

At SOS the chlorophyll concentration was also measured by the fluorometric method as described in Kratzer, 1994. This also included an acidification step with hydrochloric acid to determine the concentration of phaeopigments.

The pigment concentrations are only approximated by these methods and equations since they are a variable mixture of several compounds with different molar extinction coefficients.

2.3.4 Determination of pigments by reverse phase HPLC (High Performance Liquid Chromatography)

A full analysis of the pigment composition of selected samples from the SES cruise in 1995, and the Cirolana cruises in 1997 was obtained by reverse phase HPLC analysis carried out at PML (Barlow *et al.* 1993). If possible, the HPLC sample and the sample for the spectrophotometric determination of pigments were taken from the same oceanographic bottle, so that the two methods could be compared.

For HPLC determinations, 25 mm GF/F filters and a mild vacuum (0.2 bar) were used for filtration. 200-300 ml of sea-water were filtered, and the filters were frozen in liquid nitrogen. They were stored for up to 11 months.

The filters were extracted in 2-5 ml 90% acetone using a sonicator, and centrifuged to remove cellular debris. After 4 hours of extraction an aliquot (300µl) of clarified extract was injected into the HPLC system (Shimadzu LC-6A Liquid Chromatograph with SCL-6B system controller, and auto sampler Spectra System AS3000). The HPLC system was fitted with a 3-µm Pecosphere column (3.5 x 0.45 cm, Perkin-Elmer). For the detection of pigments a Shimadzu Fluorescence HPLC Monitor (RF-535, Xe-lamp) was used with excitation set to 405 nm, and emission set to 670 nm, as well as a Shimadzu UV-VIS spectrophotometric detector (440 nm, W- lamp).

Pigments were separated by a linear gradient changing from 0% to 100% of solvent B over 10 minutes. This was followed by a hold at 100% of solvent B for 7.5 min, at a flow rate of 1 ml m^{-1}. Solvent A consisted of 80% methanol and 20% ammonium acetate (buffer); solvent B consisted of 60% methanol, 40% acetone.

Pigments were identified by comparison with retention times of various pigments isolated from well-documented microalgal species (Barlow *et al.* 1993). The pigments were identified according to the specific retention time, and the pigment concentrations were calculated from the area under the curve of the chromatogram. In order to check the calibration, chlorophyll a and b standards were co-eluted with the samples. I performed the chemical analysis of the samples from the SES cruise (May 1995) in November 1995, with the help of Denise Cummings (PML). I calculated the pigment concentrations, and the results were used in Smith (1999). The samples from 1997 were completely processed by Denise Cummings.

2.3.5 Filter pad technique

The absorption spectra of the living phytoplankton and other SPM were measured spectrophotometrically using the wet filter pad technique (Yentsch 1957). 1-2 l of sea water were filtered through a GF/F filter. After filtration the water-saturated filter was scanned from 350 to 750 nm using a dual beam scanning spectrophotometer (UV-1601 for Irish Sea and Menai Strait samples, UV-2401 for Baltic Sea samples). A GF/F filter saturated with deionised water was used as a blank. The sample filter and blank filters were both put on microscopic slides which were fixed in front of the detector windows. Great care was given to have both filters saturated with deionised water so that no air bubbles could develop. For the sample filters, filtered sea water was used for saturation.

The sample filter was then decolourised with methanol (Kishino *et al.* 1985). The filter was placed on a Whatman glass filtering apparatus, and 30-60 ml methanol were added. The methanol was left to filter through by gravitation. After 30 minutes, the decolourised filter was rinsed with 50 ml of deionized water, and scanned in the same way as described above.

For the samples from the Baltic Sea during summer (when filamentous cyanobacteria were present) the decolourised spectrum was corrected for the presence of phycobilin pigments (which do not extract in organic solvents) by fitting an exponential curve to the lower envelope of the spectrum from 400 to 700 nm. The best fit was assumed to represent the spectrum of total SPM excluding the total pigment fraction (chlorophylls, carotenoids, and phycobilin pigments).

The decolourised spectrum was taken to be that of total SPM excluding photosynthetic pigments, and the difference between the initial and decolourised spectra was taken as the *in vivo* spectrum of the phytoplankton. All spectra were corrected for internal scattering (β-correction) by an algorithm provided by Cleveland and Weidemann (1993). The spectral optical density of the sample, $OD(\lambda)$, was corrected for the optical density at 750 nm, OD_{750}:

$$OD'(\lambda) = OD(\lambda) - OD_{750}$$

The corrected optical density, $OD'(\lambda)$, was then converted to the equivalent optical density in suspension:

$$D_{susp}(\lambda) = 0.378\ OD'(\lambda) + 0.523\ (OD'(\lambda))^2$$

From this term the absorption spectrum per unit pathlength, a(λ) was calculated:

$$a(\lambda) = (2.3026\ OD_{susp}(\lambda)\ A\ )\ V^{-1} \qquad m^{-1}$$

where the factor 2.3026 converts from $\log_{10}$ to natural logarithm, A is the soiled area of the filter in m^2 and V the volume of the filtered sample in m^3.

Chlorophyll-specific absorption spectra were then obtained for all four colour sensor centre wavelengths by regressing the absorption coefficient against the chlorophyll-a concentration, [chl]:

$$a_{ph}^*(\lambda) = a(\lambda)\ [chl]^{-1} \qquad m^2\ (mg\ chl)^{-1}$$

SPM-specific absorption coefficients were obtained for the four colour sensor wavebands by regressing the β-corrected, decolourised absorption coefficients against the concentration of SPM, [SPM]:

$$a_{SPM}^*(\lambda) = a(\lambda)\ [SPM]^{-1} \qquad m^2\ (g\ SPM)^{-1}$$

2.3.5 Phytoplankton analysis

For phytoplankton analysis, samples of unfiltered water were preserved with acetic Lugol's Iodine and, in some cases, buffered formaldehyde (Throndsen 1978). During the Baltic Sea cruises on R.V. Argos, a phytoplankton net (25μm mesh) was used to sample microplankton down to 20 m depth. The dominant phytoplankton groups (and/or the predominant species) were identified under a light microscope. (inverted microscope at SOS, standard high power microscope during Cirolana cruises). For analysing filamentous cyanobacteria at the field station in Gotland, 250-500 ml of sea water was filtered onto a 0.2 μm membrane filter and analysed under a low power stereo microscope.

2.4 Discussion of methods

2.4.1 Pigment analysis

The standard spectrophotometric and fluorometric equations for chlorophyll a are rather inaccurate giving values within +/-20% of true chlorophyll a concentration (JGOFS Report No. 6). In addition, there is the matter of precision. Tett and Grantham (1980) quoted an error of 2% for the chlorophyll a measured by the fluorometric method. This value was based on replicates from the same sampling bottle, and is a coefficient of

variation (CV) derived from log-transformed data. Taking small scale patchiness into account, the error increased to 11 %. This is the result of using samples from different bottles. Parsons *et al.* (1984) quoted an error of 1% for their spectrophotometric method in the laboratory, based on replicate extracts from the same water sample. Jeffrey and Welschmeyer quote an error of 1-3 % for the same method. The error of the chlorophyll measurements during the course of this thesis (based on samples from different bottles) ranged from 10% (Menai Strait 1996), 9% (Cirolana cruises) to 7% (Baltic Sea measurements). These values were calculated from log-transformed data and correspond to CVs. They suggest that the error got less as I became more familiar with the method. Table 2.2 summarizes the error of the chlorophyll, as well as the SPM, analyses.

	Chlorophyll ($\mu g\ l^{-1}$)	SPM ($g\ m^{-3}$)
Menai Strait (1996)	10%	13%
Cirolana cruises (1996-1997)	9%	12%
Baltic Sea (Argos cruises and Gotland, 1998)	7%	10%

Table 2.2 Percent error (=standard deviation/mean) for chlorophyll and SPM measurements during the course of the investigation. The chlorophyll data were log -transformed.

The overall deviation for the SPM measurements was 0.90 $g\ m^{-3}$ for the Menai Stait, and 0.75 $g\ m^{-3}$ for the Irish Sea. This compares well with Weeks (1989), who obtained a standard deviation of 1.8 $g\ m^{-3}$.

Absorption and fluorescence are largely properties of the porphyrin ring, which is part of the chlorophyll molecule, as well as of its breakdown products chlorophyllide, phaeophorbide and phaeophytin. Chlorophyll a can be transferred into chlorophyllide a by chlorophyllase (Jeffrey and Hallegraeff 1987). Chlorophyllase activity can be induced by harvesting techniques (filtration and centrifugation) which might give a distorted view of the original chlorophyll a and chlorophyllide a concentration in the sample. Chlorophyllide a is also one of the intermediates in the biosynthesis of chlorophyll a and there might be exchange between these two pigments under certain conditions, reflecting changes in the physiological or nutrient status (Riper *et al.* 1979). Chlorophyll a can be distinguished from phaeopigments by fluorometry including an acidification step with 2N HCL (Tett 1987). However, the fluorescence of chlorophyll a

and chlorophyllide a can not be distinguished using fluorometry only. Gowen *et al.* (1982) investigated the problem of degradation pigments in the estimation of chlorophyll by fluorescence in two Scottish sea-lochs. They used thin layer chromatography (TLC) to separate chlorophyll from its breakdown products, and then measured the fluorescence of the different components. They found that chlorophyllide a may represent up to 50% of the total chlorophyll a-like pigments.

2.4.2 HPLC versus spectrophotometric and fluorometric methods

The SeaWiFS protocols recommend reverse phase HPLC for high accuracy determination of chlorophyll a, b, and c, as well as for carotenoid concentration. However, this technique is very expensive. Peters (1991) discussed the use of HPLC versus the use of the more crude spectrophotometric determination of chlorophyll a as a proxy of biomass. He puts them in the context of applied science against pure science. According to Peters, HPLC (pure science) is assumed to be the most reliable method for measuring chlorophyll a. However, the crude estimates are often far more informative as they appear in predictive relationships for transparency, fish production, zooplankton biomass, as well as primary production. HPLC estimates, can not be introduced into such equations, because they have no consistent relation to the crude extractions on which the informative regressions are based. Peters claims that the crude extracts may reflect the range of biological important properties of the phytoplankton community better than the sophisticated HPLC measurements. He suggests giving up the claim that the traditional techniques actually measure 'chlorophyll a' and to adopt a different term for the object of the crude extraction.

In this investigation the spectrophotometric method was used as the main method for determination of pigments and checked against the HPLC method. A total of 36 water samples was divided into two samples, and the chlorophyll a and total carotenoid concentration was measured both by the spectrophotometric method, as well as by HPLC. The samples were gathered during the SES cruise in 1995, and the Cirolana cruises in 1997. The results are shown in Figures 2.4a and 2.4b. The correlation coefficient was 0.92, degree of freedom, df = 34. The intercept was significantly different from 0, which indicates, that there were other pigments present which were measured by the spectrophotometer. These are likely to be pheaopigments from non-living algal cells. The slope of the regression of chlorophyll a concentration measured by the spectrophotometric method against the chlorophyll a concentration measured by HPLC was significantly different from 1; and the chlorophyll a concentrations were

underestimated by about 31% by the spectrophotometric method (Figure 2.4a). This means that the chlorophyll specific absorption spectra calculated for the models in Chapters 5 and 6 will be overestimated by about 45% compared to published studies that use HPLC as a standard method (note: 100/100 = 1; 100/69 = 1.45).

The slope of the regression of total carotenoid concentration measured by the spectrophotometric method against the total carotenoid concentration measured by HPLC was not significantly different from 1, indicating that the spectrophotometric method worked better for total carotenoid concentration than for the chlorophyll a concentration (Figure 2.4b). The correlation coefficient was 0.93, and the intercept was only just significantly different from 0. The data set from the SES cruise only (see Figure 4.4, Chapter 4) had a correlation coefficient of 0.94, and the slope was not significantly different from 1, and the intercept was not significantly different from 0.

2.4.3 Filter storage

The storage of filters is an important issue as measurements cannot always be carried out straight after sampling. Pigments degrade when stored for long periods of time in the freezer. Freeze drying does not help because this may activate the enzyme chlorophyllase which breaks down chlorophyll (personal communication from Fauzi Mantoura, 1996). The SeaWiFS protocols refer to the JGOFS protocols for pigment analysis and storage (Joint Global Ocean Flux Study 1991). They recommend storage at lower than -20°C, preferably in liquid nitrogen. The SCOR (Scientific Community on Oceanographic Research) WG78 workshops found 75% recovery of chlorophyll a from a mixture of cultured microalgae after four weeks of storage at -20 °C, and 109% from natural phytoplankton, using HPLC (Mantoura *et al.* 1997). Including chlorophyllide a (which would be indistinguishable from chlorophyll a by fluorometry), these figures increased to 91% and 114% respectively. (Values > 100% were reproducible - the authors attributed this to enhancement of chlorophyll a extractability in methanol by the freezing process). Freezing at -90°C or in liquid nitrogen (at -196°C) recovered about 110% after a month, and using liquid nitrogen gave recovery of 88% - 100% after 328 days for different species (unreplicated). There was some variability between species and experiments. The authors concluded that the filters should be stored at least at -90°C, if not colder (Mantaura *et. al.* 1997).

2.4.4 CDOM and SPM measurements

The SeaWiFS protocols require the use of 0.2 μm membrane filters for measuring CDOM. However, our colleagues from the Limnology Department at Uppsala University used GF/F filters for measuring CDOM, because of lower costs. Their argument was that CDOM was so high in lakes as well as in the Baltic Sea, that it did not really matter which sort of filters were used. I decided to compare the two measurements during the Argos cruise in May/June 1998. I filtered samples from the same glass bottle through GF/F filters, as well as through 0.2 μm membrane filters and measured CDOM in a spectrophotometer as described before. A total of 18 samples was compared. The results are shown in Figure 2.5. The slope of the regression of GF/F g_{440} against 0.2 μm g_{440} was not significantly different from 1, but there was an offset (0.02 +/- 0.01). The correlation coefficient was 0.92, the degree of freedom was 16. The use of GF/F filters therefore leads to a consistent overestimation of CDOM. This is probably caused by scattering, partly due to the bigger nominal pore size of GF/F filters (0.7 μm) allowing more particles through, and partly due to glass fibres washed out by the filter. The constancy of the overestimation favours the latter explanation.

The storage of CDOM samples is possible without freezing. CDOM samples may be kept for several months in the dark in a refrigerator. This is based on inter-comparisons of hundreds of samples (personal communication with Nils Højerslev, 1999). The SeaWiFS protocols suggest freezing the filtrate in an amber bottle. I compared refrigerator and freezer storage in 1999. The shape of the spectra changed after freezing compared to the fresh samples. I also used mercuric chloride solution as a preservative for two samples, and kept them in the fridge for one week. The result was very encouraging: the spectra looked the same, and I got the same values for g_{440} as for the samples that were measured straight away. However, further work is needed to investigate the storage with mercuric chloride.

During this research CDOM samples were measured on the same day, except for some samples during the Menai Strait time series, and during the Argos cruise in May/June 1998, where they were stored (after filtration) in a refrigerator for up to one week.

During the ARGOS cruises in the Baltic Sea the humic content was measured by fluorometry (RF-5001 PC spectrofluorometer), using excitation at 350 nm, and measuring the emission at 450 nm. Quinine sulphate (QS) in 0.05 M sulphuric acid

was used for calibration. A mean conversion factor of 0.4 mg l^{-1} of humic substance per µg l^{-1} of QS was used to derive humic content from the fluorescent signal (Wedborg *et al.*1994). The samples for both measurements were filtered through 0.2 µm membrane filters. I compared 8 samples from the ARGOS cruise in August 1998 using both methods. The samples were mostly from the open Baltic Sea, but one sample was from the Skagerrak, and two from the Kattegat. Figure 2.6 shows the relationship of CDOM absorption to the fluorometrically derived humus content. There was a good correlation between the g_{440} values, and the concentration of humic substances. The regression equation was:

g_{440} = - 0.017 (+/-0.041) + 0.090 (+/-0.016) [humus] , r^2 = 0.84, df =6

where [humus] is the concentration of humic substances in mg l^{-1}.

Using this relationship, g_{440} values can be estimated from the fluorometric measurements. This may be useful for optical studies of the Baltic Sea, as humic substances are measured on a regular basis by SMHI (Swedish Meteorological and Hydrological Institute), but CDOM-g_{440} is not part of the monitoring program.

According to the methodology used here, CDOM is whatever passes a 0.22 µm filter. The particulate spectra, and the masses of SPM, were measured on a GF/F filter with a nominal size of 0.7 µm. Therefore, particles between 0.22 µm and 0.7 µm are not accounted for with these methods. It would be better to have one pore size to differentiate between suspended and dissolved material. The World Meteorological Organization recommends using a single pore size of membrane filters (0.45 µm) to distinguish between dissolved and suspended material (WMO, 1981). This method is also recommended in 'Water Quality Assessment' (Chapman 1998). It would increase the size of dissolved matter, which would probably cause a stronger scatter when scanned by the spectrophotometer, and therefore reduce the signal and overestimate absorption. For suspended matter it would slow down the filtering process, especially in Case-2 waters. It may reduce the sensitivity of the method as the filters might clog quickly with fine material. And there would be a problem with gravimetric determination of the organic and inorganic fraction of SPM because the membrane filter would combust.

2.4.5 Measuring *in vivo* absorption of phytoplankton

Allali *et al.* (1995) proposed a technique for measuring the spectral absorption coefficient on a membrane filter. The sediment is filtered on a 0.4 μm Nucleopore filter which is then transferred onto a microscope slide, the sediment side of the filter facing downwards. Filtered sea water is used to avoid air bubbles. The whole slide is then placed onto a metal box filled with liquid nitrogen, and the material on the filter freezes instantaneously. After a few seconds, the slide is removed from the metal box. Just at the moment when the sediment starts to thaw, the filter can be peeled off from the sediment. With this method, there is no path-length amplification due to the filter material, and the only scattering caused is due to the particles themselves. I tried this method with algal cultures (*Tetraselmis chui* and *Skeletonema costatum*) in the laboratory, as well as on Cirolana during a *Phaeocystis pouchetii* bloom in the Irish Sea. Each time the sample did not transfer properly, and some of the algae were still stuck to the filter after the filter had been peeled off. The method was therefore not quantitative. There were, also, safety problems involved in handling liquid nitrogen on the ship.

One way of checking the validity of the Cleveland and Weidemann (1993) β-correction would be to measure total absorption *in situ*, e.g. with a WetLabs AC9 (absorption and attenuation meter), and then to compare the total absorption of all OICs as measured spectrophotometrically, plus the total absorption by water (as derived from the literature) with the absorption at nine wavebands of the AC9. Another way of getting round the problem of scattering is to use an integrating sphere (Kirk 1994). However, these are very expensive, and there is still some backscatter that will be lost.

Finally, there was a minor problem in the use of methanol for decolourisation (Kishino *et al.* 1995). It was very difficult to get the filter to stick to the microscopic slide when soaked in methanol. It was necessary to rinse the filter with deionized water after decolourisation with methanol. If not the filter would not stick to the glass, and air bubbles might develop, causing internal reflection between filter and microscopic slide.

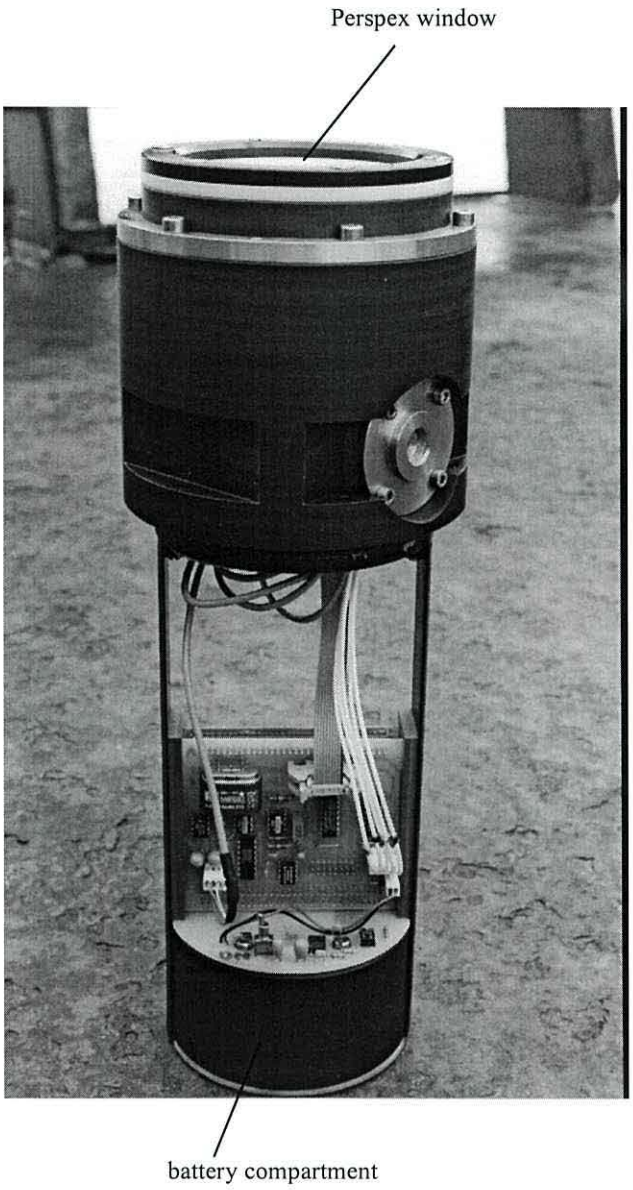

Figure 2.1 Colour sensor CS23 with housing removed.

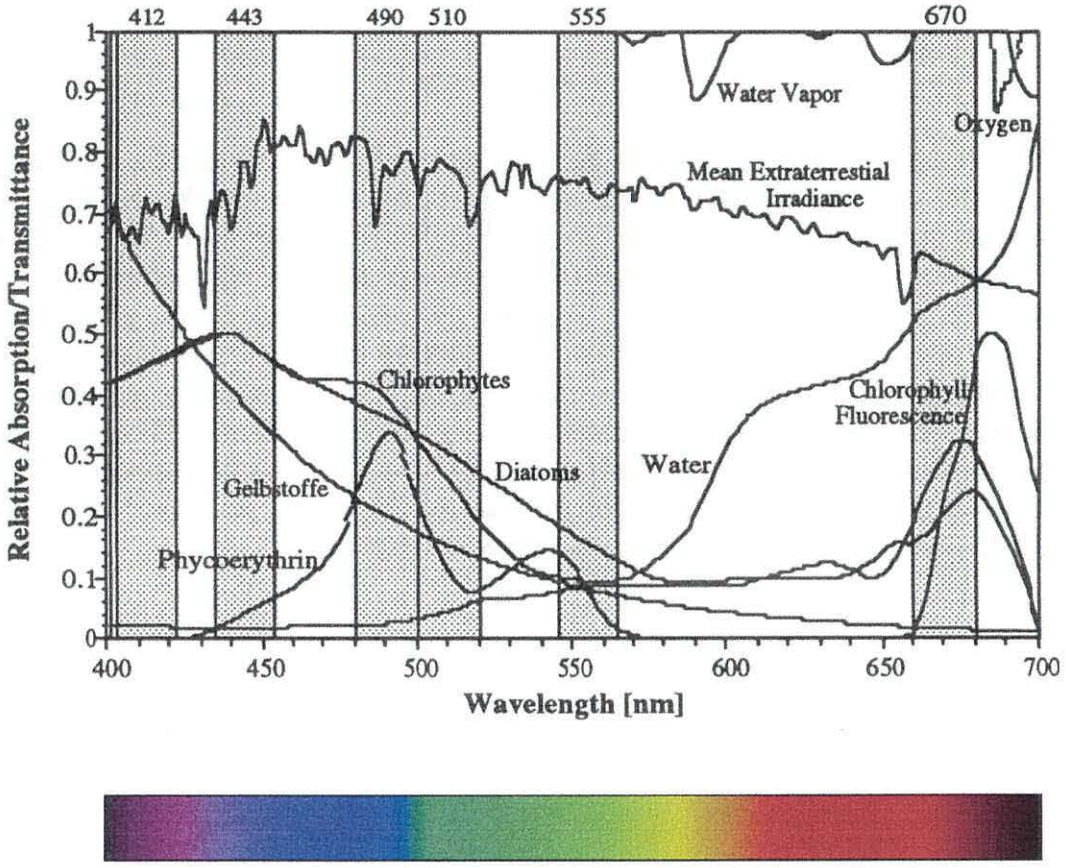

Figure 2.2 SeaWiFS visible bands, from Hooker *et al.* (1992)

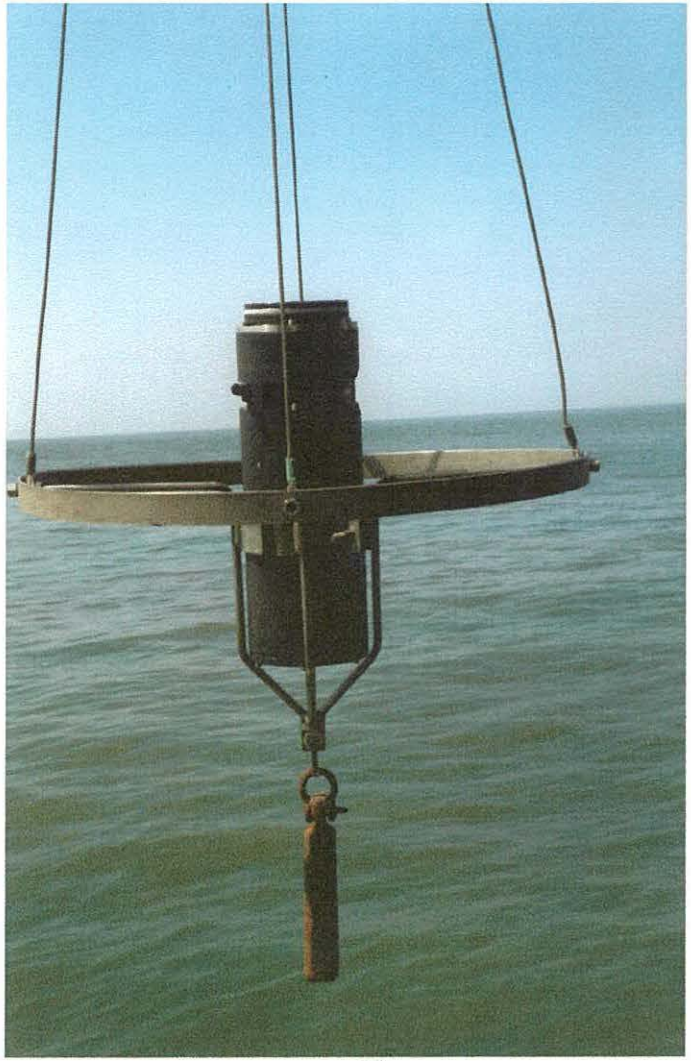

(a)

(b)

Figure 2.3

(a) CS23 in downwelling profile mode and

(b) in upwelling surface mode during Cirolana cruises 1997.

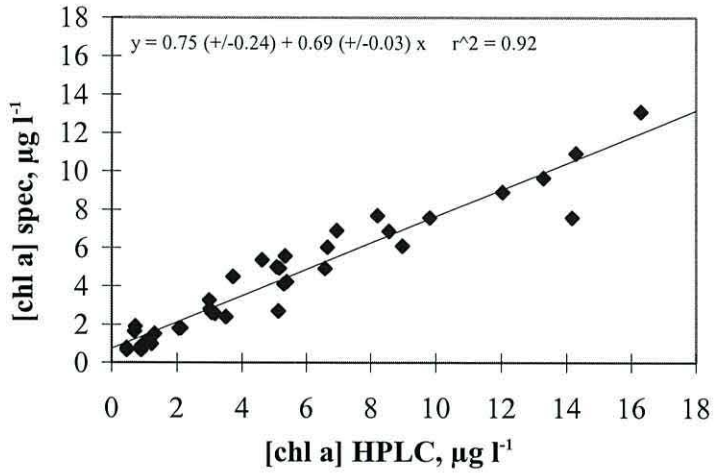

Figure 2.4a Regression of the chlorophyll a concentration measured by the spectrophotometric method against the chlorophyll a concentration measured by HPLC.

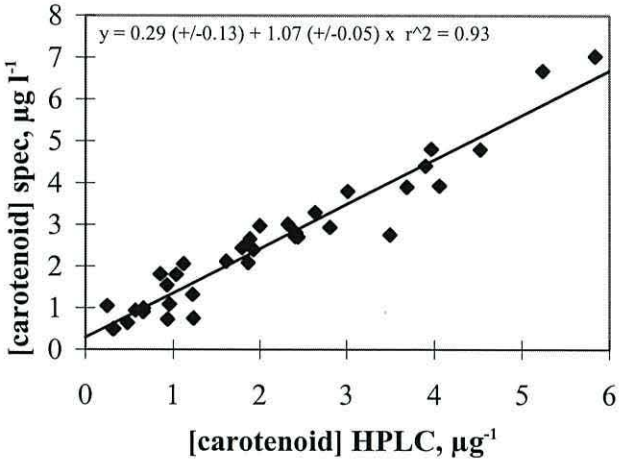

Figure 2.4b Regression of the total carotenoid concentration measured by the spectrophotometric method against the total carotenoid concentration measured by HPLC.

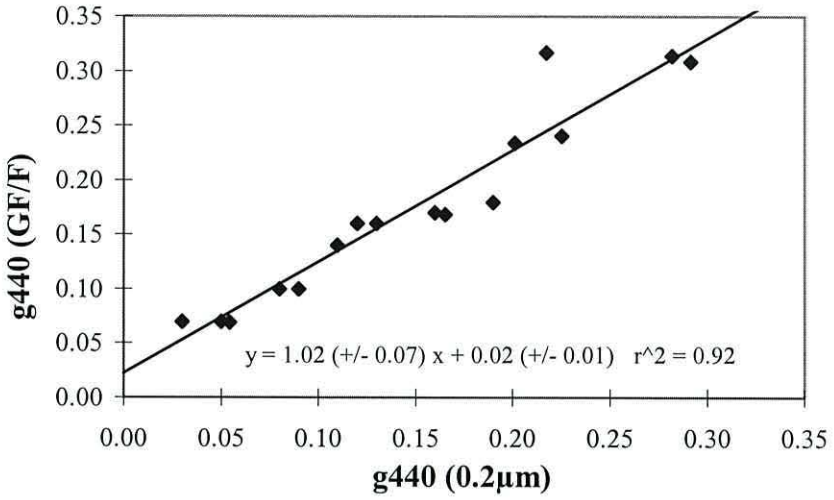

Figure 2.5 Comparison of g_{440} measurements using 0.2 µm membrane and GF/F filters.

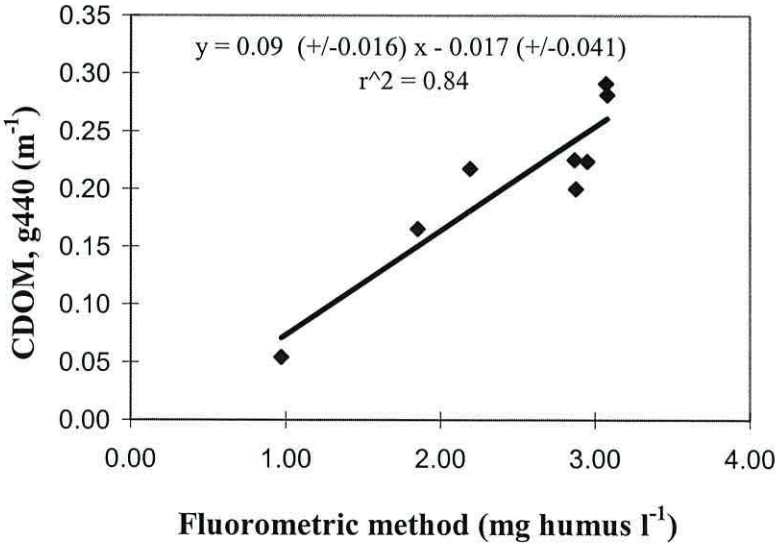

Figure 2.6 Approximate relationship between g_{440} and the concentration of humic substances determined by fluorescence.

Chapter 3 - Colour sensor calibration

3.1 Introduction

The SeaWiFS protocols describe strict procedures for radiometer calibration. I used them as a guideline for measuring the spectral response of CS23, as well as for making an absolute calibration, and checking the cosine response, and the linearity of response.

The response curves of the filters in the CS2/3 and CS4 series were measured by the supplier (Ealing Electro-Optics) in September 1993. The specifications of the two sets of filters are remarkably similar (see Table 3.1).

When discussing the different channels within MOG we felt the need to use different colour codes for defining each channel. The 'green' channel really was in the yellow-green part of the spectrum but because most algorithms refer to red:green ratios, we decided to call the channel at 570 nm 'green'.

The cosine response of CS2 had been checked underwater in a black tank using an underwater torch at the School of Ocean Sciences by Ru Morrison. It was found that a thin transparent Perspex sheet, that was meant to protect the cosine collector from scratches, caused a drastic deterioration in the cosine response at photon incidence angles greater than 41° from the vertical. This was presumably due to increased reflection. As a result of this test, the colour sensor design was modified to leave off the protective sheet, and further testing showed an improvement of the cosine response.

The relative spectral response of CS2 was measured in 1995 at the NERC field spectroscopy unit at the University of Southampton, by Genevra Harker. According to this calibration, the peak transmittance of the filters occurred at 435 nm, 485 nm, 565 nm, and 665 nm. The cyan channel (485 nm) had a leakage in the red part of the spectrum, but this may have been an artefact of the measurement, because the measurements were performed on the sensor head after it had been removed from the case of the instrument.

In January 1997, I carried out more precise optical calibrations using a dedicated calibration room at PML (Plymouth Marine Laboratory). I am grateful to Gerald Moore for advice and for letting me use these facilities.

3.2 Methods

The calibration room had been painted black in order to avoid reflection from bright surfaces. The facility had been validated in SIRREX-6 (SeaWiFS Intercalibration Round-Robin Experiment). The relative spectral response of the colour sensor was measured with a monochromator, which in turn was calibrated with a standard diode.

A calibration bench with a standard 1000 W lamp with constant power supply was used to measure the absolute response of each channel. The same bench was used to check the linearity of response, as well as the cosine response in air. For the latter two measurements a car lamp was used with constant power supply because of the cost of running the 1000 W lamp.

3.2.1 Spectral calibration

A monochromator was used to measure the spectral response of the colour sensor. The monochromator (Hilger and Watts, Monospec 600) used at PML had a 600 lines per inch diffraction grating and focusing optics with a spectral bandwidth of 3 nm. It was fitted with a quartz halogen lamp with peak output at 900 nm, declining towards the blue. The spectral output of grating monochromators changes over time and has to be measured and corrected for. This was done by measuring the monochromator light power output with a silicon diode supplied by Bentham Instruments Ltd, UK. The diode response was referenced to an NPL (National Physical Laboratory) supplied diode, and is thus traceable to NPL standards. Cross comparison amongst national laboratories has shown an accuracy within 2% for such secondary standards. Gerald Moore tested the diode against a NIST (National Institute of Standards and Technology) sourced quantum trap and it yielded an accuracy within 1%.

The colour sensor was placed on a holder in front of the monochromator, facing the window of the monochromator. The holder was too small in diameter to hold the colour sensor firmly, and careful handling was needed to keep the colour sensor in line with the monochromator's light source. In order to find the centre of each diode, a small torch was first used to detect each individual channel under the diffuser plate. For this, the colour sensor was connected to a computer so that the output of the four channels could be monitored. Once a channel had been located under the diffuser plate, this area of the diffuser was aligned with the window of the monochromator. The monochromator was then set to the channel centre waveband, in order to gain maximum sensitivity. The next step was to align the monochromator exactly with the geometric

centre of the channel, by adjusting the colour sensor on the holder, whilst checking the colour sensor's output on the computer. Once this centre was located, the monochromator was run from 20 nm below to 20 nm above the nominal centre wavelength of the channel. The monochromator wheel was moved manually in 1 nm steps around the peak waveband, and in 2 nm steps further away from the peak waveband. The colour sensor reading at each step was noted. This procedure was repeated for all four channels. Because it was so difficult to find the peak waveband, each channel was checked several times. Colour sensor output was also recorded for wavelengths outside the channel wavebands and used to correct the readings within the wavebands. Spectral bands are usually characterised by the centre wavelength and the full-width at half-maximum (FWHM) of each band. The centre wavelength may be defined as the wavelength halfway between wavelengths at which the normalised response is 50 % and the FWHM as their difference. The FWHM was calculated for each channel. The procedure took a day for each sensor.

CS23 and CS3 were the only instruments that had an external RS232 interface, but CS3 was not sensitive enough for the low output from the monochromator. Therefore, CS23 was chosen for a complete calibration. The other two instruments (CS21 and CS22, which were designed for use at a mooring) had to be connected to the computer by opening the case and running a cable from the motherboard of the colour sensor to the computer. A black cloth was used to cut out the light. This combined with the cable, made it difficult to move an instrument without getting it out of line with the monochromator, and without getting any stray light onto the photodiodes through the gap between the case and the sensor head. These practical constraints made it impossible to locate the centre of the tunnel leading to each photodiode and thus correctly to determine the waveband of each channel in these instruments.

It was, however, feasible to check if there was a leakage of red light into the cyan channel as detected in the calibration of CS2 in Southampton. CS21 was used for this purpose.

3.2.2 Absolute calibration of the sensor

After having measured the spectral response of CS23, it was calibrated with a 1000 W seasoned FEL (a type of standard lamp for irradiance and radiance calibration) supplied by the Hoffman company (Germany) and calibrated against a NIST FEL in SIRREX 3 (SeaWiFS Intercalibration Round-Robin Experiment 3). The lamp was connected to a constant power supply. It had been calibrated at 50 cm distance, and therefore the

calibration should have been performed at the same distance. The calibration bench at PML, however, was set up for smaller instruments than the colour sensor. Therefore, only about 1cm^2 of the diffuser surface was exposed to the correct irradiance at a distance of 50 cm. The aim was, however, to illuminate the entire surface of the diffuser during calibration. In order to achieve this, the distance between sensor and light source needed to be at least 1 m. Using the inverse-square law, however, the colour sensor could still be calibrated: the irradiance of a point source is proportional to $1/r^2$, where r is the distance to the point source. Therefore, applying the inverse square law, the irradiance at 1 m distance equals the calibrated irradiance at 0.5 m distance divided by four.

The colour sensor was set to sample for 10 seconds and aimed at the light source. A measurement of the stray light was taken by blocking the direct light with an opaque plate. The colour sensor readings were corrected for the stray light readings.

The irradiance spectrum of the calibration lamp was known, which together with the relative spectral calibration of the colour sensor, allowed for an absolute calibration of the instrument (in $\mu W\ m^{-2}\ nm^{-1} count^{-1}$).

3.2.3 Linearity of response of CS23 and CS21

This test was done with the same set-up as for measuring the absolute response, apart from using a car lamp with a constant power supply instead of the 1000 W lamp. Measurements were made with the sensors at two or three distances between 1 and 2 metres. The reading at 1 m was set to 1, and all other readings were normalised to this. The inverse square law was used to calculate the theoretical change in irradiance, and this was compared with change in measured signal.

3.2.4 Cosine response of CS23

The instrument response of a cosine collector should follow a cosine function when it is rotated from the normal (0°) to a 90° angle. The cosine response of CS23 was measured in air using the same equipment as used for the test of linearity. The colour sensor was set to measure every 10 sec and mounted on a rotating plate facing the light bulb. The plate was turned in increments of 10° from 0° to 90°. At each 10° step the sensor logged for approximately 1 minute. Stray light measurements were taken after each step, blocking out the direct light from the colour sensor with an opaque plate. Average

readings at each step were corrected for average stray light. All readings were normalised to 1 at an angle of 0°.

3.2.5 Immersion effect

When a diffuser is immersed in water, its light transmission is less than in air (Mueller and Austin, 1995). Two separate processes lead to this immersion effect: first the change of reflection of light at the upper surface of the collector, and second internal scattering and reflections from the collector's lower surface. A small part of the light flux falling on the collector is reflected at the air-plastic or water-plastic interface. The majority of the flux passes into the collector body. The reflectance depends on the relative difference in refractive indices between the diffuser material and the surrounding material. Since the instrument's irradiance response is calibrated in air, a correction for the immersion in water should be applied.

The immersion effect was measured using CS23 on board RV Cirolana just after the arrival back in Lowestoft, 1 May 1997 (end of Cirolana cruise 4/97). The apparatus consisted of an elongated tank, and a light source which was situated behind a window at one end of the tank. The light source was a tungsten bulb, and a neutral density filter was placed in front of the window inside the tank to keep the colour sensor from saturating. The colour sensor was placed horizontally facing the light source, about 0.5 cm away from the window. It was set to log every 10 min. The response was measured for two minutes in air. Then the tank was filled with water, and the colour sensor submersed completely, and the response was measured again for 2 min. The colour sensor had to be held down and kept in place, because it was slightly buoyant. Dark readings were taken, and corrected for. Then the mean colour ratios (blue:green, cyan:green, red: green) were calculated for both the measurements in air, and in water. The ratio of the colour ratios in air to the colour ratios in water was calculated.

3.2.5 Temperature effects

On 20 August 1996, a temperature experiment was performed on CS23 to check if there was any temperature effect on the colour ratios. This day was chosen because there was absolutely clear skies, and the downwelling irradiance could be assumed to be relatively constant over short periods of time. The light is most constant around noon, but a test the day before had shown that the colour sensor saturated in the red and green channel at noon, even when set to log only for 1 second. The measurements were therefore performed early in the morning between 7:45 and 8:15 am. The colour sensor was set

up on the lawn at Rhyddgaer Bach in Dwyran, Anglesey, well away from any shading. It was set to log every second and was placed in a black refuse bin facing the sun. The refuse bin was filled with tap water, and the colour sensor was submersed by about 10 cm. The temperature was measured to be 17.4 °C. The colour sensor was left to equilibrate for 5 minutes, and then the colour sensor readings were registered for 2 min. After this, the water was cooled down to 12.3 °C, using ice cubes. The water was stirred and the water level was kept the same. Colour sensor readings were registered for 2 min, again. I had intended to cool down the water even more, because I wanted to have a similar temperature range to that in the Menai Strait over the year (from about 5 to 15 °C). However, I ran out of ice cubes. I decided then to heat the water up to 14.5 °C, using boiling water. The measurements were repeated in the same way at each temperature step. Dark readings were taken before and after each step, and corrected for. The mean and standard deviation of the temperature was calculated for each step.

3.3 Results

3.3.1 Relative spectral response and absolute calibration of CS23

The leakage in the red that was observed for the cyan channel during the previous calibration in Southampton was neither found in CS21 nor in CS23.

Figure 3.1 shows the relative spectral response of the four channels of CS23.

Table 3.2 shows the FWHM and the measured centre wavebands of each channel, as well as the results of the absolute calibration (spectral irradiance per count, unit:Wm^{-2} nm^{-1}). The FWHM was 10 nm +/- 2 nm as specified by the SeaWiFS protocols.

3.3.2 Linearity of response

For both CS21, and CS23 the measured relative brightness was within 5% of the expected relative brightness. Figure 3.2 shows the results of the test of linearity for CS21 as an example.

3.3.3 Cosine response

Figure 3.3 shows the normalised sensor response at a given angle as a proportion of the nominal cosine response (i.e. the cosine of that angle).

3.3.4 Immersion effect

The results for the immersion effect measurements are listed in the following table:

	red:green	cyan:green	blue:green
measurement in air	1.45	0.24	0.06
measurement in water	1.57	0.20	0.04
ratios in water/ratios in air	1.08	0.82	0.8

Table 3.3 Results of the immersion effect measurements

3.3.5 Temperature effect

The results of the temperature experiments using CS23 are listed below. No significant temperature effect was observed on the colour ratios within the temperature range between 12.3 and 17.4 °C.

	red:green	cyan:green	blue:green
measurement at 12.3 °C	1.45	0.50	0.22
measurement at 14.5 °C	1.45	0.50	0.22
measurement at 17.4 °C	1.43	0.50	0.23

Table 3.4 Results of the temperature measurements

3.4 Discussion

The relative response of each colour sensor channel depends on the filter transmission and the photo-diode efficiency at each channel. Overall, the red channel is most sensitive, followed by green (61% of red in the case of CS23), cyan (26%), and blue (only 12%). This calibration confirmed linearity of response over a range of irradiances, and can be used, in the case of CS23, to quantify absolute upwelling or downwelling irradiances in each channel (Bowers *et al.,* 2000).

The sensor's relative response when rotated in air is within 90% of an ideal cosine response up to an angle of 40°, within 80% up to 70°, and within 75% between 80° and 90° from the direction of a point source. The cosine response differed slightly between the different channels, which may have depended on the orientation of the instrument. The response did not quite match SeaWiFS requirements (which specify at least 90% of cosine between 65° and 90°), but the sensors were not built primarily for SeaWiFS validation. However, the cosine response is very important when deploying an instrument with the diffuser looking downwards. If the sensor is deployed looking downwards most of the light will come from the sides, in the region of near-grazing angles (Mueller and Austin, 1995). The main problem with this deployment mode is the ring around the diffuser plate (Figure 2.1) which casts a shadow onto the diffuser. Whilst measuring the cosine response it was evident how the shade of the ring increased with increasing angle away from the light source. The different channels of the sensor may have been affected differently by this shading effect depending on the situation of each channel in relation to the shade. In future versions of the colour sensor, the cosine response could be improved by changing the design of the housing either by flattening the sensor head with the protective ring, so that the window does not get shaded by the ring when most of the light comes from the side; or by mounting a slightly convex diffuser plate. In the calibration laboratory at PML the standard procedure is to calibrate the cosine response in air. The cosine response should, however, have been measured under water, as the sensor is used underwater. Ru Morrison had attempted to measure the cosine response of CS2 with an underwater torch, but without access to proper calibration facilities. His results suggested an improvement in the cosine response between 80° and 90°, though this does not seem very likely because of the problems related to the ring around the diffuser.

The Temperature induced variations include the changes of dark readings, as well as scale responsitivity changes. According to the SeaWiFS protocols, each underwater

instrument should be individually characterised over the range of -2 to 40 ° C. For deck cells this range should be extended to -10 to 45 ° C. The temperature experiment should be repeated using a greater range in temperature. The dark readings of the instruments used in this PhD were very consistent even when comparing dark readings taken during cruises performed in different years, for example when comparing the dark readings measured during the Cirolana cruises in July 1996 and July 1997. In order to comply with the SeaWiFS protocols each sensor would have had to have been characterised individually, and temperature effects would have had to have been investigated in a wider range. The colour sensor calibration was performed at room temperature, but was mostly used in waters colder than that. However, the temperature effects seem small, at least over the range tested (see Figure 3.4).

Most instruments for ground truthing of satellite imagery (e.g. TSRB from Satlantic, or PRR 800 from Biospherical) measure upwelling radiance, and downwelling irradiance for deriving remote sensing reflectance. In order to make the instrument applicable and comparable to these applications it would have to be redesigned completely. The field has advanced so much since the development of the colour sensor, and there are much better instruments available on the market to suit the purpose of ground truthing for SeaWiFS. Nevertheless, the colour sensors have proved robust and reliable for their intended purpose of in-water measurements and time-series (see Chapters 5 and 6).

Given further use of this sort, the design of the colour sensors could be further improved. Self-shading would be reduced if the diameter of the instrument was less. It would help calibration if all instruments were fitted with an external RS232 connection, so that any sensor can be aimed accurately at a monochromator whilst connected to a computer. It would be good if it was possible for the user to change the internal clock of the instrument, without having to visit SOS.

In order to use the instrument properly it should be supplied with a very detailed user manual with all specifications: appendix 1 offers a first step towards this. Finally, all instruments should be calibrated regularly. This requires access to a good calibration bench (similar to the one in Plymouth) with customised holders for the diameter of the colour sensor.

colour sensor		CS2/3		CS4	
assigned colour	nominal centre wavelength [nm]	centre wavelength [nm]	FWHM [nm]	centre wavelength [nm]	FWHM [nm]
blue	440	440.7	6.9	440.7	6.9
cyan	490	489.5	7.5	489.3	7.5
green	570	571.1	10.4	570.9	10.3
red	670	670.5	11.7	669.5	11.5

Table 3.1 Filter specifications CS2/3, and CS4 series as provided by the supplier (September 1993).

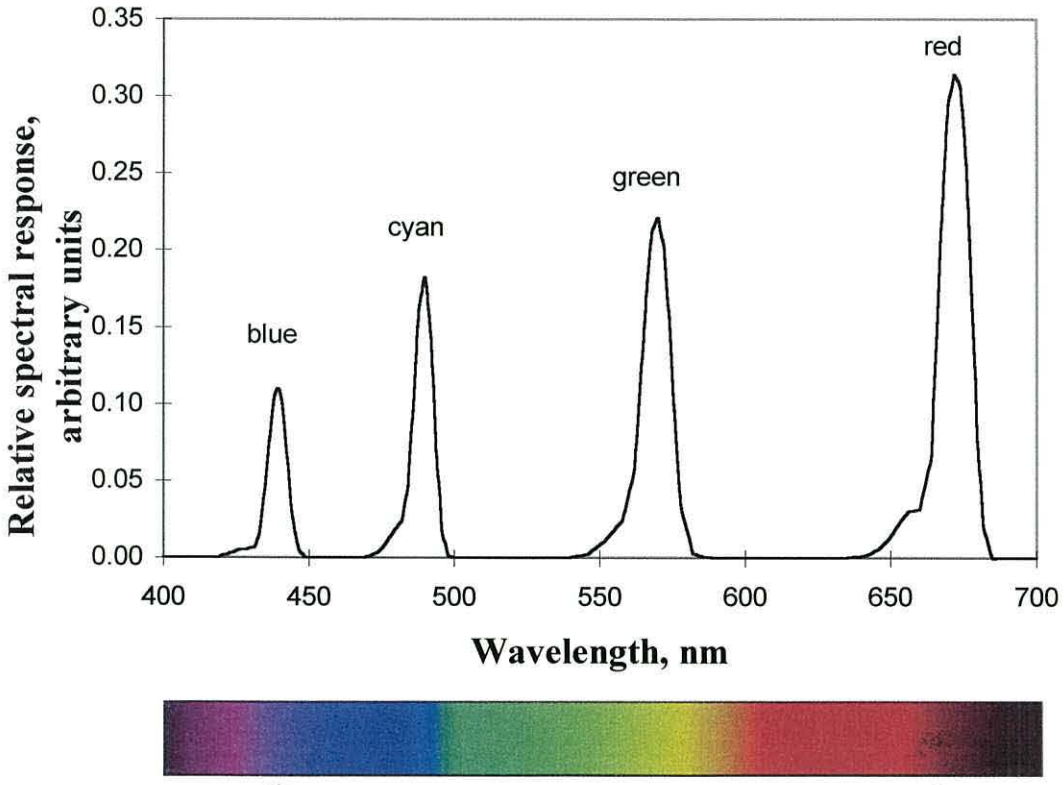

Figure 3.1 Spectral response of CS23: monochromator measurements

Colour sensor	channel	centre wavelength	FWHM	irradiance per count
CS23	colour	[nm]	[nm]	[W / nm*m2]
	blue	439.6	8.9	0.00149
	cyan	490.1	9.3	0.00070
	green	569.3	11.0	0.00030
	red	668.1	11.7	0.00018

Table 3.2 Absolute calibration of CS23

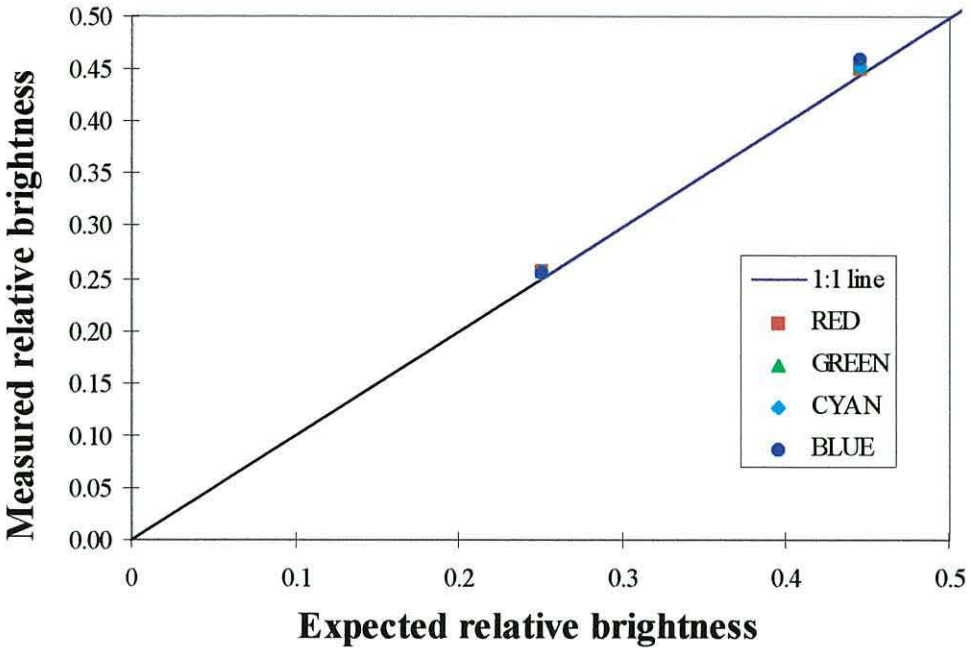

Fig. 3.2 Test of linearity for CS21. The brightness at 1 m was set to one. The expected relative brightness at each distance was calculated by the inverse-square law.

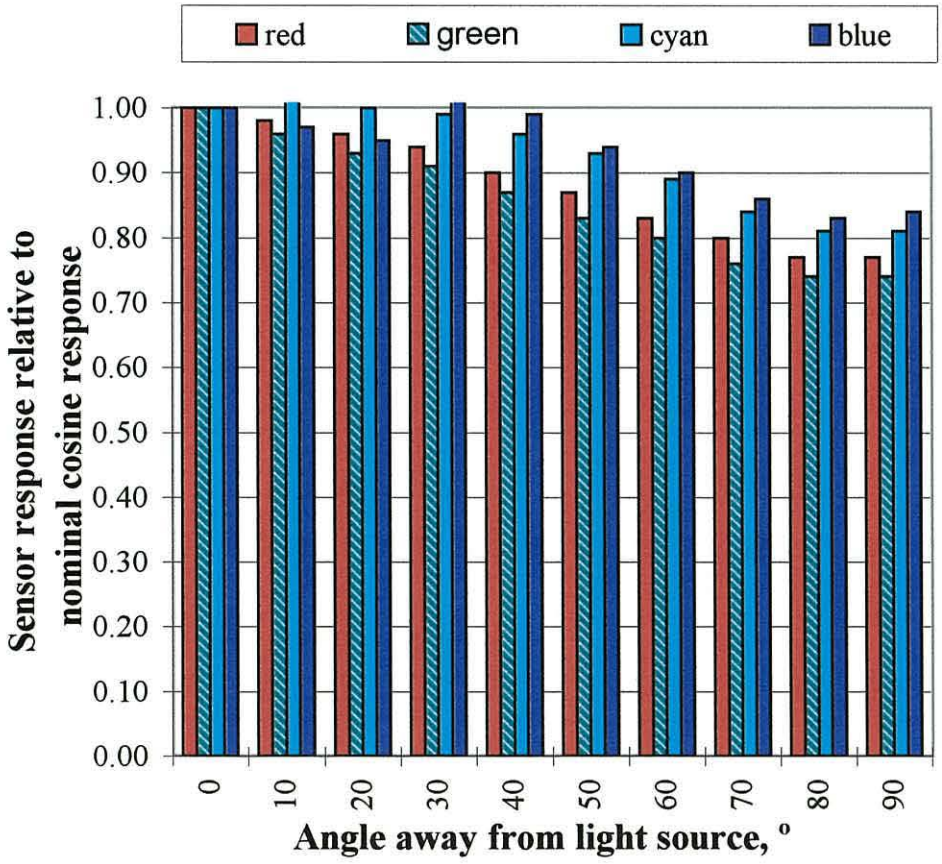

Fig. 3.3 Cosine response, CS23, 20 sec logging

Chapter 4 - Colour ratios in Case-1 and Case-2 waters

Abstract

A four-channel colour sensor was used to estimate chlorophyll concentrations from colour ratios. A relationship was sought between the logarithm of colour ratios and the logarithm of pigment concentrations. Unlike Gordon and Morel (1983) who took the surface reflectance ratios, the ratio of upwelling irradiance was used. Using upwelling irradiances in the cyan (490 nm) and green (570 nm), a good correlation was found between spectrophotometrically determined chlorophyll a concentrations and the cyan:green ratio over a wide range of concentrations in optical Case-1 waters where phytoplankton play a key role in the absorption of light. The main absorbing pigments in the cyan waveband, however, are not chlorophyll a but the carotenoid pigments. Carotenoid concentration, as measured by spectrophotometry, is highly correlated to the concentration of chlorophyll a, as well as to the cyan to green ratio. In Case-2 waters, however, the algal pigment signal may be overwhelmed by the signal due to high concentrations of CDOM and/or SPM.

4.1 Introduction

Optical measurements from *in situ* profiling radiometers, moorings, aircraft and satellites provide information about phytoplankton distribution at a temporal and spatial resolution that is not possible with traditional techniques in biological oceanography. Satellite measurements of water-leaving radiance have been widely used to map concentrations of phytoplankton pigments. Gordon and Morel (1983) used the blue-green (440: 560 nm) reflectance ratio to derive chlorophyll concentration from CZCS (Coastal Zone Colour Scanner) data. The ratio of reflection coefficients in the green and in the blue part of the spectrum was related to the pigment concentration on a log-log plot. This worked very well for Case-1 waters (mostly oceanic waters) where there is little absorbance from other OICs but phytoplankton. Using a 6-channel profiling radiometer Mitchelson *et al.* (1986) showed that in Case-2 waters, the blue-green reflectance ratio was less sensitive to changes in chlorophyll a concentration than in the open sea. Brown and Simpson (1990) showed empirically that the slope of the log of chlorophyll a concentration against the log of the blue-green ratio (440:550 nm) changed in proportion to the concentration of inorganic sediments. Later, Tett *et al.* (2000) estimated the phytoplankton chlorophyll concentration from the ratio of the blue to green (440: 524 nm) from submarine irradiance using a 2-channel instrument. It was compared with two recording Chelsea Instruments Aquatracka I fluorometers and proved to be as reliable as the *in vivo* fluorometers for the estimation of chlorophyll a concentration. In 1991, studies were begun with 4-channel versions of this colour sensor. The aim was to develop simple (hence cheap) and robust instruments for use at

moorings and thus complement remotely sensed observations. The instruments were described in detail in Chapter 2, section 2.1 and Chapter 3.

4.2 Materials and methods

The instruments were deployed in a wide range of different water types: in the subtropical Atlantic Ocean South West of Gran Canaria, where CS3 was deployed on a drifting buoy (Wild-Allen, 1997); in Loch Striven (W. Scotland) CS2 and CS3 were deployed on a mooring during a phytoplankton spring bloom in April 1994; and during the Summers of 1993 and 1994 in the Menai Strait, North Wales. The sensors were deployed looking downwards in order to measure the ratios of upwelling irradiance. Several, notionally identical, versions of CS4 were used from the RRS Charles Darwin in the Malin Shelf (Outer Hebrides, Scotland) in May 1995, and from RV Cirolana (MAFF) in the Irish Sea and the North Sea (May and July 1996), deployed on a floating frame, looking downwards. In summer 1995 one of the CS4 sensors was used from the pier in Menai Bridge and CS3 was deployed between March and November 1996 on a floating raft in the Menai Strait (see Chapter 5). Because of the lack of adequate optical calibration facilities at the School of Ocean Sciences, the colour sensors were not calibrated until much later in January 1997 (see Chapter 3). Therefore, the primary function of the instruments was to provide colour ratios from which to estimate changes in pigment concentrations. A relationship between the logarithm of the colour ratios and the logarithm of pigment concentrations was sought (Bowers *et al.* 2000). Unlike Gordon and Morel (1983), who took the surface reflectance ratios, the ratio of upwelling irradiance was used, measured at depths between 0.2 and 2 m, depending on the platform used to support the instruments. Data from 5 different sensors is reported here. Despite differences in their absolute sensitivity, all were constructed to have the same relative response when the output from one channel was compared with another.

Because continuous time-series show a systematic daily change in colour ratios around dusk and dawn (Abbott *et al.* 1995; Tett *et. al.* 2000), only colour ratios within 2 hours of local noon were used for this investigation. At corresponding times, water samples were taken for measurement of chlorophyll a and total carotenoid concentrations by spectrophotometry, as well as by HPLC (see Chapter 2).

4.3 Results

Because the instruments were used across a wide range of pigment and SPM concentrations, the readings in the blue channel were sometimes too low for the satisfactory calculation of colour ratios. The blue channel was not sensitive enough for these waters, and the readings were too close to the noise signal. A good correlation, however, was found between spectrophotometrically determined chlorophyll a concentrations and the ratio of upwelling irradiances in the cyan (490 nm) and green (570 nm) wavebands over a wide range of concentrations in optical Case-1 waters (see Fig. 4.1), where phytoplankton play a key role in the absorption of light.

The regression equation (for Case-1 data) was:

$$\log(490{:}570) = -0.13(\pm 0.04) - 0.51(\pm 0.05)\ \log [\text{chl}]\ r^2 = 0.94;\ df = 8,$$

where df stands for degree of freedom, r^2 is the coefficient of determination (the proportion of variance in the dependent variable explained by a regression), and p the probability (of there being a correlation by mere chance)

The main absorbing pigments in the cyan waveband, however, are not chlorophyll a but the carotenoid pigments. These, as measured by spectrophotometry, also showed a good correlation to the cyan:green ratio (Figure 4.2). The regression equation (for Case-1 data) was:

$$\log(490{:}570) = -0.23(\pm 0.05) - 0.63(\pm 0.07)\ \log [\text{carot}]\ r^2 = 0.92;\ df = 8,$$

where [carot] stands for total carotenoid concentration as measured by spectrophotometry.

Fig. 4.3 shows that there was a strong correlation between chlorophyll a and carotenoid concentrations.

A whole range of carotenoid pigments absorb at 480 and 510 nm. However, the carotenoid pigments measured by the spectrophotometric method showed a good correlation with the correspondent samples measured by HPLC. The spectrophotometric method underestimated the carotenoid concentration slightly, but the slope of the line was not significantly different from 1.

The regression equation was:

$$[\text{carotenoid}]_{\text{spec}} = -0.06(\pm 0.08) + 0.99(\pm 0.05)\ [\text{carotenoid}]_{\text{HPLC}}$$

There was also a good correlation between the chlorophyll a concentration measured by HPLC and the chlorophyll a measured by the standard fluorometric method:

$$r^2 = 0.88, \quad df = 25 \qquad \text{(data SES cruise, May 1995).}$$

In respect of the optical Case-2 waters of the Menai Strait, the Irish Sea, and the North Sea the correlation between colour ratio and either chlorophyll or carotenoid was not significant (Figure 4.1 and 4.2; all points sampled in Case-2 waters are marked as +).

The correlation coefficient in Figure 4.1 for chlorophyll a was

$$r = -0.18, \qquad p = 0.26; \; df = 39,$$

where r is the (Pearson product-moment) correlation coefficient, and p stands for the probability of obtaining the observed result by chance, given a null hypothesis of no relationship.

For total carotenoid concentration in Fig. 4.2 the correlation coefficient was

$$r = -0.093; \qquad p = 0.051; \; df = 24.$$

4.4 Discussion

Much current bio-optical work (Gordon 1995; Doerffer and Fisher 1994) is aimed at providing algorithms, or models for remote sensing of ocean colour by the SeaWiFS and similar sensors, once these are operational. Another body of work focuses on the absorption spectra of suspended sediment retained on a filter (Bricaud *et al.* 1995; Cleveland, 1995), with aims which include the decomposition of fully resolved spectra into components due to each particulate fraction. The aim of the work presented here is intermediate between these approaches. The School of Ocean Sciences have made efficient and relatively simple colour sensors for deployment at moorings and on drifters in order to provide time series with the daily resolution that is unlikely to be obtained by satellites in regions subject to frequent cloud cover.

As with remotely sensed ocean colour, the interpretation of *in situ* optical data poses many difficulties, although these do not include atmospheric effects. The work reported here is part of a, mainly, empirical study with the objective of a universal calibration of our colour sensors. Such a calibration should apply across a range of pigment concentrations and in waters with high and fluctuating concentrations of suspended non-phytoplankton particles, as well as in optical Case-1 waters.

The first step in this work reported here was to consider the power of simple ratios of two reflected colours to explain variation in 'chlorophyll-like' pigments over a range of

conditions in Case-1 waters. Observations were made over the widest range of concentrations likely to exist outside of a Red Tide, from oligotrophic sub-tropical waters to a eutrophic fjord during the spring bloom. Because high concentrations of chlorophyll attenuate blue light strongly, the cyan:green ratio was found a better single index than blue:green, in that it could be used over the whole of this range. Clark (1981) also proposed an algorithm switch from blue:green to cyan:green in remote sensing applications at higher chlorophyll concentrations.

This chapter has largely been concerned with explaining the observed correlation between chlorophyll concentration and cyan:green ratio, when the latter should not be directly sensitive to chlorophyll a concentrations. The pigments absorbing in the blue to green part of the spectrum are part of light harvesting complex II (LHC II). This contains chlorophyll a, together with an accessory chlorophyll b or c, and in addition the major light-harvesting xanthophyll carotenoid(s) characteristic of the algal class (see Chapter 1). Its main absorption is that of the chlorophyll Soret band. The absorption in the cyan waveband, however is not caused by chlorophyll a, but by a mixture of carotenoid pigments (Johnson *et al.* 1994). Chlorophyll b also absorbs in this waveband but can be ignored when dealing with phytoplankton communities dominated by diatoms and dinoflagellates (which do not contain chlorophyll b).

The results show that the spectrophotometric method for deriving carotenoid concentration is in good agreement with the HPLC method, but underestimates the concentration slightly. Fig. 4.1 and 4.2 show the difficulties of developing a calibration of colour ratios for Case-2 waters, where the pigment signal may be overwhelmed by that due to CDOM and SPM. It is not enough to use simple colour ratios to predict chlorophyll a in Case-2 waters. This conclusion led to a re-definition of the aims and objectives of this thesis (see Chapter 1, section 1.6 - Aims and Objectives). The use of the colour sensor in Case-2 waters for estimating OICs may be possible by combining colour sensor measurements with optical models (see Chapter 5 and 7).

Another conclusion was that the colour sensor was not sensitive enough in the blue channel. A way to deal with this problem was to make the instrument log for longer when measuring in highly turbid waters. This, however, slows down the speed of the measurements, and makes the instrument less useful for profiling.

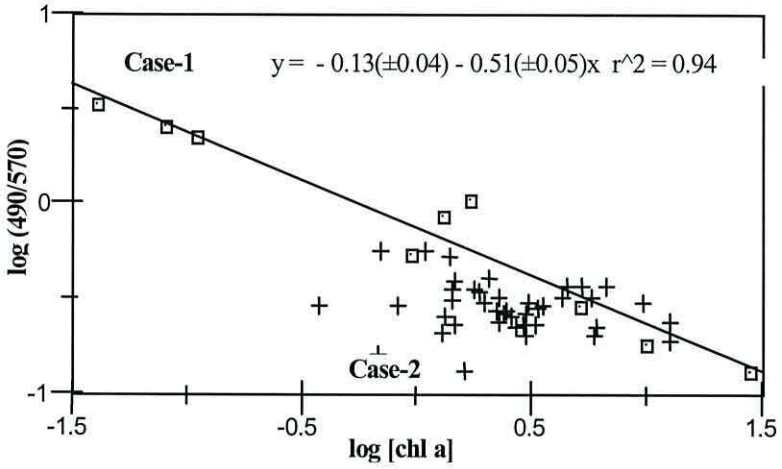

Fig. 4.1 For Case-1 (□) waters (Canary Islands, Outer Hebrides, spring bloom in Loch Striven), there is a good correlation between the logarithm of the cyan:green ratio and the logarithm of the chlorophyll concentration. For Case-2 (+) waters (Menai Straits, Irish Sea, North Sea), there was no significant correlation.

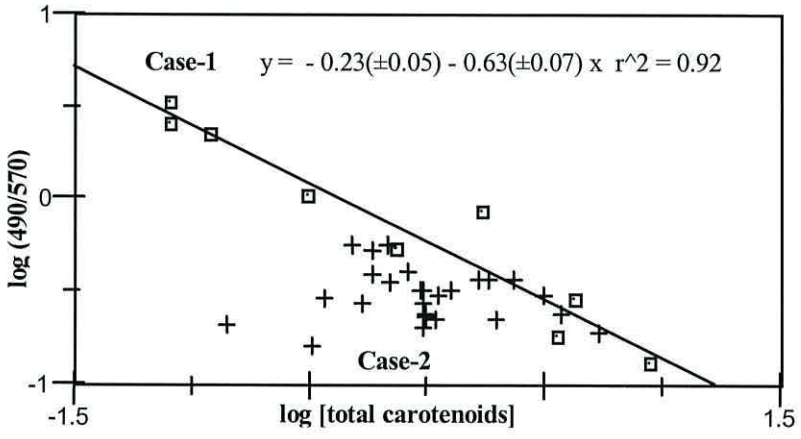

Fig. 4.2 Case-1 waters (□) show a similar correlation between the logarithm of the cyan:green ratio and the logarithm of the carotenoid concentration for the same sites as in Fig 4.1

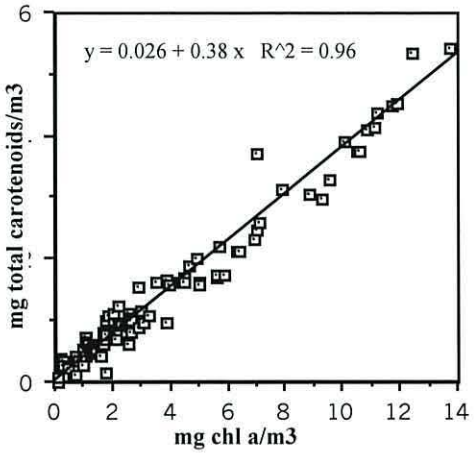

Fig 4.3 There was a good correlation between the chlorophyll and carotenoid concentration measured by the trichromatic method (data from Canary Islands, Loch Striven, Outer Hebrides, Menai Strait, Irish Sea, and North Sea)

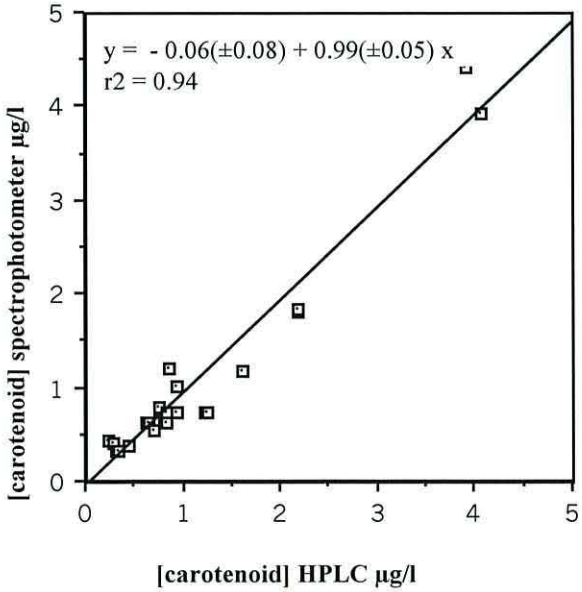

Fig. 4.4 A regression of carotenoid concentration as measured by the spectrophotometric method, using the absorbance at 480 and 510 nm, on total carotenoid concentration measured by HPLC. Data from SES cruise, May 1995.

Chapter 5 - Bio-optical properties of the Menai Strait

Abstract

A time series was conducted in the Menai Strait from March to December 1996 combining optical measurements by a colour sensor with measurements of optically-active in-water constituents (OICs). In order to improve estimations of pigment concentration in Case-2 waters, a semi-empirical optical model was used to synthesise the spectrum of water-leaving radiance from the absorption properties of pure sea water, CDOM, SPM, and phytoplankton. The original model was tested and improved by using a different set of parameters. Multiple regression analysis (MRA) was used to empirically relate colour ratios to pigments and SPM.

5.1 Introduction

Submarine optical instruments can directly monitor changes in OICs as well as provide sea-truth for remote sensing. For biologists, the most important such OICs are phytoplankton photosynthetic pigments, especially chlorophyll a, which indicate both the abundance of phytoplankton and the potential for primary production. Sea-truth in respect of these pigments may involve: water-leaving radiance (Gordon and Morel 1983); measurements of submarine optical properties, such as diffuse attenuation (Smith *et al.* 1991) or stimulated fluorescence (Fasham *et al.* 1983), which are proportional to pigment concentrations; or chemical-optical measurement of pigments extracted from water samples (Jeffrey *et al.* 1997).

Because of the relatively fast rate at which pigment concentrations can change (typically in the order of order 10 % per day, i.e. 0.1 d^{-1}) and the infrequency with which research ships can visit particular locations, both sea-truth for remote sensing and *in situ* pigment concentration monitoring need at least semi-continuous recording.

In situ recording fluorometers have been used for recording time series of phytoplankton biomass and have confirmed substantial variations on time-scales of days (Mills and Tett 1990; Whitledge and Wirrick 1986). The instruments can be made specific to chlorophyll-type pigments and can distinguish low concentrations of chlorophyll in the presence of large amounts of other optically active components. There are, however, disadvantages to their use as self-recording instruments. Firstly, they must be re-calibrated on each deployment as the relationship of chlorophyll and fluorescence is

highly variable. Diel cycles of fluorescence yield also have to be taken into account (Abbott *et al.* 1982; Setser *et al.* 1982; Pingree and Harris 1988; Prezelin and Sweeney 1977). Secondly, fluorometers view only a relatively small volume of water. Thirdly, they need a lot of power for both a strong light source for stimulating fluorescence and a sensitive detector of emitted fluorescence. Passive radiometers view larger volumes of water than fluorometers, are easier to construct and deploy, and record for a longer period of time (Booth and Smith 1988). Although high-specification instruments (Mueller and Austin 1995) have recently become available commercially there is also a need for relatively simple, inexpensive and robust instruments for deployment at moorings.

The colour sensor described in the previous chapters was built with these criteria in mind. For Case-1 waters, a good correlation was found between the logarithm of the ratio of the upwelling irradiances at 490 nm (cyan) to 570 nm (green) and the logarithm of the chlorophyll a concentration (Kratzer *et al.* 1997 and Chapter 4). In order to investigate the use of the colour sensor in Case-2 waters, the instrument was deployed on a raft in the Menai Strait, North Wales, from March to December 1996 (Figures 5.1a and 5.2).

The water flowing through the Menai Strait usually carries a heavy load of suspended material (Buchan *et al.* 1967), and is strongly Case-2. There is a diel as well as a lunar variation in the concentration of suspended particles which shows highest loads of SPM at spring tides. The water derives mainly from North Wales coastal water, although it may also occasionally include a proportion of temporary incursions of waters from the more central parts of the Irish Sea.

The phytoplankton in the Menai Straits tends to follow a pattern. It starts off with a two-peaked spring bloom (Blight *et al.* 1995). The start of the spring bloom varies from year to year, but usually occurs around April/May. It may be delayed by the persistence of high turbidity in the water. The first part of the bloom tends to consist of a mixture of diatoms, often dominated by *Rhizosolenia* species (Jones and Spencer 1970). The second peak tends to be a mixture of various diatoms, and colonies of *Phaeocystis*. The numbers of ciliates and dinoflagellates increase just after the end of the diatom/*Phaeocystis* bloom (Blight *et al.* 1995), but after the spring bloom the phytoplankton biomass remains low. During the summer the phytoplankton is dominated by small flagellates. El Hag and Fogg (1986) observed a peak of coccoid

cyanobacteria in late July / early August. In autumn, individual diatom species tend to show a second burst of growth (Jones and Spencer 1970).

This Chapter reports a time-series of colour ratios and OICs in the Menai Strait during 1996. The ratios use the Colour sensor's green channel, providing three independent records of colour (red:green, cyan:green, blue:green). The first aim of this chapter is to examine relationships amongst the OICs, and between them and the three colour ratios. In addition, an optical model is used (Harker 1997) in the Menai Strait to synthesise the spectrum of water-leaving radiance from the *in situ* measurements of concentrations of chlorophyll a, CDOM and SPM. The second aim of this work is to test the model on an independent dataset, and to improve the model parameters, as well as to explore the extent to which the data can be inverted and used to predict in-water concentrations. Successful inversion would also be encouraging for remote sensing of the optical components in coastal waters.

5.2 Methods

5.2.1 Colour sensor deployment and sampling

Between March and December 1996 CS22 and CS3 were deployed continuously on a moored (but otherwise free-floating) raft (Figure 5.1a) in the Menai Strait near the School of Ocean Science in Menai Bridge (see Figure 5.2). CS4 was used from 1st March to 1st April 1997, and was set to sample every 20 minutes, CS3 was deployed from 1st April to 3rd December 1997, and was set to sample every 10 minutes (for 20 sec). The instruments were mounted vertically on a purpose-built frame with the window facing downwards in order to measure upwelling irradiance. The sensor head was fixed at a constant depth of 0.5 m in relation to the surface level. The frame was built from scaffolding pipes to resist tidal flows and provide protection from boats visiting the raft. A 25 cm self-recording beam attenuation transmissometer (UWB, Figure 5.1b) with a red (660 nm) LED (light emitting diode) was mounted horizontally on the same frame.

Once a month, data were downloaded, the instruments were cleaned of fouling, and the batteries were changed. For the colour sensor data values recorded in air, during this monthly maintenance, were removed from the record. Compared with mid-day counts of several thousand, night-time values were less than ten in all channels, hence the "dark current" reading of the instrument was taken to be zero (personal communication with Dave Bowers).

Water samples for measurements of OICs were taken at noon, initially every 2 weeks, 2-3 days before maximum spring tide, although it should be noted that the amplitude of these tides changed during the year. The aim was to obtain a consistent series of samples from the water that enters the Menai Strait on the flood tide from North Wales coastal waters. In late autumn, the sampling interval was reduced to 1 week in order to collect additional data 2-3 days before minimum neap tide. In August, samples were taken at an interval of 2 days over a spring-neap cycle. As the water column in the Menai Strait is always well mixed it was enough to take samples just below the surface (Harker 1997).

Water temperature was measured with a digital thermometer with a precision of 0.1 °C. For salinity measurements, samples were taken every 2 weeks in 200 ml medical bottles and stored to be processed in the CEFAS laboratory (Lowestoft, UK) using a Guildline Autosal 8400b laboratory salinometer. The tidal range was measured at each sampling day, but was taken from the tidal time table for the Menai Strait (Sherwin 1996) for a continuous time series.

SPM, CDOM, chlorophyll a, total carotenoids were measured as described in Chapter 2, section 2.3.1, section 2.3.2, section 2.3.3 and section 2.3.5. Phytoplankton was analysed as described in section 2.3.5. Because of the need of distinguishing between organic and inorganic SPM in the Menai Strait the terms mineral suspended solids (MSS) and organic suspended solids (OSS) are used. To be consistent with this terminology, the term total suspended solids (TSS) will be used in this chapter in place of SPM.

In order to avoid bias due to fouling, water samples for measuring the in-water constituents were taken after downloading and cleaning of the instruments.

5.2.2 The semi-empirical model

The model of the colour of shelf seas of Harker (1997) computed ratios of sea-surface reflectance coefficients at two wavelengths. This model was modified to predict upwelling reflectance ratios measured by a colour sensor at a depth z below the sea surface:

colour ratio $[1,2] = ((b_b[1]/a[1])/(b_b[2]/a[2]))\ \exp(-z.(a[1]-a[2])/\mu)\ f[1,2]$ (equation 5.1)

where μ is the mean cosine of the angles that downwards photons make with the vertical. Initially μ=0.7 was used according to Bowers and Mitchelson-Jacob (1996). [1] and [2] refer to wavelengths. The factor f corrects for differences in the sensitivity of each channel of the pair, as found during the instrument calibration operation described in section Chapter 3. In the case of the Menai Strait data, z was 0.5 m.

The model assumes that each reflection coefficient is proportional to the ratio of backscattering b_b to absorption a at that wavelength (Kirk 1994). Backscattering is assumed to be wavelength-independent and thus the ratio of reflection coefficients at any pair of wavelengths is mainly dependent on the absorption coefficients at the same two wavelengths. The model calculates absorption as the sum of absorption by water, phytoplankton pigments, mineral suspended solids (MSS), and CDOM. At a given wavelength,

$$a = a_w + a^*_{ph}\,[\text{chl a}] + a^*_{MSS}\,[\text{MSS}] + a^*_{CDOM}\,g_{440} \qquad (m^{-1}) \quad \text{(equation 5.2)}$$

where a_w (m^{-1}) is the absorption by sea water, a^*_{ph} and a^*_{MSS} are specific absorption coefficients of, respectively, phytoplankton pigments (m^2 (mg chl a)$^{-1}$) and mineral suspended solids (m^2 (g dry weight)$^{-1}$), and a^*_{CDOM} is a dimensionless specific absorption coefficient for CDOM.

Scattering is assumed to depend only on concentrations of MSS:

$$b = b^*_{MSS}\,[\text{MSS}] \qquad (m^{-1}) \qquad \text{(equation 5.3)}$$

where, according to Harker (1997), b^*_{MSS} is 0.26 (blue), 0.24 (cyan), 0.28 (green), 0.25 (red). The ratio of backscattering to total scattering is assumed to be wavelength independent, so that the b_b terms disappear from equation 5.1. Figure 6.7 in Chapter 6 shows a schematic illustration of the model.

Using the model to predict colour ratios for comparison with those observed by the colour sensor required values of the wavelength-dependent parameters for the central wavelengths of the colour sensor channels. Initially, values were obtained from the literature: sea water absorption from Morel and Prieur (1977); a^*_{ph} from Gallegos *et al.* (1990); and a^*_{MSS} from an exponential curve fitted by Bowers *et al.* (1997) to observed spectra of combusted filters. The function $e^{-0.014(\lambda-440)}$, where λ is wavelength, was used for a^*_{CDOM} values (Kirk 1994).

In a new version of the model, some of these parameters were changed as described in section 5.3.4. The parameters of the model were derived empirically, but the structure of the model is partly theoretical, partly empirical. The model may therefore be described as semi-empirical.

5.3 Results

5.3.1 Deployment problems

Mussels and *Laminaria* growing on the raft itself changed in amount and colour during the year. In order to keep the reflectance of the raft constant, the fouling was cleared regularly. In the strong currents of the Menai Strait, drifting seaweed was sometimes caught by the frame and the optical instruments themselves and contributed to the shading of the instruments. Especially during the summer months, the colour sensor window began to develop a brown algal film (possibly diatoms) after 2 weeks. It was cleaned as often as possible, and at least every 2 weeks. Trapped seaweed fronds were removed at the same time. Fortunately, barnacles seemed to prefer the dark surface of the colour sensor housing, and therefore were not a problem on the light irradiance window. The transmissometer was more affected by fouling (Figure 5.1b), with the barnacles settling on the detector window.

The transmissometer data was analysed, but did not give any satisfactory results, as the effects of fouling were too strong on the signal (personal communication with Dave Bowers 1997).

5.3.2 Optically-active in-water constituents (OICs)

Figure 5.3 shows the time series of salinity and temperature. The temperature showed a typical variation for temperate waters, rising from about 5°C in spring to about 17°C in mid-summer. The water temperature started to decline as the air temperature decreased in autumn. The salinity curve showed a small increase over the summer, with lowest readings in early spring and late autumn.

The chlorophyll a concentrations (Figure 5.4) showed a typical pattern for the Menai Strait with a first spring peak in mid April 1996 (identified microscopically as a *Rhizosolenia* bloom), and higher a second peak (up to about 13 $\mu g\ l^{-1}$) in mid May, which was a combination of a *Phaeocystis* and a diatom bloom. After the spring bloom, the chlorophyll concentrations dropped sharply around day 180 (the end of June) and then varied between 2 and 4 $\mu g\ l^{-1}$ between mid July and late September. The

phytoplankton over the summer was a mixed community of diatoms, flagellates and dinoflagellates. In autumn, the community was dominated by diatoms, with *Phaeocystis* reappearing at the end of September. In the beginning of October, the chlorophyll concentration reached another minor peak of about 6µg l^{-1}, which was due to a rise of diatoms.

Total carotenoids followed a pattern similar to that of chlorophyll, though at lower concentrations. Phaeopigment concentrations were low (in relation to chlorophyll) in spring and summer with an increase in total amount, and in the ratio to chlorophyll, in autumn.

Figure 5.5 shows the change in OSS and MSS concentrations during the course of the year 1996, as well as the change in tidal height (tidal range) during each sampling occasion. The concentration of MSS was on average about three times the concentration of OSS; only on a few occasions did the organics make up more than half of the TSS (e.g. during the spring bloom). On these occasions chlorophyll a was measured at more than 4 mg/m^{-3}. The concentration of TSS increased significantly with tidal range (the Spearman rank correlation coefficients were 0.57 for MSS and 0.49 for organic particulates, $n = 26$, and were above the critical level of 0.47 (for $p = 0.01$), presumably a result of greater resuspension during periods of stronger tidal flows. Observations of particularly high concentrations of MSS in autumn followed a sustained period (days 285 to 315) of strong winds from the south-west. The concentration of CDOM was least at the beginning and at the end of the time-series (Figure 5.6). The highest values were found over the summer and were not simultaneous with the phytoplankton spring bloom. The Spearman rank correlation between g_{440} and chlorophyll was only 0.19, well below the critical level 0.47 (for $p = 0.01$).

Figures 5.7 a)-c) show examples of absorption spectra on filters. In all cases the dominating effects of non-phytoplankton-pigment material (NPPM), which may include organic detritus as well as inorganic sediments, are apparent. These effects are shown by the methanol decolourised spectra which decay approximately exponentially with increasing wavelength, indicating material which should appear red. However, although combusted filters were generally reddish in hue, the decolourised filters appeared greyish-brown. The NPPM was most evident in October, at a time when there were large quantities of MSS in the water. Under all conditions, however, a recognizable spectrum of phytoplankton pigments was recovered by subtracting the methanol-

decolourised spectra from the initial spectra. The relationship between the difference spectrum and chlorophyll was variable, however, as shown by the a^*_{ph} spectra plotted in Figure 5.7d.

5.3.3 Colour sensor results

The time series of colour ratios in the Menai Strait for nearly the whole of 1996 is shown in Figure 5.8. The most striking feature is the seasonal variation in the red:green ratio, with high values (> 0.5) at the beginning and end of the year and much lower values during summer. There is no obvious seasonal trend in the cyan:green ratio, which stays in the range 0.1 to 0.4 for most of the year. Figure 5.9 shows examples of variability during 10-day periods. Most obvious is a diel cycle in all ratios. This has appeared in other colour sensor records (Wild-Allen *et al.*, 1997) and may be related to colour changes in sea-surface or submarine light, but it has not been fully explained yet. There is some evidence of semi-diurnal tidal effects, e.g. in the decrease in the red:green ratio during the day on most days in Figure 5.9a, or in the twin-peak pattern in the red:green ratio towards the end of the time series in Figure 5.9b, and the cyan:green ratio in Figure 5.9c. The blue:green ratio had low values compared to the other ratios because of (i) lower sensitivity of the blue channel and (ii) greater attenuation of blue light (compared to other wavelengths) by water, CDOM and plant pigments. Particularly low values in autumn might be due to increased concentration of MSS at this time.

Changes during the spring-neap tidal cycle are clear in Figure 5.9a. This record from April shows a clear inverse relationship between the red:green and cyan:green ratios. At the beginning of the April plot it is spring tide, and the red:green ratio is somewhat higher than the cyan:green ratio. As the days advance, the tidal range decreases, tidal flows and stirring lessen, MSS settles out, the red:green ratio decreases and the cyan:green ratio increases, so that by neap tides, the cyan:green ratio is 2-3 times the red:green ratio. No similar changes are apparent in Figure 5.9b (July), but they reappear in Figure 5.9c (November). Although the tidal range on 4 November (the last day shown in Figure 5.9c was low, the relatively high red:green ratios may be explained by sediment resuspension associated with wind-wave stirring.

5.3.4 Model results

(i) Multiple regression analysis

The possibility of empirically relating the concentrations of OICs to colour ratios was investigated using multiple regression analysis (Table 5.1). Log-log regression with the red:green ratio as a single dependent variable gave good results for TSS concentrations: 73% of the variance could be explained. For MSS the best single regression was a linear equation also using the red:green ratio, explaining up to 67% of the variance; whereas for OSS only 48% of the variance could be explained using the same ratio. For the other OICs, single regressions scored rather poor results. The best results overall were obtained by fitting polynomial equations in all the colour ratios. These explained 51% of CDOM, 55% of carotenoid, 62% of chlorophyll, 66% of OSS, 87% of MSS, and 89% of TSS variance.

The time-series of section 5.3.2 demonstrates the strong influence of TSS on water colour in the optical Case-2 waters of the Menai Strait. The results in Table 5.1 show that the four channels of data recorded by the colour sensors can be analysed using MRA to allow satisfactory prediction of TSS as well as of chlorophyll a, despite the dominance of the optical signal by TSS. This is because some ratios are more sensitive to plant pigments and others to TSS and yellow substance.

Figure 5.10 shows how well (a) TSS and (b) chlorophyll concentrations are predicted by the MRA algorithms described in Table 5.1.

Figure 5.11a and 5.11b show the time series of TSS and chlorophyll a as derived from this MRA. The predicted chlorophyll values derived from the MRA represent daily means, the measured values are, each, the mean of two samples. Both time series are well in agreement with historical data (Spencer 1970; Blight *et al.* 1995; Buchan *et al.* 1967; Kratzer *et al.* ms). Comparing these figures to Figures 5.4 and 5.5 shows that the chlorophyll peak of about 25 $\mu g\ l^{-1}$, and the TSS peak of about 50 $g\ m^{-3}$ as measured continuously with a 1-day resolution by the colour sensor would have been missed with the conventional method of measuring these constituents by taking water samples at intervals and analysing them in the laboratory.

Figure 5.12a shows a comparison of the mean TSS values from the time series in 1996 compared to the mean values from the time series measured by Buchan *et al.* (1967).

The figure demonstrates that the mean values from the 1996 time series were well within the range of values (mean +/- standard deviation) from the time series in 1963/1964. Figure 5.12b shows the MSS/TSS ratio, and the tidal range. In August there was a strong relationship between tidal range and MSS/TSS ratio.

The empirical equations given in the Table 5.1 may not be applicable to other Case-2 waters or even to other years in the Menai Strait. It is the need to find a general relationship between colour and OICs that suggests the use of a semi-empirical model, such as that given in section 5.2.2.

(ii) Semi-empirical model

In this section the model's prediction of colour ratios in the Menai Strait is tested using, first, the original parameterisation of Harker (1997), and then with some improved parameter values. As explained in section 5.2.2., the water colour model of Harker (1997) predicts sets of ratios of reflectance coefficients. The original parameterisation (Table 2) used spectra for sea water from Morel and Prieur (1977); for phytoplankton from Gallegos *et al.* (1990); for MSS from Harker (1997) based on measurements of combusted TSS on filters; and for CDOM from Kirk (1994) with an exponent measured by Harker (1997).

Observed colour ratios were averaged over the 6 hours from 10:00 to 16:00 GMT on the days on which water samples were taken. Earlier and later values were excluded to avoid the effect on colour ratios of low sun angles reported by Wild-Allen *et al.* (1997).

The original model by Harker (1997) was tested on the Menai Strait data set from 1996, inputting g_{440}, chlorophyll, and MSS concentration. In the following section the model's prediction are evaluated (a) in terms of the (Pearson) correlation coefficient for a given set of pairs of observed and predicted ratios, and (b) the root mean square (RMS) deviation of observed from predicted ratios, measured in the direction of the vertical axis. Figure 5.13(a) shows a plot of predicted against measured colour ratios, with an overall RMS error of 0.114. The overall correlation was high ($r = 0.91$). However, because of the different ranges and the different principal axes for each colour ratio, the individual r for each ratio was calculated. The red:green was highly correlated between predictions and correlations ($r=0.88$), whereas the cyan:green was less well correlated ($r = 0.35$), and the blue:green ratio was actually inversely correlated ($r= -0.28$). The

agreement between observations and predictions was not improved by substituting colour ratios observed at the actual time of sampling.

In the new model, μ was corrected for the diffuse nature of the light, according to Kirk (1994):

$$\mu = 1/ ((1 + 0.256 \ b / a)^{0.5})$$

where a and b were computed as described in section 5.2.2.

All model parameters were re-evaluated, using the dataset from the Menai Strait time series 1996 (Table 5.2). Harker (1997) took values of a^*_{CDOM} from an exponential decay curve fitted to plots of the absorption of filtered sea water against wavelength. She used data from samples taken in 1995. The value of the CDOM coefficient for exponential decay with wavelength measured with Menai Strait water in 1996 was ranging from - 0.011 to -0.017 nm^{-1}, with a mean of -0.014 nm^{-1} and was found to be the same as Harker's mean value (1997).

A site-specific chlorophyll-specific absorption spectrum was calculated for the Menai Strait. Sixteen difference spectra were used for this analysis, another 10 from the total of 26 being excluded because the difference spectrum was not always realistic (i.e. the decolourised spectrum showed higher absorbance than the spectrum of total sediment, giving the pigment spectrum an untypical shape). Because the distribution of the a^*_{ph} values for a given wavelength was not normal, a simple ranking procedure was used to estimate a median (rather than a mean) and an interquartile range (IQR), rather than a standard deviation, for each waveband. The IQR gives the range of the central 50% of the values. Table 5.2 shows the median values, as well as the 25% and 75% range of values for a^*_{ph}. The median values are 2-3 times higher than the values given by Gallegos *et al.* (1990).

As the model by Harker (1997) neglected the organic fraction of TSS, a new TSS-specific absorption coefficient was determined for the Menai Strait. The absorption spectra from the decolourisation method were divided by the measured TSS concentration in order to derive the TSS-specific absorption coefficient. The same number of samples and the same analysis was used as outlined for the chlorophyll-specific absorption coefficient.

For the water absorption, the spectrum given by Morel and Prieur (1977), and that given by Buiteveld *et al.* (1994) were used as alternatives.
The model of equations 5.1-3 (in section 5.2.2) was then used with the new parameter values in Table 5.2 and the time series of observations of g_{440}, chlorophyll and TSS to predict blue:green, cyan:green and red:green ratios for comparison with the colour ratios observed at the time of water-sampling. In equation 5.2 and 5.3 the concentration of MSS was replaced by the concentration of TSS, and the a^*_{MSS}, and the b^*_{MSS} terms were replaced by a^*_{TSS} and the b^*_{TSS}. The new parameter values improved the agreement of predictions with observations (Figure 5.13b), resulting in a new RMS error of 0.081. Again, the correlation between predicted and measured ratio was best for the red:green ratio ($r = 0.91$). The cyan:green ratio was less well predicted ($r = 0.42$) and blue:green ratios remained least well predicted ($r = 0.09$).

The water absorption coefficients both of Morel and Prieur (1977) and Buiteveld *et al.* (1994) gave the same RMS value. A sensitivity analysis of the model using the median values (Table 5.2) derived from the Menai Strait time series, the values given by Gallegos *et al.* (1990), and the 25 % values for a^*_{ph}, showed how sensitive the model was to changing the parameter: the RMS value changed from 0.081, to 0.086 and to 0.142 respectively.

5.4. Discussion

5.4.1 Seasonal changes in water-sampled OICs, and their relationship with colour ratios

The succession of phytoplankton in 1996 showed a similar pattern as described by Jones and Spencer (1970) and Blight *et al.* (1995). However, the reoccurrence of *Phaeocystis* in autumn was not described by these authors, but has been observed during recent years by a monitoring program of North Wales coastal waters by MBCC (Marine Biological and Chemical Consultants, Bangor, personal communication with Brian Egan, Mentec, Bangor, 1997). It is noticeable that the actual chlorophyll a and TSS peaks were missed with the conventional methods. The colour sensor, however, registered a peak for both on day 117 (26 April 1996). It registered an even earlier peak of TSS concentration on day 69 (3 March 96), which seemed very high at first (49 g m^{-3}) but was well within the measurements performed in the 1960s by Buchan *et al.* (1967).
A sustained period of strong winds from the south-west (days 285 to 315) could be related to the increase in sediment load during a time of low tidal range. In August there was a strong relationship between tidal range and sediment load (Figure 5.12b). The TSS time series (Figures 5.5 and 5.11a) may partially be explained by these physical processes (tidal and wind stirring, especially in autumn), partially by the phytoplankton

productivity (spring and autumn blooms), which in turn is governed not only by physical processes but also by the availability of light and nutrients.

Although Carder *et al.* (1989) found a link between chlorophyll and CDOM concentration, there was no correlation between the phytoplankton biomass and the amount of CDOM in this time series. The increase of chlorophyll a during the spring bloom does not cause an immediate increase in concentration of CDOM. When carrying out experiments in mesocosms, Rochelle-Newall *et al.* (1999) also could not find a significant correlation between dissolved organic carbon and chlorophyll a concentration, even though there was a large phytoplankton bloom in their mesocosm. They also rejected the idea that the sediment could be a source of dissolved organic matter, which has been observed in the Baltic by Skoog *et al.* (1996).

Although there is no direct link between phytoplankton concentration and CDOM, the increase of CDOM over the summer might still be explained in connection to phytoplankton biomass and bacterial activity. Blight *et al.* (1995) observed a respiration maximum about 1-2 weeks after the *Pheaocystis* bloom in the Menai Strait which they explained with an increase of bacterioplankton. The bacterial numbers decreased after this peak, but returned to higher concentrations over the summer. Rochelle-Newall *et al.* (1999) and Nelson *et al.* (1998) found bacteria to be a source of CDOM, even though there was no obvious correlation between bacteria number and dissolved organic carbon. In their mesocosm experiment, Rochelle-Newall *et al.* (1999) could not observe any effect of nitrogen source on the concentration of CDOM, using nitrate, ammonia and urea as nitrogen source. Being nitrogen poor and extremely difficult to break down, and thus not providing an attractive food source for bacteria, the more stable fraction of the CDOM (refractory CDOM) increases over the summer months. It is possible that these molecules get adsorbed mostly to smaller inorganic particles (because of their high surface area) during the course of the year, forming bonds amongst one another. They then get drawn down into the sediment. In autumn, increased wind stirring leads to a resuspension of these particles and increased OSS was measured, together with an increase of MSS and phaeopigment concentration.

For most of the year, the optical signal in the Menai Strait seemed to be dominated by the high concentration of TSS. An increase of TSS concentration during spring tides and during autumn led to an increase of the red:green ratio. Table 5.1 shows a positive relationship between TSS and the red:green ratio, i.e. the slope of the single regression

is positive. This means the more TSS, the higher the red:green ratio. This can be explained by the stronger absorption of TSS in the green than in the red part of the spectrum (and will be further discussed in Chapter 8).

The cyan:green ratio seemed to be inversely related to the red:green ratio during most of the year. This is clearly shown in Figure 5.8 and 5.9 a. Only during the summer months did this relationship not hold: during these months the cyan:green and red:green ratio changed together. This might indicate that phytoplankton influence the colour of the Menai Strait more in summer than during the rest of the year, as phytoplankton absorb both red and cyan light.

The single regression for chlorophyll a in Table 5.1 shows that chlorophyll a and the red:green ratio were inversely related (i.e. the slope of the regression line is negative), and thus that an increase in chlorophyll a concentration tended to result in to a decrease in the red:green ratio. The inverse relationship between the chlorophyll a and the red:green ratio is presumably caused by the strong absorption in the red, and the low absorption in the green, of the chlorophyll molecule. The same should hold for the relationship between chlorophyll a and the blue:green ratio, as chlorophyll a also absorbs in the blue. However, the variation of the blue:green ratio may have been too small, for it to have been a good predictor in a single regression.

The linear regression in Table 5.1 also shows that the carotenoid concentration and the cyan:green ratio were inversely related, which can be explained by the absorption of carotenoids in the blue-green (=cyan) part of the spectrum. A similar relationship was shown in Figure 4.2 (Chapter 4).

The multiple regression analysis showed that the inclusion of the blue:green ratio as variable improved the predictive power of the regressions. This means that, although low in range, the blue:green ratio nevertheless included some usable information about OICs.

To conclude, the optical effects of the phytoplankton, TSS and CDOM were mixed in the recorded colour ratios. Theory suggests, and observation supports the idea that an increase in chlorophyll concentration (which is linked to an increase to carotenoid concentration) should tend to reduce both the red:green, and the cyan:green, ratio. Nevertheless, the optical signal of the phytoplankton in the Menai Strait is relatively

weak in comparison to the signal of the high concentrations of TSS. It is encouraging, however, that the chlorophyll, TSS and MSS components, at least, can be unravelled from the signal using MRA with cubed values of colour ratios. However, this reduced the degree of freedom from 22 (linear regression, n = 26, four variables) to 16 (cubic regression, n = 26, 10 variables), not a problem in the case of the Menai Strait data set, but a reduction that did cause difficulties in the Baltic Sea data set (Chapter 6).

The use of these empirical relationships to estimate OICs requires more investigations, as the coefficients may be expected to be site-specific. The simple regression of log TSS and log MSS on log red:green is significant, presumably because TSS and mostly MSS dominated the colour signal in the Strait. This is possibly the reason why all the other simple regressions were not so significant. However, in order to be able to test the predictive power of the algorithms in Table 5.1, the algorithms should be tested on an independent data set. The relationship between CDOM and colour ratio had a low significance, even when using MRA. This may be because the range of g_{440} values was too small for the CDOM signal to be extracted from the data set. It is possible that the colour sensor could be used for estimating CDOM, as well as chlorophyll a and TSS, if the same method was used for an environment that had more variations in the concentration of CDOM (for example the Baltic Sea). This question will be considered in Chapter 6, section 6.2.

Finally, it is interesting that the best fits to these optical Case-2 data were obtained with polynomial rather than logarithmic equations. The case of using logarithmic equations derives in part from the ocean colour algorithm of Gordon and Morel (1983), and the MOG have found good agreement between log (phytoplankton pigments) and log (colour ratio) using similar colour sensors in optical Case-1 waters (Wild-Allen *et al.* 1997; Kratzer *et al.* 1997).

5.4.2 Semi-empirical model

The model produced by Harker (1997) was tested and improved by the optical time series in the Menai Strait. Using the new parameters resulted in an improvement (from 0.114 to 0.081) in the RMS difference between predicted and observed colour ratios, and the predictions were less biased (Figures 5.13a and 5.13b). The model tends to over-predict the colour ratio, particularly at lower values of each ratio. Nevertheless, the red:green ratio in these optically complicated waters can be predicted surprisingly well, given knowledge of the concentrations of three OICs. The cyan:green ratio shows

consistent deviations from the model prediction that are not seen in the red:green ratio, suggesting an effect in the cyan channel that is not included in the model. The blue:green ratio shows no obvious trends. These results imply that only one constituent can be retrieved using the model. This suggest that the MRA has more predictive power than the model.

The chlorophyll-specific absorption coefficients for the Menai Strait are 2-3 times higher for all channels than the ones given by Morel and Prieur (1977) for oceanic phytoplankton and the ones given by Gallegos *et al.* (1990) for estuarine waters. However, replacing the new site-specific values by those given by Gallegos does not improve the model prediction (RMS changes from 0.081 to 0.086). Using the 25 % values from Table 2 makes the prediction even worse (RMS=0.142), which shows how sensitive the model is to the chlorophyll specific absorption spectrum.

The original model by Harker (1997) included a term for MSS but ignored the organic fraction of TSS. The new model replaces a^*_{MSS} (in equation 5.2) by a^*_{TSS}. The absorption spectrum a_{TSS} was determined from decolourised filter measurements, whereas a_{MSS} was estimated by Harker from the spectra of ashed filters. Combustion during the ashing procedure may have changed filter colour by oxidising iron. All other things being equal a^*_{TSS} may be expected to be less than corresponding a^*_{MSS}, because the former result from division of absorption by [TSS], which was always greater than [MSS]. However, as Table 5.2 shows, the new procedure for filter treatment resulted in a a^*_{TSS} spectrum that differed in shape from that for a^*_{MSS} given by Harker (see Chapter 9: Conclusions). It seems that further study of the optical properties of non-phytoplankton particulates in Case-2 waters is needed.

Figure 5.1a Raft in the Menai Strait. The colour sensor and a transmissometer were deployed on a scaffolding frame which was protected from boats using old car tyres.

Figure 5.1b After 2 weeks of deployment in the Menai Strait in summer 1996, the transmissometer was fouled by benthic organisms. After each download the instruments were cleaned using high-pressure water.

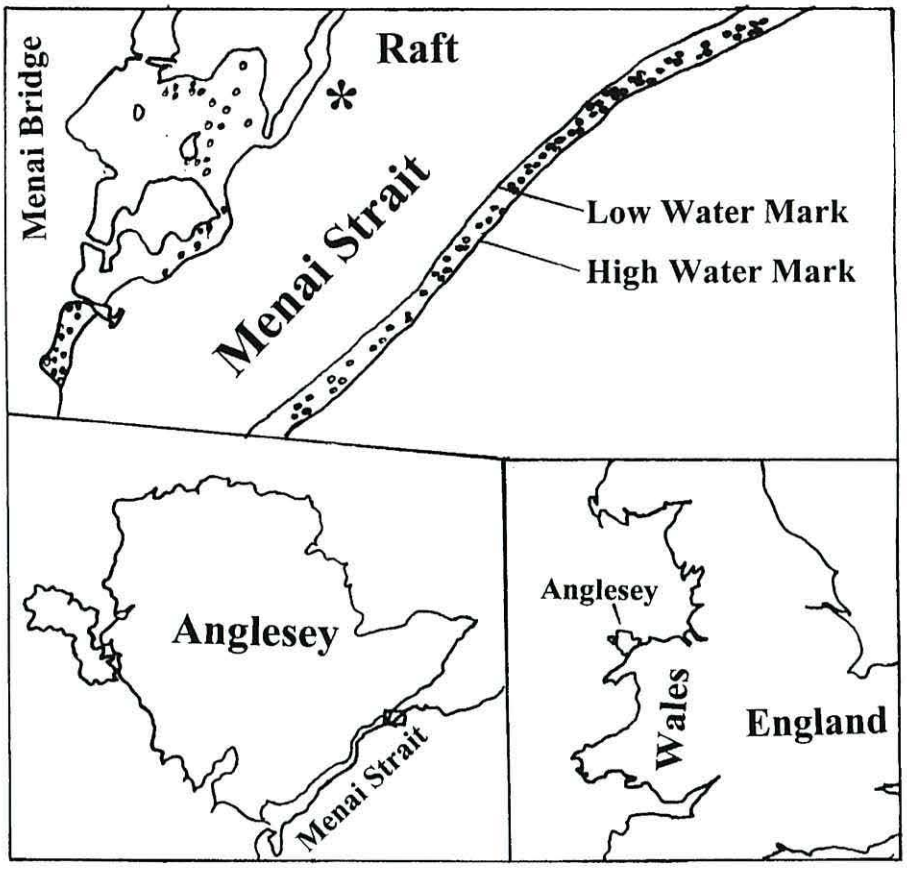

Figure 5.2 Map of the Menai Strait between the Island of Anglesey and North Wales (map drawn from Ordnance Survey map).

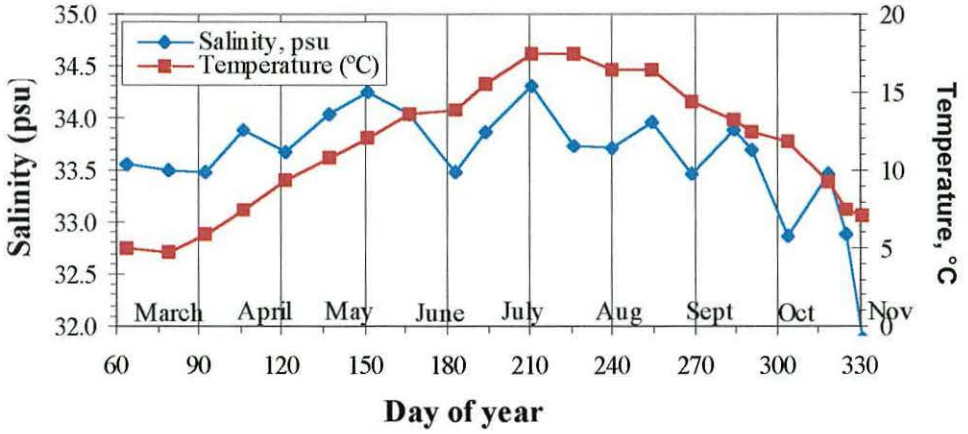

Figure 5.3 Time series (4 March - 29 November 1996) of water temperature and salinity in Menai Strait surface water.

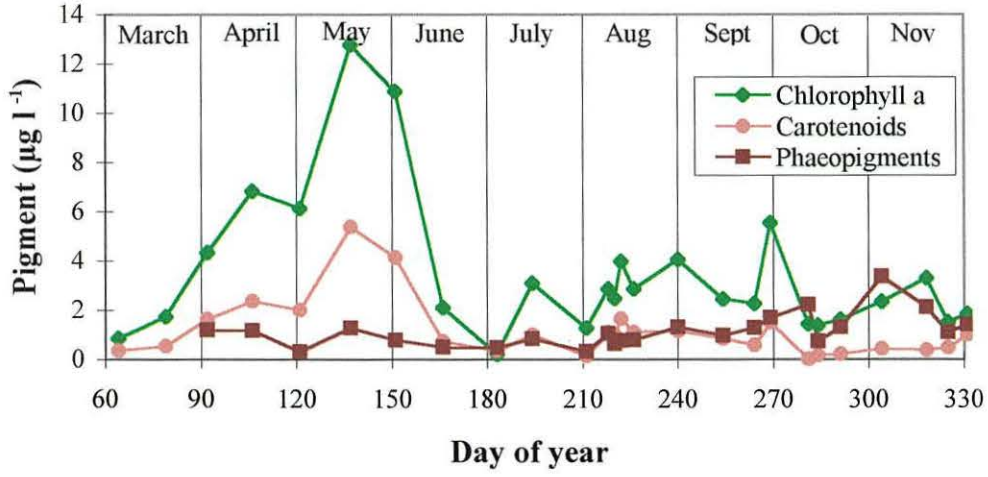

Figure 5.4 Concentrations of chlorophyll a, phaeopigments and total carotenoids as measured *in vitro* using a spectrophotometer.

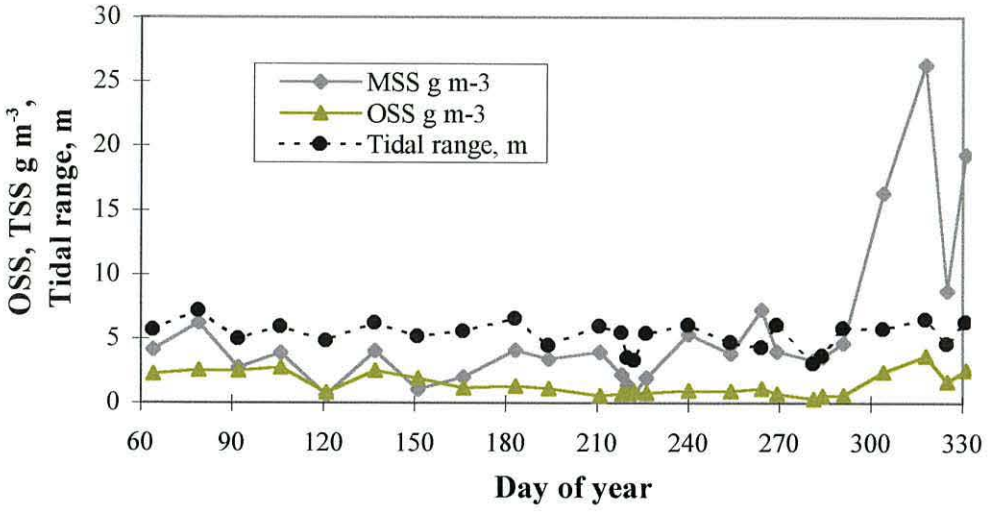

Figure 5.5 Tidal range and the concentrations of MSS and OSS at sampling time.

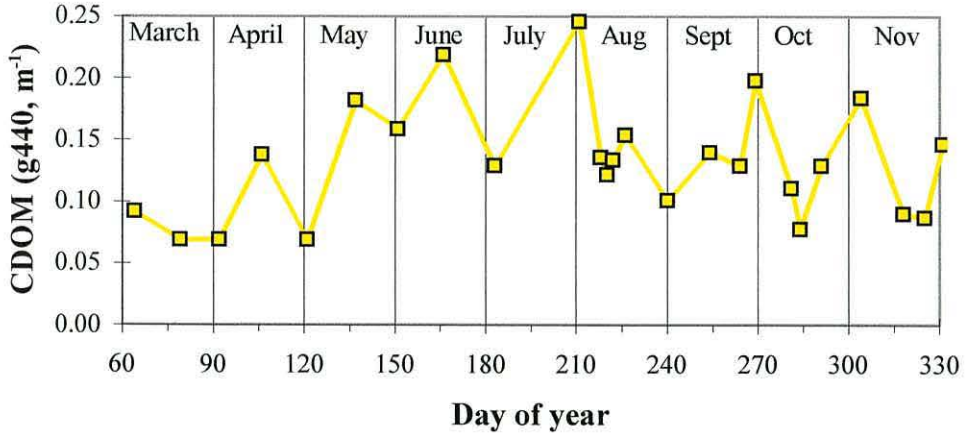

Figure 5.6 The concentration of CDOM as represented by the absorption coefficient at 440 nm (g440). Note the slight increase over the summer.

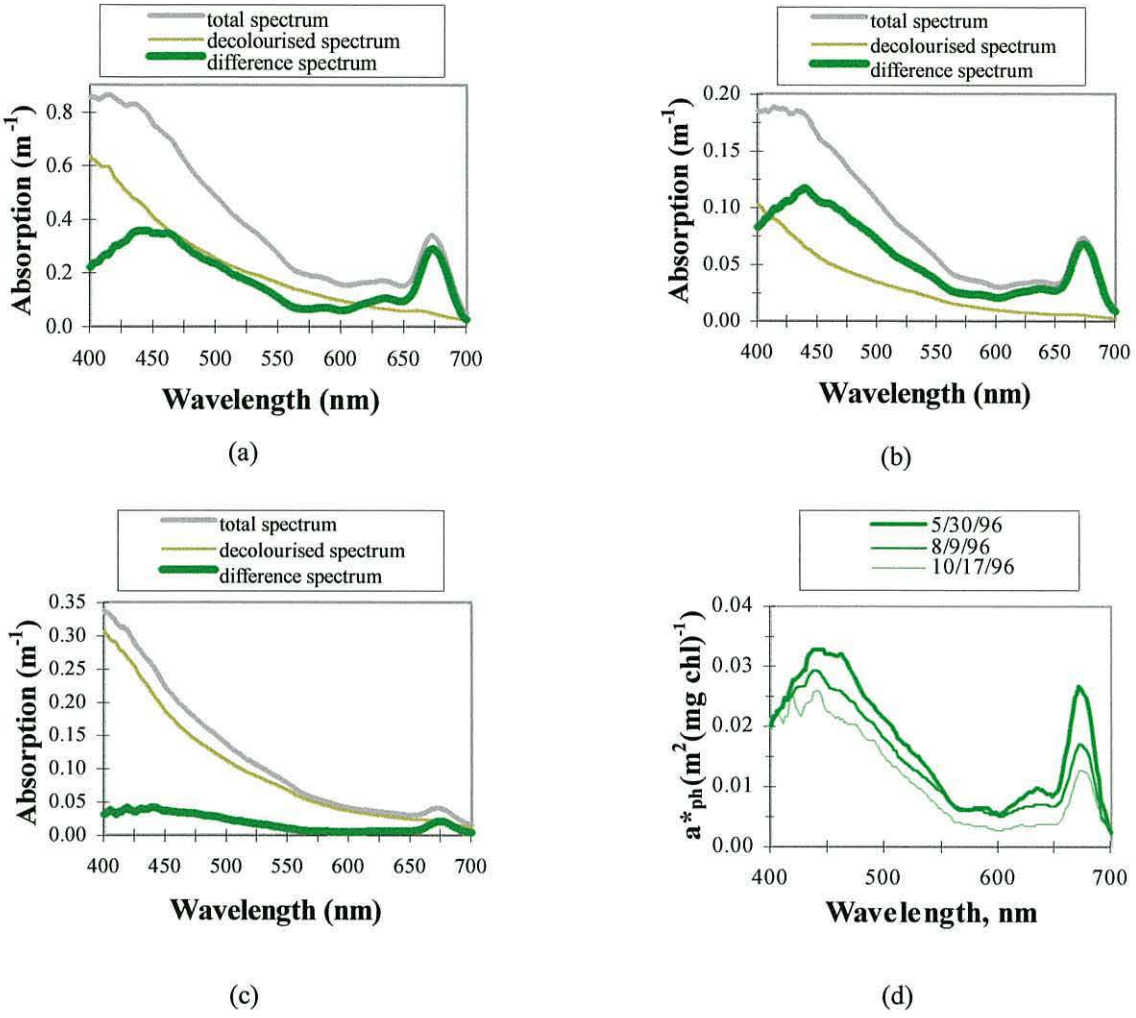

Figure 5.7 *In vivo* spectra: typical initial wet-filter and decolourised spectra for:

(a) 30 May, 1996, at a time when diatoms (especially *Rhizosolenia*) were dominant following the end of the *Phaeocystis* bloom; [chl] = 10.9 mg m^{-3}; [TSS] = 3.0 g m^{-3}; [MSS] = 1.1 g m^{-3}; [OSS] = 1.9 g m^{-3}.

(b) 9 August 1996, phytoplankton mixed (diatoms, cryptophytes and dinoflagellates); [chl] = 4.0 mg m^{-3} ; [TSS] = 1.6 g m^{-3}; [MSS] = 0.7 g m^{-3}; [OSS] = 0.9 g m^{-3}.

(c) 17 October 1996, a time of high MSS; phytoplankton diatom dominated, but also cryptophytes and some *Phaeocystis*). [chl] = 1.6 mg m^{-3}; [TSS] = 5.2 g m^{-3}; [MSS] = 4.6 g m^{-3}; [OSS] = 0.6 g m^{-3}. The 'difference spectra' (phytoplankton pigment spectra) were obtained by subtracting the decolourised from the initial spectra.

(d) shows the chlorophyll-normalised absorption spectra of phytoplankton pigments for these three dates, obtained by dividing the difference spectrum in (a)-(c) by spectrophotometrically-determined 'chlorophyll a' after applying the Cleveland and Weidemann (1993) correction for effects of concentrating material onto a filter.

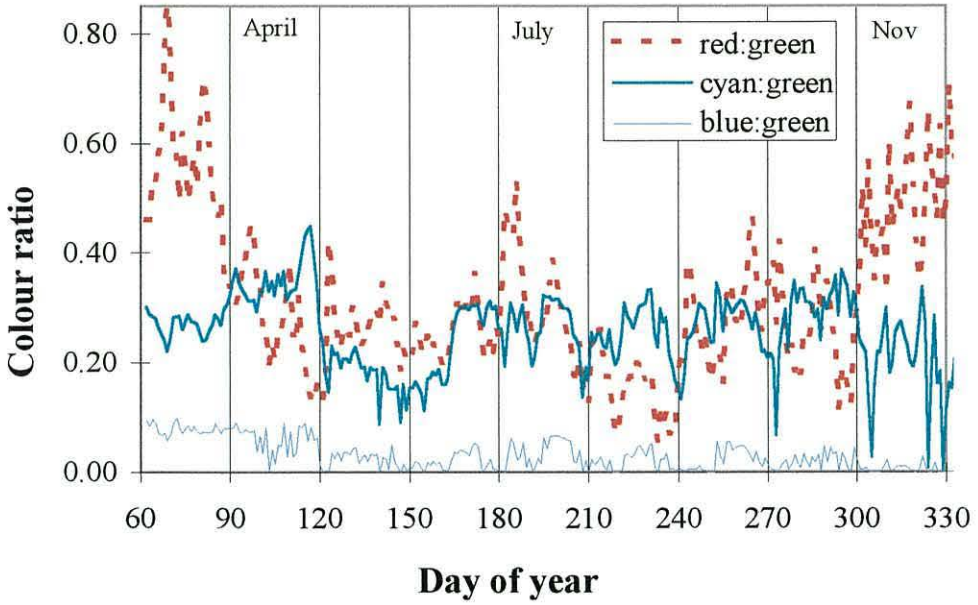

Figure 5.8 Time series of daily mean colour ratios in the Menai Strait, between 3 March and 3 December 1996. The means are of ratios of counts recorded between 10:00 and 16:00 GMT. A change of instrument (from CS4 to CS3 series) occurred on April 1 1996 (day 92), but caused no detectable changes in the ratios. The CS4 instrument recorded every 20 minutes, the CS3 instrument recorded every 10 minutes. Readings obtained in air (during instrument servicing) have been removed, but no correction for differences in channel sensitivity have been applied.

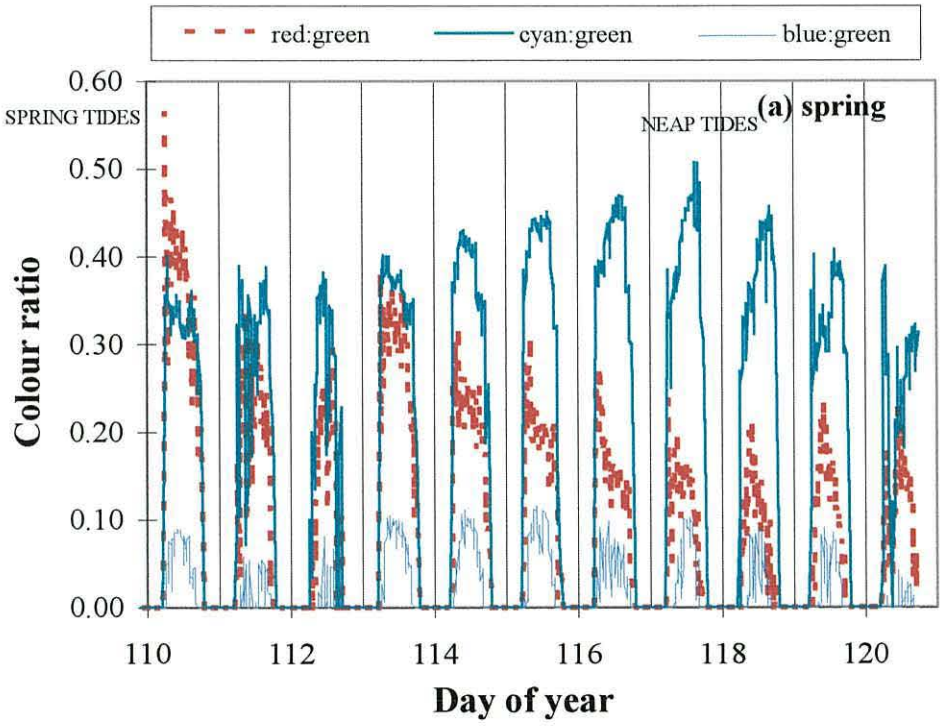

(a)

Figure 5.9 Time series of colour ratios during 10-day periods. The ratios are of counts recorded in each channel during each sampling interval (6 hr^{-1}). Ratios have been set to zero during the night-time. (a) Spring, 18 to 28 April 1996.

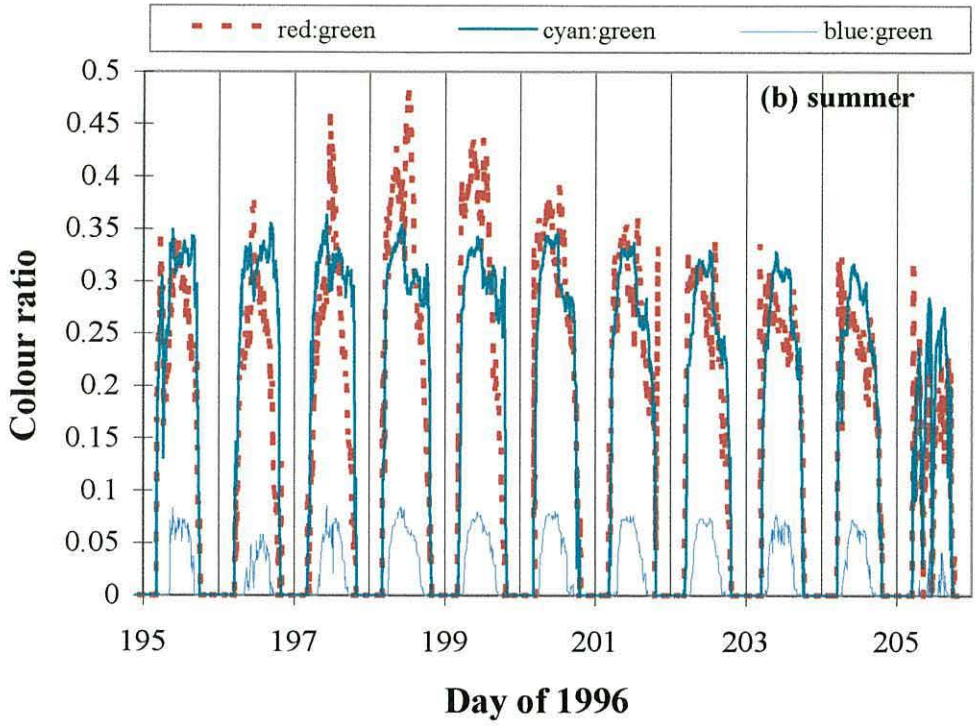

(b)

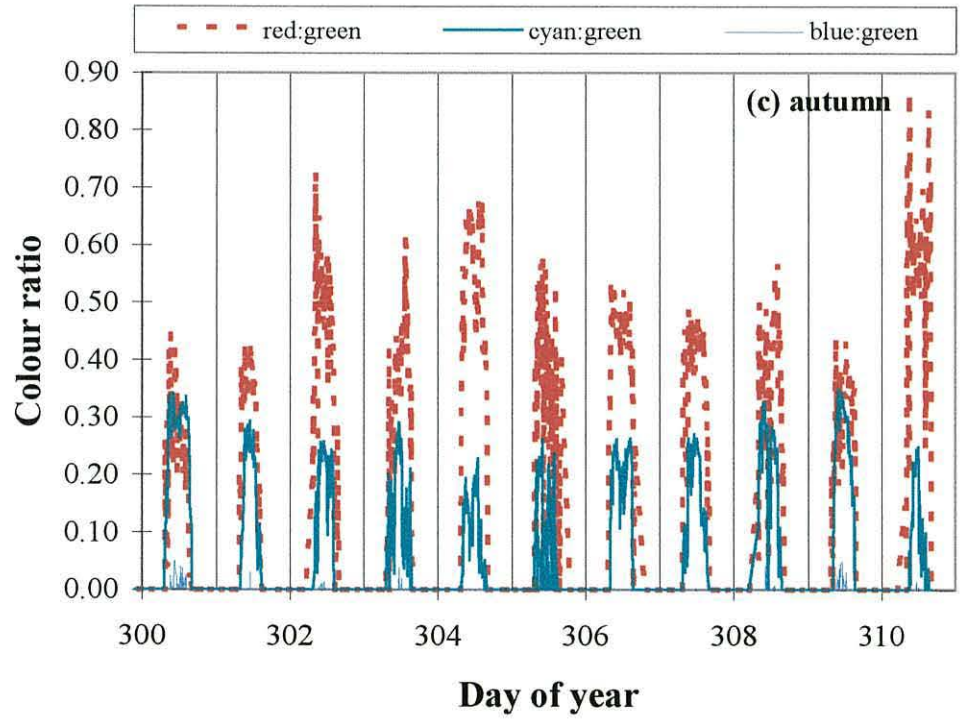

(c)

Figure 5.9 (continued)
(b) Summer, 12 to 22 July 1996;
(c) Autumn, 25 October to 4 November, 1996.

best single regressions:

equation: $y = a + b\,x$

constituent	y	x	a	b	r^2	p	n
TSS	ln [TSS]	ln (r/g)	1.35	1.15	0.73	0.000	26
MSS	[MSS]	(r/g)	-3.40	28.2	0.67	0.000	26
OSS	[OSS]	(r/g)	0.154	3.60	0.48	0.000	26
chlorophyll	ln [chl]	ln (r/g)	0.161	-0.466	0.10	0.124	26
carotenoids	ln [caroten]	ln (c/g)	-0.606	-1.060	0.14	0.066	26
CDOM	[g440]	(c/g)	0.167	-0.136	0.04	0.344	25

best multiple regressions:

example: $[TSS] = 0.79 - 12\,(r/g) + 117\,(c/g) + 183\,(b/g) + 17\,(r/g)^2 - 806\,(c/g)^2 - 4675\,(b/g)^2 + 63\,(r/g)^3 + 1457\,(c/g)^3 + 26059\,(b/g)^3$

constituent:	y	a	(r/g)	(c/g)	(b/g)	$(r/g)^2$	$(c/g)^2$	$(b/g)^2$	$(r/g)^3$	$(c/g)^3$	$(b/g)^3$	r^2	p	n
TSS	[TSS]	0.79	-12.0	117.3	183.2	17.3	-806.2	-4675	62.6	1457	26059	0.88	0.000	26
MSS	[MSS]	-4.95	3.07	148.4	109.7	-16.2	-882.5	-2657	77.9	1505	11059	0.87	0.000	26
OSS	[OSS]	5.74	-15.1	-31.1	73.5	33.5	76.4	-2018	-15.3	-48.0	14999	0.66	0.014	26
chlorophyll	[chl]	-28.3	47.1	480.8	117.7	-155.4	-2317	-367.8	126.9	3266	-4567	0.62	0.031	26
carotenoids	[car]	1.78	5.21	52.5	58.8	-22.5	-415.7	-454.1	20.6	713.8	-392.9	0.55	0.080	26
CDOM	g440	0.43	0.09	-3.28	6.45	-0.58	10.9	-140.1	0.64	-13.0	794.9	0.51	0.164	25

Table 5.1 Results of single and multiple regression analyses. r^2 is the coefficient of determination (the proportion of variance in the dependent variable explained by a regression), and p the probability (of there being a correlation by mere chance)

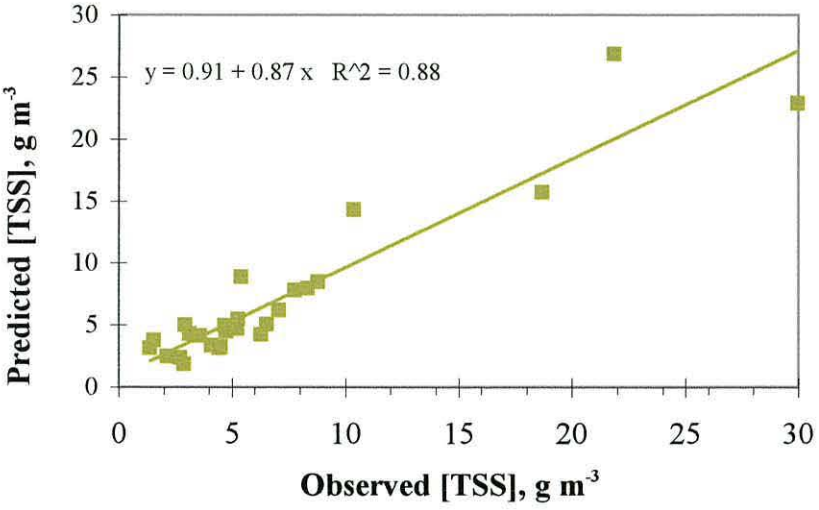

(a)

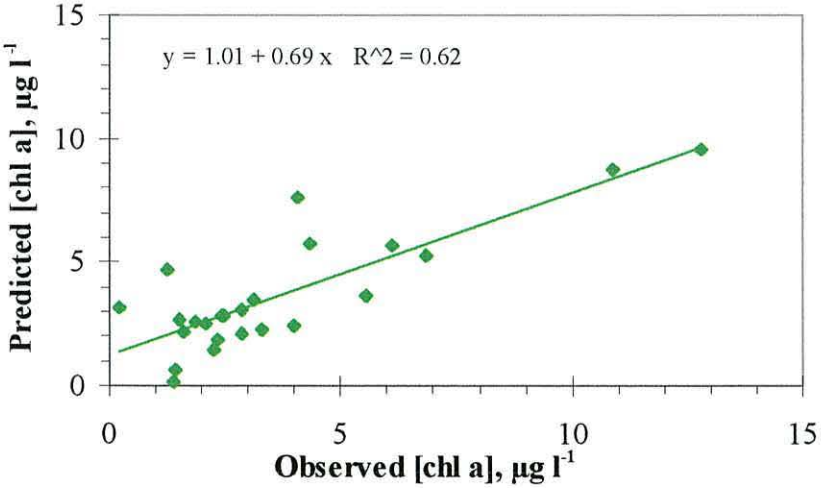

(b)

Figure 5.10 Observed concentrations of OICs, and those predicted from the MRA algorithms of (a) TSS and (b) chlorophyll concentration (Table 5.1).

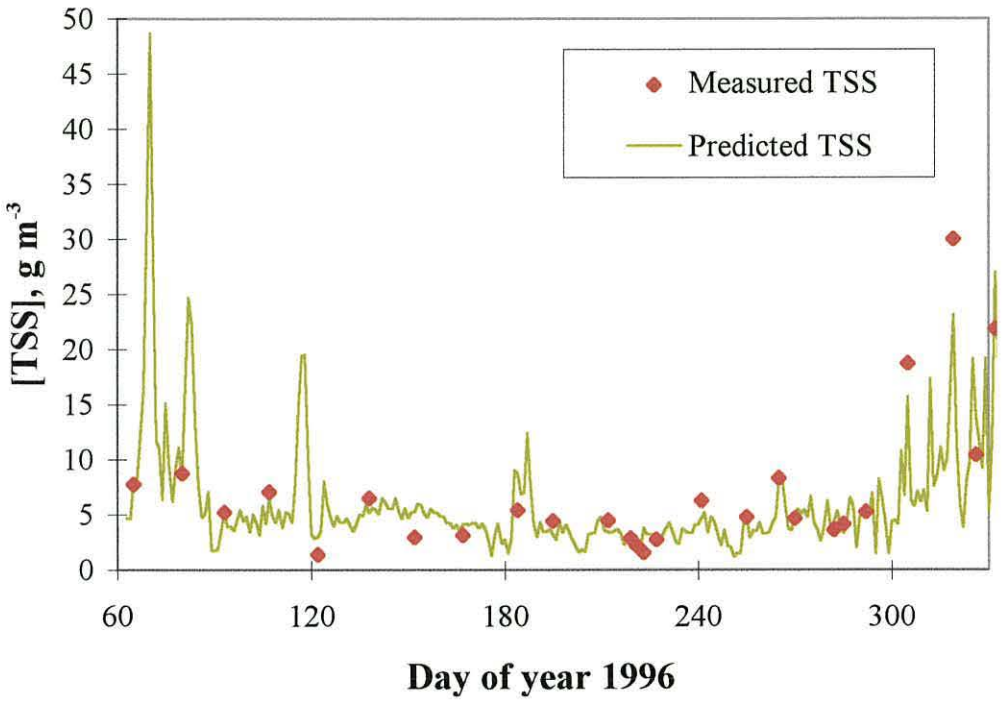

Figure 5.11a TSS time series Menai Strait 1996.

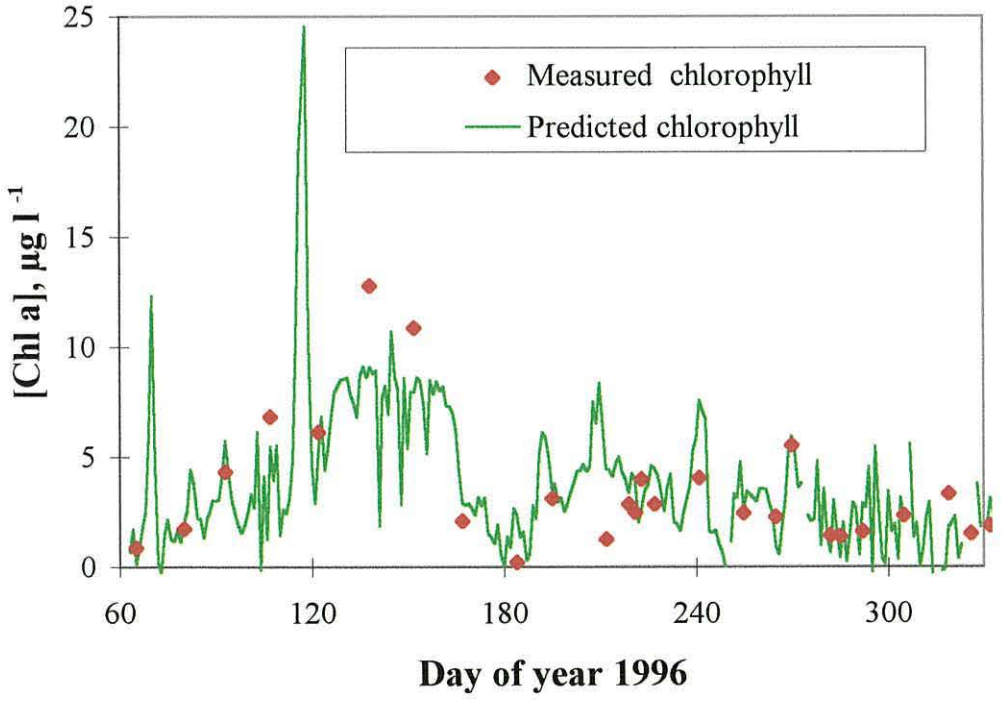

Figure 5.11b Chlorophyll a time series Menai Strait 1996.

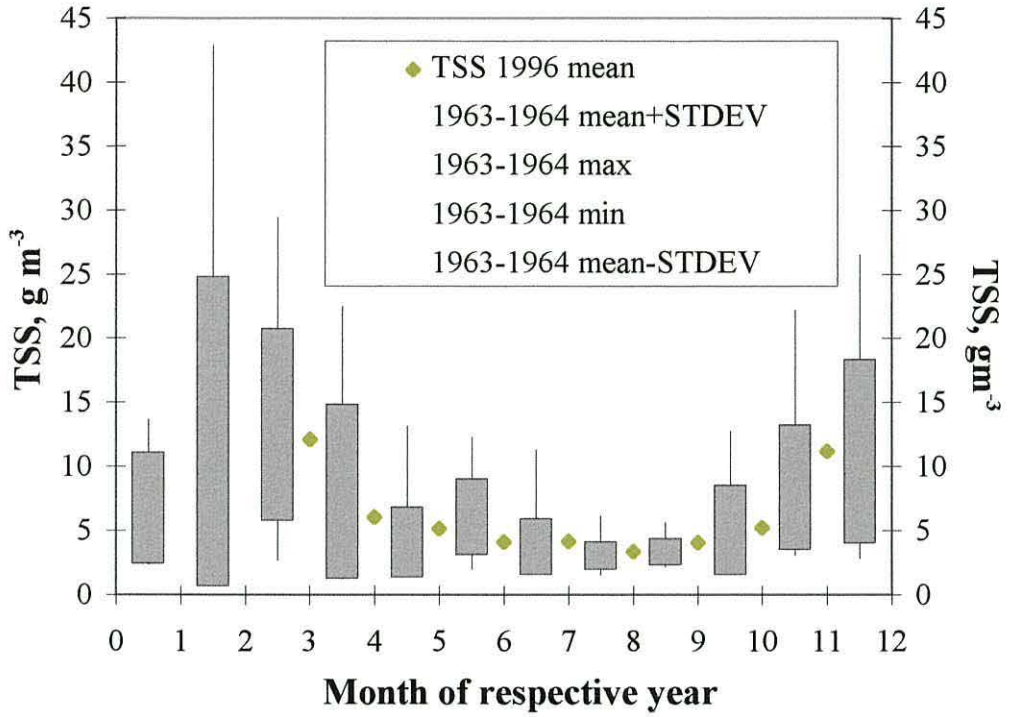

Figure 5.12a Comparison of mean TSS in 1996 to TSS in 1963 and 1964. Data from the 1960s by courtesy of Sinclair Buchan.

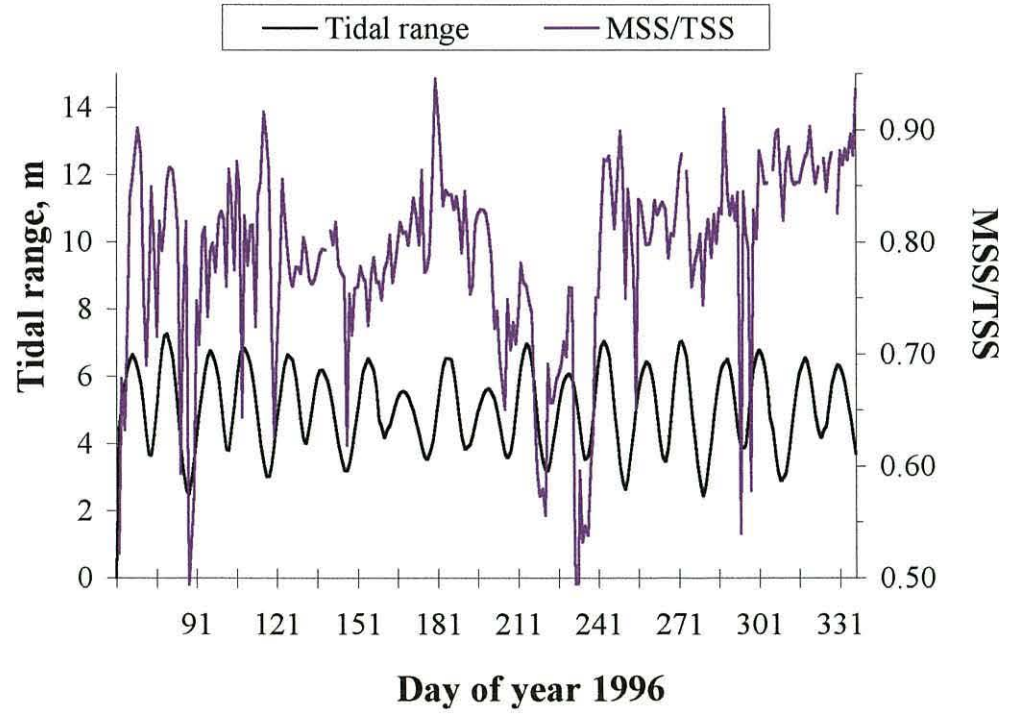

Figure 5.12b Change of the MSS/TSS ratio in the Menai Strait over the year 1996. From late July to late August (from day 210-240) the change in the MSS/TSS ratio is closely related to the change in tidal range.

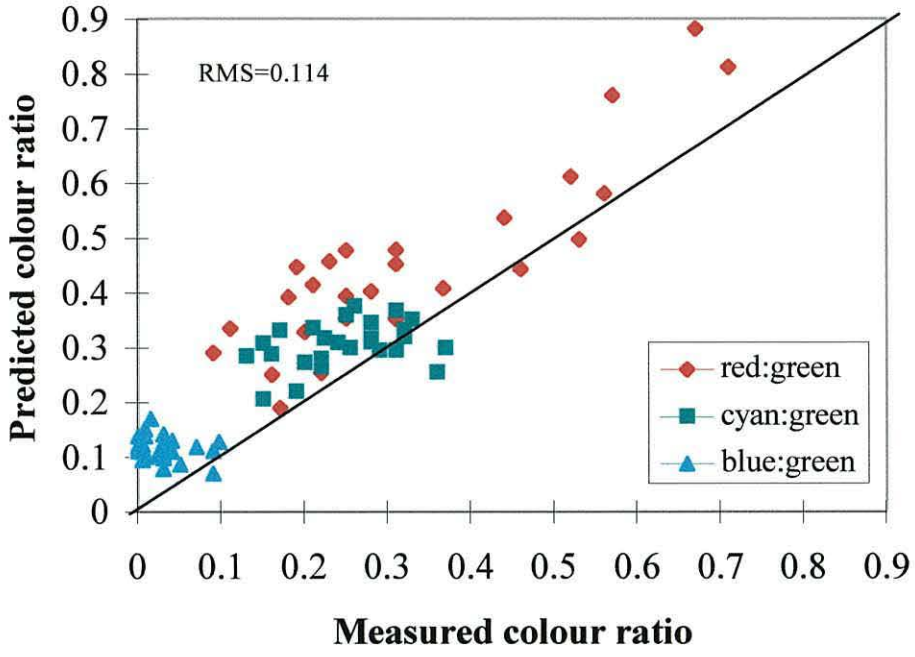

(a)

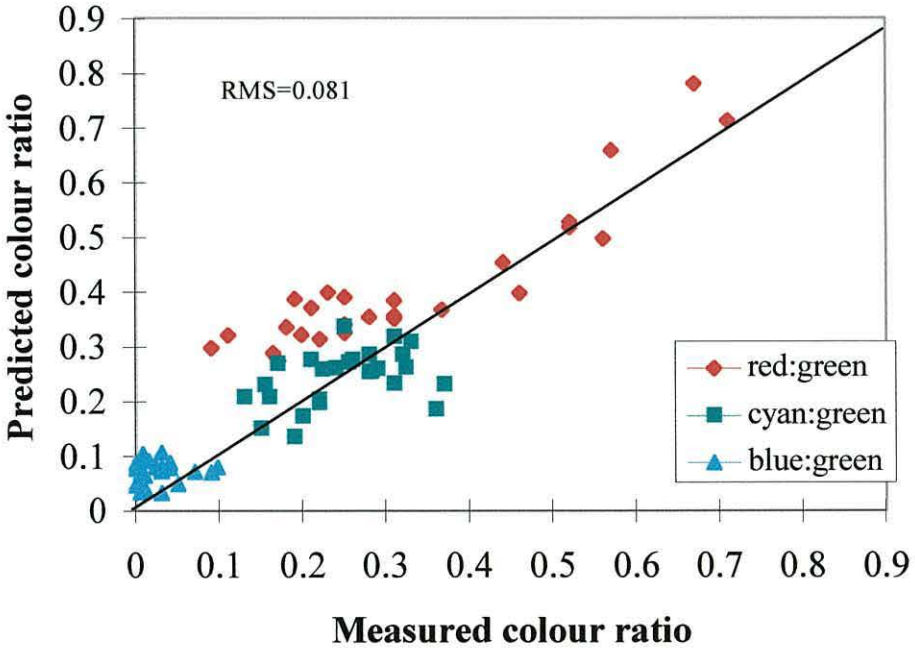

(b)

Figure 5.13 Predictions of colour ratios made from the model of Harker (1997) using water-sampled data for CDOM, chlorophyll and MSS, compared with colour ratios recorded by the colour sensor at the same time as the sampling. The graphs make use of all reliable data from the Menai Strait in 1996. (Different symbols distinguish red:green, cyan:green and blue:green ratios.) (a) Model using original parameter values of Harker. (b) Model using parameter values modified as discussed in this paper.

Specific absorption coefficient	Source	440 nm	490 nm	570 nm	670 nm	Unit
	Parameters from literature					
a^*_w	Morel & Prieur (1977)	0.015	0.02	0.08	0.43	m^{-1}
a^*_w	Buiteveld *et al.* (1994)	0.0104	0.0181	0.0759	0.4122	m^{-1}
a^*_{CDOM}	Harker (1997)	1	0.533	0.174	0.043	
a^*_{ph}	Gallegos *et al.* (1990)	0.025	0.019	0.005	0.018	m^2 (mg chl)$^{-1}$
a^*_{MSS}	Harker (1997)	0.06	0.055	0.045	0.037	m^2 (gMSS)$^{-1}$
b^*_{MSS}	Harker (1997)	0.26	0.24	0.28	0.25	m^2 (gMSS)$^{-1}$
	New parameters					
a^*_{ph}	25%	0.0540	0.0366	0.0084	0.0179	m^2 (mg chl)$^{-1}$
	median	0.0888	0.0592	0.0170	0.0382	m^2 (mg chl)$^{-1}$
	75%	0.1169	0.1083	0.0244	0.0626	m^2 (mg chl)$^{-1}$
a^*_{TSS}	25%	0.0474	0.0324	0.0183	0.0129	m^2 (gTSS)$^{-1}$
	median	0.0659	0.0456	0.0285	0.0207	m^2 (gTSS)$^{-1}$
	75%	0.1038	0.0736	0.0472	0.0338	m^2 (gTSS)$^{-1}$

Table 5.2 Specific absorption coefficients used in the two different models. The new model uses a new set of absorption coefficients for phytoplankton and total suspended matter, the coefficients for CDOM and water are the same as in Harker (1997).

Chapter 6 - Optical properties of the Baltic Sea

This chapter consists of two parts. The first part is a general review of remote sensing and optical monitoring in the Baltic Sea. The review takes ecological considerations into account, and is an attempt to link remote sensing with more conventional methods of Baltic Sea monitoring. The second part is a modelling paper presented at Ocean Optics XIV, Kailua-Kona, Hawaii, USA, 10-13 November 1998 (Kratzer *et al.* 1998). The model developed for the Menai Strait (Kratzer *et al.* 2000; Chapter 5) was adapted to Baltic Sea conditions, using parameters specific to the Baltic Sea.

6.1 Remote sensing and optical monitoring of toxic algal blooms in the Baltic Sea. A review.

Abstract

Due to its spatial coverage remote sensing provides a powerful tool for improving the monitoring of toxic algal blooms in the Baltic Sea. The main restrictions for using visible radiometry for the detection of algal blooms are cloud cover and the fact that it is only sensitive to the uppermost layer of the sea. Overcoming these requires the combination of remote sensing with other techniques such as *in situ* monitoring and bio-optical and dynamical models. These models need to incorporate the optical characteristics of the different OICs as well as the interaction with their environment. This review introduces the reader into the ecology of cyanobacteria blooms in the Baltic Sea and looks at the contributions remote sensing and optical monitoring can make to the more conventional methods in monitoring.

6.1.1 Introduction

The Baltic Sea is connected to the North Sea via the Skagerrak and the Kattegatt. The bottom topography separates the Baltic Sea into basins which vary widely in their biogeochemistry (HELCOM 1996). Figure 6.1 shows the depth distribution of these different basins. The Baltic Sea is characterised by a permanent salinity stratification with a brackish surface layer caused by the high freshwater input from rivers and more saline deep and bottom waters coming in from the North Sea. In the Baltic Proper the halocline ranges between 40 and 70 m depth. During spring and summer, a thermocline at depths between 15 and 20 m develops in most parts of the Baltic Sea, providing another density barrier for vertical exchange (Voipio 1981). The depth of the euphotic zone in general coincides with the depth of the surface mixed layer. Apart from vertical density stratification, the high fluvial input from the north and the saline input of water

from the North Sea also produce a strong horizontal salinity gradient across the whole Baltic Sea.

The Baltic Sea has a large freshwater input, and a slow exchange with the North Sea, and is therefore brackish in nature. The salinity is low compared to other seas, and the large freshwater content is associated with a high content of coloured dissolved organic matter. Because of the low tidal range in the Baltic Sea, and the strong salinity stratification, there is little resuspension of sediment. This, from a marine optics point of view, makes the Baltic Sea and the Menai Strait an interesting comparison. Both the Baltic Sea and the Menai Strait are optical Case-2 waters. However, they differ substantially in the nature of the OICs. In the Menai Strait the optical properties are dominated by SPM, including minerals, which get resuspended by tidal flows, and by the strong currents (Chapter 5).

The aim of this chapter is to characterise the OICs of the Baltic Sea, and to test the hypothesis that the colour sensor can be used for measurements of chlorophyll and/ or other OICs in the Baltic Sea (see section 1.6. Aims and objectives). Furthermore, to adapt the Case-2 model developed for the Menai Strait to optical conditions in the Baltic Sea, and to improve the model by including immersion and shading effects, as well as scattering and backscattering. The data used to test these hypotheses were collected in 1998 during two cruises across the Baltic Sea and at a field station in the north of Gotland (see section 6.2.2). The immersion effect was measured in 1997 during a Cirolana cruise in the Irish Sea (see section 3.2.5). During the spring cruise in the Baltic Sea, measurements of scattering, and of spectral K_d were made with additional instruments in order to improve the model (see section 6.2.2).

6.1.2 Phytoplankton Blooms in the Baltic Proper

The phytoplankton succession in the Baltic Proper has a similar pattern every year. There is a spring bloom dominated by a mixture of diatoms and dinoflagellates, and a summer bloom of filamentous nitrogen-fixing (diazotrophic) cyanobacteria. The spring bloom in the southern and central parts of the Baltic Proper generally occurs in the second half of April. From July onwards (sometimes from the end of June) blooms of nitrogen-fixing, filamentous cyanobacteria may be formed by *Nodularia spumigena, Aphanizomenon flos-aquae*, and, in low-salinity areas, several *Anabaena* species. Until early autumn these species may give rise to extensive blooms, dependant on calm and stable weather conditions. There are scientific reports of such blooms in the Baltic Sea dating back to the middle of the 19th century. The blooms can be traced by satellite

(Horstmann 1975; Horstmann *et al.* 1986; Håkansson and Moberg 1994). They can cover up to about 15% of the total Baltic Sea area as shown by satellite imagery (Rud and Kahru 1995; HELCOM 1996). Figure 6.2 shows an example of an AVHRR image of a cyanobacteria bloom from the NOAA-14 satellite.

During the summer cyanobacteria blooms *N. spumigena* and *A. flos-aquae* make up the bulk of the biomass (Kononen and Leppänen 1997). Figure 6.3 shows pictures of *N. spumigena* and *A. flos-aquae* as seen under the microscope using different magnifications. *Nodularia spumigena* tends to be toxic, whereas *A. flos-aquae* is not toxic (personal communication with Edna Graneli, 2000). In the Gulf of Finland, *N. spumigena* was only found in small numbers. In laboratory experiments, the toxin production has been shown to be dependant on the phosphate concentration, and for one toxic strain even the salinity had an influence on the toxicity (Lehtimäki 1994).

The two species are functionally similar because of their ability to fix nitrogen. Field measurements, however, suggest that *N. spumigena* is more efficient in nitrogen fixation (Kononen and Leppänen 1997). *Aphanizomenon flos-aquae* may benefit from nutrient pulse events and is often found in frontal and upwelling zones (Kononen *et al.* 1996). The two species also differ in their temperature, salinity and light requirements. *Aphanizomenon flos-aquae* occurs throughout the growth season (March to October in the southern parts, April/May to September in the northern parts), and is dominant when considering total biomass across all seasons. It usually has its biomass peak at around 10 m depth (personal communication with Susanne Hajdu, 2000). *Nodularia spumigena* appears only in the warmer months (Kononen and Leppänen 1997), and tends to dominate surface accumulations. *Aphanizomenon flos-aquae* has a temperature optimum of 16-22 °C. The temperature optimum of *N. spumigena* is higher (25-28 °C), and its temperature tolerance limits are narrower than for *A. flos-aquae.* Knowledge of Sea Surface Temperature (SST) distribution from AVHRR (Advanced Very High Resolution Radiometer) imagery may therefore be a useful tool for the prediction of the occurrence of either species. The optimum range of salinity is also higher for *N. spumigena* (10-15 psu, practical salinity unit) than for *A. flos-aquae* (0-5 psu), and *N. spumigena* also tolerates higher irradiances. In general the salinity decreases with increasing CDOM concentrations, because of the higher proportions of CDOM in fresh water. Therefore, remote sensing imagery in the visible may also provide a tool for mapping areas of possible distribution of either species, inferring the change in salinity from a decrease of reflectance in the blue, and taking the salinity tolerance of the species

into account. However, the relationship is very complicated, because of the complex variety and structures of CDOM molecules. Another complication is the change of molecular charge due to changes in the salinity which may cause CDOM molecules to coagulate and settle out on the sediment.

The massive blooms are probably facilitated by upwelling of phosphate-rich deep water (Leppänen *et al.* 1988). Anoxic bottom areas and bottom waters with low oxygen content may result in the release of phosphorus from the sediment. In the deep basins of the Baltic Proper and the Gulf of Finland the stable stratification of the water and the slow and irregular exchange of bottom waters enhance the build up of stagnant conditions. This causes oxygen depletion, which in turn leads to a decrease in inorganic nitrogen reserves by denitrification. It also causes the trapping of inorganic phosphorus in the bottom water, and a phosphorus flux from the sediment, resulting in a decrease in the ratio of dissolved inorganic nitrogen (DIN) to dissolved inorganic phosphorus (DIP). The DIN:DIP ratio is especially low in the open Baltic Sea and is believed to be one of the key factors for the occurrence of blooms of filamentous nitrogen-fixing cyanobacteria. The buoyancy provided by gas vesicles is also thought to give a selective advantage to cyanobacteria by enabling them to float into higher irradiances close to the surface (Walsby *et al.* 1995), and this is advantageous in calm conditions. Thus, two properties of cyanobacteria (i.e. nitrogen fixation ability, and floating ability) fit them particularly for the prevailing conditions in the Baltic Sea in summer. A more detailed review of the physiology, ecology and toxic properties of *N. spumigena* and *A. flos-aquae* (as well as *Trichodesmium* spp.) is given by Sellner (1997); also Kononen 1992 and Kononen *et al.* 1995.

6.1.3 CDOM and SPM in the Baltic Sea

The optical properties of the Baltic Sea are dominated by CDOM. Compared to other seas the concentration of CDOM is relatively high in the Baltic. This is because of the high fluvial inputs of humic and fulvic acids, and little exchange with the North Sea. CDOM absorbs strongly in the blue, a feature that is usually modelled as an exponential decrease with increasing wavelength. Both the magnitude and the exponent show very high variability in the Baltic. In the open Baltic Sea, the absorption due to CDOM is higher than in Bay waters, or close to river mouths (Siegel *et al.* 1996; Kowalczuk and Kaczmarec 1996). According to Kowalczuk and Kaczmarec 1996, the absorption spectrum of CDOM decayed exponentially with an exponent ranging between -0.014 and -0.022 nm^{-1}. This agrees well with measurements performed by Højerslev and Aas,

1998. The latter concluded that because of the source and site dependence of the CDOM it may be very difficult to derive CDOM concentration from remotely sensed imagery.

Recent models of total absorption in Case-1 waters work on the basis of treating the absorption of CDOM and NCP (Non Chlorophyllous Particulates) as one unit (Carder *et al.* 1991; Aiken *et al.* 1995). The principal reasons for this grouping are that, in the open ocean, the absorption by these two components covary implicitly with phytoplankton absorption, and that they have similar spectral properties: they can both be described by an exponential decrease of absorption with wavelength (Roesler and Perry 1995).

However, Dowell *et al.* (1996) showed for the Baltic and the Adriatic, that the spectral absorption of NCP and CDOM vary independently in these two examples of Case-2 waters, and therefore, that they should be treated as two separate components when modelling the total absorption of Case-2 waters. This agrees with Højerslev's (1989) finding that biological activities such as primary productivity and organic decay were unrelated to the formation of CDOM in the Baltic Sea. Dowell *et al.* showed that the absorption in the Baltic is clearly dominated by CDOM, and to a lesser extent by phytoplankton, depending on the time of year and the location. The absorption by the three components (CDOM, pigments and NCP) show the largest degree of variability in absorption at around 670 nm, and the red part of the spectrum in general. This may be of great importance for modelling the three components in Case-2 waters.

6.1.4 Optical properties of phytoplankton in the Baltic Sea

The chlorophyll a concentration is commonly used as an indicator of phytoplankton biomass. It is also one of the input parameters for optical modelling. Averaged over the period from 1993-1997, the mean chlorophyll values in the Baltic Proper were 2.9 $\mu g\ l^{-1}$ in spring, 2.3 $\mu g\ l^{-1}$ in summer, and 2.2 $\mu g\ l^{-1}$ in winter (HELCOM 1996). The highest value was 27.3 $\mu g\ l^{-1}$ during a spring bloom. Much higher values are to be expected for dense surface accumulations in summer (Subramanium *et al.* 2000).

The dominant phytoplankton groups during blooms in the Baltic Sea are diatoms and dinoflagellates in the spring bloom, as well as filamentous cyanobacteria in the summer blooms. All these species contain chlorophyll a and a mixture of accessory pigments. Because of the similarities in pigmentation, the spectra of *in vivo* absorption for diatoms and dinoflagellates are very similar (see Johnsen *et al.* 1994). However, the characteristic carotenoid pigment of diatoms is fucoxanthin, whereas that of

dinoflagellates is peridinin (Wright *et al.* 1991). Cyanobacteria possess phycobilins but no accessory chlorophylls. The possession of phycobilins leads to characteristic absorption bands in the yellow / orange part of the spectrum. However, not only the absorption properties of phytoplankton have to be considered when trying to model the light field in the Baltic Sea, but also its scattering properties. Gas-vacuole containing filamentous cyanobacteria cause a strong scatter of light which also increases the amount of back-scatter. Roesler (1998) pointed out that in some toxic algal blooms the colour of the water may be attributed to the unique set of conditions associated with algal blooms: enhanced cell concentration, distribution close to the surface, uniform cell size distribution, as well as their inherent optical properties.

6.1.5 Remote sensing of the Baltic Sea

Due to its spatial and temporal coverage, remote sensing of ocean colour has greatly advanced our understanding of the oceans, in ways which could not have been achieved by conventional oceanographic methods. Visible radiometry is the only remote sensing technique which can penetrate the sea surface. However, it is only sensitive to the upper part of the euphotic zone. The biggest restriction for remote sensing in the Baltic Sea area seems to be the extent of cloud cover, which is about 40-50 % in summer, and about 60-70 % in winter (Karlsson 1996). Another challenge is atmospheric correction, which is extremely difficult in coastal areas because of the high variability of aerosol concentration and distribution, and the increased occurrence of significant water-leaving radiance in the near infrared.

Horstmann *et al.* (1986) used CZCS (Coastal Zone Colour Scanner) imagery for mapping chlorophyll and SPM distribution in the Baltic and for demonstrating the influence of river run-off on the south-eastern Baltic Sea at different times of the year. The (443:550) reflectance ratio was used to derive chlorophyll a concentration. However, the algorithm used does not strictly apply to Case-2 waters. AVHRR imagery is increasingly used for near-real time monitoring of the Baltic Sea (Rud and Kahru 1994). Ove Rud and Miho Ishii at the Department of Physical Geography at Stockholm University combine AVHRR imagery and Meteosat data for monitoring SST and cyanobacteria in the Baltic Sea. During summer, they process and interpret AVHRR images twice a day. The images can be seen on their web page browser (http://wwwmarin.natgeo.su.se/~ab/). The images are also used by the Information Centre for the Baltic Proper at the country administration in Stockholm, and by the Finnish Institute of Marine Research in Helsinki. Thus, near-real time information of

the location and spatial distribution of a bloom can be transferred within one hour to the relevant local authorities for appropriate action. However, the spectral resolution is very low, and the visible band (580-680 nm) is too broad to retrieve the information contained in ocean colour and to allow the development of specific algorithms for quantitative estimation of OICs.

AVHRR has also been used for examining the sea surface temperature (SST) variability in the northern and central Baltic Sea (Kahru *et al.* 1995) and helped to identify the major frontal areas along the eastern coast of the Bothnian Sea and along the north-western coast of the Gulf of Finland. Victorov (1996) gives a good overview on the development and occurrence of seasonal fronts, coastal upwelling and eddies as observed by satellite imagery. Håkansson and Moberg (1994) demonstrated how AVHRR imagery can be used for detecting cyanobacterial blooms. The cyanobacteria are good scatterers of visible light and therefore cause a high signal in the visible channel. High concentrations of these surface accumulations show up as bright areas in the image. Rud and Kahru (1994) estimated the AVHRR band 1 albedo of these cyanobacteria accumulations to be between 2.3 % and 4 %. The algae are dispersed by currents and act as a tracer for the flow field. The images, however, may only reflect the conditions close to the sea surface. Kahru *et al.* (1993) used AVHRR imagery combined with ship measurements to demonstrate that surface accumulations of toxic algal blooms cause an increase in the satellite-derived SST by up to 1.5 ° C. They attributed this phenomenon to increased absorption of sunlight due to increased phytoplankton pigment concentration. These sea surface temperature anomalies (hot spots) which were associated with increased reflectance in the visible channel of the AVHRR could be correlated with chlorophyll concentrations at 5 m depth. The hot spots followed the detailed boundaries of the cyanobacterial plumes and probably represented a shallow, diurnally heated top layer appearing in the late afternoon during low wind and weak mixing conditions. They disappeared during the night due to thermal convection and were hardly detectable on days with wind speed between 6 and 8 m s^{-1}.

Kahru *et al.* (1994) examined a long-term series of AVHRR imagery of the Baltic Proper, and mapped annual surface accumulations of cyanobacterial blooms between 1982 and 1993. There was no obvious shift in the time of bloom, but substantial increase in phytoplankton coverage was observed in the years 1982-1984, and 1990-1993 (also Kahru 1997). This was possibly a result of calm weather conditions

observed over this time range, which allowed the gas-vesicle-containing cyanobacteria to float up to the surface. Some of the interannual variations in the extent of surface accumulations can be explained by the variation in the total amount of sunshine during the summer period. The high frequency of cloud coverage has lead to a very irregular collection of useful images. In some years only four to five images of surface accumulations could be retrieved, whereas in more recent years composite images were made up from up to 50 images.

In 1997, the surface accumulations over the whole Baltic covered an area larger than that ever observed before. They even extended into the Bothnian Sea, and included massive blooms in the Gulf of Finland. The summer of 1998 was relatively cold and there were only a few surface accumulations as shown by satellite. The summer of 1999, was exceptionally warm, again, and the extend of the surface accumulations may have been even more than in 1997 (personal communication with Ove Rud). It is very difficult to explain why these blooms appear and reappear in certain areas at a certain time. They may require a combination of low wind stress, high insolation leading to warming of the surface layers, and a shift to a low DIN:DIP ratio (DIN: Dissolved Inorganic Nitrogen; DIP: Dissolved Inorganic Phosphorus).

Ekstrand (1992) used TM (Thematic Mapper on LANDSAT) imagery combined with sea- truthing to map chlorophyll a in Himmersfjärden bay on the Swedish east coast from 10 May 1988 to 7 May 1990. The disturbing spectral influence from SPM was reduced by using an existing algorithm for TM sediment retrieval combined with *a priori* knowledge about water depths, bottom sediments and river outlets. The author suggested the use of a ratio of TM bands (TM1/(log TM3+1) in Case-2 waters, and the earlier suggested ratio of TM bands 1/2 only in Case-1 waters. The discriminating power of the data analysis indicated the capability to quantify chlorophyll a in bloom situations. Unfortunately, the bands are rather broad which makes the TM less applicable for the development of specific algorithms. However, its spatial resolution (30 m) is very good compared to that of ocean colour sensors (about 1 km). In combination with AVHRR, TM is still of great use for bloom monitoring and for studying surface accumulations in more detail (Rud and Kahru 1994).

A new generation of ocean colour sensors is under development. Some have already been launched in the last few years: e.g. SeaWiFS (Sea-Viewing Wide Field of View Sensor), MOS (Modular Optical Scanner), OCTS (Ocean Colour and Temperature Scanner). These are multispectral instruments with improved sensitivity compared to

CZCS. The sensitivity of ocean colour sensors is adapted to the dark signal of water, which leads to saturation over bright targets over land and clouds. When moving from a bright target to the sea most sensors need some time to recover. This effect is termed bright target recovery (BTR) which usually shows up in the image as bright regions adjacent to the coast or cloud. The new generation of ocean colour sensors has been designed to recover much more quickly from this effect than CZCS (Barnes *et al.* 1995).

The launch of SeaWiFS was delayed by several years, but it was successfully launched in August 1997. The blue band centred around 443 nm is affected by strong absorption from both chlorophyll a and CDOM. Chlorophyll a *in vivo* absorption peaks around 443 nm in the blue. However, the chlorophyll a absorption band decreases, whereas CDOM absorption still increases exponentially towards the lower wavelengths in the blue (Prieur and Sathyendranath 1981). Algorithms including both blue bands (at 412 nm and 443 nm) may therefore help to discriminate between chlorophyll a and CDOM. The 412 nm band may also be used to discriminate between photosynthetically active chlorophyll a and phaeopigments (Darecki and Kowalczuk 1996). However, it was mostly aimed at producing algorithms for the quantification of CDOM, which is particularly important for remote sensing in the Baltic Sea. The spectral resolution of SeaWiFS is better than that of CZCS, and will probably be sufficient for algorithm development for OICs in Case-1 waters. However, because of the interference of CDOM and SPM in Case-2 waters, the spectral resolution might not be enough for any detailed information about phytoplankton composition. There is also a problem with the spatial resolution of about 1 km, which is more than adequate for remote sensing of the open ocean, but insufficient for many coastal areas and lakes. NASA produced a map for the global ocean chlorophyll concentrations as derived from SeaWiFS data acquired between September 4 and October 28 (SeaWiFS project 1997). The values in the Baltic Sea are highly over-estimated, and the map looks more like a distribution map for CDOM. A new SeaWiFS reprocessing round was performed in August-September 1998, and another round was performed in spring 2000. The aim was to improve the derived products, especially in the coastal and high latitude zones where negative water-leaving radiances and erroneously high chlorophyll values have hampered research.

6.1.6 Combining remote sensing with other monitoring techniques

Since 1992, the Algaline project at the Finnish Institute of Marine Research has been monitoring the variability in phytoplankton biomass and species composition, as well as surface temperature, salinity and nutrient concentrations. Water samples are taken at

5 m depth using unattended recordings of *in vivo* fluorescence, and automatic water samplers, on passenger ferries (also called ships-of-opportunity). Most recordings are carried out on the ferry Finnpartner which crosses the Southern Baltic from Helsinki to Lübeck (previously Finnjet from Helsinki to Travemünde; Leppänen *et al.* 1991; Rantajärvi and Leppänen 1994).

The *in vivo* fluorescence gets converted to chlorophyll a concentration, and the species composition of the water samples is determined by microscopic analysis. Kononen and Leppänen (1997) describe the application of a multi-scale research strategy for monitoring the patchiness, scales and controlling mechanisms of cyanobacterial blooms by combining different techniques such as ship-of-opportunity, satellite imagery, intensive case studies by research vessels, and information from laboratory experiments.

In order to improve the monitoring of the Baltic Sea environment Victorov (1996) suggested the creation of an integrated Baltic Europe GIS based on existing national databases, combining the knowledge of a variety of disciplines including cartography, geology, meteorology, as well as municipal, agricultural and demographic statistics, etc. He suggested that this database consisted of permanent parts (e.g. historical information), and operational parts which may become permanent after a detailed assessment procedure (Victorov 1996). The operational network data may include a subsystem of different alarm levels which he terms alarm level 1 and alarm level 2. The idea is that alarm level 1 is used as a preliminary one, and requires additional observations to either generate an alarm signal of level 2 or to switch off the alarm subsystem.

6.1.7 Discussion

Remote sensing provides a powerful tool for monitoring toxic algal blooms due to its spatial and temporal coverage and the variety of sensors available, provided the data can be interpreted successfully. For example, measurements of SST can help to identify upwelling or frontal regions, which tend to be areas of increased productivity. AVHRR imagery has helped us to understand bloom development, dynamics and coverage. It may also have the potential of monitoring the effects of eutrophication.

The limitations of AVHRR, CZCS and TM for monitoring algal blooms in the Baltic are obvious: the limited spectral resolution (small number of bands) and the broad band widths do not allow for any detailed spectral information about the OICs in Case-2 waters. The algorithms produced for CZCS were successful for retrieving the sum of

chlorophyll a and phaeopigments in Case-1 waters. When applied to the optically more complicated Case-2 waters, several problems interfere with the retrieval. Firstly, it is difficult to separate the water-leaving radiance from the radiance scattered by the atmosphere. Secondly, absorption in the Baltic Sea is not only affected by phytoplankton pigments, but also by CDOM, as well as SPM in the coastal areas. Thirdly, backscattering due to particles in the water may become the most important factor determining the ocean colour signal, as opposed to pigment absorption. With the advent of new ocean colour sensors with higher spectral resolution such as MOS, OCTS and SeaWiFS, it should be possible to retrieve much more detailed information from the spectral composition of the water leaving radiance using more channels with smaller defined band widths, and after correcting for atmospheric effects. The improved spectral resolution may help to discriminate between the major light-absorbing and scattering constituents encountered (CDOM, SPM and phytoplankton pigments), and maybe even between different phytoplankton groups such as diatoms and cyanobacteria.

This type of satellite imagery has inherent limitations for the remote sensing of toxic algal blooms because of the frequent cloud cover in the Baltic Sea region, and because the sensors can only detect blooms close to the surface. In the case of toxic cyanobacteria the blooms are only detected under certain weather conditions (low wind, clear sky). This makes it difficult to predict any new formations rather than just monitoring the movement or the dispersal of the bloom. Another complication is that *A. flos-aquae* tends to accumulate at 10 m depth, which may be too deep to be detected by satellite.

In order to advance the use of remote sensing there is a need for better understanding of the optical properties that contribute to the remotely sensed signal, and the general properties of the observed water body. Unfortunately, measurements of CDOM and SPM are not included in routine monitoring programs of the Baltic Sea (HELCOM 1996). However, CDOM is spectrally dominant in the blue part of the absorption spectrum, except in blooms, and highly variable. SPM concentration and particle size-distribution are vital parameters for describing the volume-scattering function, and ultimately linking backscatter to the spectral remote sensing reflectance of the water. In order to improve the interpretation of Baltic Sea imagery we need to know the range of variability of all optical in-water parameters. Optical modelling, then, can be used to predict remote sensing reflectance from information about a particular set of OICs. In the following part of this chapter the Menai Strait model described in Chapter 5 is

adapted to the Baltic Sea. Furthermore, MPA is used as a form of inverse modelling to derive OICs from measured colour ratios.

6.2 Optical modelling of Baltic Sea water

Abstract

A semi-empirical optical in-water model developed for the use of a four-channel colour sensor in the Menai Strait (characterised by high mineral suspended sediments) is adapted for use in the Baltic Sea (characterised by high CDOM and lower sediment). The model predicts colour ratios from the absorption properties of pure sea water, CDOM, SPM, and phytoplankton, and the back-scattering properties of water and SPM, including corrections for sensor depth and self-shading. Specific absorption coefficients for the OICs were derived from laboratory measurements. The specific absorption coefficient of phytoplankton was divided into two categories: (a) phytoplankton dominated by diatoms/dinoflagellates, (b) phytoplankton dominated by cyanobacteria. The model was tested with cruise data and with data from an optical field station north of Gotland. The RMS of the model predicted against the measured colour ratios was 0.096. Multiple regression analysis was used to derive OICs from colour sensor data (inverse modelling).

6.2.1 Introduction

For modelling the optical characteristics of the Baltic Sea a semi-empirical optical model was used which was originally developed for the Irish Sea and later the Menai Strait (Harker 1997; Kratzer *et al.* 2000 - see Chapter 5).

6.2.2 Materials and methods

Field work and laboratory methods

The data used for this work were gathered during two cruises across the Baltic Sea on RV Argos (SMHI Oceanographic Laboratory), in late May/early June 1998 and late August 1998 (see Table 2.1, Chapter 2), and at an optical field station close to Ar on the north coast of Gotland, in July-August 1998. Figure 6.4 shows the position of the Ar field station, and of the cruise stations. The two cruises were aimed at studying the spatial changes of the bio-optical properties across the Baltic Sea, while the field station was set up to investigate the optical properties of Baltic Sea waters during summer. The field station is well situated for optical investigations because the absence of significant

river run-off and the proximity of the Gotland Deep cause the water to be comparatively clear, i.e. with low sediment input.

The colour sensor CS22 was used during the May/June cruise to measure upwelling irradiance at 27 cm below the surface (Figure 6.5a). Figure 6.5b shows CS24 measuring downwelling irradiance while CS22 was measuring upwelling irradiance in the water. The sensors were always deployed on the sunny side of the ship (Mueller and Austin, 1995) in order to avoid ship shading. Another measure to avoid ship shading was to deploy the in-water colour sensor vertically in a floating frame, so it could float away from the ship during measurements, attached to the ship by a rope (see Figure 6.5a).

CS22 was also deployed in summer 1998 on a moored platform at the same depth, about 1 km offshore from Ar (see Figure 6.4). Great care was taken to avoid shading by the platform. The platform was built in a triangular fashion, and the colour sensor was deployed on a vertical, south facing steel rod (Figure 6.6 a) with the colour sensor facing downwards measuring upwelling irradiance at about 27 cm depth below the sea surface (Figure 6.6b, Kratzer *et al.* 1998). The colour sensor was logging every 10 minutes, with a sampling time of 30 sec. A Thermistor chain (Aandera Instruments, Bergen) was deployed on the same raft, measuring at 1 m increments down to 11 m depth. The Thermistor chain was set to log once every hour. Both instruments had their internal clocks set to GMT. Over a period of about two weeks (day 204-216), water samples were taken close to the mooring every other day if the weather allowed. A Secchi disk reading was taken prior to sampling in order to be able to judge how much water volume would be needed for filtration.

All OICs, i.e. coloured dissolved organic matter (CDOM), phytoplankton pigments, and suspended particulate matter (SPM), were measured on board ship during the Argos cruises, and in the laboratory in Ar during the colour sensor deployment near Gotland. For consistency and comparability of the data sets, the same optical measurements were performed as described in Chapter 2, section 2.3 and Chapter 5. A small boat was used to take water samples close by the moored platform. There were no severe problems with fouling of the colour sensor during the deployment in Gotland, but in order to prevent any possible fouling, the sensor head was cleaned weekly.

During the Argos cruises in May/June, profiles of downwelling irradiance were made with a GER 1500 spectroradiometer (Geophysical and Environmental Research Corp.), and a LI-190SZ quantum sensor (LI-COR, inc.) was used for measuring downwelling

irradiance above the surface (photosynthetically active radiation, PAR). These data belong to the Limnology Department at Uppsala University, but Don Pierson and Nicklas Strömbeck kindly provided the data for inclusion into our Baltic Sea model. The hyperspectral GER 1500 instrument was used to derive the downwelling diffuse attenuation coefficient K_d for the four colour sensor channels. These values were used to derive the spectral average cosine, which was then included into the semi-empirical model. A profiling Hydroscat-6 spectral backscatterometer (HOBI Labs) was used in the Skagerrak to measure profiles of b_b at six wavelengths, which were then weighted by $\exp(-2 K_d z)$, where z is depth, to obtain the surface equivalent value for b_b. These values were then interpolated to the colour sensor wavelengths and regressed against the concentration of SPM to find b_b*SPM. These values for b_b were also included into the new version of the model.

The measurements with the GER 1500, LI-190SZ and Hydroscat-6 were performed by Niklas Stömbeck. The data were calibrated by Don Pierson, and incorporated into the model by Peter Land (see below). Peter Land and I transferred the Menai Strait model which had been written by Dave Bowers in Basic into an Excel spreadsheet.

The model

The original model of Harker (1997) computed ratios of subsurface irradiance reflectance R at two wavelengths. Kratzer *et al.* 2000 (see also Chapter 5) modified it to predict ratios of upwelling irradiance measured by the colour sensor at a depth z below the sea surface. The model assumes that R is proportional to the ratio of backscattering, b_b and absorption, a (Chapter 5).

$$\text{colour ratio}[1,2] = \{(b_b[1] / a[1]) / (b_b[2] / a[2])\}.\exp\{-z.(K_d[1] - K_d[2])\}.f[1,2]$$

where [1] and [2] refer to colour sensor channels. The factor f corrects for differences in sensitivity between channels, based on measurements of above water downwelling irradiance in cloudy conditions, and measurements of the immersion effect (as described in Chapter 3).

The Baltic Sea version of the model calculates b_b as the sum of contributions from water and SPM:

$$b_b(\lambda) = b_{bw}(\lambda) + b_b{*}SPM(\lambda)\cdot[SPM],$$

and absorption as the sum of absorption by water, phytoplankton pigments, SPM, and CDOM:

$$a(\lambda) = a_w(\lambda) + a^*_{ph}(\lambda)\cdot[\text{chl a}] + a^*_{SPM}(\lambda)\cdot[\text{SPM}] + a^*_{CDOM}(\lambda)\cdot g_{440}$$

where a_w is the absorption by sea-water, a^*_{ph} and a^*_{SPM} are respective specific absorption coefficients of phytoplankton pigments (m^2 (mg chl a)$^{-1}$) and SPM (m^2 (g dry weight)$^{-1}$), and a^*_{CDOM} is a dimensionless specific absorption coefficient for CDOM (see Chapter 5). The absorption by sea water was taken from Pope and Fry (1997).

The model was further developed (Kratzer *et al.* 1998) to include the immersion effect on downwelling irradiance, instrument self-shading, spectral variation in the diffuse attenuation coefficient K_d, and the effect of backscattering on K_d. Figure 6.7 shows a schematic illustration of the semi-empirical model and its input parameters.

The use of the model for prediction of colour sensor ratios required knowledge of the wavelength-dependent parameters for the four different colour sensor channels, corrected for the colour sensor's spectral response. These are sea water absorption (as obtained from Pope and Fry 1997); backscatter of water, b_{bw}, which was interpolated by Peter Land from the SeaWiFS wavelengths (Gregg *et al.* 1993) using a power law, as well as the specific absorption coefficients a^*_{ph}, a^*_{SPM}, a^*_{CDOM}, $b_b{}^*_{SPM}$, and μ, which were derived from laboratory and field measurements. I derived Baltic Sea specific a^*_{ph}, a^*_{SPM}, and a^*_{CDOM} using a spectrophotometer as described in Chapter 2 and 5.

Peter Land derived K_d from the GER 1500 measurements, and then used K_d to calculate μ from a modification of Gershun's law, to account for backscattering:

$$\mu = a_w + b_{bw} + (a - a_w) / K_d$$

The total absorption coefficient (which I had calculated) excluding water, $a - a_w$, was regressed against $K_d - K_{dw}$, where $K_{dw} = a_w + b_{bw}$ (Smith and Baker 1978), to find a value of the average cosine μ. This is a simplification of Gershun's law, modified to account for backscattering. The original form of Gershun's law ($a \approx K_d\,\mu$) was found not to fit the data in the green and red channels. K_d was then used in the model to extrapolate the colour sensor readings to the surface. Sensor self-shading was also corrected for by Peter Land using the method of Gordon and Ding (1992). This self-

shading had not been accounted for in the Menai Strait model. Figure 6.8 summarises the different corrections applied to the raw data set. The sensitivity and immersion correction (box a and b) was worked out by myself whereas Peter Land performed the depth and the shading correction (box c and d).

The colour ratios predicted by the model were then plotted against the measured colour ratios.

Regression analysis

Both simple and multiple regression analysis were used to derive a time series of chlorophyll, CDOM, and SPM from the colour ratios of the radiometer moored in the north of Gotland. The same analysis was applied as described in Chapter 5 for the Menai Strait data (Kratzer *et al.* 2000). For data analysis, the colour sensor data were averaged daily over two hours before and two hours after local noon (Wild-Allen *et al.* 1997; Kratzer *et al.* 2000). The temperature at 1 m depth was averaged in the same way as the colour sensor data in order to see if there was a correlation between the chlorophyll concentration and temperature.

6.2.3 Results

Field work and laboratory measurements

The phytoplankton absorption spectra were divided in two shape categories: (a) diatom/dinoflagellate dominated spectra, and (b) cyanobacteria dominated spectra (see Figure 6.9). This was a step towards working out regional as well as seasonal chlorophyll-specific absorption coefficients for the Baltic Sea model. All spectra from the May/June cruise belonged to the first category, whereas the spectra from the Gotland station belonged to the second category. The data from the cruise in August had to be divided into both categories: all samples from the Kattegatt/Skagerrak area belonged to category (a), whereas samples gathered in the Baltic Sea (all BY stations, as well as SSI and SSII) belonged to category (b). In category (b) samples, decolourisation by methanol left a pink hue on the filter, possibly due to phycoerythrocyanin, a pigment characteristic of cyanobacteria (see Chapter 7). During filtration it was possible to detect the cyanobacteria filaments by eye.

As an example, Figure 6.10 shows the total absorption coefficient, and contributions due to water, CDOM, SPM, and *in vivo* pigments as derived from spectrophotometric

measurements for station Å16 (26 May 98) in the Skagerrak. Figure 7.5 (see next chapter) shows the same for the optical station in Ar, 5 August 98. Both figures illustrate the importance of CDOM in the blue part of the spectrum. However, in the Baltic Sea, the absorption coefficient for CDOM in the blue is higher by about a third compared to the one in the Skagerrak.

In order to calculate the relative contribution of each OICs for the whole data set, the proportion of a - a_w due to CDOM, SPM, and *in vivo* pigments was calculated at each station (surface samples only). The data set was again divided into the categories (a) and (b) mentioned above.

During the spring cruise, CDOM was mostly the dominant absorber. It accounted for 60-90% of absorption from 400-600 nm, and even around the chlorophyll peak at 670 nm, it still accounted for 10-40%. The g_{440} values varied from 0.21 to 1.89, with a mean of 0.53, higher in the central Baltic Sea than in the Skagerrak, except close to river outlets. The exponent varied from -0.0149 to -0.0191 nm^{-1}, with a mean of - 0.0171 nm^{-1}. The pigment absorption was only dominant around the 670 nm peak, with 50-90% of total absorption. In the blue to green (470-600 nm) it made up 10-50% of the total absorption, and in the blue only about 20%. The surface chlorophyll values during this cruise were rather low, ranging from 1.0 to 2.6 $\mu g\ l^{-1}$, mean: 1.85 $\mu g\ l^{-1}$, in the Kattegatt/Skagerrak area, and from 1.2 to 2.3 $\mu g\ l^{-1}$, mean: 1.7 $\mu g\ l^{-1}$ in the central Baltic Sea. SPM was the weakest absorber, with 0-20%. The concentrations of SPM were low, ranging from 0.4 to 2.0 $g\ m^{-3}$, with a mean of 0.9 $g\ m^{-3}$ in the Baltic Sea area, and from 0.5 to 3.4 $g\ m^{-3}$, with a mean of 1.8 $g\ m^{-3}$, in the Kattegatt/Skagerrak. The highest SPM concentrations were found in the Skagerrak in Singlefjorden (east of Oslofjorden). Compared to the SPM concentrations in the Menai Strait (Chapter 5), however, these concentrations were low.

Both in Gotland and at the Baltic Sea stations of the August cruise, CDOM was again the main absorbing OIC in the blue (see Figure 6.10 and 7.5), accounting for about 80% of total absorption at 400 nm, with a broadly linear decrease to about 5% at 675 nm. The g_{440} values ranged from 0.05 to 0.3 with a mean of 0.24, lower than the mean spring value. The exponent varied from -0.0191 to -0.0230 nm^{-1}, with a mean of -0.0204 nm^{-1}, and was higher than in spring. The pigment absorption made up 10 to 15% at 400nm. Absorption by phycobilins was apparent in a distinct double feature with a shoulder

around 500 nm, with 40-60% of total absorption, and a distinct shoulder around 570 nm, with 55-75%. At 675 nm, pigment absorption ranged from 85 to 95%.

The chlorophyll values ranged from 2.2 to 3.9 $\mu g\ l^{-1}$, with a mean of 2.9 $\mu g\ l^{-1}$ for the measurements in Gotland, and from 2.5 to 3.4 $\mu g\ l^{-1}$, with a mean of 2.8 $\mu g\ l^{-1}$ at the Baltic Sea stations of the August cruise. Chlorophyll values in the Kattegatt/Skagerrak area were much lower during this cruise: they ranged between 0.4 and 1.4 $\mu g\ l^{-1}$, mean 0.8 $\mu g\ l^{-1}$. The SPM fraction was again the weakest absorber, accounting for less than 10% at 400 nm and 675 nm, and 30% at 600 nm. SPM ranged from 0.6 to 1.3 $g\ m^{-3}$ in Gotland (mean: 1.0 $g\ m^{-3}$), from 0.8 to 1.0 $g\ m^{-3}$ (mean: 0.9 $g\ m^{-3}$) in the Baltic Sea, and from 0.5 to 2.0 $g\ m^{-3}$ (mean:0.9) at the Kattegatt/Skagerrak stations during the August cruise. The exponent for CDOM was found to vary little over the three data sets with an overall mean of -0.0191 nm^{-1}, and a standard deviation of 0.0021 nm^{-1}.

The summer of 1998 was relatively cool, and the water at the station off Gotland was quite well mixed down to 11 m (Figure 6.11) with water temperatures at 1 m depth ranging from 13.2 to 17.2 °C, with a mean of 15.7 °C from day 181 to day 216. The upper panel in Figure 6.11 shows short periods of stratification (comparing the water temperature at 1m and 11 m depth). The cyanobacteria filaments in the water were visible by eye due to their size and scattering properties. They seemed well distributed within the water column. As seen under a stereoscope microscope the cells looked very healthy, and were green in hue, with the *A. flos-aquae* cells being of a slightly darker green. Both *A. flos-aquae* and *N. spumigena* were present in approximately equal amounts.

Results of semi-empirical model

The SPM-specific backscatter coefficient, $b_b^*{}_{SPM}$, as derived from the Hydroscat measurements in the Skagerrak was dependent on waverlength. It was 0.072 $m^2\ (g\ SPM)^{-1}$) in the blue, 0.038 $m^2\ (g\ SPM)^{-1}$) in the cyan, 0.015 $m^2\ (g\ SPM)^{-1}$) in the green and 0.005 $m^2\ (g\ SPM)^{-1}$) in the red channel.

The average cosine, μ, as derived from the GER 1500 measurements, also changed spectrally. It was 0.8 in the blue, 0.7 in the cyan, 0.46 in the green, and 0.26 in the red channel.

The shading correction, derived from these data, decreased the red:green ratio by 5.38%, and increased the cyan:geen and blue:green ratios by 1.8% and 1.82% respectively.

The model-predicted colour ratios were plotted against the measured ratios (Figure 6.12) for comparison with the ideal 1:1 line. The overall correlation was high (r = 0.82). The red:green ratio was very highly correlated (r = 0.97), but all points were situated under the 1:1 line. The cyan:green ratio was well correlated (r = 0.61), but most points were situated above the 1:1 line. The blue:green ratio was least well correlated (r = 0.56), and most points were above the 1:1 line. However, considering the low range of blue:green values, the blue:green ratio was quite well predicted, especially when compared to the results of the Menai Strait model.

The overall RMS of the errors was 0.096, most of the error being due to the red:green ratio, which had an RMS error of 0.150. The RMS errors of the cyan: green and blue:green ratios were 0.072 and 0.034, respectively. The high RMS value for the red:green ratio can be explained with the higher range of values (from about 0.25 to 0.9). The cyan:green ratio ranged from about 0.1 to 0.4, whereas the blue:green ranged only from 0 to about 0.1. Dividing the RMS by the appropriate range, the relative values for the three ratios were 0.26, 0.18, and 0.3, respectively, the cyan:green ratio value being lowest.

Multiple regression analysis

Table 6.1 shows the results of the best single, and multiple regression analyses of all OICs. They were all best described using multiple regression, and in the case of chlorophyll and SPM a $\log_e$ transformation gave the best correlation. Initial MRA of the whole Baltic Sat data set had shown that the algorithms differed according to region. Therefore, the algorithm of the Gotland series reported in this thesis was used to predict the time series of OICs from the colour sensor ratios. The coefficient of determination for chlorophyll and CDOM was very high, which may be a result of the low degree of freedom (n = 6, 4 variables to predict, leaves only 2 df). However, MRA of the whole Baltic Sea data set from 1998 (including samples from spring as well as the Kattegatt and Skagerrak) showed very high correlations using the same number of variables.

It is notable that (in the Gotland data set) there was a good correlation between SPM and chlorophyll a concentration, which means that most of the suspended matter was of biological origin (probably from cyanobacteria). This was confirmed by the combustion of the SPM filters. The filters turned from green to white after baking, and no trace of inorganic particles was visible. G_{440} was not correlated to the chlorophyll concentration,

which is to be expected in Case-2 waters. It is also notable that there was no significant correlation between chlorophyll and temperature during this survey.

Figure 6.13 shows the time series of colour ratios as derived from the colour sensor measurements at the raft. Figure 6.14 shows the time series of chlorophyll a, CDOM and SPM as derived from the colour sensor measurements using multiple regression analysis (Table 6.1). The chlorophyll concentration of the water samples from Gotland ranged only from 2.2 to 4.0 µg/l (measured values taken between day 201 and day 215), with a mean of 2.9 (+/- 0.6) µg/l. However, the predicted values of the Gotland time series (day 181 to day 216) went as high as 9.8 µg/l. The time series shows that there was not much variability in the concentrations of all OICs which implies a rather constant light field around noon.

6.2.4 Discussion

The results in Section 6.2.3 emphasise the dominance of CDOM in Baltic spectral absorption. The strong absorption by CDOM may pose a severe restriction in terms of satellite remote sensing. The sensitivity of current ocean colour sensors may not be adequate for water bodies with high contents of CDOM. The exponent of the CDOM spectrum is different in the Baltic Sea (mean of -0.0191 nm^{-1}) compared to the one in the Menai Strait (mean -0.014 nm^{-1}). According to Carder *et al.* 1991, this may indicate that the CDOM molecules in the Baltic Sea consists mostly of fulvic rather than humic acids.

Figure 6.9 shows the spectral shape of a typical cyanobacteria dominated spectrum, and that of a diatom/dinoflagellate dominated spectrum. There is a well-defined shoulder in the cyanobacteria-dominated spectrum at 570 nm, which is an indication for phycobiliproteins. This result illustrates that it was necessary to divide the chlorophyll-specific absorption spectra into separate categories which imply a regional, as well as seasonal split. The chlorophyll values in summer were much higher in the Baltic Sea area than in the Kattegatt/Skagerrak area. This coincides with the presence of cyanobacteria which seem to imply a relatively high chlorophyll standing stock in summer, with chlorophyll values ranging from 2.2 µg l^{-1} (after a stormy period in Gotland) to 4.0 µg l^{-1}.

The SPM values show a distinct difference between two regions: in the Baltic Sea the values are lower and less variable than in the Kattegatt/Skagerrak area. Furthermore,

the SPM values are consistent in spring and summer in the Baltic Sea, whereas there is a big difference between the spring and the summer values for the Kattegatt/Skagerrak area. This may be due to increased river discharge in the Skagerrak during spring.

Semi-empirical model

The colour ratio model aims to predict remote sensing reflectance from colour sensor ratios of up-welling irradiance. The model results were not satisfactory. A distinct improvement was made by putting in the corrections for the immersion effect: the RMS of the model errors was improved from 0.117 to 0.096 (see Figure 6.12). However, a sensitivity test on the Menai Strait model showed an increase in the RMS values when the immersion effect was included into the Menai Strait model. It will therefore be necessary to test inclusion of the immersion effect on an additional, independent data set.

The model might also be improved by including downwelling irradiance, because R could then be directly derived from the ratio of upwelling to downwelling irradiance. This would also increase the number of possible OICs that can be derived from the data set, as one would not have to use colour ratios, which would allow for the estimation of another variable.

Attenuation of light in the water is a decrease in the energy of light due to absorption and scattering combined. In order to model the light field of the Baltic Proper accurately one would need to consider the scattering properties of particles (which consist mostly of phytoplankton in the open Baltic), as well as the absorption properties of water, CDOM, phytoplankton and its pigments, and suspended particulate matter (SPM). Most optical models have the concentrations of Chlorophyll a, SPM and CDOM as input parameters. Figure 6.15 illustrates in a simplified manner the way in which these models work. Many of the complicated relationships can be derived from theory and from the literature (e.g. Kirk 1994). However, little is known about the scatter and backscatter properties of cyanobacterial blooms. It is possible that the mismatch between ratios measured in the Baltic, and those predicted by the semi-empirical model was because of one or more false assumptions, such as assuming scattering to be wavelength independent.

The Baltic Sea version of the model included a term for backscatter which was derived from stations in the Skagerrak in spring 1998. However, scattering is likely to change

over time and over different regions (because of change in sediment load, occurrence of blooms etc.).

Improved instrumentation will make it possible to improve the model by measuring additional parameters. For example, the AC9 (WETLabs) measures absorption and attenuation at nine wavelengths. It will be possible to derive spectral scattering from those two measurements. The ECO VSF (WETLabs), a volume scattering function meter, will allow to account for a more accurate measure for backscatter than derived from theory. With the information from both instruments it should be possible to derive backscatter for 9 wavelengths, and to improve the Baltic Sea model.

Regression analysis

The best single predictor for chlorophyll was the blue:green ratio (see Table 6.1). This is surprising because of the low range of the blue:green ratio, and the strong absorption of CDOM in the blue part of the spectrum. The explanation may be that the CDOM values at the station in Ar were not very variable. The single regression for chlorophyll a in Table 6.1 has a negative slope, showing that chlorophyll a and the blue:green ratio were inversely related and that an increase in chlorophyll a concentration led to a decrease in the blue:green ratio, which is to be expected because of the strong absorption of chlorophyll in the blue.

The best single predictor for CDOM was the red:green ratio. Table 6.1 shows a positive relationship between CDOM and the red:green ratio, i.e. the slope of the single regression is positive. This means the more CDOM, the higher the red:green ratio. This may be explained by the stronger absorption of CDOM in the green than in the red part of the spectrum. The best single predictor for SPM was also the cyan:green ratio. However, the proportion of explained variance was very low (0.28). Chapter 5 showed that the red:green ratio was the best predictor for SPM in the Manai Strait (which was optically dominated by SPM). The explanation for cyan:green being the best single predictor for SPM in the Baltic Sea may be explained by the strong correlation between SPM and chlorophyll.

The multiple regression analysis showed that it was possible to derive chlorophyll, CDOM as well as SPM for the Gotland data set, and that the colour sensor is well suited for estimating OICs directly from colour ratios. This makes the instrument a very good tool for in-water monitoring over long periods of time. In combination with a semi-analytical model the colour sensor may be a powerful tool for the analysis of remote

sensing data because all the derived OICs are input parameters for semi-analytical models that predict remote sensing reflectance.

The comparison between the algorithms for the Gotland data set (Table 6.1) with the Menai Strait data set (table 5.1) demonstrates that algorithms have to be regional. The algorithm produced for the Gotland time series is not necessarily valid for the whole of the Baltic Sea, or even for all seasons at Gotland. Because of the higher variability in sediment load, CDOM concentrations, and pigment composition of phytoplankton, a universal algorithm for the whole of the Baltic Sea is unlikely to predict local conditions as accurately. An analysis of the whole Baltic Sea data set (which is not reported here in the thesis) also showed that the algorithms were regional.

A multi-scale research strategy

The cyanobacteria did not bloom during the monitoring station in the north of Gotland. In the Baltic Sea as a whole blooms only developed in very restricted areas in 1998. During the sampling period in Gotland, there was a bloom in the Northern Baltic proper (21 July 1998), NE of Gotland and in the Gulf of Finland (23 July 1998) as shown by AVHRR algal bloom imagery (Ove Rud and Miho Ishii, Department of Physical Geography, Stockholm, http://www.natgeo.su.se/~ab3). The blooms did not occur at the field station, which is unusual (Lars Westin, personal communication). However, both *N. spumigena*, and *A. flos-aquae* were dominant throughout the period of investigation. Therefore, the data set may be representative of pre-bloom conditions. This may help to determine the optical conditions leading to a toxic bloom, which in turn may help with the prediction of toxic blooms.

During a cruise on R.V. Searcher in the Baltic Sea in summer 1999 (Kratzer and Subramanium 2000), the water temperature at 1 m depth was significantly higher (with a mean of 17. 4 °C) than during the investigation in Ar (mean 15.7), and *Nodularia spumigena* blooms developed all over the Baltic Proper (Subramanium *et al.* 2000). I investigated these dense blooms by snorkelling and was surprised how much the water temperature changed from pleasantly warm to quite cold as I was snorkelling from a dense patch into a less dense part of the bloom. The visibility increased from a few centimetres to a few metres. I also looked at the vertical structure of these dense filaments by snorkelling down to a depth of about 5 m, and slowly coming back up to the surface. There was a strong density gradient, especially in the last 50 cm: the bloom got denser towards the surface. The water was also noticeable warmer in the upper half

metre. These observations, although only qualitative, show that in order to understand bloom development and dynamics it is necessary to combine measurements on different scales. For improved interpretation of satellite remote sensing and for optical monitoring, it would be desirable to include all OICs into routine monitoring programs. Figure 6.16 is an attempt to put the idea of a multi-scale research strategy as proposed by Kononen and Leppänen (1997) into a broader context aiming to match up remote sensing with monitoring, and ultimately to provide the end-user with necessary information for environmental policies and decision making. Prediction of toxic blooms may require the combination of remote sensing with other techniques such as *in situ* monitoring and bio-optical and dynamical models in order to predict toxic algal blooms in the Baltic Sea. These models need to incorporate the optical characteristics of the different OICs as well as the interaction with their environment.

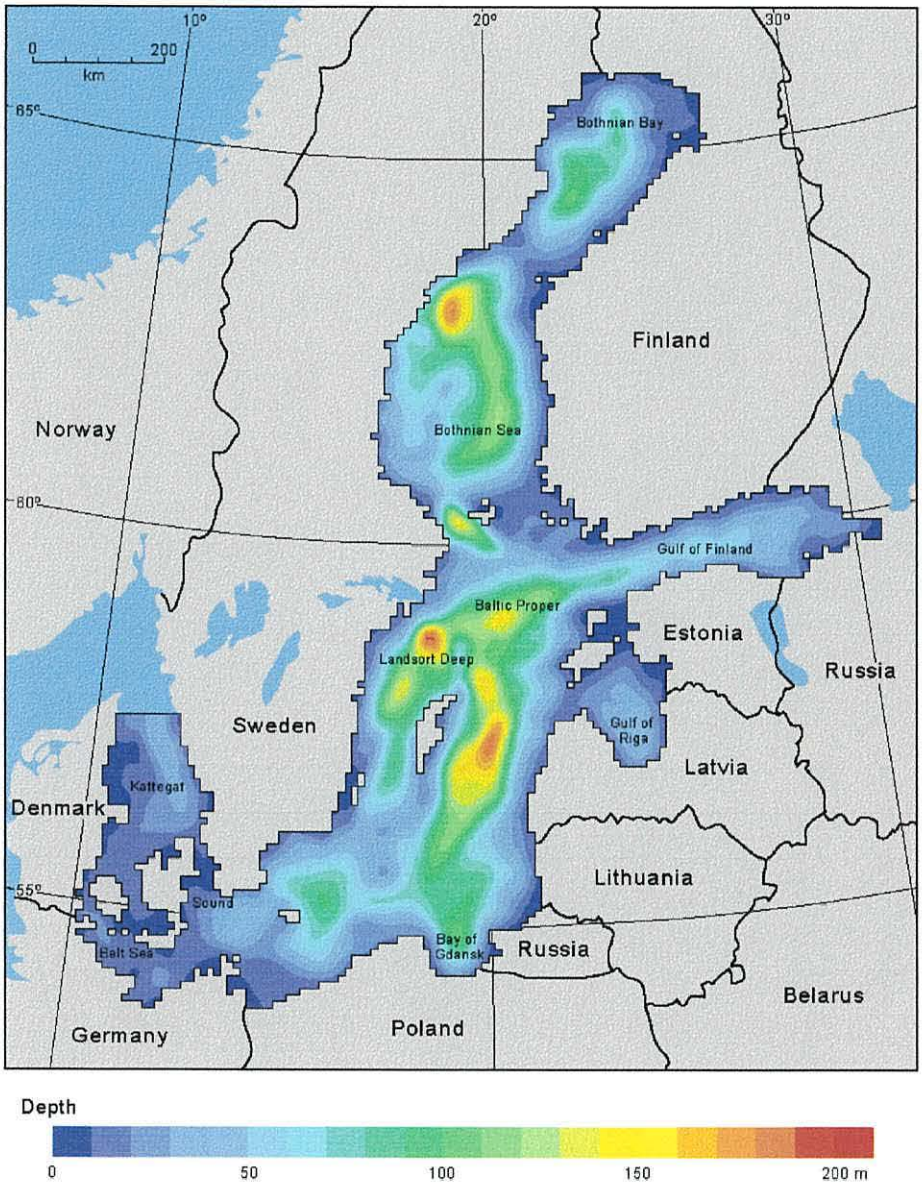

Figure 6.1 Depth distribution of the Baltic Sea. With a mean depth of 52 m the Baltic Sea is very shallow. Landsort Deep is the deepest part in the Baltic Proper, with a depth of 459 m. Map from http://data.ecology.su.se/baltic96/depth.htm, geo-referenced by Ivonne Anders.

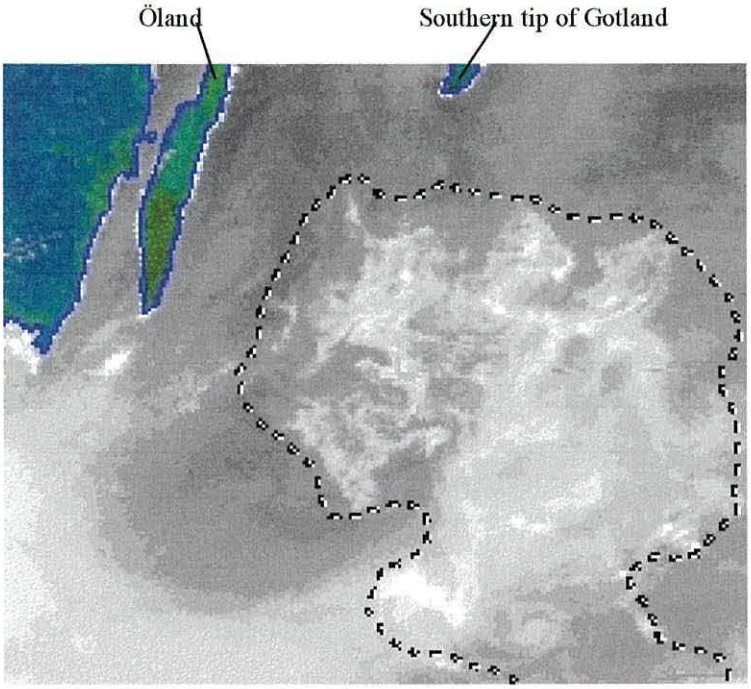

Figure 6.2 Algal bloom from space. Mosaic image made from satellite data registered 8 August, 1997 by NOAA-14. Land areas: false colour composite of AVHRR channel -1,2 and 4; water areas show only channel-1. Image by courtesy of Ove Rud.

Aphanizomenon flos-aquae

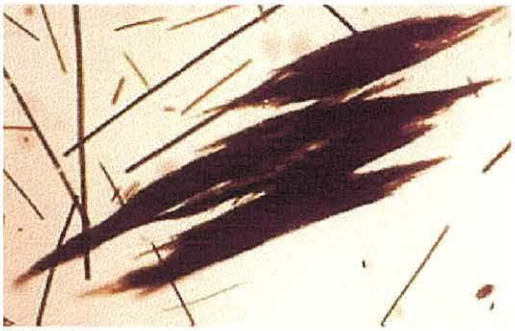

Colonies.
Measurement unavailable; probably 100x.
from: http://www-cyanosite

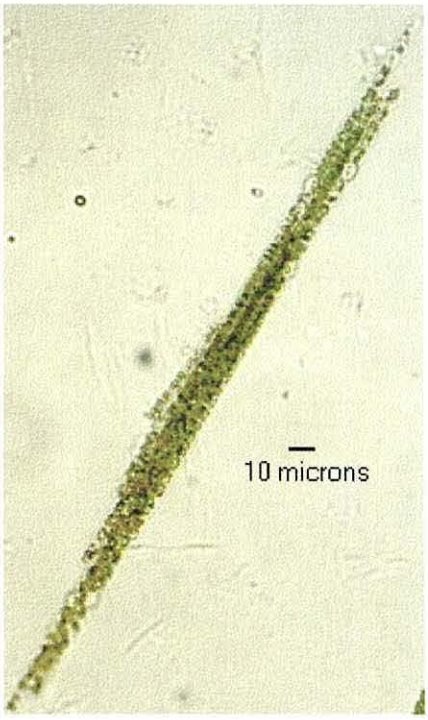

Colony. Akinetes absent. 400x
from: http://www-cyanosite

Nodularia spumigena

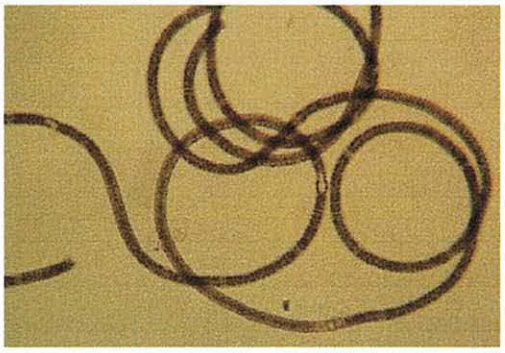

(filament diameter ca 10μm)
http://www.botan.su.se
Photograph by courtesy of
Birgitta Bergman.

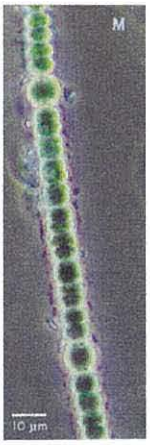

***Nodularia* sp.**
from: http://www-cyanosite

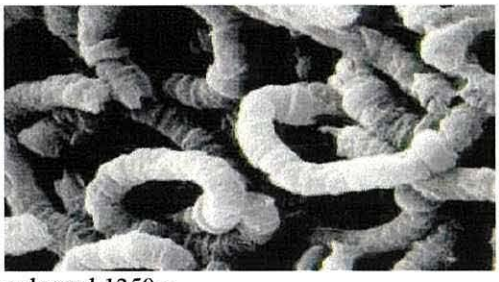

enlarged 1250 x
from: http://www-cyanosite

Figure 6.3 *Aphanizomenon flos-aquae* and *Nodularia spumigena* -the most common filamentous cyanobacteria species in the open Baltic Sea. *A. flos-aquae* can be found over the whole year, whereas *N. spumigena* produces extensive surface accumulations in late summer.

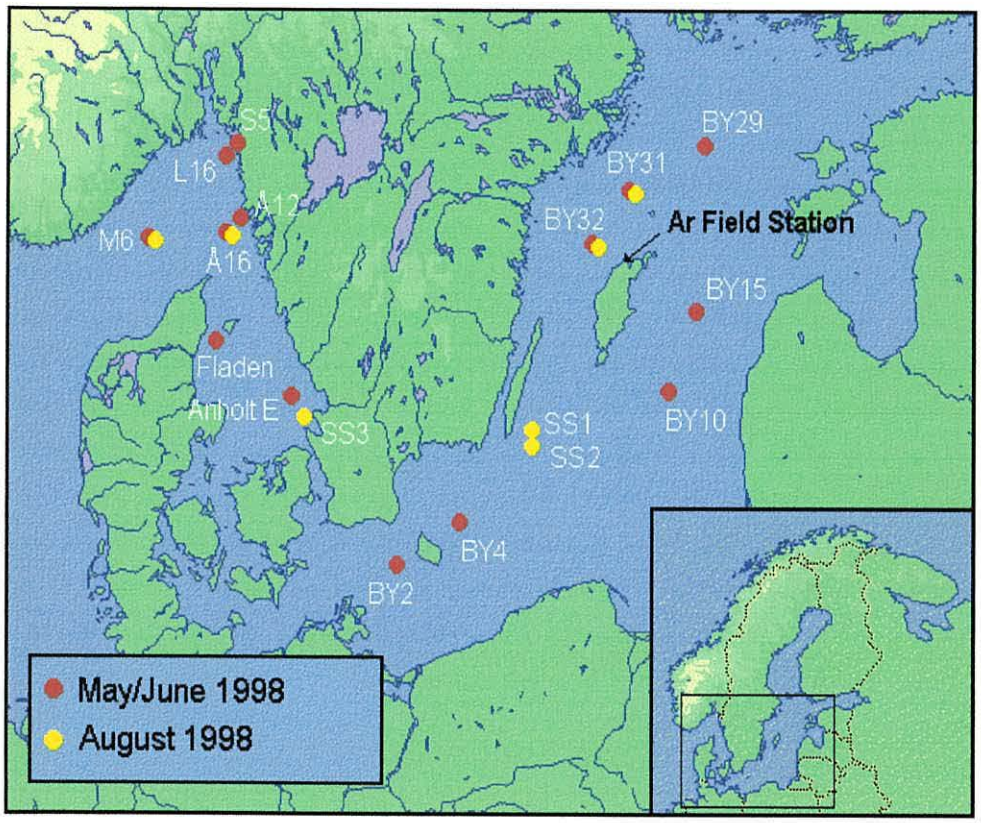

Fig. 6.4 Map of the Baltic Sea showing the positions of the two cruises and of the optical field station in Ar, Gotland. The map in the right hand corner shows an overview of the Baltic Sea area. This map was produced by Niklas Strömbeck.

Figure 6.5 a During the ARGOS cruises in 1998 CS22 was deployed in a floating frame to measure upwelling irradiance.

Figure 6.5 b CS24 was deployed on deck to measure downwelling irradiance. The sensor was held upright on a wooden frame. The sensor saturated in clear skies.

Figure 6.6a Henrik Lindh from SMHI with his triangular raft construction. The design of the raft was aimed at avoiding shading of the colour sensor. CS 22 was deployed on the aluminium rod, facing south.

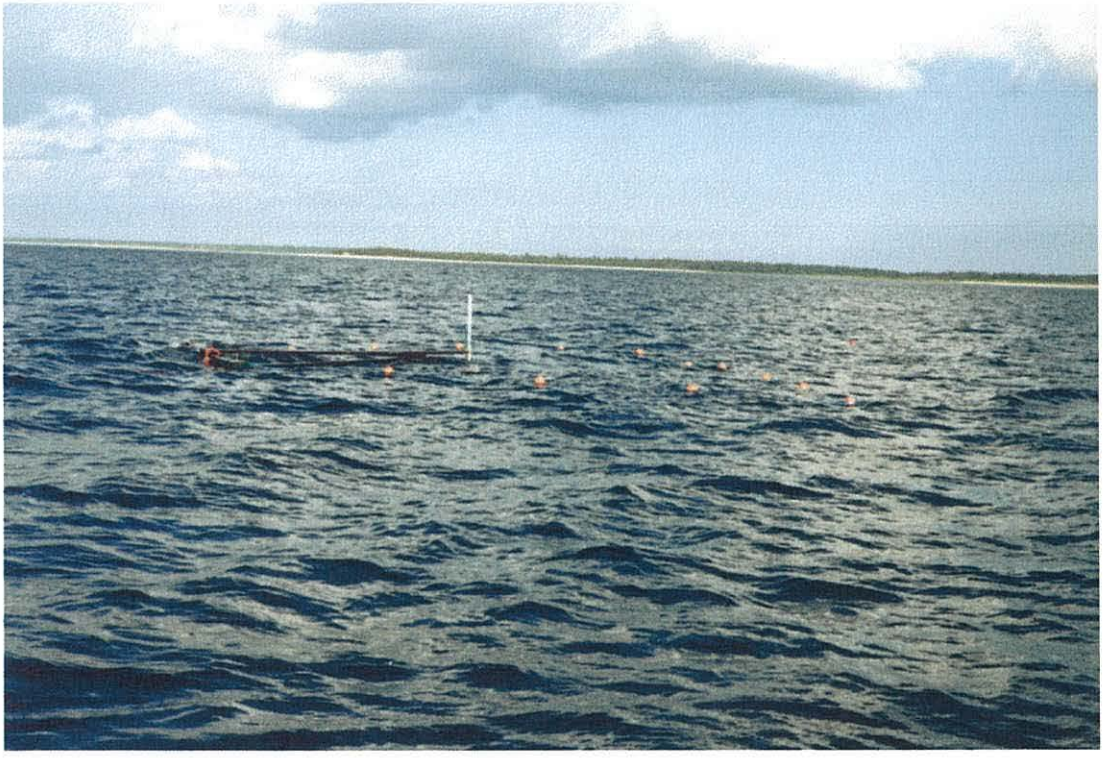

Figure 6.6b The raft after deployment. The area was not heavily in use by shipping.

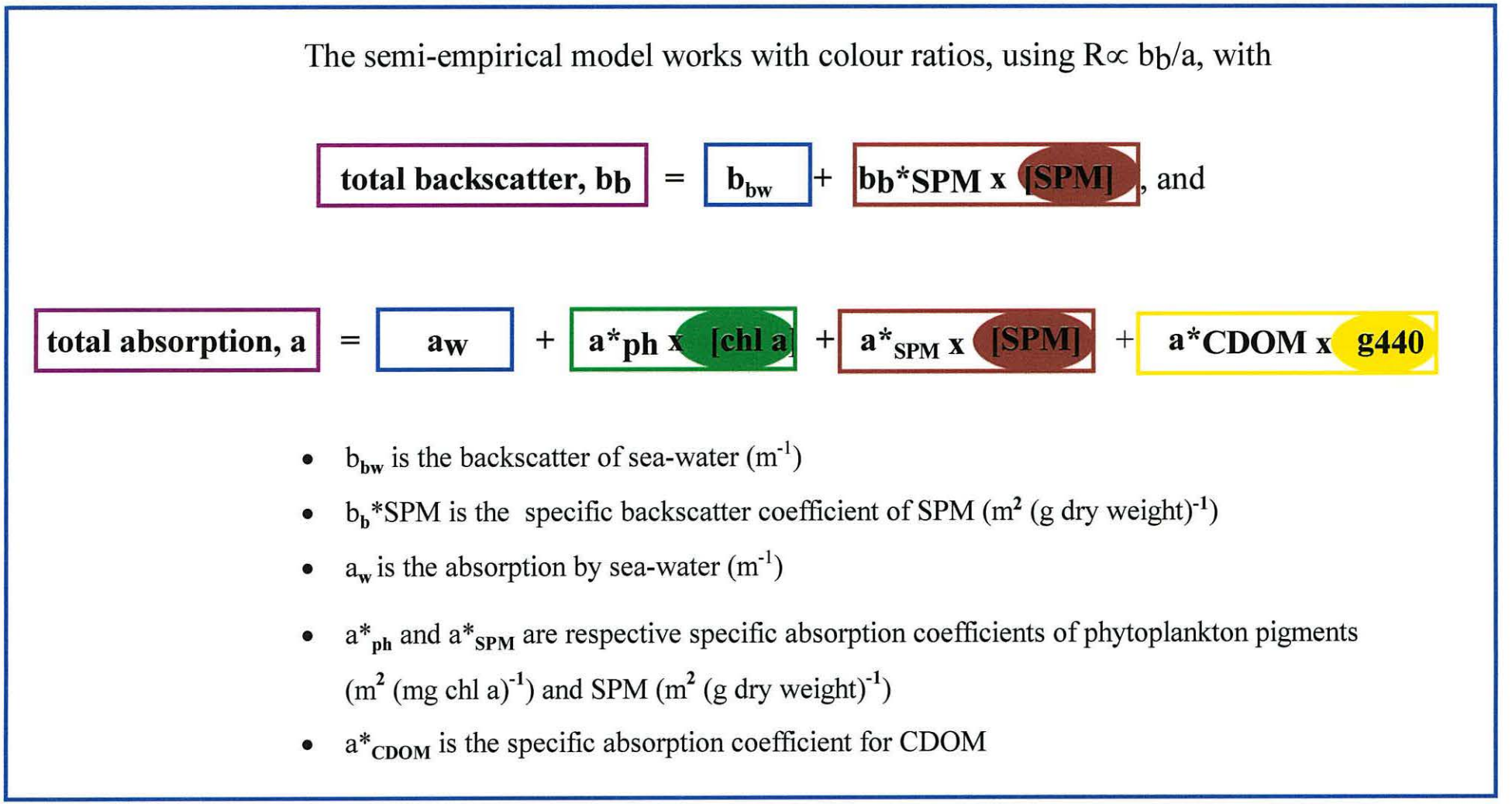

Figure 6.7 Schematic illustration of the semi-empirical model originally developed for the Menai Strait (Chapter 5), and adapted to the Baltic Sea.

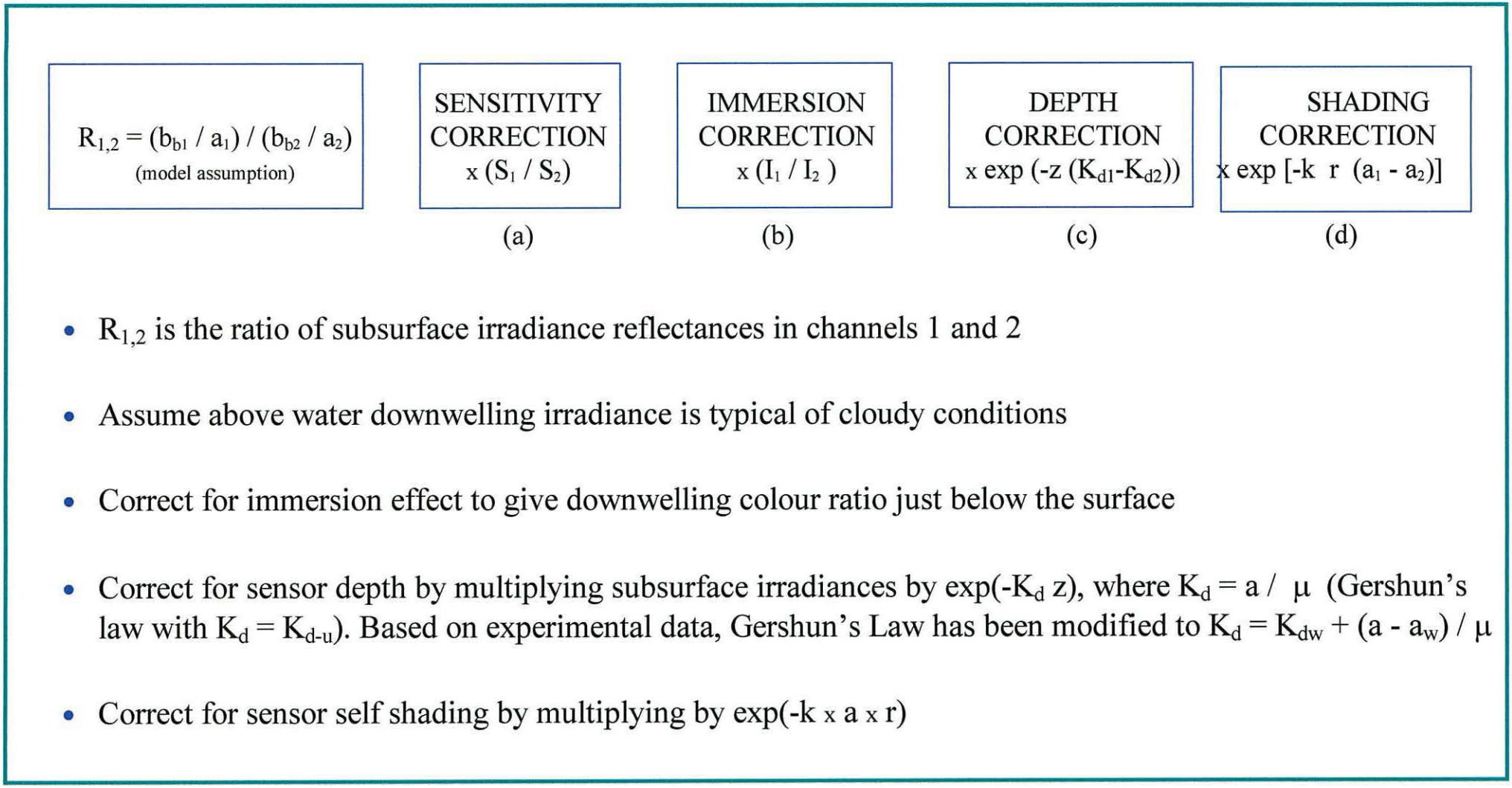

Figure 6.8 Summary of corrections applied to the raw colour sensor ratios.

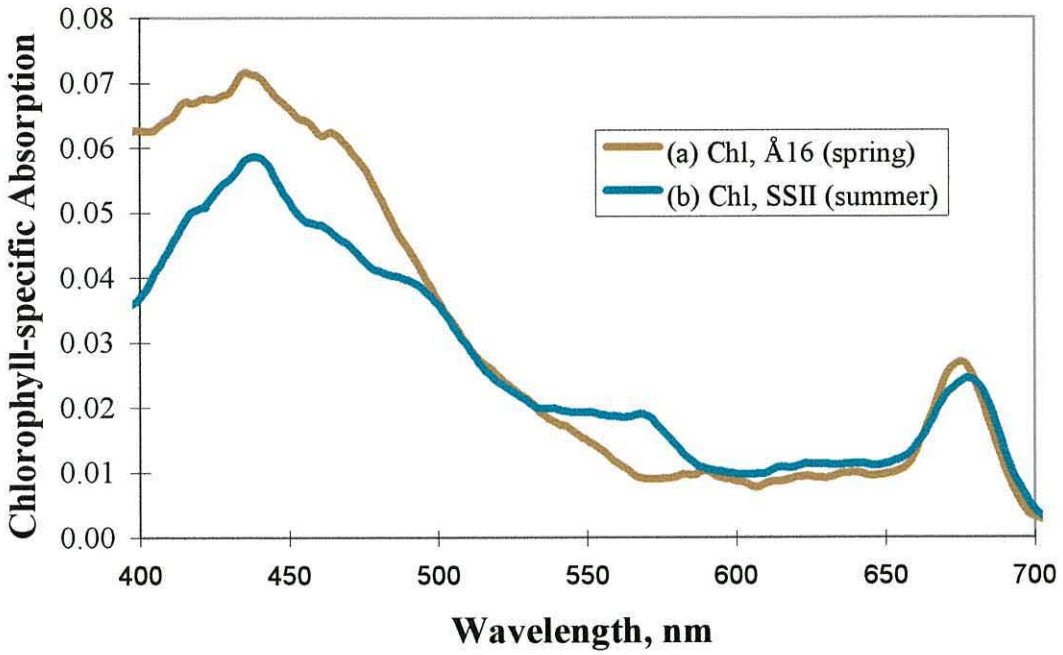

Fig. 6.9 (a) chlorophyll-specific absorption spectrum for diatom/dinoflagellate dominated phytoplankton in spring (brown line)
(b) chlorophyll specific absorption of cyanobacteria-dominated phytoplankton (green line).

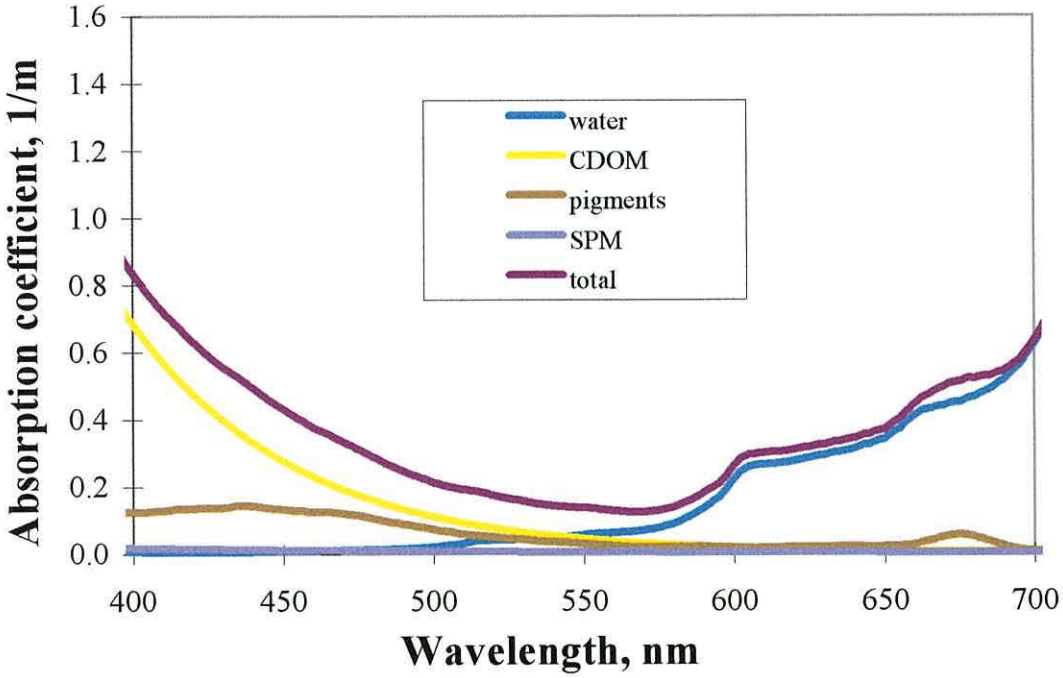

Fig. 6.10 Specific absorption coefficients for STN Å16 (Skagerrak, see Figure 6.4) during the May/June 1998 cruise on research vessel Argos. The absorption spectrum for water was taken from Pope and Fry, 1997. The absorption in the blue is strongly dominated by CDOM. This tendency increases with decreasing salinity.
Figure 7.5 shows the same set of optical parameters for a station in the Baltic Sea. Note the increase of CDOM absorption by approximately a third.

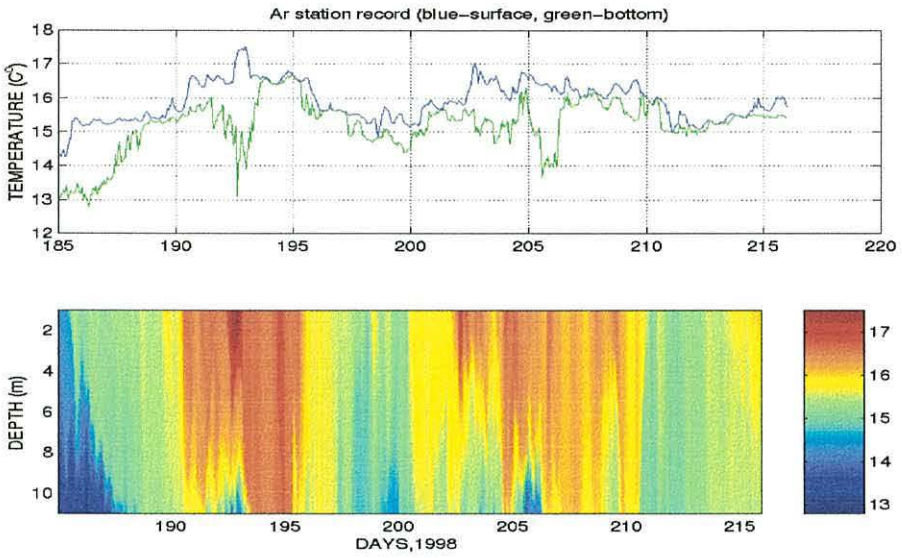

Figure 6.11 Temperature-depth chart for day 185-216, year 1998 at the optical station in Ar. The water was fairly well mixed. The upper chart of temperature at 1m, and 11 m depth respectively shows short periods of stratification. Chart by courtesy of Bertil Håkansson.

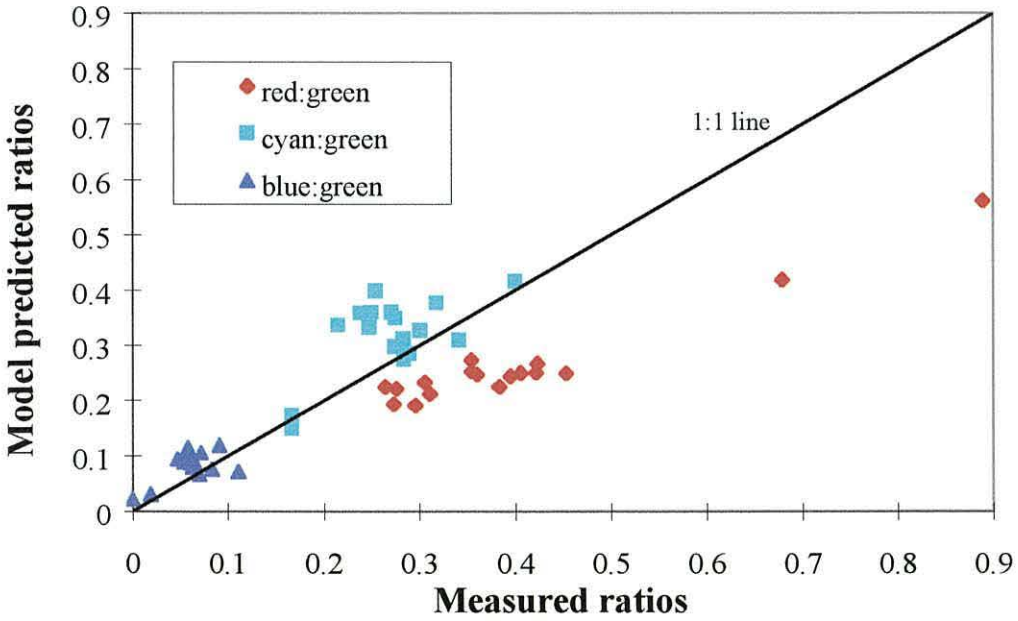

Figure 6.12 Predicted versus measured colour ratios using semi-empirical Baltic Sea model.

best single regressions:	**equation: y = a + b x**						
constituent	**y**	**x**	**a**	**b**	**r^2**	**p**	**n**
chlorophyll	[chl]	ln (b/g)	-15.3	-6.35	0.71	0.037	6
CDOM	g440	ln (r/g)	0.642	0.369	0.70	0.038	6
SPM	[SPM]	ln (b/g)	-3.14	-1.43	0.28	0.276	6
SPM	[SPM]	[chl]	0.131	0.288	0.66	0.051	6

best multiple regressions:	**example: ln [chl] = - 9.48 + 3.11 ln (r/g) + 1.8 ln (c/g) - 5.66 ln (b/g)**							
constituent:	**y**	**a**	**ln (r/g)**	**ln (c/g)**	**ln (b/g)**	**r^2**	**p**	**n**
chlorophyll	ln [chl]	-9.48	3.11	1.8	-5.66	0.99	0.019	6
CDOM	g440	-0.596	0.318	0.618	-0.713	0.96	0.055	6
SPM	ln [SPM]	-10.9	4.65	2.63	-6.74	0.79	0.301	6

Table 6.1 Result of single and multiple regression analyses of colour ratios and optical in-water constituents as derived from the four-channel colour sensor.

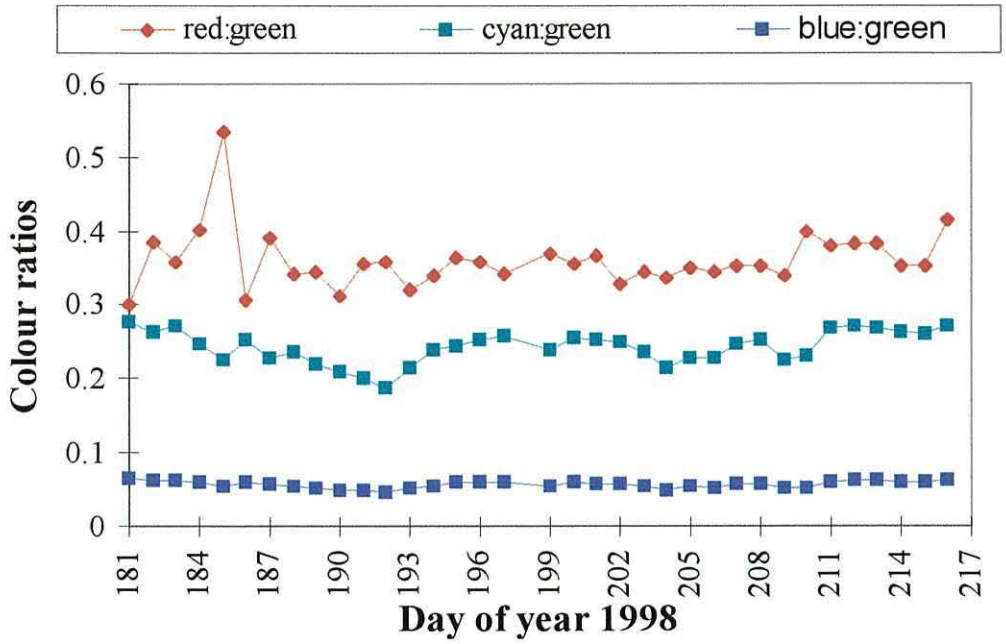

Figure 6.13 Colour ratios as derived from CS22 measurements from the time series in 1998 in Gotland.

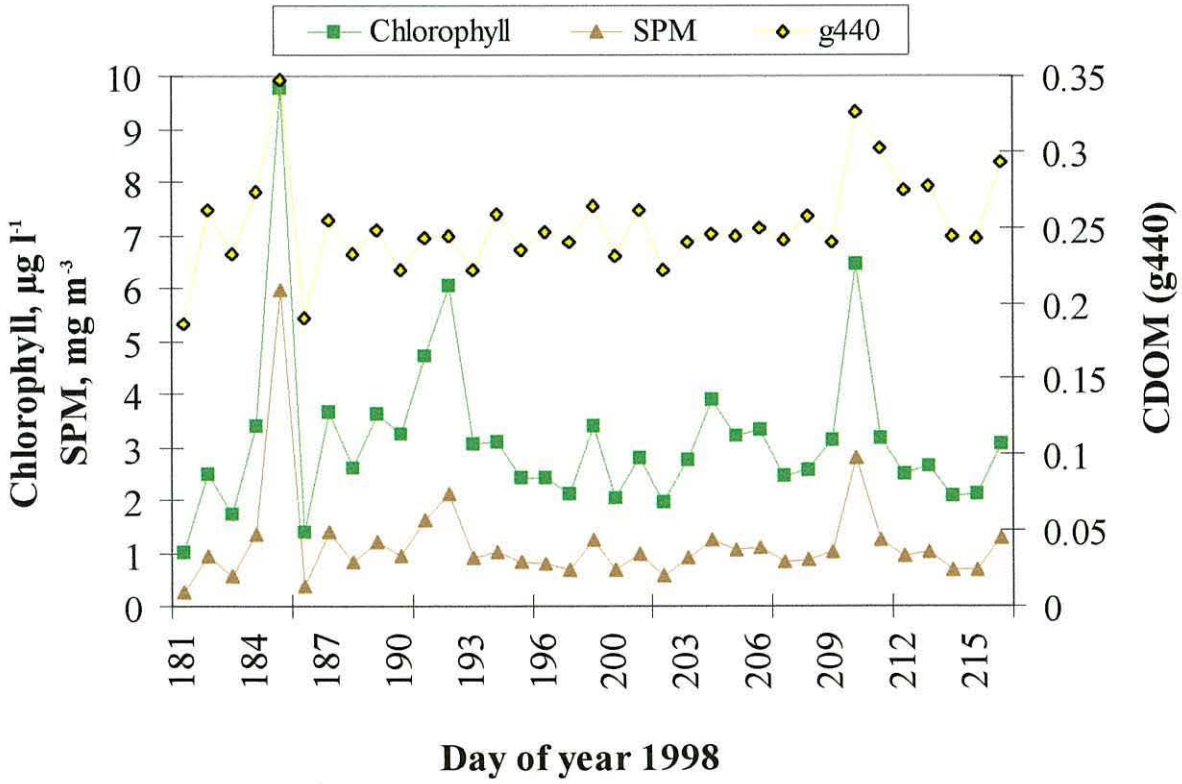

Figure 6.14 Time series of chlorophyll a and SPM concentration, as well as for g440 as derived from colour ratios using the multiple regression algorithms shown in Table 6.1.

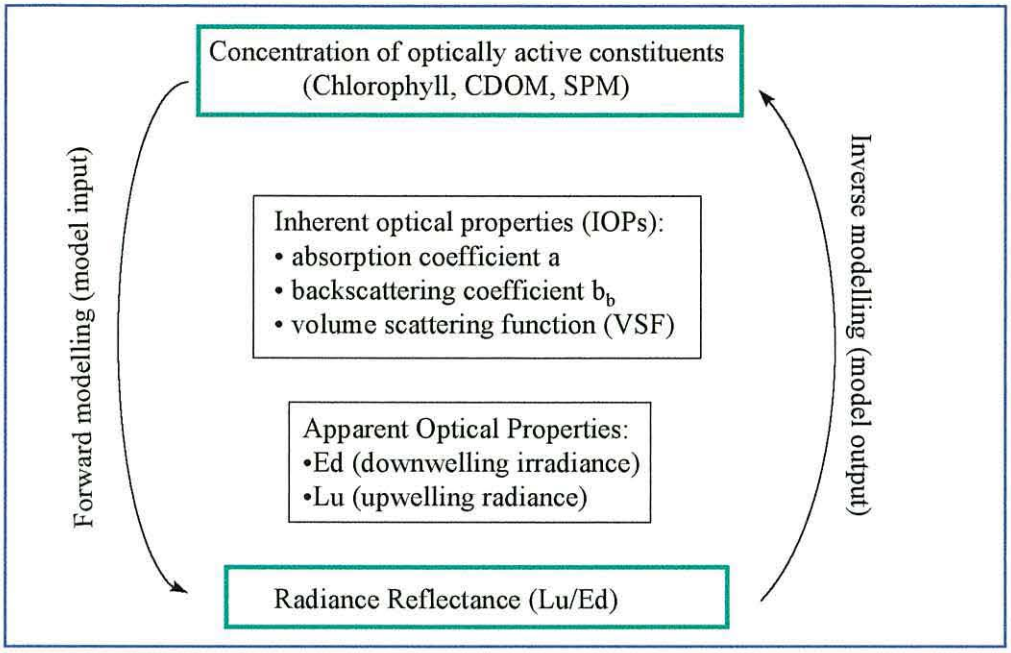

Figure 6.15 A simplified description of optical in-water modelling. The ultimate aim is to predict optically active constituents from the remote sensing reflectance.

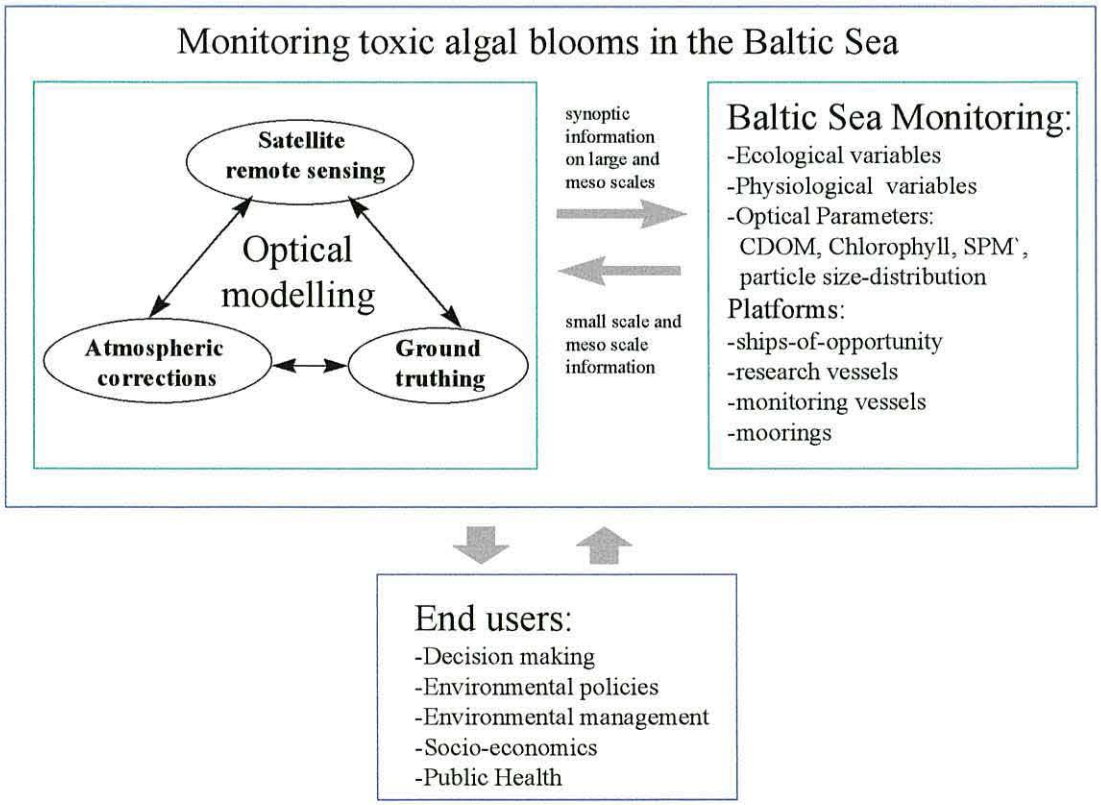

Figure 6.16 A multi-scale approach to improve Baltic Sea monitoring.

Chapter 7 Bio-optical investigations in the Baltic Sea suggest complementary chromatic adaptation of Nodularia *spumigena* and *Aphanizomenon flos-aquae*

This Chapter is based on a talk I gave at the ASLO Aquatic Science Meeting: Research across boundaries, 5-9 June 2000, Copenhagen, Denmark. It deals with the absorption characteristics of *N. spumigena* and *A. flos-aquae* from the Baltic Sea compared to laboratory cultures. Figure 6.9 in Chapter 6 showed that it was possible to distinguish phytoplankton dominated by diatoms and dinoflagellates from phytoplankton dominated by cyanobacteria using spectrophotometry. This is because of the spectral signature caused by a different set of accessory pigments, notably phycobilin pigments in the case of cyanobacteria (for description of different accessory pigments see Chapter 1). During the time series in Gotland both *N. spumigena* and *A. flos-aquae* were present in approximately equal amounts, and the spectrum in Figure 6.9 resulted from a mixture of both species. It may, however, be that *N. spumigena* and *A. flos-aquae* have different absorption properties, and that they therefore can be distinguished spectrally, which may help to distinguish the two species by remote sensing. In order to test the hypothesis that the two species may differ in their spectral signatures, laboratory cultures of both species were measured spectrally, and the resulting individual spectra were compared. In addition, I used these results to investigate the hypothesis that cyanobacteria can adapt the relative concentrations of different phycobilin pigments to prevailing spectral conditions.

Abstract

The chlorophyll-specific absorption spectra of natural Baltic Sea samples dominated by *Nodularia spumigena* and *Aphanizomenon flos-aquae* samples was compared to the spectra of laboratory cultures of the two species. The laboratory samples of both species showed a distinct absorption peak in the light red (630-640 nm), which indicates the presence of phycocyanin. The spectra from the field samples did not show any distinct feature in that area of the spectrum, but had a shoulder in the green part of the spectrum (at about 570 nm), indicating the presence of phycoerythrocyanin. Absorption measurements of all OICs showed a distinct trough in the same part of the spectrum which coincided with the peak in transmission. Due to the mixing of the water column the cyanobacteria were exposed predominantly to yellow-green light. The shoulder at 570 nm therefore suggests complementary chromatic adaptation to the prevailing light field. Samples taken from surface accumulations during a *N. spumigena* bloom showed an increase of phycocyanin, and the loss of the shoulder at 570 nm. This, again, may be interpreted as complementary chromatic adaptation to the increased proportion of red light close to the surface. Nitrogen fixation is a highly energy demanding process. Therefore, the ability to adapt to the light field may be another reason for these species being so successful in the open Baltic Sea during summer compared to other phytoplankton species. The chapter examines the distinct absorption spectra of the two species and discusses some implications for remote sensing.

7.1 Introduction

The phycobilisomes of cyanobacteria are highly organised complexes of various biliproteins and linker polypeptides (MacColl 1998). Phycobilisomes are made up of rods and a core (see Figure 7.1). The rods radiate out from the core, and contain phycocyanin, and, if present, phycoerythrin or phycoerythrocyanin. The biliproteins have their bilins (chromophores) arranged to produce rapid and directional energy migration to chlorophyll a in the thylakoid membrane. According to their absorption properties biliproteins are categorised into three different types: those of high energy (phycoerythrins and phycoerythrocyanins), intermediate energy (phycocyanins), and low energy (allophycocyanin). The transfer of excitation energy is one-directional and always flows from the highest- to the lowest-energy pigment. This is also the way the phycobilisomes are organised: the highest-energy pigment (phycoerythrin or phycoerythrocyanin) is situated furthest away from the core, followed by phycocyanin. The core contains allophycocyanin and is attached to photosystem II (PSII) in the thylakoid membrane. Under certain light conditions the energy transfer may occur directly from phycobilisomes to photosystem I (PSI) which is situated in the thylakoid membrane on either side of PSII. Table 7.1 shows some biliproteins of cyanobacteria. Beale and Cornejo, 1991, found evidence that phycoerythrobilin may be a precursor in the biosynthesis of phycocyanobilin. According to Ducret *et al.*, 1994, phycoerythrocyanin is a phycocyanin-related phycobiliprotein.

The full spectrum of white light (400-700 nm) is only found within the first meter of the surface of clear ocean water. Most of the euphotic zone of clear ocean water exhibits a blue-green spectrum (450-500 nm), whereas shallow coastal waters receive mostly green (550 nm) to yellow (580-590 nm) light (Jerlov 1976). Cyanobacterial phycobilisomes can acclimatise to the spectral quality of light by changing the ratio of phycocyanin to phycoerythrin in the rods of their phycobilisomes to improve light harvesting in changing habitats. Lüning (1990) termed this phenomenon 'complementary chromatic adaptation', referring to the predominant synthesis of phycocyanin in red light, and of phycoerythrin in green light. In deep oceanic waters (blue light), the concentration of phycoerythrin is higher than the concentration of phycocyanin. Some species photoregulate the rate of phycoerythrin synthesis only, whereas other species modulate the synthesis of both phycoerythrin and phycocyanin (Lüning, 1990). When a cyanobacterium exhibits complementary chromatic adaptation the rods of the phycobilisome change with irradiation (MacColl, 1998). The change within each rod may include one or both biliproteins attached to the phycocyanin chromophore. Dependant on the species and the quality of light the second chromophore in the rod may be either phycocyanin

or phycoerythrin, followed by the third chromophore, which may be phycoerythrin or phycoerythrocyanin, if present.

Another interesting phenomenon in the photochemistry of certain phycobiliproteins is photoreversibility. For example, different light regimes may change the relative absorption of the phycoviolobilin (PVB) absorption peak in the blue-green (503 nm) compared to the PVB peak in the yellow-green (570 nm; Sai *et al.* 1992). The phycourobilin (PUB) of CU-phycoerythrin is known to be an excellent absorber of blue light (MacColl 1998). Studying colonies of *Trichodesmium* in the Caribbean Sea, Subramaniam *et al.* (1999) observed a reversible interconversion of phycourobilin and phycoerythrobilin (PEB). They also found a clear diel cycle in the ratio of PUB to PEB. The observed relative increase of PUB under high light conditions suggested that the pigment may serve as a photoprotectant. Hoge (1999) developed an algorithm for the satellite retrieval (MODIS) of both PUB- and PEB-rich phycobilins in Case-1 waters.

7.2 Methods

7.2.1 Field measurements

Absorption spectra of a natural population of *N. spumigena* and *A. flos-aquae* were measured spectrophotometrically on GF/F filters. The chlorophyll-specific absorption coefficient was derived as described in Chapter 2, section 2.3, and Chapter 6 (Kratzer *et al.* 1998). Most of the spectra were measured during the optical time series in Gotland (Chapter 6) during which a colour sensor and a Thermistor chain were deployed on a raft. Four additional absorption spectra were measured during a cruise on R.V. Argos (25/26 August 1998). These stations were BY29 and BY 31, as well as SS1 and SS2 (Figure 6.4). The time series in Gotland was repeated in 1999, and a cruise on R.V. Searcher was undertaken in order to investigate the optical properties of a cyanobacteria bloom.

7.2.2 Laboratory spectra

Cyanobacteria cultures

Absorption spectra of *N. spumigena* and *A. flos-aquae* were measured in March 1999 using laboratory cultures from a stock collection of the Botany Department at Stockholm University. The stocks were kept in Z8X nutrient medium, which does not contain nitrogen. The salinity of the *A. flos-aquae* medium was 0 psu, whereas the salinity of the of *N. spumigena* medium was approximately 7 psu. For dilution, the stock culture was transferred to fresh medium about once every month. The cultures were grown at 24 °C under constant white light (fluorescent lamp). *N. spumigena* was grown under 30 $\mu E\ m^{-2}s^{-1}$, whereas *A. flos-aquae* was grown under lower irradiances (5-10 $\mu E\ m^{-2}s^{-1}$). The stocks were kept in

Erlenmeyer flasks which were continuously and gently agitated to ensure that the filaments were exposed to the same light conditions on average. The layer of the stock culture was 1-2 cm thick. The cultures were not axenic.

Spectrophotometric measurements

Twenty-two ml of each stock culture were diluted with 78 ml filtered sea water and filtered on a GF/F filter using a hand pump (Sartorius). The filter was scanned on a GF/F filter and extracted into 90% acetone. The extracts were scanned the next day. The chlorophyll concentration as well as the chlorophyll-specific absorption spectra were determined for both the *in vivo* spectra, and the extracts as described in Chapter 2, section 2.3. Decolourisation was not performed on these samples. Spectral *in vivo* signatures from both species cultured in the laboratory were compared to the ones found in the open Baltic Sea.

7.3 Results

As described in Chapter 6, the natural population of phytoplankton during the optical time series in Gotland was dominated by *N. spumigena* and *A. flos-aquae.* As seen under a stereoscope microscope the cells looked very healthy, and were green in hue, with the *A. flos-aquae* cells being of a slightly darker green. Both *A. flos-aquae* and *N. spumigena* were present in approximately equal amounts. The chlorophyll concentration of the water samples was low, ranging from 2.16 to 3.9 $\mu g\ l^{-1}$. There was no significant correlation between chlorophyll and temperature during this survey. The time series in Chapter 6 (Figure 6.14) shows that there was not much variability in the concentrations of all OICs which implies a rather constant light field around noon. Figure 7.2 shows the temperature at 1m and at 2m depth over the period of investigation. There was no significant stratification close to the surface during the time of observation. During the Argos cruises the water column was well mixed down to about 15 m depth. The weather conditions in summer 1998 were in general relatively cool and cloudy. Only a few localised surface accumulations were observed by satellite.

The chlorophyll specific *in vivo* absorption spectra of all samples in Ar, and a few more samples from the Argos cruise in August 1998 are shown in Figure 7.3. Note the shift of the chlorophyll peak in the blue to the left on 30 July 1998. This was after a stormy day, and the cyanobacteria filaments were broken down to smaller units when investigated under the microscope. The shift to the left indicates an increase in phaeopigments. The chlorophyll peak in the red was centred around 677 nm. According to Hoepffner and Sathyendranath (1991) this indicates a high proportion of the PSI reaction centre (677 to 680 nm). The reaction centre of PSII has an absorption peak at shorter wavelengths (670 to 675 nm). The *in*

vivo spectra all have a more or less pronounced peak in the green (at about 570 nm), indicating the presence of phycoerythrocyanin. As mentioned before, PVB which is present in phycoerythrocyanin, has a peak around 570 nm, as well as another peak at around 503-510 nm, dependent on the species (Sai *et al.* 1992; Hong *et al.*1993; MacColl 1998). The *in vivo* spectra show a slight shoulder around 500 nm which may be due to the peak of PVB for these species, as well as some carotenoids. The samples were pink in colour after decolourisation with methanol.

The chlorophyll concentrations of both cultures were high, even after dilution: 238 $\mu g\ l^{-1}$ for the *A. flos-aquae* culture, and 766 $\mu g\ l^{-1}$ for the *N. spumigena* culture. The chlorophyll-specific absorption spectra were similar in shape. However, the *in vivo* spectra of both species differed markedly from the spectra of the natural populations. The cultures showed a distinct absorption peak in the red (630-640 nm), indicating the presence of substantial amounts of phycocyanin (Figure 7.4a). Neither culture had the shoulder around 570 nm as shown in the natural Baltic Sea samples, but instead a shoulder around 500 nm. This may indicate the presence of phycoviolobilin, and therefore a different form of phycoerythrocyanin. As mentioned earlier, phycoerythrocyanin contains phycocyanin and phycoviolobilin. Phycoviolobilin peaks at 503 and 570 nm. However, dependent on the spectral quality of the light, it can change the relative height of its peaks (photoreversibility).

In addition, there were slight differences between the *in vivo* spectra of the two species. *N. spumigena* had a higher peak at 630 nm, indicating a higher proportion of phycocyanin in the phycoerythrocyanin component, and *A. flos-aquae* had a higher shoulder between 450 and 500 nm which may be due to a higher proportion of the 500 nm PVB absorption, and a higher proportion of photoprotective carotenoid pigments.

Figure 7.4b shows the chlorophyll-specific absorption spectra of the acetone extracts. It is notable that the extracts have completely different signatures in the blue to blue-green part of the spectrum (400-500 nm). This may be of use for identification purposes. *A. flos-aquae* shows a much higher peak around 490 nm, which may be β-carotene, and an additional feature around 455 nm, which may be zeaxanthin (Jeffrey *et al.* 1997). Zeaxanthin is known to be a photoprotective pigment which may indicate that *A. flos-aquae* may prefer slightly lower irradiances. Both carotenoid pigments are known to be present in cyanobacteria (Jeffrey and Vesk 1997), and β-carotene is known to be a precursor in the synthesis of zeaxanthin (Porra *et al.* 1997).

7.4 Discussion

The following conclusion may be drawn from the chlorophyll-specific absorption spectra of the laboratory cultures and the open Baltic Sea samples:

I) There is a slight difference between the spectrum of the two laboratory cultures, but the difference seems to imply a difference in phycobilin concentration, rather than in the nature of phycobilin. This makes it unlikely that the two species can be distinguished on the basis of their absorption spectra, as the variation of phycobilin concentration within a given species may be more variable than between two species.

II) The spectral shape of the two species was different after extraction in acetone. However, this difference is not useful for remote sensing.

III) The two species seem to be able to adapt their phycobilin make-up to the environment, as shown by the difference in spectral shape between laboratory and Baltic Sea samples.

Alternative explanation for the difference in spectral shape would be changes within the physiology of algal cells, e.g. senescence or pigment packaging effect. Senescence is unlikely to be a plausible explanation for the observed change in spectral shape because it would also cause a shift of the chlorophyll peak in the blue to a lower wavelength (around 412 nm) as observed after the stormy period in Gotland (Figure 7.3, spectra from 30 July 1998). Pigment packacking effect is unlikely to cause a shift in absorption bands. It does not tend to cause drastic changes in the spectral shape, but rather tends to fill up the valleys more in relation to the peaks (Lüning, 1990).

As mentioned earlier, cyanobacteria are known to be able to adapt to the light field. The following discussion is an attempt to explain the difference between laboratory and Baltic Sea samples in relation to their environment, particularly in relation to the light field and temperature.

Figure 7.5 shows the spectral absorption coefficient of all optical constituents for 5 August 1998 at the station in Gotland. The absorption spectrum for water was obtained from Pope and Fry (1997). The minimum of total absorption occurred in the yellow-green part of the spectrum at about 570 nm which coincides with the phycoerythrin peak of the absorption spectra of both cyanobacteria species from the open Baltic Sea.

According to Jerlov, 1976, the Baltic Sea belongs to coastal water 9 (Figure 7.6), which belongs to optical Case-2 waters. Due to the high fresh water input, the optical properties of

the Baltic Sea are strongly determined by very high concentrations of CDOM, especially in the blue part of the spectrum (Figure 7.5). The absorption of the red part of the spectrum is dominated by the absorption of water itself. When compared to Case-1 water, which has the highest transmittance in the blue, the maximum of transmittance of Baltic Sea water is strongly shifted towards the yellow-green part of the spectrum (Figure 7.6 taken from Jerlov 1976). The absorption spectra of all optical constituents show a distinct trough in the same part of the spectrum (see Figure 7.5). The peak of transmission (as measured by Jerlov 1976) and the lowest absorption occur in the same spectral region, which implies that the attenuation in the open Baltic Sea is spectrally determined mostly by absorption, and less by scattering. Due to their gas vacuoles the cyanobacteria cause strong scattering of visible light. The backscatter also increases, and causes a high signal in the visible channel of AVHRR imagery. High concentrations of these surface accumulations show up as bright areas in the image (Figure 6.2).

The spectra of total absorption as derived from the absorption spectra of all optical constituents indicate that the light field was dominated by yellow-green light (570 nm). As the water was relatively well mixed they were less exposed to red and blue light close to the surface. The deeper the cyanobacteria are mixed into the surface mixed layer, the more they will be exposed to yellow-green light. It is well known from other investigations that cyanobacteria can adapt chromatically to the prevailing light field (Vesk and Jeffrey 1977; Lüning 1990; Hausschild *et al.* 1991).

When decolourised with methanol the field samples of the natural populations of *A. flos-aquae* and *N. spumigena* turned faint pink. At first sight this appeared to be an indication of phycoerythrin. However, phycoerythobilins have a double peak absorption at 545 and 565 nm, which is not shown in the *in vivo* spectra. Phycoerythrocyanin has a peak of absorption in the yellow, at 570 nm. It is therefore likely, that the phycobilin pigment found in the natural population of *A. flos-aquae* and *N. spumigena* is actually phycoerythrocyanin. Phycoerythocyanin is lavender to the eye, but it may be that the molecule was denatured because of the methanol extraction, and subsequently changed colour. In order to be more certain about the nature of the phycobiliprotein the cyanobacteria could be scanned in a scanning fluorometer. The fluorescence emission peak of phycoerythrocyanin is at 625 nm. Ducret *et al.* (1994) suggested that phycoerythrocyanins are specialised phycocyanins that are adapted to green-light absorption. Sai *et al.* (1992) isolated phycoerythrocyanin from the filamentous cyanobacteria, *Westiellopsis prolifica* ARM 365 and *Nostoc rivulare* ARM 212. Both show photoreversibility (absorption maxima at 503 and 570 nm) characteristic of this

pigment which is related to the phycoviolobilin chromophore. The authors showed that the energy transfer from the violobilin chromophores to the cyanin chromophores was efficient only in the 570 nm form. This may be another clue as to why the cyanobacteria in the Baltic Sea use this absorption band.

It is known that *N. spumigena* and *A. flos-aquae* are especially well adapted to the low DIN:DIP ratio in the open Baltic during summer (see Chapter 6). The ability to fix nitrogen will be the prime competitive factor for these species being so successful over the summer months. However, as soon as the internal phosphate reservoirs of the cells are used up, it is unlikely that the cyanobacteria will have a competitive advantage in terms of nutrients compared to other phytoplankton, unless additional phosphate is provided from up-welling of bottom waters. Based on laboratory studies of *N. spumigena* and *A. flos-aquae*, Kononen and Leppänen (1997) found that neither *N. spumigena* nor *A. flos-aquae* appear to grow in optimal conditions in the Baltic Sea, taking their growth optima in terms of temperature, salinity and irradiances into account. The optimum irradiance for *N. spumigena* was in the range of 105-155 $\mu E\ m^{-2}s^{-1}$in the laboratory, whereas the optimum range for *A. flos-aquae* was 24-45 $\mu E\ m^{-2}s^{-1}$.

Due to its high CDOM content, the Baltic Sea is very turbid compared to other seas (see Figure 7.6), and therefore light may be another key limiting factor. Sanden and Håkansson (1996) showed that the Secchi depths are consistently low in the Baltic Sea during summer. This means that the light levels are especially low in summer, and light is even more likely to become a limiting factor for photosynthesis than during the rest of the year. It may be possible that the ability to absorb in the yellow-green part of the spectrum is yet another factor that makes these cyanobacteria species so competitive. Nitrogen fixation is a highly energy consuming process (Figure 7.7). It may therefore be crucial for nitrogen fixing cyanobacteria to make the best use of the little light available in the Baltic Sea. It may be possible that under light limiting conditions cyanobacteria prefer the synthesis of the phycobilin pigment that absorbs in the least attenuated part of the spectrum. The choice of adequate absorption bands for light harvesting pigments may be a strategy for cyanobacteria to yield enough energy for nitrogen fixation. In principle it should be possible to calculate a daily mean for PAR at typical depths and to model the quantum needs for carbon and nitrogen fixation as well as the compensation depth.

In summer 1999 the time series in the North of Gotland was repeated, and the *in vivo* spectra showed the same signature with a distinct shoulder around 570 nm. CTD profiles showed that the water column in that area was well mixed. The decolourised filters were also red. During

this survey, a size fractionation was performed on chlorophyll samples in order to get an idea of how much picoplanktonic cyanobacteria contribute to the total biomass. The scans of the acetone extracts indicate that the biomass of phytoplankton ranging from 0.6 µm to 3 µm was in the same range as the biomass of the fraction greater than 3 µm. It is therefore likely that both filamentous cyanobacteria (which were dominant in the fraction > 3µm) and picoplanktonic cyanobacteria, if present in the smaller fraction, use the same strategy of adapting to the light field in the Baltic Sea.

The measurements of the laboratory cultures were repeated with the same experimental set-up as in summer 1999 (more than a year later) and showed the same spectral signature (Subramanium *et al.* 2000). The comparison of the absorption spectra of the field samples to the samples from the laboratory (*A. flos-aquae* and *N. spumigena* scanned individually), suggests that the two species are able to adapt chromatically to the prevailing light field. In the laboratory the two species were exposed to 'white' light (fluorescent lamps), which have a rather broad distribution between 500 and 700 nm. Both species showed a distinct phycocyanin peak. It is unnatural for the species to be grown under constant light (without a night cycle), and this may be another reason why they have such a different signature compared to the samples from the open Baltic Sea. It may be possible that phycocyanin synthesis is connected to the lack of a night cycle (which may have a similar effect as the exposure to high irradiances). Vesk and Jeffrey (1977) showed that different light regimes (i.e. change of the day:night cycle) may change the relative proportion of pigments, e.g. the proportion of photoprotective to photosynthetic pigments. Another example of how the light regime can change the relative amount of different phycobilin pigments is shown in Johnsen *et al.*, 1994. The authors observed an increase of Cr- phycoerythrin 545 in the cryptophyte *Rhodomonas baltica* when exposed to high light. The low light adapted cultures had a less pronounced peak in the green part of the spectrum.

Phycocyanin synthesis may also be temperature related. The laboratory cultures were grown at relatively high temperatures (24°C) compared to Baltic Sea waters, even during a hot summer. During a cruise on R.V. Searcher in the Baltic Sea in summer 1999 (Kratzer and Subramanium, 2000), the water temperature at 1 m depth was significantly higher (with a mean of 17. 4 °C) than during our investigation in Ar in 1998 (mean 15.7°C). The weather was calm with blue skies during the whole expedition, and *Nodularia spumigena* blooms developed all over the Baltic Proper (Subramanium *et al.* 2000). An example of surface accumulations during this cruise is shown in Figure 7.8a and b. The absorption spectra of filamentous cyanobacteria looked different during this cruise: the shoulder around 570 nm

(phycoerythocyanin) was only present in one sample which may have originated from a deeper depth and may have been stirred up by the ship's movement. None of the other samples had the shoulder at 570 nm. Instead they had a pronounced peak in the red, peaking at around 630 nm, which is an indication for phycocyanin. In the samples from Ar this peak was also visible, but much less pronounced. The phycocyanin peak as observed during the Searcher cruise, again, may be interpreted as complementary chromatic adaptation, as the cyanobacteria were situated very close to the surface during strong stratification and may have been exposed to relatively more red light. The filters were colourless after decolourisation which may be due to the lower optical density. However, during a two-day cruise later in August 1999 on R.V. Baltica the *in vivo* spectra looked blue after decolourisation, again, an indication for phycocyanin. The CTD casts showed that the water column was clearly stratified. The data sets from 1999 have not been fully analysed yet.

The shift from one phycobilin band to another may also be temperature related. During the Searcher expedition, the surface layer as derived from SST measurements by AVHRR measurements had an average of about 22 °C during the Searcher cruise (http://wwwmarin.natgeo.su.se/~ab/). The blooms looked yellow in hue, and the filament aggregates were in the range of centimetres (see Figure 7.9). Under the microscope the *N. spumigena* filaments did not look as healthy as the ones found during the investigation in Ar. The samples from Searcher consisted of filament aggregates which were strongly interwoven, and they looked somewhat bleached. It may be possible that this was partly due to leaching of pigments into the water.

Phycobilin pigments may also be a way to store nitrate, as nitrate is present in the chromophores. It may be possible that the synthesis of phycobilin proteins is governed by a complex relationship of nutrients, temperature, irradiance, as well as light quality. This process may be species depended, taking optimum temperature as well as light adaptation of the species under consideration into account.

Another interesting perspective is gained by comparing the pigment composition of *Trichodesmium* in Case-1 waters (Subramanium *et al.* 1999) to the pigment composition of *A. flos-aquae* and *N. spumigena* in the Baltic Sea (Case-2 water). As mentioned before clear ocean water is dominated by blue-green light. CU-phycoerythrins contain PUB and PEB as chromophores which absorb in the blue to green (see Table 7.1). From a broader perspective, the CU-phycoerythrin pigments may be an evolutionary adaptation to Case-1 water conditions, and yet another example of complementary chromatic adaptation. The cyanobacteria may be able to photoregulate their capacity to capture photons of a certain

energy by choosing the appropriate band. On the other hand, the choice of a specific absorption band may also be used for photoprotective purposes.

In Case-2 waters the relative proportion of green light increases with depth. As discussed earlier, an increase of phycoerythrocyanin may be an adaptation to relative more green light. In evolutionary terms, this may be an adaptation of accessory pigment composition to Case-2 under-water light conditions. This hypothesis is backed up by the observation, that the filamentous freshwater cyanobacteria *Westiellopsis prolifica* and *Nostoc rivulare* also contain phycoerythrocyanin (Sai *et al.* 1992). Hashimoto *et al.* (1995) found that the genus *Microcystis* in Lake Kasimugaura, Japan, also contain a phycoerythrocyanin-like pigment.

Further work needs to be done to prove these hypotheses. We are planning a more detailed analysis of the Baltic Sea data from summer 1999, and another Searcher cruise is planned for August 2000. It should be possible to derive a Case-2 algorithm for phycoerythrocyanin rich cyanobacteria, which may be a step towards the prediction of blooms before a bloom event, as the phycoerythrocyanin rich cyanobacteria tend to be dominant in mixed waters, which tend to be before the development of a strong thermocline, and the occurrence of surface accumulations.

Biliprotein	Absorption	Reference	Bilin (chromophore)
Allophycocyanin	650 nm	MacColl, 1998	phycocyanobilin (PCB)
C-phycocyanin	614 to 638 nm	MacColl, 1998	phycocyanobilin (PCB)
C-phycoerythrin	545 nm, 565 nm	MacColl, 1998	phycoerythrobilin (PEB)
CU-phycoerythrins	545 nm, 565nm	Fujita and Shimaru,	phycoerythrobilin (PEB)
	495 nm	1974	phycourobilin (PUB)
Phycoerythrocyanin	503 nm, 570 nm	Sai *et. al*, 1992	phycoviolobilin (PVB)
	614 to 638 nm	MacColl, 1998	phycocyanobilin (PCB)

Table 7.1 Biliproteins of cyanobacteria

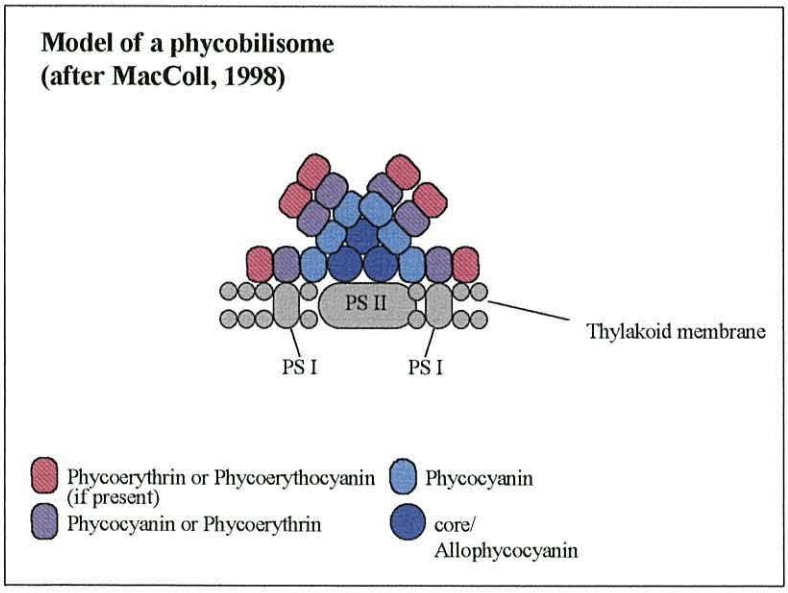

Figure 7.1 Model of a phycobilisome with its core attached to photosystem II.

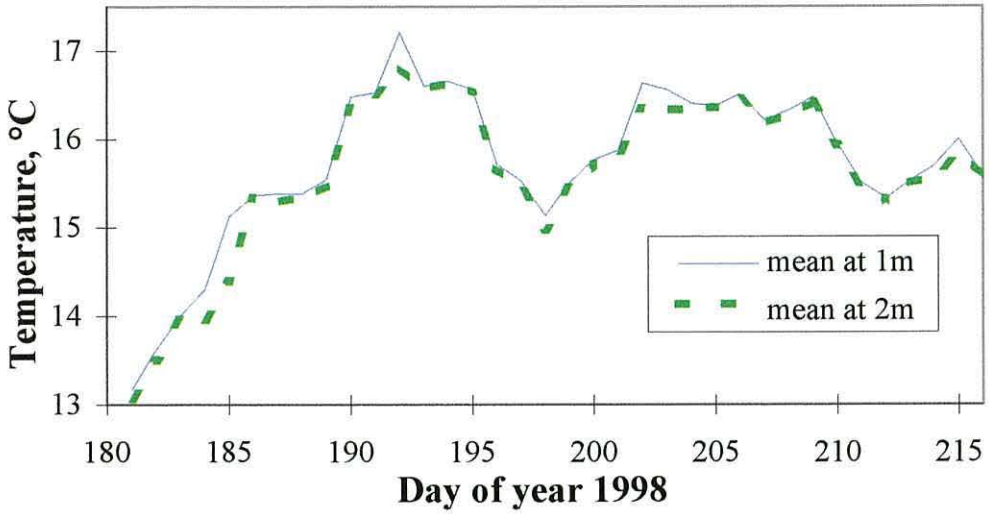

Figure 7.2 Temperature chart for day 185-216, year 1998 at the optical station in Ar at 1m and 2m depth respectively. The water was well mixed close to the surface.

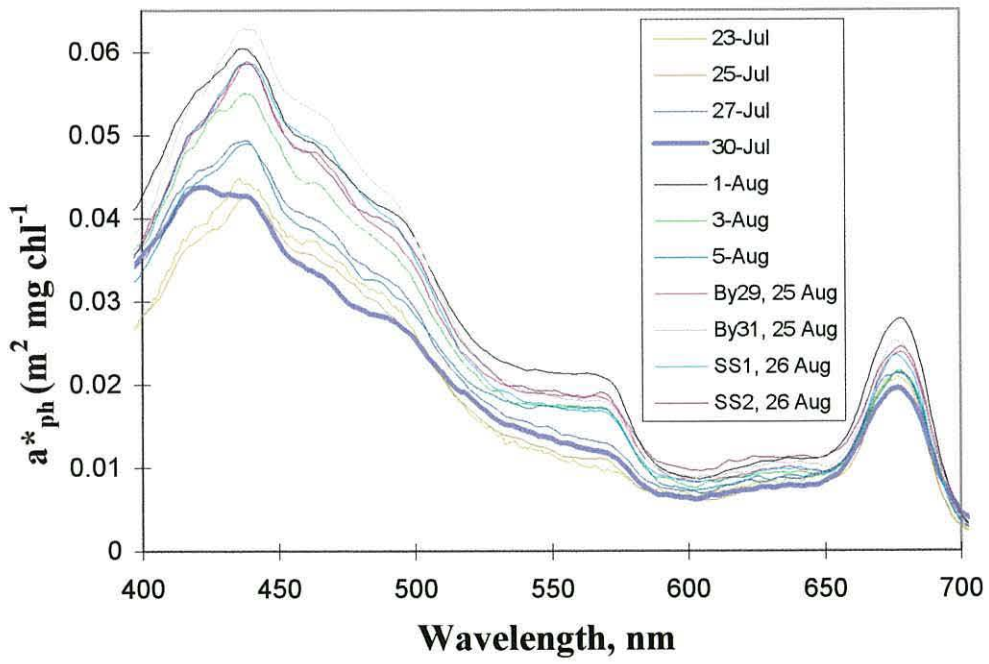

Figure 7.3 Chlorophyll-specific absorption spectra of natural Baltic Sea samples from 1998 as derived from spectrophotometric measurements (filter pad method). Both *N. spumigena* and *A. flos-aquae* were present during these observations. Note the absorption shoulder around 570 nm.

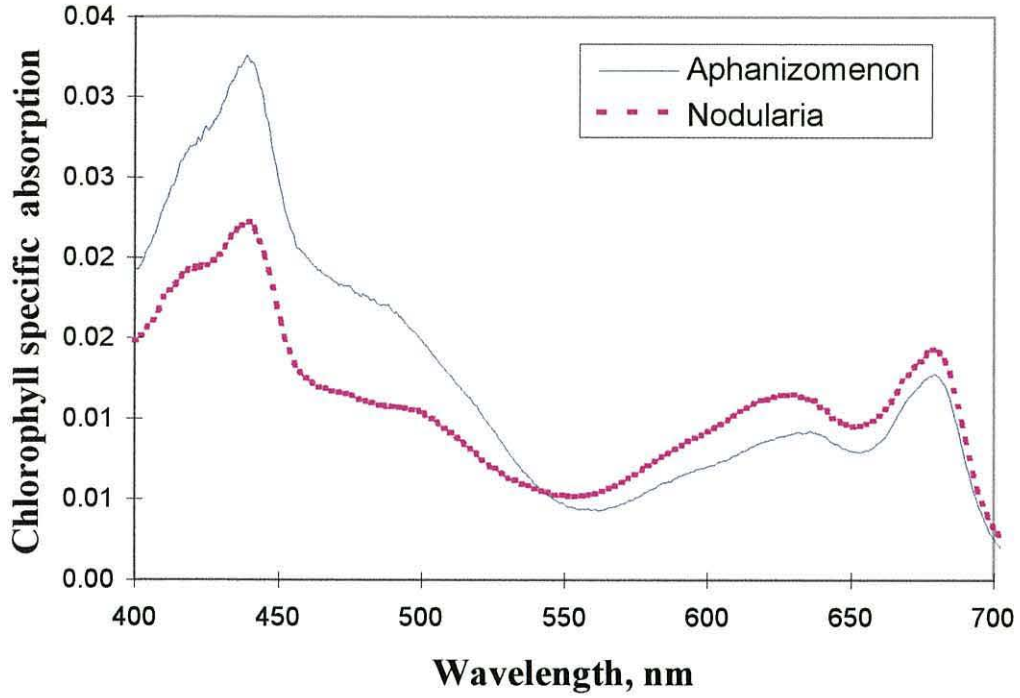

Figure 7.4a Chlorophyll-specific absorption spectra of *A. flos-aquae* and *N. spumigena* cultures as derived from spectrophotometric measurements using the filter pad method. Note the phycocyanin peak around 630 nm. The decoulorisation method was not applied for these spectra.

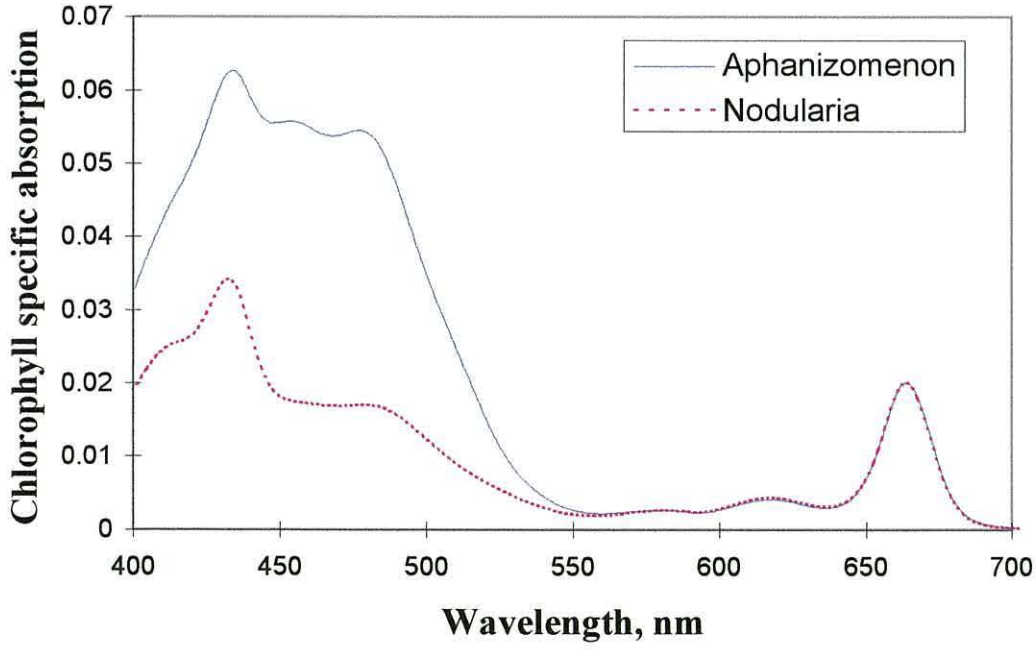

Figure 7.4b Chlorophyll-specific absorption spectra of the acetone extracts of *A. flos-aquae* and *N. spumigena* cultures as derived from spectrophotometric measurements.

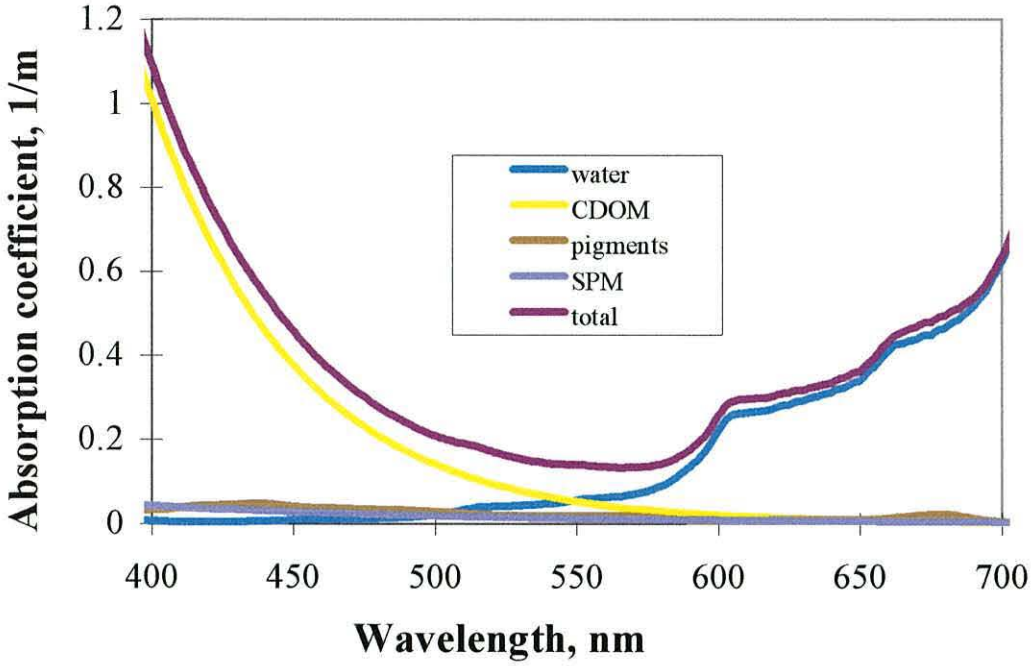

Figure 7.5 Absorption coefficients from field station Ar, 5 August 98, as derived from spectrophotometric measurements of all optical in-water constituents. Note the strong CDOM absorption in the blue. The absorption spectrum for water was taken from Pope and Fry, 1997.

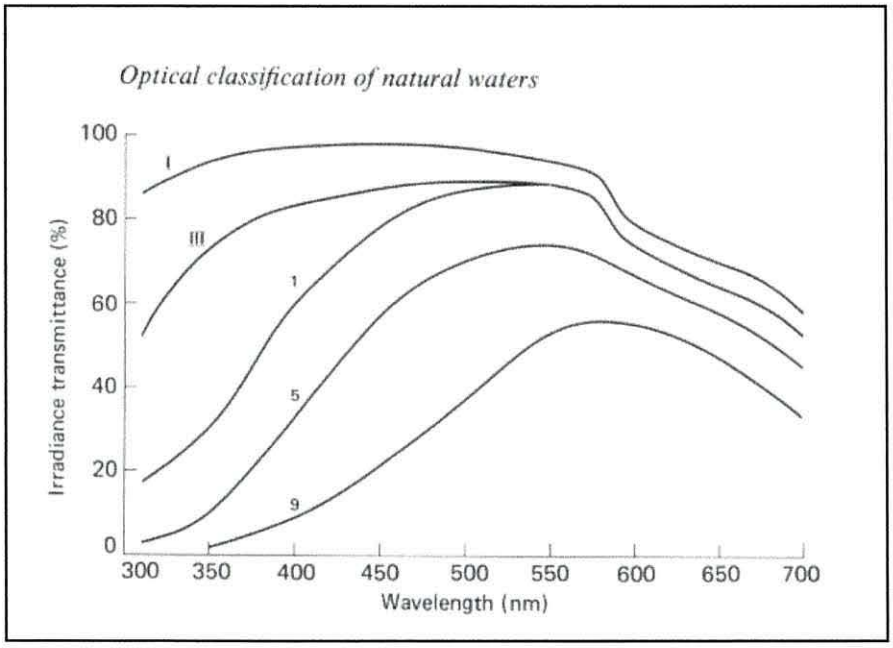

Figure 7.6 Jerlov's optical classification of natural waters (from Kirk 1994, based on Jerlov 1976). Note the peak of transmission for coastal waters 9 (Baltic Sea)which coincides with the lowest absorption in Figure 7.5.

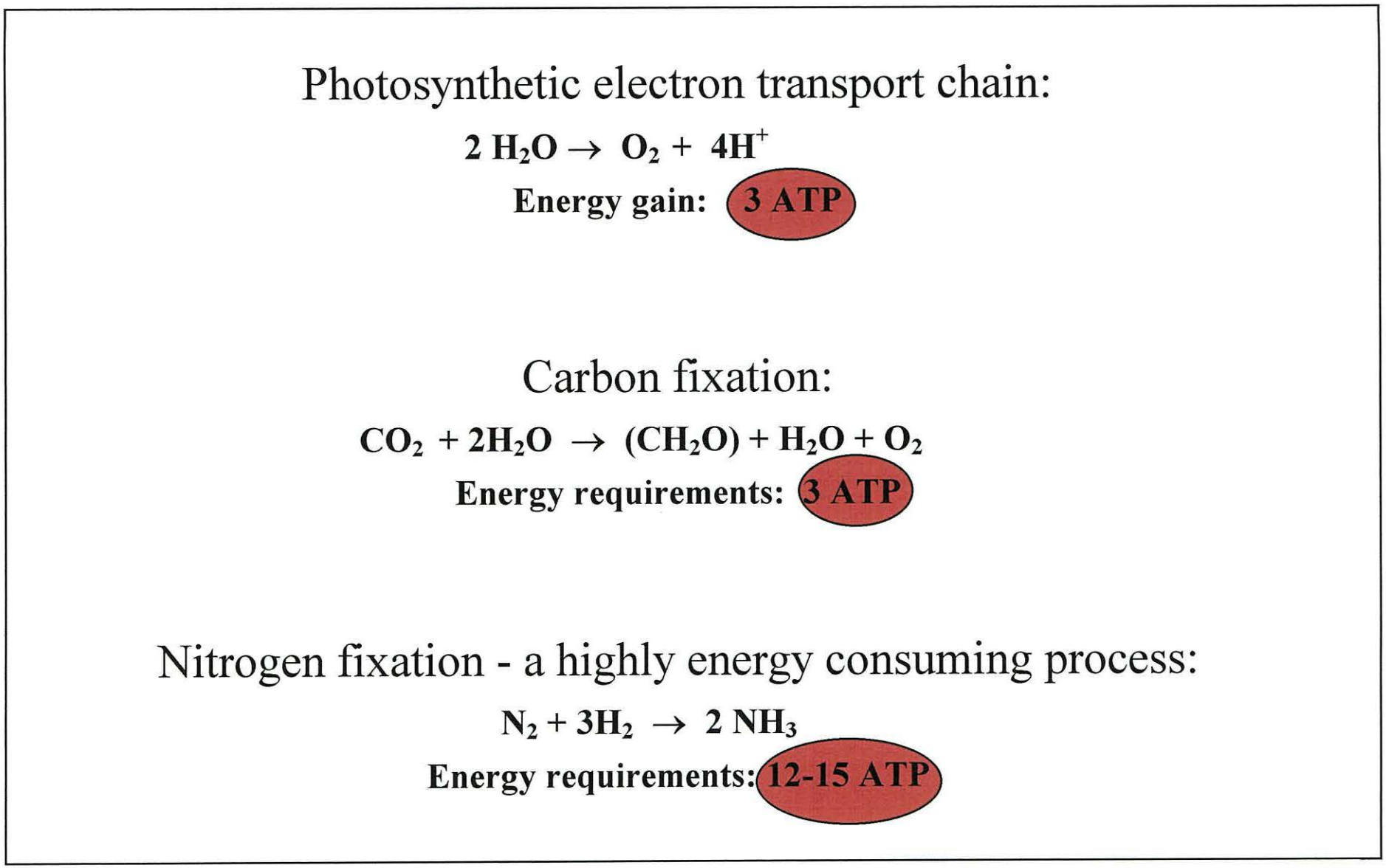

Figure 7.7 Energy requirements for nitrogen fixation in terms of mole ATP in comparison to the energy generation by the photosynthetic electron transport chain, and the energy requirements for the assimilation of carbon (Falkowski and Raven 1997). Only net reactions are shown.

(a)

Figure 7.8 Surface accumulations during Searcher cruise August 1999. The cyanobacteria discoloured the water yellow-brown. The water temperatures in a bloom patch (filament) was substantially higher than in the more mixed surface layers.

(b)

Figure 7.8 continued

Figure 7.8 *Nodularia spumigena* bloom as taken from the under-water port hole on Searcher, 2 August, 1999. The porthole of Searcher was situated 40-60 cm below the sea surface. The diameter of the glass screen was 21 cm. The width of the ruler shown in the photograph was 18 mm. However, it was not directly attached to the window.

Chapter 8 - Conclusions

8.1 Aims

The original aim of the MAFF-funded part of this study was to use the four-channel colour sensor to distinguish different algal groups. However, initial work showed that this was not possible in Case-2 waters, where a fundamental challenge was to measure chlorophyll in the presence of high SPM and/or CDOM. Much of the work of this thesis has therefore been methodological, concerned with the use of the colour sensor, the methods to measure OICs, and the algorithms used to interpret the colour sensor measurements. In addition, however, there are some substantive findings concerned with variability in OICs in the Menai Strait and comparisons between the bio-optics of the SPM-dominated waters of the Menai Strait and the CDOM-dominated waters of the Baltic Sea. Finally, the findings concerning supposed complementary chromatic adaptation in Baltic Sea cyanobacteria have implications for chromatic separation of the main phytoplankton taxa relating the ending of this work to its beginning.

8.2 Laboratory measurements of OICs

Reasonable agreement has been found between HPLC and spectrophotometric measurements of chlorophyll a and carotenoid concentration (see Chapter 2). The results showed that the spectrophotometric method underestimated the chlorophyll a concentration as measured by HPLC by about 31%. As the chlorophyll concentration is used for deriving the chlorophyll specific absorption spectra for the models in Chapters 5 and 6, this means an overestimation of this parameter by about 45% compared to published studies that use HPLC as a standard method (note: 100/100 = 1; 100/69 = 1.45). HPLC is very expensive, though, and not very widely used, even though this should change with increasing use of the SeaWiFS protocols.

The SeaWiFS protocols specify the use of 0.45 μm membrane filters for measuring SPM, and the use of 0.2 μm membrane filters for measuring CDOM. Because of the need to distinguish between organic and inorganic particles, GF/F filters were used for SPM during this study. This implies the lack of the 0.2 to 0.7 μm fraction in the semi-empirical model which has CDOM and SPM as input variables. It would therefore be better to use one pore size to separate these two optical components. Practically, it would be easiest to use GF/F filters for this, as the filtration is fast, and because of lower costs. The comparison of g_{440} values from 0.2 μm filtered sea water with g_{440} values from GF/F filtered sea water, however, showed that the g_{440} filtered sea water

had a consistent off-set when compared to the 0.2 μm filtered sea water. This was explained by scattering processes caused by glass fibres in the GF/F filtered fraction. The increase in scattering could be reduced by pre-washing the GF/F filters with deionised water before filtration.

A relationship was derived in Chapter 2 for fluorometrically measured humic substances (by SMHI) and g_{440}. With some precaution this relationship can be used to derive g_{440} values from fluorometrically measured concentrations of humic substances. This has implications for optical modelling of the Baltic Sea, as the fluorometric method is part of a standard monitoring program performed by SMHI. There is an inherent problem with this approach, though, as the humic substances in the Baltic Sea are very variable, and the fluorescence fingerprint as well as the conversion factor used are likely to change with the region, as well as the season. Furthermore, it was shown in Chapter 6 that the slope of CDOM also varied dependant on region and season. The correlation coefficient between g_{440} and CDOM fluorescence was nevertheless very high, probably because the measurements were taken over a strong geographic gradient.

The Harker (1997) model described in Chapter 5 used a standard chlorophyll-specific absorption spectrum derived from Kirk (1994). This was replaced during the present study by a regional chlorophyll-specific absorption spectrum using data collected during the Menai Strait time-series in 1996.

Harker (1997) had used combusted filters to derive the SPM-specific absorption coefficient. In this thesis, however, the decolourisation method with methanol (Kishino 1985) was applied to derive the SPM-specific absorption. It was shown that the method has been successfully applied to distinguish the optical contribution from fat-soluble phytoplankton pigments from the part of the spectra of non-phytoplankton-pigment material. Interestingly, it resulted in greyish-brown filters, which changed to reddish in colour after combustion. The colour change suggested oxidation of ferrous (Fe^{2+}) to ferric iron (Fe^{3+}). This implies that the combustion method causes a change in the spectral quality of SPM which would not be observed in nature, and therefore that the derived spectrum should not be used for optical in-water modelling.

Figure 8.1a shows a number of absorbance spectra of combusted filters from the Menai Strait time series. Compared to the decolourised spectra (Figure 8.1b) the combusted filters have a relative lower absorbance in the red (compared to the absorbance in the blue). The stronger absorbance in the blue gives the samples their reddish colour. In contrast to this, the decolourised spectra show a much flatter spectrum, with less

difference between the red and the blue wavebands, which makes these samples look more greyish-brown. Figure 8.2a shows that the combusted filters do not follow a straight line on a logarithmic scale. The resulting lines show at least two different slopes, whereas for the decolourised spectra (Figure 8.2b), the log transformation looks closer to a straight line. This implies that the spectrum of combusted filters gave an inaccurate impression of the spectrum of MSS, a hypothesis with implications for modelling the effects of inorganic sediment in optical Case-2 waters. Figure 8.1b also demonstrates that decolourisation method was rather efficient in terms of extracting chlorophyll and carotenoid pigments. The absorption spectra used by Bowers *et al.* (1996) and Harker (1997) did not take the changes in colour due to combustion into consideration.

In the Baltic Sea samples the spectral signature of the phycobilin pigments had to be removed mathematically from the decolourised spectrum, as these pigments are not soluble in methanol (see Chapter 6).

8.3 Field methods and colour sensor engineering

Part of the aims of this PhD was to improve the use and the design of the Colour sensor. The design and engineering was improved by Ray Wilton and Anne Hammerstein at SOS, UWB. The sensitivity of the instruments was adjusted for measuring up-welling irradiance using improved photocells. In addition, some of the instruments were fitted with external RS232 connectors. This made it easier to download ASCII data to an external computer, and to adjust sampling parameters from the external computer by interacting with the controlling software in the Colour Sensors' s microprocessors. The external connector also proved to be necessary for spectral calibration of the instrument.

As there was no simultaneous measurement of downwelling irradiance the colour sensor measurements had to be restricted to times within +/- 2 hrs of local noon This ensured that the upwelling irradiance was rather constant (see Chapter 2, section 2.2). During this investigation the ranges of the logging start and end times were 4.00-9.00 GMT and 16.00-21.00 GMT respectively. The data collected before 9 and after 16 GMT was in fact useless as it included mostly information about changes in sun-angle, and not much relevant information about OICs. The sampling scheme of the instruments would be improved by changing the range of the logging start and end times. It would be better if the logging start time ranged between 6.00-11.00 GMT, and the stop time between 13.00-18.00 GMT (accounting for measurements in different time zones as well).

The colour sensor was tested in different modes of deployment, and it was found that the instrument was very good for mooring applications. The moorings in the Menai Strait and the Baltic Sea showed that the instruments were robust enough to withstand deployment for several weeks in a row, the only restriction being the fouling of the diffuser window. During the deployment in the summer in the Menai Strait the instrument body (which was black) was fouled with barnacles, whereas the white and smooth Perspex window was not attacked by barnacles, but had a thin film of microalgae (brown in hue, possibly diatoms) after 2 weeks. However, a comparison with a transmissometer that was deployed on the same platform during the time series in the Menai Strait showed that the colour sensor was much less susceptible to fouling than the transmissometer. One reason for this may be due to the uneven and scratched surface of the old transmissometer that was used. In some places the paint of the housing was peeling off, and this may have been a good surface for benthic organisms to settle on. During this deployment in the Menai Strait, macro algae were also a practical problem as they got caught by the sensor and its frame.

During the deployment in the Baltic Sea the instrument's window was cleaned at least once a week. This seemed a restriction in the first place, because in meant a rather tight schedule for servicing in the instruments. However, MPA showed that for producing viable algorithms a sufficient number of OIC measurements had to be available. This number depends on the algorithm used (if linear, squared or cubed), and the number of degrees of freedom required. For example, during the Gotland measurements there were six data points in all. The multiple regression used up four degrees of freedom (Table 6.1), so there were only two degrees of freedom left. It would therefore have been preferable to have more measurements.

The strong tidal currents in the Menai Strait caused difficulties. In order to withstand the tidal force, and to protect the instrument, a very strong frame was built from scaffolding pipes. The frame, however, caused shading. In the Baltic Sea the design was improved for maximum avoidance of shading. However, this was only possible because there was no strong tidal force, and the area in the North of Gotland was not heavily in use by shipping.

All instruments, were found sufficiently sensitive for measuring upwelling irradiance even in strongly turbid waters, although the digital output from the blue channel was low relative to the other channels. This could be explained by the increasing sensitivity when moving from the blue to the red channel (see Figure 3.1), and the higher

absorption of SPM and CDOM in the blue.

A comprehensive calibration of CS23 at PML provided an absolute calibration of the instrument, and confirmed the linearity of response. The use of a monochromator for spectral calibration has confirmed that the peak wavelengths of each colour channel in CS21 and CS23 were within 2 nm of the design wavelengths. Using these calibration results, absolute irradiances can be calculated for each channel. Following the requirements of the SeaWiFS protocols (Mueller and Austin 1995) the cosine response was found to be non-satisfactory, and detailed suggestions for improvement of the cosine response were made (Chapter 3). The effect of submersion of the instrument on colour ratios was measured, but sensitivity analyses on both the Menai Strait and the Baltic Sea model were inconclusive considering the immersion effect.

8.4 OICs in the Menai Strait and the open Baltic Sea as measured by the spectrophotometric method

The time series in the Menai Strait showed that all OICs followed a seasonal cycle.

The chlorophyll a and total carotenoid concentration indicated a spring bloom, and some smaller autumn blooms.

The SPM concentration showed both a seasonal, as well as a tidal signal: the concentrations were distinctively high in spring and autumn, but also increased with tidal range. This may be explained by increasing wind and tidal stirring. Another cause for the seasonality of the SPM signal was the phytoplankton spring bloom, which increased the relative proportion of OSS. The SPM (TSS) concentrations ranged from 1.6 to 30.0 g m^{-3} (MSS: 0.7 to 26.3 g m^{-3}; 0SS: 0.3 to 3.6 g m^{-3}), and the mean was 6.4 g m^{-3} (MSS: 5.3 g m^{-3}; OSS: 1.1 g m^{-3}). Figure 8.3a shows an example of the specific absorption spectra of all OICs on the 17 October 1996. The absorption in the blue was dominated by SPM, and CDOM had a minor effect on total absorption. Note that the chlorophyll concentration was low on that day (1.6 µg l^{-1}). Figure 5.7a-c (Chapter 5) shows how the contribution of the phytoplankton to TSS changed dependent on chlorophyll a and SPM concentration.

The g_{440} values ranged from 0.07 to 0.25 m^{-1}, with a mean of 0.13 m^{-1}. The CDOM fraction, although comparatively low (if compared to the Baltic Sea), peaked in summer (Figure 5.5). The summer peak occurred at a time of maximum salinity (Figure 5.2) and so cannot be explained by increasing terrigenous CDOM in run-off. No relationship between g_{440} and accumulative amount of rain was found. There was also no

relationship between phytoplankton biomass and g_{440} which means that CDOM is not directly related to phytoplankton biomass. Although there is no direct link between phytoplankton concentration and CDOM, the increase of CDOM over the summer might still be explained in connection to phytoplankton biomass and bacterial activity. Blight *et al.* (1995) observed a respiration maximum about 1-2 weeks after the *Pheaocystis* bloom in the Menai Strait which they explained with an increase of bacterioplankton. The bacterial numbers decreased after this peak, but returned to higher concentrations over the summer. Rochelle-Newall *et al.* (1999) and Nelson *et al.* (1998) found bacteria to be a source of CDOM, even though there was no obvious correlation between bacteria number and dissolved organic carbon. In their mesocosm experiment, Rochelle-Newall *et al.* (1999) could not observe any effect of nitrogen source on the concentration of CDOM, using nitrate, ammonia and urea as nitrogen source. Being nitrogen poor and extremely difficult to break down, and thus not providing an attractive food source for bacteria, the more-stable fraction of the CDOM (refractory CDOM) increases over the summer months. It is possible that these molecules get adsorbed mostly to smaller inorganic particles (because of their high surface area) during the course of the year, forming bonds amongst one another. They then get drawn down into the sediment. In autumn, increased wind stirring leads to a resuspension of these particles and increased OSS was measured, together with an increase of MSS and phaeopigment concentration.

In the Baltic Sea in general, and at the station in Gotland the optical signal was clearly dominated by CDOM (60-90% of total absorption in the blue, and 5-40 % in the red (Chapter 6.2). At the Gotland station CDOM made up 60-70% of the total absorption in the blue, 30-40% in the green channel, and 5-15 % in the red channel.

The exponent of the CDOM spectrum in 1998 was -0.020 nm^{-1} for the open Baltic Sea in summer, and -0.019 nm^{-1} for the whole data set, and the absolute value of the exponent was therefore larger than in the Menai Strait (ranging only from -0.011 to -0.017 nm^{-1}, with a mean of -0.014 nm^{-1}). According to Carder *et al.* 1991 this may indicate that in the Baltic Sea CDOM consists mostly of smaller fulvic, rather than humic, acids.

The CDOM signal in the Baltic showed a seasonal signal with higher values in spring than in summer: the mean of all g_{440} values measured in 1998 was 0.53 m^{-1} in spring, and 0.24 m^{-1} in summer. At the Gotland station in summer the CDOM values were rather consistent, with a mean of 0.27 (+/- 0.03).

Phytoplankton pigments, although only sampled outside bloom situations, also contributed significantly to the total absorption (about 20% in the blue, 50-90% in the red). Figure 8.3b shows the specific absorption spectra for all optical constituents for a station in spring in the Skagerrak. When moving towards the open Baltic Sea the concentrations of CDOM increase, and the absorption by CDOM increases by about one third (compare Figure 7.5 and Figure 8.3b). This tendency should increase with decreasing salinity when moving further north along the Gulf of Bothnia.

The concentration of SPM was generally very low in the open Baltic Sea when compared to the Menai Strait. During the time series in Gotland the SPM concentration was found to covary with the chlorophyll a concentration. This has implications for modelling the open Baltic Sea, where it may be justifiable to use the SPM and phytoplankton fraction as one unit. This would make the decolourisation by methanol unnecessary for open Baltic Sea samples. For coastal areas, however, decolourisation would still be useful, as SPM and chlorophyll a are unlikely to be correlated.

8.5 Algorithms for estimating OICs from in situ optical measurements with the colour sensor

MRA was used to derive a time series of OICs in Case-2 waters. In the Menai Strait, the cubed multiple algorithm gave the best fit for TSS ($r^2 = 0.89$, Table 5.1), and even when using a linear regression the fit was still good ($r^2 = 0.73$), which was consistent with the fact that TSS were the dominant absorber in the Menai Strait. The red:green ratio yielded the highest predictive power for TSS, which may be explained by figure 8.1a. The non-pigmented sediment fraction still absorbs significantly in the red. In the blue this signal may be overwhelmed by phytoplankton and to a lesser extent by CDOM. There was no significant relationship between the chlorophyll a and the TSS concentration. The MSS fraction was dominating TSS most of the year, but during the phytoplankton bloom OSS reached up to 50% of TSS. This means that the organic fraction must not be neglected in optical models, and the models should use TSS rather than MSS as an input variable for suspended matter. For chlorophyll, the prediction was less reliable, with $r^2 = 0.66$. However, the algorithm produced predicted a chlorophyll time series that was well in agreement with historical data (Figure 5.11b). The chlorophyll time series derived from MRA of colour ratios is the first continuous time series of the Menai Strait that covers the whole period of phytoplankton growth and decay (with a daily resolution). This makes the colour sensor a very good instrument for monitoring chlorophyll and suspended matter in the Menai Strait. For CDOM a less

satisfactory algorithm could be derived from colour ratios. The reason for this was that CDOM did not contribute substantially to the total absorption (Figure 8.3a), but was overwhelmed by the SPM signal. This means that the colour sensor could only give satisfactory information about the two dominant OICs. The time series of SPM derived from the colour sensor was used to compare the sediment loads measured during a time series by Sinclair Buchan in the Nineteen-Sixties (Buchan *et al.* 1967; Kratzer *et al.* ms). It was concluded that the sediment load has not increased significantly, which may be of value for environmental management.

The MRA of the Gotland data showed that chlorophyll a, CDOM and SPM could be derived from 3 colour ratios (Table 6.1). Both chlorophyll a and CDOM yielded very high values of r^2 (0.99 and 0.96 respectively). The r^2 for SPM was 0.79. This was explained by the good correlation between phytoplankton biomass and total SPM.

The best single predictor for CDOM in the Baltic Sea was the red:green ratio, which is very surprising as CDOM mostly absorbs in the blue and the cyan, and less in the red.

The linear regressions worked best using the blue:green ratio for chlorophyll a (see Table 6.1) which is also surprising, as the blue:green ratio was not changing substantially (see Figure 6.13). The same problem was shown by the semi-empirical model: the blue:green ratio was mostly representing instrument noise (see Figure 6.12).

A general conclusion that can be drawn from the MRA for both types of Case-2 waters is that the algorithms are regional (compare Tables 5.1, Menai Strait and Tables 6.1, Baltic Sea).

8.6 Semi-empirical optical model

The algorithms mentioned in the previous section represent an empirical relationship between the measured concentration of OICs, and optical *in situ* measurements, and can be used to predict the former from the latter. In contrast, the model originally developed by Harker for the Irish Sea attempts to predict sea-surface reflectance ratios on the basis of optical theory, as well as on empirical measurements (Bowers *et al.* 1996, Harker 1997). The model was therefore semi-empirical, and synthesised the spectrum of sea-leaving radiance from known optical properties of pure seawater, CDOM (using g_{440} as a proxy), mineral SPM (measured gravimetrically) and the chlorophyll-specific absorption spectrum of phytoplankton. Some of the parameters in the model were changed because of the findings mentioned above (change of colour by combustion process, significant contribution of organic SPM to the optical signal).

However, although improved and made more specific to the Menai Strait, the model output was still not satisfactory. The Baltic Sea model in Chapter 6 was a complete revision of the model presented in the Chapter about the Menai Strait. It included not only specific parameters for the Baltic Sea (e.g. chlorophyll-specific absorption, SPM-specific absorption etc, but also included spectral backscatter, a spectral mean cosine, as well as corrections for self-shading and immersion effect. However, Figure 6.12 showed that the model still had a rather low predictive power when comparing predicted and measured values.

In both types of optical Case-2 waters, the Baltic Sea and the Menai Strait, it was not possible to reverse the semi-empirical model to estimate, reliably, concentrations of phytoplankton pigments, SPM and CDOM. This may be due to the missing information about appropriate regional values of scatter and backscatter coefficients. In the Menai Strait model backscatter was assumed to be wavelength independent. The scattering coefficients were measured by Harker (1997), and we used the mean of these measurements for the model. However, b changes over the year due to the seasonal and tidal changes in SPM concentrations, and these changes might need to be taken into account. Furthermore, scattering is generally thought to be wavelength dependent, and b_b to change proportionally to scattering. Therefore, b_b should also vary with wavelength. This may be one of the reasons why the Menai Strait version of the model did not predict so well.

In the Baltic Sea model we had some information about backscatter (as derived from measurements made with the Hydroscat instrument at four stations in the Skagerrak), but no information about scattering. It seems likely that the backscatter coefficients vary regionally and thus that their values should be appropriate to the different regions as well as seasons for inclusion into the Baltic Sea model. The backscatter properties of cyanobacteria blooms, for example, are known from satellite imagery to be distinctive (see Chapter 6).

During a sensitivity analysis of the Baltic Sea model, it was found that the model was very sensitive to changes in backscatter, b_b. The sensitivity analysis showed that when the model's values for b_b were made spectrally neutral, the predictive power of the model improved. Figure 8.4 shows the comparison between the two model runs, with Figure 8.4a the same as Figure 6.12 (spectrally varying b_b), and Figure 8.4b, assuming b_b to be spectrally neutral (by setting $b_b^* = 0.02\ m^2\ (g\ SPM)^{-1}$ for all the channels).

This suggests that the way forward, for model improvement, lies in further work on

particle scattering in Case-2 waters.

8.7 Colour sensor channel prescription

When the four-channel colour sensor was designed by Bowers and Tett (Bowers *et al.* 2000) it was intended that four channels of (uncalibrated) irradiance would give three independent colour ratios, allowing the estimation of two phytoplankton chromatic groups and SPM.

Chapter 4 verified that in Case-1 waters the sensors can be used to derive pigments concentrations from the cyan: green ratio. There was a good relationship between the logarithm of upwelling cyan:green ratio and the logarithm of the chlorophyll a concentration, over the range of chlorophyll concentrations from below 0.05 to more than 30 $\mu g\ l^{-1}$. This wide-range relationship, in essence gave a universal calibration for the instruments in Case-1 waters. The MOG at UWB chose to work with the cyan:green, rather than the blue:green, ratio because the sensor response to blue light was very low at the highest concentrations of chlorophyll. In a way using the cyan:green seemed like a paradox initially, as chlorophyll does not absorb significantly in the cyan. However, it was proven by Figure 4.3 (Chapter 4) that there was a good correlation between chlorophyll a and carotenoid concentration, despite the fact that the regression included data from different types of waters (Canary Islands, Loch Striven, Outer Hebrides, Menai Strait, Irish Sea, and North Sea). This is to be expected, as the chlorophyll to total carotenoid concentration are known to be tightly coupled, despite the change in the carotenoid composition over different bio-geographical (bio-optical) provinces (Aiken *et al.* 1995). For reflectance ratios Clark (1981) suggested an algorithm switch from R(443)/ R(555) to R(490)/ R(555) to derive chlorophyll concentrations when moving from low to high chlorophyll values (see below). Theoretically it should be possible to use the same switch for the upwelling irradiance ratios from the colour sensor.

There was no significant relationship between logarithm of the cyan:green ratio and the logarithm of the chlorophyll a concentration or the logarithm of the total carotenoid concentration in the Irish Sea, the southern North Sea, and the Menai Strait, although some of the data from the Western Irish Sea fell on the Case-1 line (see Figures 4.1 and 4.2). The lack of a significant correlation in Case-2 waters may be explained by additional light absorption and scattering processes by non-phytoplankton SPM, and yellow-substance, present in varying amounts and often dominating the optical in-water

conditions. Theory suggests that the colour ratios and pigment concentrations should correlate when the other OICs remain constant.

The IOCCG working group (IOCCG, 1998) recommended the choice of the following visible channels for algorithm development in Case-1 waters (assuming a minimum of four channels): 410 nm, 443 nm, 490 nm, 555 nm. As mentioned before the R(443)/R(555) and R(490)/ R(555) ratios can both be used to derive chlorophyll a, the R(443)/ R(555) ratio being favourable for lower chlorophyll concentrations. At high chlorophyll values a switch to R(490)/ R(555) is recommended (Clark, 1981).
A combination of the R(410)/ R(555) and R(443)/ R(555) could help to distinguish between CDOM and chlorophyll a absorption. For additional information about other pigments or about species composition one needs more channels. Johnsen *et al.* (1994) showed by means of discriminant analysis that if only taking the absorption spectra of marine phytoplankton into account the following wavebands are highly predictive for different algal groups and specific pigments: 481 nm, 535 nm, 649 nm. The predictions improved when adding on another two wavebands: 586 nm, and 628 nm. However, these wavebands would have to be rather narrow to exclude information from other pigments. Another problem is that scattering could also influence the spectral signature, as discussed by Roesler (1998).

8.8 New instruments

Most current radiometers (e.g. from Satlantic or Biospherical) measure Ed and Lu for deriving the reflectance ratio and sea-truthing of satellite remote sensing. My suggestions for a relatively robust and simple instrument would be a colour sensor with 4 Ed and 4 Lu sensors. The sensor heads should both be situated at the same level close to the surface, so that one does not need to regress back to the surface. For cruises, the instrument would have wings so it could be used for profiling well away from the ship in free-falling mode to avoid ship shadow (like the SPMR from Satlantic, or the PRR 800 from Biospherical). Alternatively, it could be used on a floating frame as the ones shown in Figures 2.3b, and 6.5. Additionally, if one wanted to use the instrument not only for MRA, but also somewhat more sophisticated models (e.g. semi-empirical models), one should also have information about b_b. The WETLabs ECO VSF meter is a low-cost volume-scattering function meter from which b_b can be derived. It can be moored as well, and WETLabs have developed a protective shield against fouling. During measurements the shield is moved automatically off the meter's window. After measurement, it is closed automatically, again.

We are still working on our optical Baltic Sea model at Stockholm University, and with improved instrumentation it should be possible to inverse the semi-empirical model. We have recently got funding for new instrumentation. The AC9 (WETLabs), which is the state-of-the-art instrument to measure spectral attenuation and absorption (in nine channels), from which spectral scattering can be derived. Scattering is one of the weak parameters in the model. Using the AC9 in combination with the ECO VSF it should be possible to derive backscatter for nine wavelengths, and to improve the Baltic Sea model. With the TACCS (7-channel Lu, 3 Ed channel radiometer; Satlantic) we will be able to measure the reflectance ratio at SeaWiFS channels, as well as K_d at 490 nm. The combination of improved spectral information from our radiometers, as well as knowledge about the reflectance ratio, scattering, backscattering and the diffuse attenuation coefficient, should improve the predictive power of models.

8.9 Complementary chromatic adaptation

Chapter 7 showed some evidence for complementary chromatic adaptation by Baltic cyanobacteria. The idea of chromatic adaptation has a long history starting with Engelmann in the 1880s (Lüning 1990). Cyanobacteria are especially successful in adapting to the light field by complementary chromatic adaptation, i.e. they produce blue pigments in red light, and red pigments in green light (MacColl 1998).

The phenomenon has implications both for understanding the ecology of phytoplankton (and, in particular, how adaptations to the underwater light field may help to define ecological niches), and also for interpreting the results of in-water or remotely sensed measurements in terms of phytoplankton taxa. Figure 6.1 shows the chlorophyll-specific absorption spectra for a (a) diatom/dinoflagellate and (b) a cyanobacteria dominated phytoplankton community. From this it would seem possible to distinguish between those groups optically, e.g. by comparing R(570)/R(600) for both groups. However, evidence was presented in Chapter 7 that cyanobacteria seem to be able to adapt to the dominant light field in the Baltic Sea. Assuming a surface layer mixed down to 10-12 m depth a given cyanobacteria filament will be exposed to yellow-green light, as both the red and the blue to green light will get attenuated in the first few metres. Cyanobacteria found in such environments had a distinct absorption shoulder at 570 nm, an indication for phycoerythrocyanin. Phycoerythrocyanin was found to be present in a number of filamentous fresh-water bacteria (Chapter 7), and may be a physiological, or even an evolutionary adaptation to Case-2 water conditions. Data from the Searcher cruise in 1999 (Kratzer, 2000) gave evidence that cyanobacteria may

shift their phycobilin absorption band to the light red (peaking at around 630 nm) when found as surface accumulations (Figure 8.4). This peak is an indication for the presence of phycocyanin, which is usually an adaptation to red light (MacColl, 1998). This shift has implications for algorithm development. It may be necessary to use an algorithm switch from R(570)/R(600) at low SST to R(630)/R(600) at high SST to remotely sense cyanobacteria in the Baltic Sea. The IR channel from the AVHRR could be used to derive SST, and for determining the switch. None of the new ocean colour sensors have planned a waveband around 600 nm, and the closest to the 630 nm band is the MERIS 620 nm, and the GLI 625 nm channel (IOCCG 1998). For the remote sensing of the Baltic Sea it would be desirable to have an additional waveband at 600 nm. This would be especially valuable for bulk estimation of nitrogen fixation by filamentous cyanobacteria.

Another consideration for remote sensing is the absorption peak of cyanobacteria in the red at 677 nm (Figure 6.9). This may be of concern when using MERIS algorithms for the retrieval of chlorophyll concentration. The MERIS red chlorophyll band is 10 nm wide and centred at 665 nm, which may be a problem because this misses the chlorophyll peak in the red.

These examples show how an understanding of marine optics, including chromatic adaptation, can contribute towards the interpretation of remote sensing data.

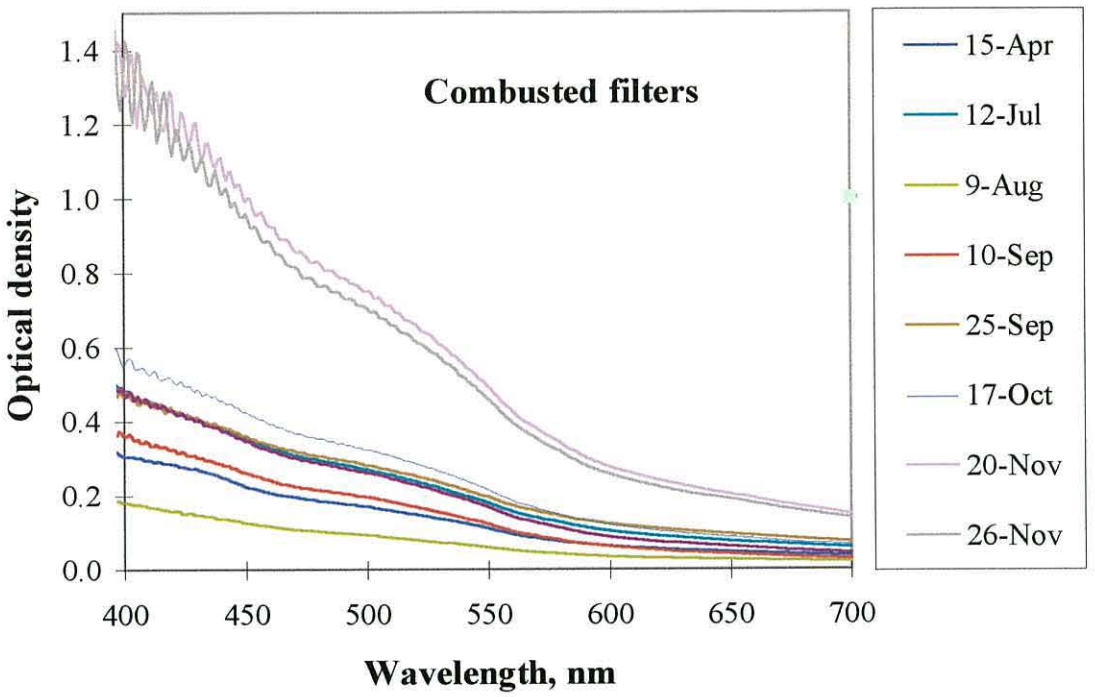

(a)

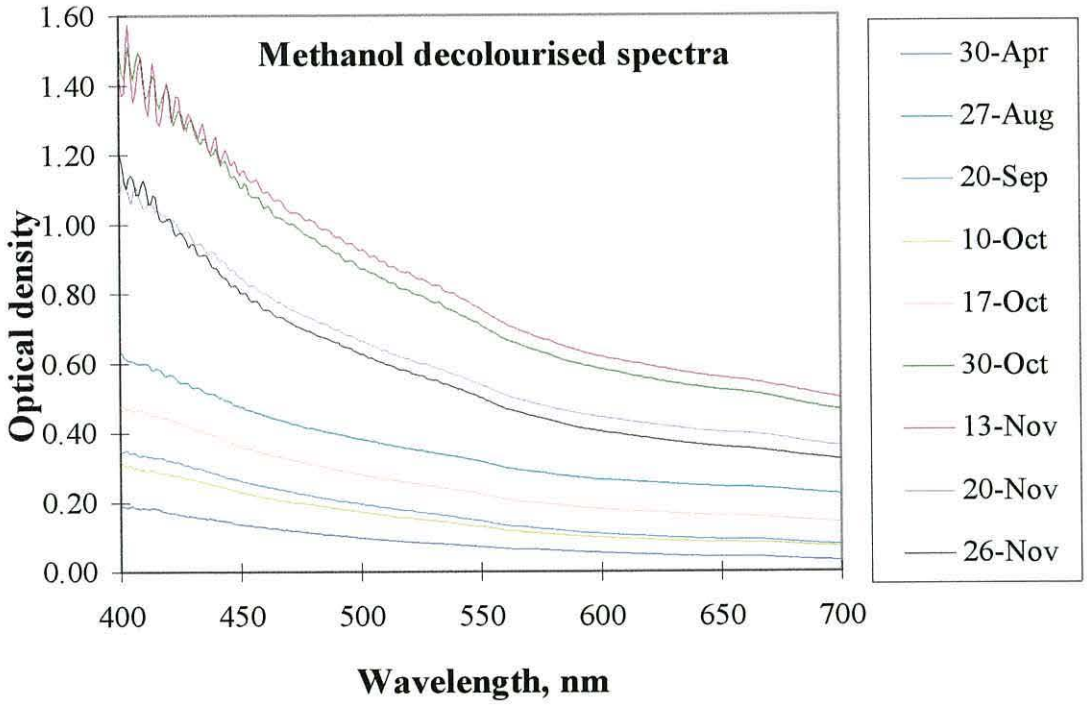

(b)

Figure 8.1 (a) Spectrum of combusted filters.
(b) Spectrum of methanol decolourised filters.

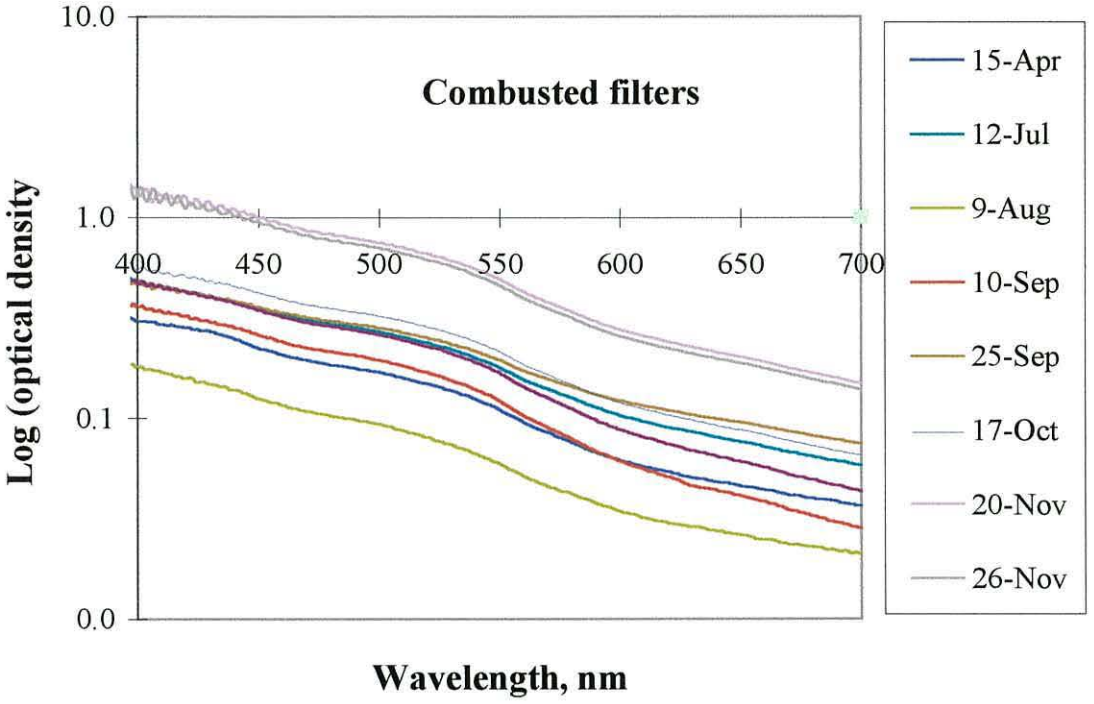

(a)

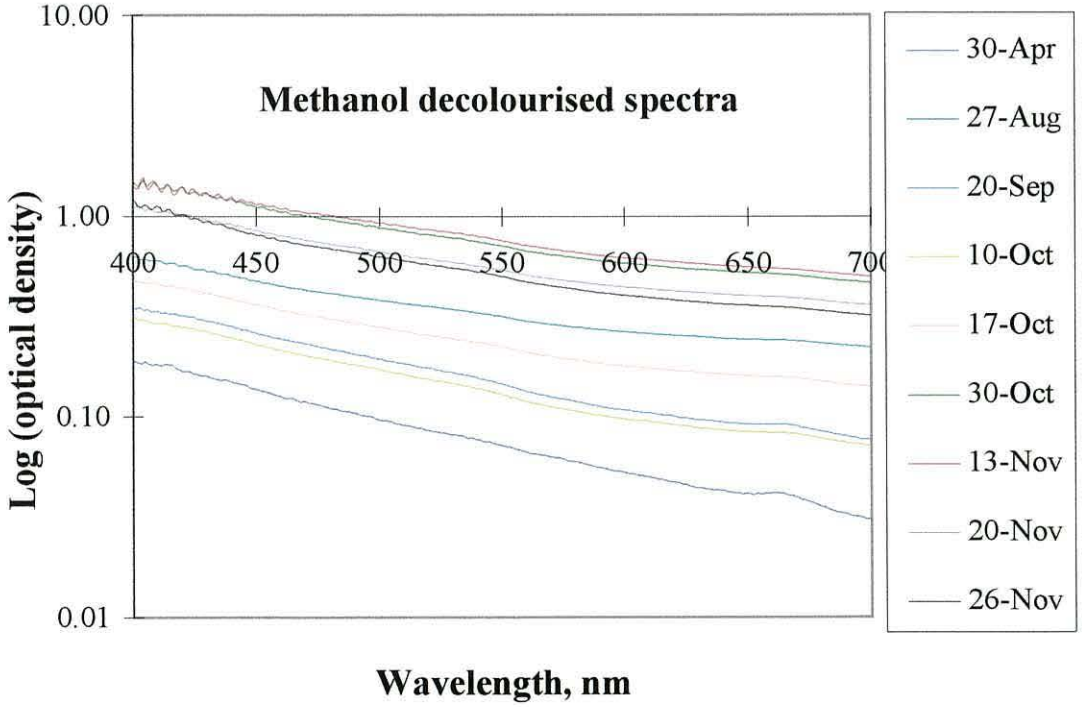

(b)

Figure 8.2 (a) Spectrum of combusted filters after log transformation of y-axis.
(b) Spectrum of methanol decolourised filters after log transformation of y-axis.

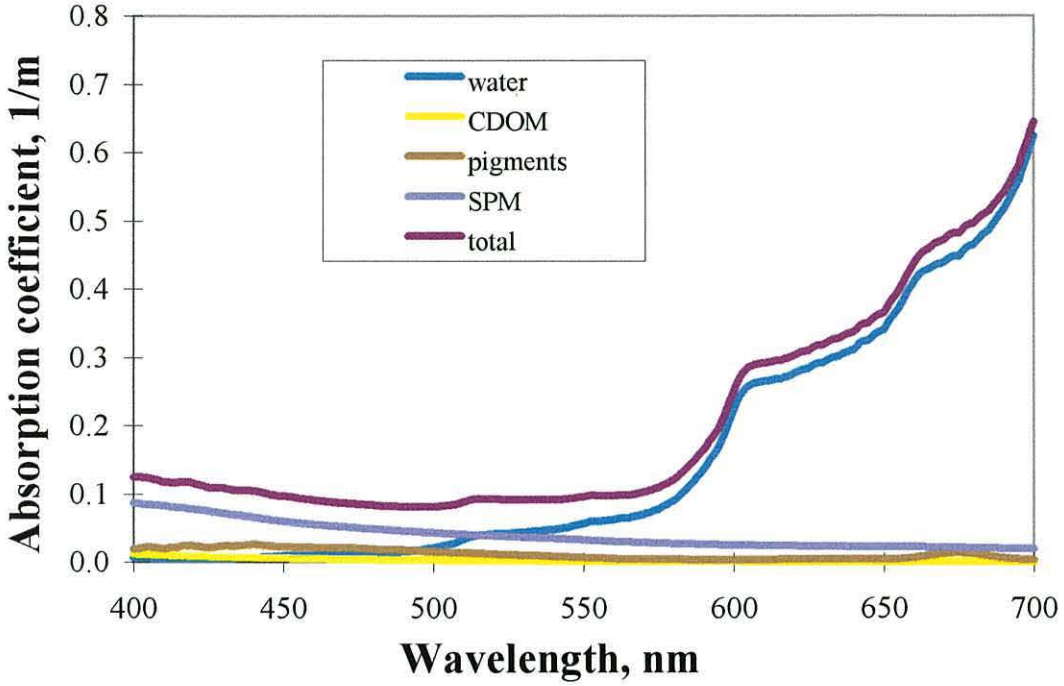

Fig. 8.3a Specific absorption coefficients Menai Strait time series, 17 October 1996. The absorption in the blue was dominated by SPM. CDOM had a minor effect on total absorption.

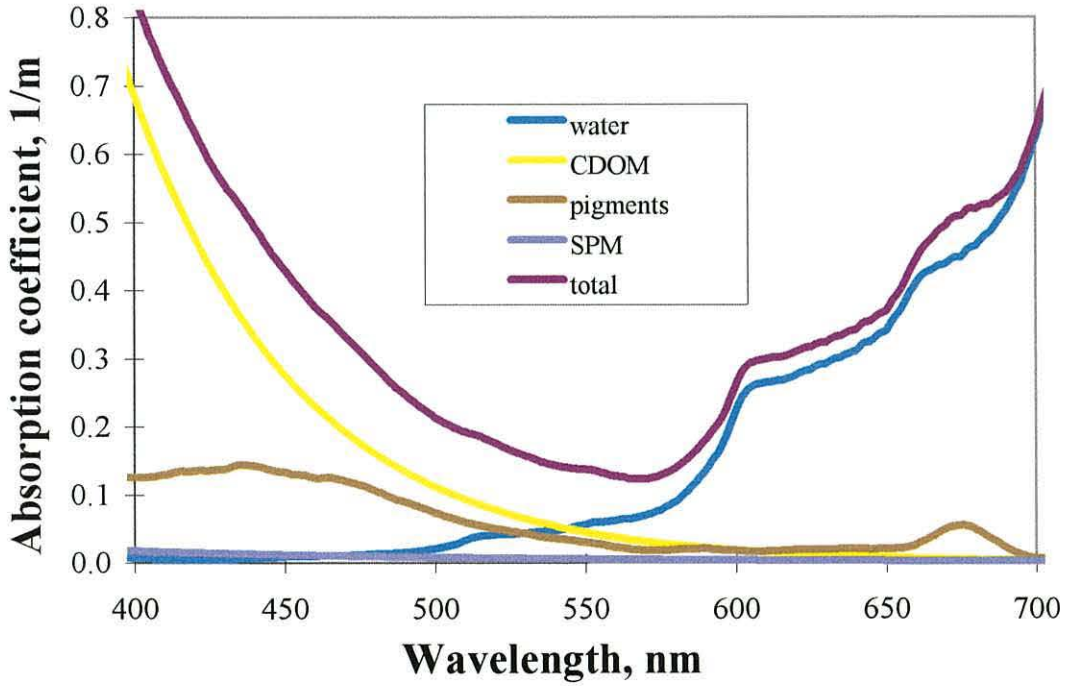

Fig. 8.3b Specific absorption coefficients for STN Å16 in the Skagerrak (same as Figure 6.10) during the May/June 1998 cruise on research vessel Argos. The absorption in the blue was strongly dominated by CDOM. SPM had a minor effect on absorption.

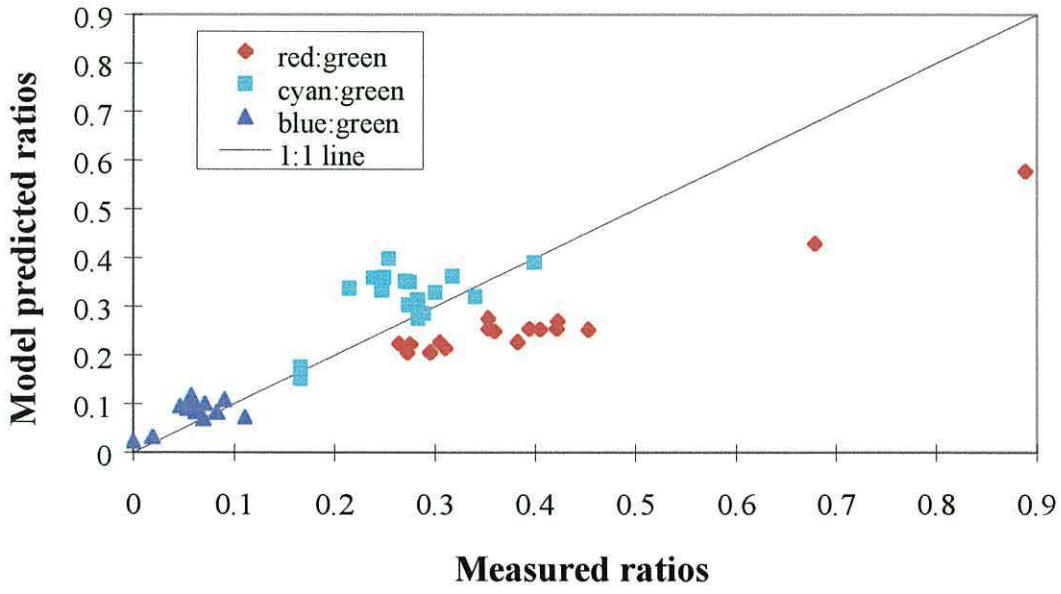

Figure 8.4 a Results from the Baltic Sea model as described in Chapter 6.

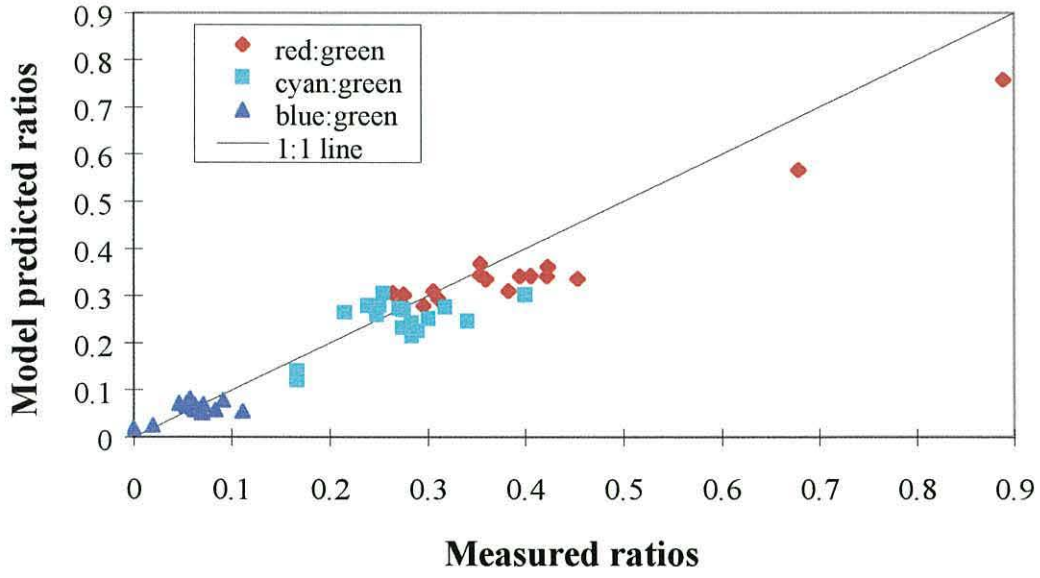

Figure 8.4 b Results from the Baltic Sea model assuming b_b to be spectrally neutral.

Appendix I

I) Instructions for using the UWB colour sensor

The CS4 colour sensors can be either used as instruments for long-term deployment on a mooring (CS2, CS3, CS20,CS21, CS23, CS24) or as profiling instruments (CS23/CS24). In contrary to the other instruments the latter two contain an internal pressure meter which measures the depth of the instrument indirectly by measuring the water pressure (output in digital numbers; DN). They also have an external RS-232 connection. A blanking plug is used for protecting the external connection during deployment.

All the CS are equipped with an internal logger and with a battery pack which lasts for up to three months. In order to start up the logging and downloading of the data the instruments must be connected to a PC with downloading software e.g. Hyperterminal (Windows program) or Smartcom (Macintosh program) with the following settings:

baud rate:	9600
bits per character:	8
stop bits:	1
parity:	none
flow control:	none.

CS23 and CS24 can be connected to an interface box via a RS-232 connection. Mooring instruments must be connected by opening the housing and connecting to the mother board. There is an additional battery supply in the interface box in order to safe battery power of the instrument during setting-up and downloading of the instrument. There is also a reset switch on the interface box of CS23 and CS24 which starts off the communication between the instrument and the computer. The mooring instruments have a blue reset switch on the mother board.

The logging mode, interval and integration period can be chosen in the main menu. The logging can be set to 'continuous mode' for the duration of 1, 10, 20, 30, 40, 50, or 60 seconds sample time, or to 'logging mode' with the option of logging in intervals of 10, 20, 30, 40, 50 or 60 minutes cycles. Continuous mode means that the colour sensor will sample and integrate over the specified sample time. In logging mode both the cycle and sample time must be set, and the colour sensor will then sample in the specified intervals, for the specified sampling time, e.g. every 10 minutes for 10 seconds. For deployment on moorings in Case-2 waters over a period of several months the logging interval may for example be 10 minutes with an integration time of

20-30 (Menai Strait), or 30-60 seconds (Baltic Sea). In logging mode, one can specify the starting and finishing time of logging in order to safe battery. The internal clock of the colour sensor is set to GMT. For example, it is possible to program the colour sensor to start logging at 10:00 GMT, and to finish logging at 16:00 GMT. After the deployment the data can be downloaded to an ASCII file and the memory can be cleared for the next deployment. The option 'power down' is used for turning the instrument off at the end of deployment.

II) The colour sensor program

The program only works with 'caps lock' on. First connect the colour sensor to a computer, and start of the communication with the reset switch, and the following window will appear:

UNIVERSITY OF WALES
SCHOOL OF OCEAN SCIENCE
MKIII IRRADIANCE LOGGER
SOFTWARE VERSION 1.20 15/01/96

MENU OPTIONS [Y/N] -

Command 'Y' takes you into the option menu, with screen:

Irradiance Logger Menu Options

1 - Setup Options

2 - Display Options

3 - Download Data

4 - Erase Memory

5 - Power Down (Battery Saving)

6 - Start Logging (Default)

Enter Option (1-6):-

To set the sampling mode and intervals use option 1. The following options will then appear:

Irradiance Logger Setup Menu

1 - Set Continuous Mode

2 - Set Logging Mode

3 - Set Cycle Time

4 - Set Sample Time

5 - Set Logging Start Time

6 - Set Logging Stop Time

7 - Exit

Enter Option (1-7) :-

You can either choose between continuous mode (for profiling) or logging mode (which you would use for a moored instrument). With option 1 (continuous mode) choose option 4 to determine the sample time in seconds:

Set Sample Time

1 - 1 sec.

2 - 10 secs.

3 - 20 secs.

4 - 30 secs. (Default)

5 - 40 secs.

6 - 50 secs.

7 - 1 min.

Enter Option (1-7) :-

On a dull day you may have to use a sampling time of 30 sec but on a very sunny day 10 sec might be sufficient to get a reasonable response.
Using any of these options will take you back into the Set-up Menu.
Use the Setup Menu's option 2 for setting the instrument to log on a mooring. Both option 3 and 4 have to be set with option 2. Option 3 sets the cycle time i.e. the time

between the start of two successive measurements, and option 4 to set the integration time during one measurement. Option 2 chooses how many seconds the instrument is logging for.

In order to set the starting time of the logging choose option 5. The following screen will show up:

Set Start Time

1 - 0400 hrs.

2 - 0500 hrs.

3 - 0600 hrs. (Default)

4 - 0700 hrs.

5 - 0800 hrs.

6 - 0900 hrs.

Enter Option (1-6) :

Choosing any option will take you back into the set-up menu.
To set the stop time of the sampling choose option 6:

Set Stop Time

1 - 1600 hrs.

2 - 1700 hrs.

3 - 1800 hrs. (Default)

4 - 1900 hrs.

5 - 2000 hrs.

6 - 2100 hrs.

Enter Option (1-6) :

Again, choosing one of the settings will take you back into the set up menu. To exit set up menu choose option 7 which takes you back into the main menu. Use option 2 to check if the logging mode is set right.
After setting up the sampling mode enter option 6 to start logging.

For CS23/CS24: once the internal logging is started put blanking plug before lowering instrument into the sea.

For profiling: Note times and keep instrument for the interval of at least 2 readings at each depth (this means 3 times the sampling time). First record up-welling profile then take instrument out and turn the sensor (by undoing and turning the cables of the frame over to the other side).

After taking the instrument out of the water measure the dark currents by completely covering up the sensor screen with a black plastic bag. I noticed that some black bags are not very dense- needs to be a good one!

III) Downloading data

For downloading data reconnect the instrument to the computer and start off the communication with the instrument again by the reset switch (switch caps lock on!).

Choose 'Y' to get to option menu.

Use option 3 to log data into the file (make sure your PC program is set up to receive a file before). If you want to erase all the data after downloading hit option 4.

In order to power down hit option 5; the following note will appear:

STANDBY POWER - PRESS RESET TO POWER UP

Take the connector off, put blanking plug in (CS23/CS24), or carefully close the housing.

The readings of the colour sensor are in DN, and the downloaded data is arranged in 7 columns:

date, time, red (670 nm), yellow (570 nm), cyan (490 nm), and blue (440 nm)

for CS23/CS24 there is also a column for depth counts (pressure counts).

In CS20-CS22 the last column contains a row of zeros.

Glossary

A&D:	Manufacturer of electronic balances and scales. Name stands for 'Analog to Digital Conversion'.
A/D:	Analog-to-Digital
AOPs:	Apparent Optical Properties
ARGOS:	Not an acronym; data collection and location system on NOAA operational satellites
ASCII:	American Standard Code for Information Interchange
ATP:	Adenosine triphosphate. Common energy 'currency' of cells.
AVHRR:	Advanced Very High Resolution Radiometer
BS:	Baltic Sea
CEFAS:	Centre for Environment, Fisheries and Aquaculture Science (Lowestoft)
CDOM:	Coloured Dissolved Organic Matter
CZCS:	Coastal Zone Colour Scanner
CS:	Colour Sensor
DIN:	Dissolved Inorganic Nitrogen
DIP:	Dissolved Inorganic Phosphorus
DN:	Digital Numbers
FWHM:	Full -Width at Half-Maximum
GF/F:	not an acronym; a specific type of glass fibre filter manufactured by Whatman nominal pore size: 0.7 μm
GMT:	Greenwich Mean Time
HELCOM:	Helsinki Commission
HPLC:	High Performance Liquid Chromatography
IOPs:	Inherent Optical Properties
IR:	Infrared
IOCCG:	International Ocean-Colour Coordinating Group
JGOFS:	Joint Global Ocean Flux Study
JONUS:	Joint Nutrient Study
MAFF:	Ministry of Agriculture Fisheries and Food
MOG:	Marine Optical Group, SOS
MOS:	Modular Optical Scanner
MRA:	Multiple Regression Analysis
ms:	manuscript
MS:	Menai Strait
MSS:	Mineral Suspended Solids, mineral part of SPM
MSS:	Multi Spectral Scanner
NCP:	Non Chlorophyllous Particulates
NERC:	Natural Environment Research Council
NIR:	Near Infrared
NIST:	National Institute of Standards and Technology (USA)
NOAA:	National Oceanic and Atmospheric Administration (USA)
NPL:	National Physical Laboratory
OICs:	Optically-active In-water Constituent
OSS :	Organic Suspended Solids, organic part of SPM
PCB:	phycocyanobilin
PEB:	phycoerythrobilin
PML:	Plymouth Marine Laboratories
psu:	practical salinity unit
PUB:	phycourobilin
PVB:	phycoviolobilin
RMS:	root mean square
SCOR:	Scientific Community on Oceanographic Research
SeaWiFS:	Sea-viewing Wide Field-of-view Sensor
SEM:	scanning electron microscope
SES:	Shelf-Edge-Study
SIRREX:	SeaWiFS Intercalibration Round-Robin Experiment
SMHI:	Swedish Meteorological and Hydrological Institute

SOS:	School of Ocean Sciences in Menai Bridge (University of Wales, Bangor)
SPM:	Suspended Particulate Matter, same as TSS
SST:	Sea Surface Temperature
TSS:	Total Suspended Solids, same as SPM
UCES:	Unit of Coastal and Estuarine Studies, SOS, Menai Bridge
UWB:	University of Wales, Bangor
UV:	Ultraviolet

Akinete:	Vegetative cell which becomes transformed into a thick-walled, resistant spore. Formed by certain cyanobacteria and some algae (e.g. some Chlorophyta).
Frustule:	The external skeleton of a diatom.
Heterocysts:	Specialised cells found in some Cyanobacteria. Larger than the vegetative cells. They are thick-walled cell inclusions that are impermeable to oxygen; they provide the anaerobic (oxygen-free) environment necessary for the operation of the nitrogen-fixing. Particularly efficient nitrogen fixers are found among the filamentous species that have specialised cells called heterocysts enzymes.

References

Abbott, MR, Brink, KH, Booth, CR, Blasco, D, Swenson, MS, Davis, CO, and Codispoti, LA , 1995, Scales of variability of bio-optical properties as observed from near-surface drifters, *Journal of Geophysical Research* **100**: 13345-13367.

Abbott, MR, Richerson, PJ and Powell, TM, 1982, *In situ* response of phytoplankton fluorescence to rapid variations in light, *Limnology and Oceanography* **27**: 218-225.

Aiken, J, Moore, G, Trees, CC, Hooker, SB, and Clark, DK, 1995, Volume 29, The SeaWiFS CZCS-Type Pigment Algorithms, *SeaWiFS Technical Report Series,* Editors: Hooker, SB, Firestone, ER, and Acker, JG, NASA Technical Memorandum 104566, Maryland, **29**: 6-13.

Allali, K, Bricaud, A, Babin, M, Morel, A, Chang, P,1995, A new method for measuring spectral absorption coefficients of marine particles, *Limnology and Oceanography* **40**(8): 1526-1532.

Barlow, RG, Mantoura, RFC, Gough, MA, and Fileman, TW, 1993, Pigment signatures of phytoplankton composition in the northeastern Atlantic during the 1990 spring bloom, *Deep-Sea Research II* **40**(1/2): 459-477.

Barnes, RA , Holmes, AW and Esaias, WE, 1995, Stray light in the SeaWiFS radiometer, *NASA Technical Memorandum 104566, SeaWiFS Technical Report Series* **31,** *edited by* S B Hooker, E R Firestone, and J G Acker (Maryland, Goddard Space Flight Centre).

Beale, SI and Cornejo, J, 1991, Biosynthesis of Phycobilins - 3(Z)-Phycoerythrobilin and 3(Z)- Phycocyanobilin are intermediates in the formation of 3(E)-phycocyanobilin from biliverdin-IX-Alpha, *Journal of Biological Chemistry*, **266** (33): 22333-22340.

Bidigare, RR, Morrow, JH, 1989, Derivative analysis of spectral absorption by photosynthetic pigments in the western Sargasso Sea, *Journal of Marine Research* **47**: 323-341.

Blight, SP, Bently, TL, Lefevre, D, Robinson, C, Rodrigues, R, Rowlands, J, and Williams, PJ leB, 1995, Phasing of autotrophic and heterotrophic plankton metabolism in a temperate coastal ecosystem, *Marine Ecology-Progress Series* **128**: 61-75.

Boney, AD, 1989, *Phytoplankton*. London, Edward Arnold.

Booth, CRB and Smith, RC, 1988, Moorable spectroradiometer in the Biowatt Experiment. In *Ocean Optics IX,* eds. SG Ackleson, R Frouin, Proceedings SPIE (The International Society of Optical Engineering), Washington, **925**: 176-188.

Bowers, DG and Mitchelson-Jacob, EG, 1996, Inherent optical properties of the Irish Sea determined from underwater irradiance measurements, *Estuarine, Coastal and Shelf Science* **43**: 433-447.

Bowers, DG, Harker, GEL, and Stephan, B, 1996, Absorption spectra of inorganic particles in the Irish Sea and their relevance to remote sensing of chlorophyll, *International Journal of Remote Sensing* **17**(12): 2449-2460.

Bowers, DG, Boudjelas, S, and Harker, GEL, 1997, The distribution of fine suspended sediments in the surface waters of the Irish Sea and its relationship to tidal stirring. *International Journal of Remote Sensing* **19** (14): 2789-2805.

Bowers, DG, Kratzer, S, Morrison, JR, Smith, PSD, Tett, PB, Walne, AW, and Wild-Allen, K, 2000, On the calibration and use of in situ ocean colour measurements for monitoring algal blooms, *International Journal of Remote Sensing*, in press.

Bricaud, A, Morel, A and Prieur, L, 1981, Absorption By Dissolved Organic-Matter of the Sea (Yellow Substance) in the UV and Visible Domains, *Limnology and Oceanography* **26** (1): 43-53.

Bricaud, A and Stramski, D, 1990, Spectral absorption coefficients of living phytoplankton and nonalgal biogenous matter: A comparison between the Peru upwelling area and Sargasso Sea, *Limnology and Oceanography* **35**: 562-582.

Bricaud, A, Babin, M, Morel, A, Claustre, H, 1995, Variability in the chlorophyll-specific absorption-coefficients of natural phytoplankton - analysis and parameterization, *Journal of Geophysical Research-Oceans* **100** (C7): 13321-13332.

Brown, J and Simpson, JH, 1990, The radiometric determination of total pigment and seston and its potential use in shelf seas, *Estuarine, Coastal and Shelf Science* **31**:1-9.

Buchan, S, Floodgate, GD, and Crisp, DJ, 1967, Studies on the seasonal variation of the suspended matter in the Menai Straits. I. The inorganic fraction, *Limnology and Oceanography* 12 (1): 419-31.

Buiteveld, H, Hakvoort, JHM, and Donze, M, 1994, The optical properties of pure water. In *Ocean Optics XII,* eds. SG Ackleson and R Frouin, SPIE Proceedings (The International Society of Optical Engineering), Washington, **2258**: 174-183.

Butler, LW, 1962, Absorption of light by turbid materials, *Journal of the Optical Society of America* **52**: 292-299.

Carder, KL, Steward, RG, Harvey, GR, and Ortner, PB, 1989, Marine humic and fulvic -acids- their effect on remote-sensing of ocean chlorophyll, *Limnology and Oceanography* **34** (1): 68-81.

Carder, KL , Hawes, SK, Baker, KA, Smith, RC, Steward, GR, and Mitchell, BG, 1991, Reflectance model for quantifying chlorophyll a in the presence of productivity degradation products, *Journal of Geophysical Research* **96**, 20599-20611.

Chapman, D, 1998, *Water Quality Assessment*, 1998, 2nd ed., E & S N Spon (Chapman and Hall).

Chrétiennot-Dinet, M-J, 1990, *Atlas du phytoplankton marin*. Paris, Éditions du centre national de la recherche scientifique.

Chrisholm, SW, Olson, RJ, Zettler, ER, Goericke,R, Waterbury, JB, and Welschmeyer, NA, 1988, A novel free-living prochlorophyte abundant in the ozeanic euphotic zone, *Nature* **334**: 340-343.

Chrisholm, SW, Frankel, SL, Goericke, R, Olson, RJ, Palenik, B, Waterbury, JB, West-Johnsrud, L, and Zettler, ER, 1992, *Prochlorococcus marinus nov.* gen. *nov.* sp. an oxytrophic marine procaryote containing divinyl chlorophyll a and b, *Archiv für Mikrobilogie* **157**: 297-300.

Clark, DK, 1981, Phytoplankton algorithms for the Nimbus-7 CZCS. In: Oceanography from space, Ed. Gower, Plenum Press, 227-238.

Cleveland, JS and Weidemann, AD, 1993, Quantifying absorption by aquatic particles: a multiple scattering correction for glass-fibre filters, *Limnology and Oceanography* **38**: 1321-1327.

Cleveland, JS, 1995, Regional models for phytoplankton absorption as a function of chlorophyll-a concentration, *Journal of Geophysical Research-Oceans* **100** (C7):13333-13344.

Coble, PG and Brophy, MM, 1994, Investigation of the geochemistry of dissolved organic matter in coastal waters using optical properties. In *Ocean Optics XII,* eds. SG Ackleson and R Frouin, SPIE Proceedings (The International Society of Optical Engineering), Washington, **2258**: 377-391.

Darecki, M and Kowalczuk, P, 1996, Upwelled spectral radiance distribution in relation to yellow substance absorption in the example of Case II waters (Baltic Sea). In

Ocean Optics XIII, eds. SG Ackleson and R Frouin, SPIE Proceedings (The International Society of Optical Engineering) **2963**: 386-391.

Dera, J and Stramski D, 1986, Maximum of sunlight focusing under wind-disturbed sea surface, *Oceanologia* **34**: 15-42.

Doerffer, R and Fischer, J, 1994, Concentrations of chlorophyll, suspended matter, and Gelbstoff in Case-II waters derived from satellite coastal zone color scanner data with inverse modelling methods, *Journal of Geophysical Research-Oceans* **99** (C4): 7457-7466.

Dowell, MD , Berthon, J-F, Hoepffner, N, and Gross*i*, S, 1996, Absorption modelling in Case II waters: the need to distinguish Coloured Dissolved Organic Matter from Non-Chlorophyllous Particulates. In *Ocean Optics XIII*, eds. SG Ackleson and R Frouin, SPIE Proceedings (The International Society of Optical Engineering) **2963**: 401-407.

Ducret A, Sidler W, Frank G, Zuber H, 1994, The complete amino-acid-sequence of r-phycocyanin-I alpha subunit and beta-subunit from the red alga *Porphyridium cruentum* - structural and phylogenetic-relationships of the phycocyanins within the phycobiliprotein families, *European Journal of Biochemistry* **221**: (1) 563-580.

Duysens, LNM, 1956, The flattening of the absorption spectrum of suspensions as compared to that of solutions, *Biochimica Biophysica Acta* **19**: 1-12.

Ekstrand, S ,1992, Landsat TM based quantification of chlorophyll-a during algae blooms in coastal waters, *International Journal of Remote Sensing* **13**(10): 1913-1926.

El Hag, AGD, and Fogg, GE , 1986, The distribution of blue-green algae (cyanobacteria) in the Menai Straits and the Irish Sea, *British Phycological Journal* **21**: 45-54.

Falkowski, PG, 1980, *Primary productivity in the sea*. New York, Plenum Press.

Falkowski, PG and Raven, JA, 1997, *Aquatic photosynthesis*. Oxford, Blackwell Science, 375 pp.

Fasham, MJR, Pugh, PR, Griffiths, D and Wheaton, JEG, 1983, A submersible fluorometer for the detection of chlorophyll, *The Radio and Electronic Engineer* **53**: 21-24.

Fujita, Y, Murakami, A, and Aizawa, K, 1974, Phycoerythrin of the marine blue-green alga *Trichodesmium thiebautii*, *Plant Cell Physiology* **15**: 939-942.

Gallegos, CL, Correll, DL and Pierce, JW, 1990, Modelling spectral diffuse attenuation, absorption and scattering coefficients in a turbid estuary, *Limnology and Oceanography* **35**: 1486-502.

Garver, SA, Siegel, DA, and Mitchell, BG, 1994, Variability in near-surface particulate absorption spectra: what can a satellite ocean colour imager see? *Limnology and Oceanography* **39**: 1349-1367.

Gieskes, WW and Kraay, GW, 1983, Unknown chlorophyll a derivatives in the North Sea and the tropical Atlantic Ocean revealed by HPLC analysis, *Limnology and Oceanography* **28**: 757-766.

Gieskes, WW and Kraay, GW, 1986, Floristic and physiological difference between the shallow and the deep nanoplankton in the euphotic zone of the open tropical Atlantic revealed by HPLC analysis of pigments, *Marine Biology* **91**: 567-576.

Glover, HA, Phinney, DA, and Yentsch, CS, 1985, Photosynthetic characteristics of picoplankton compared to those of larger phytoplankton populations in various water masses in the Gulf of Maine, *Biological Oceanography* **3**: 223-248.

Goericke, R and Repeta, DJ, 1992, The pigments of *Prochlorococcus marinus*: The presence of divinyl chlorophyll a and b in a marine prochlorophyte, *Limnology and Oceanography* **37**: 425-433.

Goericke, R and Repeta, DJ, 1993, Chlorophyll a and b and divinyl chlorophylls a and b in the open subtropical North Atlantic Ocean, *Marine Ecology Progress Series* **101-103**: 307-313.

Gordon, HR and Morel, AY , 1983, Remote assessment of ocean colour for interpretation of satellite visible imagery: A review. New York: Springer Verlag.

Gordon, HR and Ding, K, 1992, Self-shading of in-water optical instruments, *Limnology and Oceanography* **37**: 491-500.

Gordon, HR, 1995, Remote-sensing of ocean color - a methodology for dealing with broad spectral bands and significant out-of-band response, *Applied Optics* **34** (36): 8363-8374.

Gowen, RJ, Tett, P and Wood, BJB, 1982, The problem of degradation pigments in the estimation of chlorophyll by fluorescence, *Archiv für Hydrobiologie, Ergebnisse der Limnologie*, **16**: 101-106.

Gregg, WW , Chen, FC, Mezaache, AL, Chen, JD, and Whiting, JA, 1993, The Simulated SeaWiFS Data Set, Version 1. *NASA Technical Memorandum 104566*, eds, SB Hooker and ER Firestone, NASA Goddard Space Flight Center, Greenbelt, Maryland, **9:**17 pp.

Håkansson, B G and Moberg, M, 1994, The algal bloom in the Baltic during July and August 1991, as observed from the NOAA weather satellites, *International Journal of Remote Sensing* **15**(5*)* 963-965.

Harker, GEL, 1997, A comparison between optical measurements made in the field and in the laboratory, and the development of an optical model, PhD thesis, School of Ocean Sciences, University of Wales, Bangor, UK.

Hashimoto, S and Otsuki, A, 1995, Natural Occurrence of Phycoerythrocyanin-Like Pigment in Cyanobacterial Blooming Samples Dominated By Microcystis in Lake Kasumigaura, *Journal of Plankton Research* **17** (5): 907-917.

Hausschild, CA, McMurter, HJG and Pick, FR, 1991, Effects of spectral quality on growth and pigmentation of picocyanobacteria, *Journal of Phycology* **27**(6):698-702.

Heathcote, PM, Wyman, M, Carr, NG, and Beddard, GS, 1992, Partial uncoupling of energy transfer from phycoerythrin in the marine cyanobacterium *Synechococcus* sp, WH7803, *Biochimica Biophysica Acta* **1099**: 267-270.

HELCOM, 1996, Third periodic assessment of the state of the marine environment of the Baltic Sea, 1989-1993; Executive Summary. HELSINKI COMMISSION Baltic Sea Environment Protection Commission, *Baltic Sea Environment Proceedings* **64 A**.

HELCOM, 1996, Third periodic assessment of the state of the marine environment of the Baltic Sea, 1989-1993; Background Document. HELSINKI COMMISSION Baltic Sea Environment Protection Commission, *Baltic Sea Environment Proceedings* **64 B**.

Hewes, CD and Holm-Hansen, O, 1983, A method for recovering nanoplankton from filters for identification with the microscope: The filter-transfer-freeze (FTF) technique, *Limnology and Oceanography* **28**: 389-394.

Hoepffner, N and Sathyendranath, S, 1991, Effect of pigment composition on absorption properties of phytoplankton, *Marine Ecology Progress Series* **73**: 11-23.

Hoepffner, N and Sathyendranath, S, 1992, Bio-optical characteristics of coastal waters: Absorption spectra of phytoplankton and pigment distribution in the western North Atlantic, *Limnology and Oceanography* **37**(8): 1660-1679.

Hoge, FE and Swift, RN, 1990, Photosynthetic accessory pigments: evidence for the influence of phycoerythrin on the submarine light field, *Remote Sensing Environment* **34**: 19-35.

Hoge, FE, 1999, Algorithm Theoretical Basis Document MODIS Phycoerythrin Pigment Concentration, Modis phycoerythrin data product, http://modarch.gsfc.nasa.gov/MODIS/ATBD/atbd_mod27.pdf.

Højerslev, NK, 1989, Surface water quality studies in the interior marine environment of Denmark, *Limnology and Oceanography* **34** (8) 1630-1639.

Højerslev, NK and Aas, E, 1998, Spectral light absorption by Gelbstoff in coastal waters displaying highly different concentrations. *Ocean Optics XIV*, Kailua-Kona, Hawaii, USA, 10-13 November 1998.

Hong, Q, Zhao, KH and Scheer, H, 1993, 2 different types of photochemistry in phycoerythrocyanin alpha-subunit, *Photochemistry and Photobiology* **58** (5): 745-747.

Hooker, SB, Esaias, WE, Feldman, GC, Gregg, WW, and McClain, CR, 1992, An overview of SeaWiFS and ocean colour, *NASA Technical Memorandum 104566*, **1**, eds SB Hooker and DK Clark, Goddard Space Flight Centre, Maryland, 24 pp.

Horstmann, U , 1975, Eutrophication and mass production of blue-green algae in the Baltic, *Merentutkimuslaitoksen julkaisu, Havsforskningsinstitutets skrift* **239**, 83-90.

Horstmann, U, van der Piepen, H, Barrot, KW, 1986, The influence of river water on the southeastern Baltic Sea as observed by NIMBUS 7/CZCS imagery, *Ambio* **15**(5): 286-289.

Houghton, WM, Exton, RJ, Gregory, RW, 1983, Field investigation of techniques for remote laser sensing of oceanographic parameters, *Remote Sensing Environment* **13**: 17-32.

IOCCG, 1998, Minimum requirements for an operational, ocean-colour sensor for the open ocean, Reports of the international ocean-colour coordinating group, Report number 1, Report on an IOCCG working group held in Villlefranche-sur-Mer, October 6-7, 1997.

Jeffrey, SW, 1974, Profiles of photosynthetic pigments in the ocean using thin-layer chromatography, *Marine Biology* **26**: 101-110.

Jeffrey, SW and Humphrey GF, 1975, New spectrophotometric equations for determining chlorophylls a, b, c1 and c2 in higher plants, algae and natural phytoplankton, *Biochemie und Physiologie der Pflanzen* **167**: 191-194.

Jeffrey, SW and Hallegraeff, 1987, Chlorophyllase distribution in 10 classes of phytoplankton - a problem for chlorophyll analysis, *Marine Ecology Progress Series* **35**: 293-304.

Jeffrey, SW, Mantoura, RFC and Wright, SW, 1997, *Phytoplankton pigments in oceanography.* Monographs on oceanographic methodology: UNESCO Publishing, Paris.

Jeffrey, SW, Mantoura, RFC, and Bjørnland, T, 1997, Data for the identification of 47 key phytoplankton pigments. In: Phytoplankton pigments in oceanography: Guidelines to modern methods, Appendix F, eds. SW Jeffrey, RFC Mantoura, SW Wright. UNESCO. Paris, 449-559.

Jeffrey, SW and Vesk, M, 1997, Introduction to marine phytoplankton and their pigment signature. In: Phytoplankton pigments in oceanography: Guidelines to modern methods, eds. SW Jeffrey, RFC Mantoura, SW Wright. UNESCO. Paris, 37-84.

Jeffrey, SW and Welschmeyer, NA, 1997, Spectrophotometric and fluorometric equations in common use in oceanography. In: Phytoplankton pigments in oceanography: Guidelines to modern methods, eds. SW Jeffrey, RFC Mantoura, SW Wright. UNESCO, Paris, 597-615.

Jerlov, NG, 1976, *Marine Optics*. Elsevier Oceanography Series 14, Elsevier Scientific Publishing Company, Amsterdam, 231 pp.

Johnsen, G, Samset, O, Granskog, L and Sakshaug, E, 1994, *In vivo* absorption characteristics in 10 classes of bloom-forming phytoplankton: taxonomic characteristics and responses to photoadaptation by means of discriminant and HPLC analysis, *Marine Ecology Progress Series* **105**: 149-157.

Joint Global Ocean Flux Study, 1991, JGOFS Core Measurements Protocols, *JGOFS Report* **6**, Scientific Community on Oceanic Research, 40 pp.

Jones, LW and Myres, J, 1965, Pigment variations in *Anacystis nidulans* induced by light of selective wavelength, *Journal of Phycology* **1**: 7-14.

Jones, M, and Spencer, CP,1970, The phytoplankton of the Menai Straits, *Journal du Conseil International pour l'Exploration de la Mer* 33(2): 169-180.

Kahru, M, Leppänen, J-M, Rud, O, 1993, Cyanobacterial blooms heating the sea surface, *Marine Ecology Progress Series* **101**: 1-7.

Kahru, M, Horstmann, U, and Rud, O, 1994, Satellite detection of increased cyanobacterial blooms in the Baltic Sea: Natural fluctuation or ecosystem change? *Ambio* **23**(8): 469-471.

Kahru, M , Håkansson, B, and Rud, O, 1995, Distribution of sea-surface temperature fronts in the Baltic Sea as derived from satellite imagery, *Continental Shelf Research* **15**(6): 663-679.

Kahru, M, 1997, Using satellites to monitor large-scale environmental change: A case study of cyanobacteria blooms in the Baltic Sea. In: Monitoring algal blooms, New techniques for detecting large-scale environmental change, *edited by* M Kahru and C W Brown, Springer-Verlag Berlin Heidelberg New York, 43-61.

Karlsson, K-G, 1996, Cloud classifications with the SCANDIA model, SMHI Reports Meteorology and Climatology, **67**.

Kiefer, DA and Sohoo, JB, 1982, Spectral absorption by marine particles of coastal waters of Baja California, *Limnology and Oceanography* **27**: 492-499.

Kiefer, DA and Mitchell, BG, 1983, A simple, steady-state description of phytoplankton growth based on absorption cross-section and quantum efficiency, *Limnology and Oceanography* **28**: 770-776.

Kirk, JTO, 1980, Spectral absorption properties of natural waters: Contribution of the soluble and particulate fractions to light absorption in some inland waters of southeastern Australia, *Australian Journal of Marine and Freshwater Research* **31**: 287-296.

Kirk, JTO, 1994, *Light and photosynthesis in aquatic ecosystems*. Second edition, Cambridge University Press, Cambridge.

Kishino, M, Takahashi, M, Okami, N and Ichimura, S, 1985, Estimation of the spectral absorption coefficients of phytoplankton in the sea, *Bulletin of Marine Science* **37**: 634-642.

Kleppel, GS and Pieper, RE, 1984, Phytoplankton pigments in the gut contents of planktonic copepods from coastal waters off southern California, *Marine Bioliology* **78**: 193-198.

Kononen, K, 1992, Dynamics of the toxic cyanobacterial blooms in the Baltic Sea, *Finnish marine research* **261**: 3-36.

Kononen, K, Sellner, KG, Lassus, P, Arzul, G, Erard-le-Denn, E, Gentien, P, Marcaillou-Le-Baut, C, 1995, Toxic cyanobacterial blooms in marine, estuarine and coastal ecosystems. In: Harmful marine algal blooms (Paris Lavoisier), 858-860.

Kononen, K, Kuparinen, J, Makela, K, Laanemets, J, Pavelson, J, and Nommann, S, 1996, Initiation of cyanobacterial blooms in a frontal region at the entrance of the Gulf of Finland, Baltic Sea, *Limnology and Oceanography* **41** (1): 98-112.

Kononen, K and J-M Leppänen, 1997, Patchiness, scales and controlling mechanisms of cyanobacterial blooms in the Baltic Sea: Application of a multiscale research strategy. In: Monitoring algal blooms. New techniques for detecting large-scale environmental change, eds. M Kahru and CW Brown (Springer-Verlag Berlin Heidelberg New York), 63-84.

Kopelevich, OV and Burenkov, VI, 1977, Relation between the spectral values of the light absorption coefficients of the sea water, phytoplankton pigments, and the yellow substance, *Oceanology* **17**: 62-64.

Kopelevich, OV, Rodionov, VV, and Stupakova, TP, 1987, Effect of bacteria on optical characteristics of ocean water, *Oceanology,* English Translation **27**: 696-700.

Kopelevich, OV and Filippov YV, 1994, Comparison between different spectral methods of the diffuse attenuation and absorption coefficients of sea water, In *Ocean Optics XII,* eds, SG Ackleson and R Frouin, SPIE Proceedings (The International Society of Optical Engineering), Washington, **2258**: 210-221.

Kopelevich, OV and Ershova, SV, 1997, Model for seawater optical characteristics at UV spectral region. In *Ocean Optics XIII*, eds. SG Ackleson and R Frouin, SPIE Proceedings (The International Society of Optical Engineering) **2963**: 167-172.

Kowalczuk, P and Kaczmarek, S, 1996, Analysis of temporal and spatial variability of yellow substance absorption in the Southern Baltic, *Oceanologia* **38** (1): 3-32.

Kratzer, S, 1994, A comparison of the optical properties of phytoplankton from coastal and oceanic waters, Master Thesis (in English), Universität Bremen, Germany.

Kratzer, S, Tett, P, and R Wilton, 1997, The use of a four-channel colour sensor to measure chlorophyll and carotenoid concentration. In: *Ocean Optics XIII*, eds. SG Ackleson and R Frouin, SPIE Proceedings (The International Society of Optical Engineering) **2963**: 603-608.

Kratzer, S, Land, P and Strömbeck, N, 1998, An optical in-water model for the Baltic Sea, poster at Ocean Optics XIV, Kailua-Kona, Hawaii, USA, 10-13 November 1998, Ocean Optics XIV Conference Papers, Volume 2, New Insights from Ocean Color, CD-ROM prepared by the Office of Naval Research. Ocean, Atmosphere, and Space S&T Department, November 1998.

Kratzer, S, Bowers, DG and Tett, P, 2000, Seasonal changes in colour ratios and optically active constituents in the optical Case-2 waters of the Menai Strait, North Wales, *International Journal of Remote Sensing* **21**(11): 2225-2246.

Kratzer, S, Buchan, S and Bowers, DG, ms, Long term trends and cycles in turbidity in the Menai Strait, North Wales; submitted to *Limnology and Oceanography,* March 2000.

Kratzer, S, ms, Remote sensing and optical monitoring of toxic algal blooms in the Baltic Sea. A review; submitted to *Geophysica*, April 2000.

Kratzer, 2000, Absorption spectra of *Nodularia spumigena* and *Aphanizomenon flos-aquae* reveal chromatic adaptation to the light field in the Baltic Sea, talk and abstract (SS05-08) at the ASLO Aquatic Science Meeting: Research across boundaries, 5-9 June 2000, Copenhagen, Denmark.

Kratzer and Subramaniam, 2000, Remote sensing and optical in-water measurements of a cyanobateria bloom in the Baltic Sea, abstract (CS17p06) at the ASLO Aquatic Science Meeting: Research across boundaries, 5-9 June 2000, Copenhagen, Denmark.

Lehtimäki, J , Sivonen, K, Luukainen, R, and Niemelae, SI , 1994, The effects of incubation time, temperature, light, salinity and phosphorus on growth and hepatoxin production by *Nodularia* strains. *Archiv für Hydrobiologie* **130 (3)** 269-282.

Leppänen, J-M , Niemi, A, and Rinne, I, 1988, Nitrogen fixing of cyanobacteria (blue-green algae) and the nitrogen cycle of the Baltic Sea. *Symbiosis* **6 (1-2)** 181-194.

Leppänen, J-M , Kahru, M, and Nommann, S, 1991, Variability in the surface layer in the Gulf of Finland as detected by repeating continuous transect between Helsinki and Tallinn- a progress report. ICES Symposium on patchiness in the Baltic Sea, Mariehamn, Finland, 3-4 June 1991. Paper No. 30.

Lewis, MR, Ulloa, O, and Platt, T, 1988, Photosynthetic Action, Absorption, and Quantum Yield Spectra For a Natural-Population of Oscillatoria in the North-Atlantic, *Limnology and Oceanography* **33**(1): 92-98.

Lüning, K,1990, *Seaweeds, Their Environment, Biogeography, and Ecophysiology.* Chapter 6: Light. New York, John Wiley & Sons, Inc.

MacColl, R, 1998, Cyanobacterial phycobilisomes, *Journal of Structural Biology* **124**:1047-8477.

Mantoura, RFC and Llewellyn, CA, 1983, The rapid determination of algal chlorophyll and carotenoid pigments and their breakdown products in natural waters by reverse-phase high performance liquid chromatography, *Analytica Chimica Acta* **151**: 297-314.

Mantoura, RFC, Wright, SW, Jeffrey, SW, Barlow, R G, Cummings, D, 1997, Filtration and storage of pigments from microalgae. In: Phytoplankton pigments in oceanography: Guidelines to modern methods, eds. SW Jeffrey, RFC Mantoura, SW Wright. UNESCO, Paris, 283-305.

Margulis, L, 1993, *Symbiosis in cell evolution. Microbial communities in the Archean and Proterozoic eons*. New York, WH Freeman and Company.

Mills, DK and Tett, P, 1990, Use of a recording fluorometer for continuous measurements of phytoplankton concentration. *Ocean Optics X,* eds. SG Ackleson and R Frouin, SPIE Proceedings (The International Society of Optical Engineering) **1269**, 106-115.

Mitchell, BG and Kiefer, DA, 1988, Chlorophyll a specific absorption and fluorescence excitation spectra for light-limited phytoplankton, *Deep-Sea Research* **35**: 639-663.

Mitchell, BG, 1990, Algorithms for determining the absorption coefficient of aquatic particulates using the quantitative filter technique (QFT). In: *Ocean Optics X,* eds. SG Ackleson, R Frouin, Proceedings SPIE (The International Society of Optical Engineering), Washington, **1302**: 137-148.

Mitchelson, EG, Jacob, NJ and Simpson, JH, 1986, Ocean colour algorithms from the case 2 waters of the Irish Sea in comparison to algorithms from case 1 waters, *Continental Shelf Research* **5**(3): 403-415.

Morel, A & Prieur, L, 1977, Analysis of variations in ocean colour, *Limnology and Oceanography*, **22**, 709-722.

Morel, A and Bricaud, A, 1981, Theoretical results concerning light absorption in a discrete medium, and application to specific absorption of phytoplankton, *Deep-Sea Research* **28A**(11): 1375-1393.

Morel, A and Smith, RC, 1982, Terminology and units in optical oceanography, *Marine Geodesy* **5**: 335-349.

Morel, A, 1988, Optical modelling of the upper ocean in relation to its biogenous matter content (case I waters), *Journal of Geophysical Research* **93**(C9):10749-10768.

Morel, A and Ahn, YH, 1990, Optical efficiency factors of free-living marine bacteria: Influence of bacterioplankton upon the optical properties and particulate organic carbon in oceanic waters, *Journal of Marine Research* **48**: 145-175.

Morel, A and Gentili, B, 1991, Diffuse reflectance of oceanic waters: its dependence on sun angle as influenced by the molecular scattering contribution, *Applied Optics* **30**(30): 4427-4438.

Morel, A, Ahn, YH, Partensky, F, Vaulot, D, and Claustre, H, 1993, Prochlorococcus and Synechococcus - a comparative-study of their optical properties in relation to their size and pigmentation, *Journal of Marine Research* **51**(3): 617-649.

Moreth, CM and Yentsch, CS, 1970, A sensitive method for the determination of open ocean phytoplankton phycoerythrin pigments by fluorometry, *Limnology and Oceanography* **15**: 313-317.

Mueller, JL, and Austin, RW, 1995, Ocean Optics Protocols for SeaWiFS Validation, Volume 25, Revision 1, *SeaWiFS Technical Report Series,* eds. SB Hooker, ER Firestone, and JG Acker, NASA Technical Memorandum 104566, Maryland, **25**.

Nelson, NB, Siegel, DA, and Michaels, AF, 1998, Seasonal dynamics of colored dissolved material in the Sargasso Sea. *Deep-Sea Research Part I-Oceanographic Research Papers*, **45** (6): 931-957.

Parsons, T R, Maita, Y and Lalli, CM, 1984, *A manual of chemical and biological methods for seawater analysis*. Oxford, Pergamon Press.

Parsons, TR, Takanashi, M, and Hargrave, B, 1990, *Biological Oceanographic Processes*, Pergamon Press.

Peters, RH, 1991, *A critique for ecology*, Cambridge University Press, Cambridge.

Pingree, RD and Harris, RP, 1988, An in vivo fluorescence response in the Bay of Biscay in June, *Journal of the Marine Biological Association of the United Kingdom* **68**: 519-529.

Platt, T and Sathyendranath, S, 1988, Ocean primary production. Estimation by remote sensing at local and regional scales, *Science* **241**: 1613-1620.

Pope, RM and Fry, ES, 1997, Absorption spectrum (380-700 nm) of pure water. II. Integrating cavity measurements, *Applied Optics* **36** (33): 8710-8723.

Porra, RJ, Pfündel, EE, and Engel, N, 1997, Metabolism and function of photosynthetic pigments. In: Phytoplankton pigments in oceanography: Guidelines to modern methods, eds. SW Jeffrey, RFC Mantoura, SW Wright. UNESCO, Paris, 85-126.

Prezelin, BB and Sweeney, BM, 1977, Characterization of photosynthetic rhythms in marine dinoflagellates. II. Photosynthesis-irradiance curves and in vivo chlorophyll fluorescence, J*ournal of Marine Research* **38**: 687-701.

Prieur, L and Sathyendranath, S, 1981, An optical classification of coastal and oceanic waters based on the specific spectral absorption curves of phytoplankton pigments, dissolved organic matter, and other particulate materials, *Limnology and Oceanograph* **26**(4): 671-689.

Rantajärvi, E and Leppänen, JM, 1994, Unattended algal monitoring merchant ships in the Baltic Sea. Nordic Council of Ministers, TemaNord **546,** 60 pp.

Ricard, M, 1987, *Atlas du phytoplankton marin*. Paris, Éditions du centre national de la recherche scientifique.

Richter, G, 1988, *Stoffwechselphysiologie der Pflanzen. Physiologie und Biochemie des Primär- und Sekundärstoffwechsels*. Stuttgart, New York, Georg Thieme Verlag.

Riper, DM, Owens, TG, and Falkowski, PG, 1979, Chlorophyll turnover in *Skeletonema costatum*, a marine plankton diatom, *Plant Physiology* **64**: 49-54.

RochelleNewall, EJ, Fisher, TR, Fan, C, and Glibert, PM, 1999, Dynamics of chromophoric dissolved organic matter and dissolved organic carbon in experimental mesocosms, *International Journal of Remote Sensing* **20** (3): 627-641.

Roesler, CS and Perry, MJ, 1995, *In situ* phytoplankton absorption, fluorescence emission, and particulate backscattering spectra determined from reflectance, *Journal of Geophysical Research* **100**(C7): 13279-13294.

Roesler, CS , 1998, Remote detection of harmful algal blooms. Ocean Optics XIV, Kailua-Kona, Hawaii, USA, 10-13 November 1998, *SPIE*.

Rowan, KS, 1989, *Photosynthetic pigments of algae*. Cambridge, Cambridge University Press.

Rud, O and Kahru, M, 1994, Long-term series of NOAA AVHRR imagery reveals large interannual variations of surface cyanobacterial accumulations in the Baltic Sea. EARSeL workshop on Remote Sensing and GIS for Coastal Zone Management, 24-26 October 1994, Delft, The Netherlands, Rijkswaterstaat Survey Department.

Rud, O and Kahru, M, 1995, Monitoring of harmful algal blooms in the Baltic Sea, *Remote Sensing* **(26)**: 8-10.

Sai, PSM, Siebzehnrubl, S, Mahajan, S, and Scheer, H, 1992, Phycoerythrocyanins from *Westiellopsis prolifica* and *Nostoc rivulare* - Characterization of the phycoviolobilin chromophore in both states, *Photochemistry and Photobiology* **55** (1): 119-124.

Sanden, P and Håkansson, B, 1996, Long-term trends in the Secchi depth in the Baltic Sea, *Limnology and Oceanography* **41**(2): 346-351.

Sathyendranath, S, Lazzara, L, and Prieur, L, 1987, Variations in the spectral values of specific absorption of phytoplankton, *Limnology and Oceanography* **32**: 403-415.

SeaWiFS project, NASA/Goddard Space Flight Centre, 1997, Image of global ocean chlorophyll concentration (no title), *Backscatter, the magazine for the aquatic remote sensing community* **8**(4): 16-17.

Sellner, KG, 1997, Physiology, ecology, and toxic properties of marine cyanobacteria blooms, *Limnology and Oceanography* **42** (5, II): 1089-1104.

Setser, PJ, Guinasso, NLJr, and Schink, DR, 1982, Daily patterns of fluorescence *in vivo* in the central equatorial Pacific, *Journal of Marine Research* **40**: 453-471.

Sherwin, TJ, 1996, Menai Strait Tide Tables, Unit for Coastal and Estuarine Studies (UCES), SOS, University of Wales, Bangor, Menai Bridge.

Sieburth, JM, Smetacek, V, Lenz, J, 1978, Pelagic ecosystem structure: Heterotrophic components of the plankton and their relationship to plankton size-fractions, *Limnology and Oceanography* **23**: 1256-1263.

Siegel, H , Gerth, M and Beckert, M, 1996, Variation of specific optical properties and their influence on measured and modelled spectral reflectances in the Baltic Sea. In: *Ocean Optics XIII*, eds. SG Ackleson and R Frouin, SPIE Proceedings (The International Society of Optical Engineering) **2963**: 526-531.

Siegelman, HW and Kycia, JH, 1973, Algal biliproteins. In: Handbook of phycological methods. Physiological and biochemical methods, eds. JA Hellebust and JS Craigie. London, Cambridge University Press: 71-79.

Skoog, A, Hall, POJ, Hulth, S, Paxeus, N, vanderLoeff, MR, and Westerlund, S, 1996, Early diagenetic production and sediment-water exchange of fluorescent dissolved organic matter in the coastal environment. *Geochimica et Cosmochimica Acta* **60**(19): 3619-3629.

Smith, PSD, Bowers, DG and Mitchelson-Jacob, EG, 1996, The optical determination of phytoplankton floristic composition. In: *Ocean Optics XIII*, eds. SG Ackleson and R Frouin, SPIE Proceedings (The International Society of Optical Engineering) **2963**: 532-537.

Smith, PSD, 1999, Bio-Optical Observations at the Hebridean Shelf Edge, PhD thesis, School of Ocean Sciences, University of Wales, Bangor, UK.

Smith, RC and Baker, KS, 1978, The bio-optical state of ocean waters and remote sensing, *Limnology and Oceanography* **23**: 247-259.

Smith, RC and Baker, KS, 1981, Optical properties of the clearest natural waters (200-800nm), *Applied Optics* **20**: 177-84.

Smith, RC, Waters, KJ, and Baker, KS, 1991, Optical variability and pigment biomass in the Sargasso Sea as determined using deep-sea optical mooring data, *Journal of Geophysical Research-Oceans* **96** (NC5): 8665-8686.

Sosik, HM and Mitchell, BG, 1991, Absorption, fluorescence, and quantum yield for growth in nitrogen-limited *Dunaliella tertiolecta*, *Limnology and Oceanography* **36**(5): 910-921.

Sournia, A, 1986, *Atlas du phytoplankton marin*. Paris, Éditions du centre national de la recherche scientifique.

Spinrad, RV, Glover, H, Ward, BB, Codispoti, LA, and Kullenberg, G, 1989, Suspended particle and bacteria maxima in Peruvian coastal waters during a cold water anomaly, *Deep Sea Research* **36**: 211-222.

Stewart, DE and Farmer, FH, 1984, Extraction, identification, and quantification of phycobiliprotein pigments from phototrophic phytoplankton, *Limnology and Oceanography* **29**(2): 392-397.

Stramski, D and Kiefer, AD, 1990, Optical properties of marine bacteria. In: *Ocean Optics X,* eds. SG Ackleson, R Frouin, Proceedings SPIE (The International Society of Optical Engineering), Washington, **1302**: 250-268.

Stramski, D and Morel, A, 1990, Optical properties of photosynthetic picoplankton in diffrent physiological states as affected by growth irradiance, *Deep-Sea Research* **37**(2): 245-266.

Strickland, JHD and Parsons, TR, 1972, A practical handbook of sea-water analysis, *Bulletin Journal of the Fisheries research board of Canada* **167**: 185-203.

Subramaniam, A, Carpenter, EJ, Karentz, D, Falkowski, PG, 1999, Bio-optical properties of the marine diazotrophic cyanobacteria *Trichodesmium* spp. I. Absorption and photosynthetic action spectra, *Limnology and Oceanography* **44** (3): 608-617.

Subramaniam , A, Kratzer, S, Carpenter EJ and Söderbäck, E, 2000, Remote sensing and optical in-water measurements of a cyanobacteria bloom in the Baltic Sea. Presented at the Sixth International Conference on Remote Sensing for Marine and Coastal Environments, Charleston, South Carolina, 1-3 May 2000.

Tassan, F and Ferrari, GM, 1995, An alternative approach to absorption measurements of aquatic particles retained on filters, *Limnology and Oceanography* **40**(8): 1358-1368.

Tett, P and Grantham, B, 1980, Variability in Sea Loch Phytoplankton. In: Fjord Oceanography, eds. HJ Freeland, DM Farmer and CD Levings. Plenum Publishing Corporation, New York.

Tett, P, 1987, Plankton. In: Biological Survey of Estuaries and Coasts, eds. J Baker and WJ Wolff, Cambridge University Press, 280-341.

Tett, PB, 1990, The photic zone. In: Light and life in the sea, eds. PJ Herring, AK Campell, M Whitfield and L Maddock, Cambridge University Press, pp 59-87.

Tett, P, Kennaway, GM, Boon, D, Mills, DK, O'Connor, GT, Walne, AW, and Wilton, R, 2000, Optical monitoring of phytoplankton blooms in Loch Striven, an euphotic fjord, *International Journal of Remote Sensing*, in press.

Throndsen, 1978, Preservation and storage, In: Phytoplankton manual, Monographs on oceanographic methodology,ed. A Sournia, UNESCO, Paris, pp 69-74.

Trüper, H and Yentsch, CS, 1967, Use of glass fibre filters for the rapid preparation of *in vivo* absorption spectra of photosynthetic bacteria, *Journal of Bacteriolgy* **94**: 1255-1256.

Ulloa, O, Sathyendranath, S, Platt, T, and Quinones, R A, 1992, Light scattering by marine heterotrophic bacteria, *Journal of Geophysical Research* **97**(C6): 9619-9629.

Ulloa, O, Sathyendranath, S, and Platt, T, 1994, Effect of the particle size distribution on the backscattering ratio in sea water, *Applied Optics* **33**(30): 7070-7077.

Vesk, M and Jeffrey, SW, 1977, The effect of blue-green light on photosynthetic pigments and chlorophyll structure in uni-cellular marine algae from six algal classes, *Journal of Phycology* **13**: 280-288.

Victorov, SV, 1996, *Regional Satellite Oceanography* (Taylor and Francis).

Voipio, A, 1981, *The Baltic Sea* (Elsevier Science Publishers, New York).

Walsby, AE , Hayes, PK, Boje, R, 1995, The gas vesicles, buoyancy and vertical distribution of cyanobacteria in the Baltic Sea, *European Journal of Phycology* **30**: 87-94.

Walsh, JJ, Rowe, GT, Iverson, RL, and McRoy, CP, 1981, Biological export of shelf carbon is a sink of the global CO_2 cycle, *Nature* **291**: 196-201.

Waterbury, JB, Watson, SW, Guillar, RR, and Brand, LE, 1979, Widespread occurrence of a unicellular, marine phytoplanktonic cyanobacterium, *Nature* **277**: 293-294.

Wedborg, M, Skoog, A and Fogelqvist, E, 1994, Organic carbon and humic subtances in the Baltic Sea, the Kattegatt, and the Skagerrak. Eds. N Senesi and TM Miano, Humic substances in the global environment and implications on human health, Elsevier Sciences.

Weeks, AR, 1989, Seasonal and tidal cycles of suspended particulates in the Irish Sea, PhD thesis, University of Wales, Bangor.

Weidemann, AD and Bannister, TT, 1986, Absorption and scattering coefficients in Irondequoit Bay, *Limnology and Oceanography* **31**: 567-583.

Wells, ML and Goldberg, ED, 1992, Marine submicron particles, *Marine Chemistry* **40**: 5-18.

Whitledge, TE and Wirrick, CD, 1986, Development of a moored in situ fluorometer for phytoplankton studies. In: Tidal Mixing and Phytoplankton Dynamics, eds. J Bowman, M Yentsch, and WT Petersen, Springer Verlag, Berlin, 449-462.

Wild-Allen, K, Tett, PB, and Bowers, DG, 1997, Observations of diffuse upwelling irradiance and chlorophyll in case I waters near the Canary Islands (Spain), *Optics and Laser Technology* 29 (1): 3-8.

WMO, 1981, *Measurement of River Sediments*, WMO Operational Hydrology Report 16, World Meteorological Organization, Geneva, 61 pp.

Wright, SW , Jeffrey, SW, Mantoura, RFC, Llewellyn, CA, Bjørnland, T, Repeta, D, and Welschmeyer, N, 1991, Improved HPLC method for the analysis of chlorophylls and carotenoids from marine phytoplankton, *Marine Ecology Progress Series* **77**: 183-196.

Wyman, M, Gregory, RPF, and Carr, NG, 1986, Role of Phycoerythrin in Marine Picoplankton Synechococcus Spp - Response, *Science* **234**: 1423-1424.

Wyman, M, 1992, An *in vivo* method for the estimation of phycoerythrin concentrations in marine cyanobacteria (*Synechococcus* spp.), *Limnology and Oceanography* **37**(6): 1300-1306.

Yentsch, CS, 1957, A non-extractive method for the quantitative estimation of chlorophyll in algal cultures, *Nature* **179**: 1302-1304.

Yentsch, CS, 1962, Measurements of visible light absorption by particulate matter in the ocean, *Limnology and Oceanography* **7**: 207-217.

Yentsch, CS and Phinney, DA, 1989, A bridge between ocean optics and microbial ecology, *Limnology and Oceanography* **34**: 1694-1705.